Lappeenranta
University of Technology

Igor Rozhansky

RESONANT TUNNELING EFFECTS IN SEMICONDUCTOR HETEROSTRUCTURES

Thesis for the degree of Doctor of Philosophy to be presented with due permission for public examination and criticism in the Auditorium 1383 at Lappeenranta University of Technology, Lappeenranta, Finland on the 26th of September, 2014 at noon.

Acta Universitatis
Lappeenrantaensis 586

Supervisors Professor Erkki Lähderanta
Department of Mathematics and Physics
Lappeenranta University of Technology
Finland

Professor Nikita Averkiev
Sector of Theory of Optical and Electrical Phenomena in Solids
A.F. Ioffe Physical Technical Institute, Russian Academy of Sciences
St.Petersburg, Russia

Reviewers Professor Alexander Tagantsev
Materials Department
Swiss Federal Institute of Technology, EPFL
Switzerland

Professor Magnus Willander
Division of Physics and Electronics
Linköping University
Sweden

Opponent Professor Martti Puska
Department of Applied Physics
Aalto University School of Science
Finland

ISBN 978-952-265-631-5
ISBN 978-952-265-632-2 (PDF)
ISSN-L 1456-4491
ISSN 1456-4491

Lappeenrannan teknillinen yliopisto
Digipaino 2014

Abstract

Igor Rozhansky
RESONANT TUNNELING EFFECTS IN SEMICONDUCTOR HETEROSTRUCTURES
Lappeenranta, 2014
80 p.
Acta Universitatis Lappeenrantaensis 586
Diss. Lappeenranta University of Technology
ISBN 978-952-265-631-5, ISBN 978-952-265-632-2 (PDF), ISSN-L 1456-4491, ISSN 1456-4491

The thesis is devoted to a theoretical study of resonant tunneling phenomena in semiconductor heterostructures and nanostructures. It considers several problems relevant to modern solid state physics. Namely these are tunneling between 2D electron layers with spin-orbit interaction, tunnel injection into molecular solid material, resonant tunnel coupling of a bound state with continuum and resonant indirect exchange interaction mediated by a remote conducting channel.

A manifestation of spin-orbit interaction in the tunneling between two 2D electron layers is considered. General expression is obtained for the tunneling current with account of Rashba and Dresselhaus types of spin-orbit interaction and elastic scattering. It is demonstrated that the tunneling conductance is very sensitive to relation between Rashba and Dresselhaus contributions and opens possibility to determine the spin-orbit interaction parameters and electron quantum lifetime in direct tunneling experiments with no external magnetic field applied.

A microscopic mechanism of hole injection from metallic electrode into organic molecular solid (OMS) in high electric field is proposed for the case when the molecules ionization energy exceeds work function of the metal. It is shown that the main contribution to the injection current comes from direct isoenergetic transitions from localized states in OMS to empty states in the metal. Strong dependence of the injection current on applied voltage originates from variation of the number of empty states available in the metal rather than from distortion of the interface barrier.

A theory of tunnel coupling between an impurity bound state and the 2D delocalized states in the quantum well (QW) is developed. The problem is formulated in terms of Anderson-Fano model as configuration interaction between the carrier bound state at the impurity and the continuum of delocalized states in the QW. An effect of this interaction on the interband optical transitions in the QW is analyzed. The results are discussed regarding the series of experiments on the GaAs structures with a δ-Mn layer.

A new mechanism of ferromagnetism in diluted magnetic semiconductor heterosructures is considered, namely the resonant enhancement of indirect exchange interaction between paramagnetic centers via a spatially separated conducting channel. The underlying physical model is similar to the Ruderman-Kittel-Kasuya-Yosida (RKKY) interaction; however, an important difference relevant to the low-dimensional structures is a resonant hybridization of a bound state at the paramagnetic ion with the continuum of delocalized states in the conducting channel. An approach is developed, which unlike RKKY is not based on the perturbation theory and demonstrates that the resonant hybridization leads to a strong enhancement of the indirect exchange. This finding is discussed in the context of the known experimental data supporting the phenomenon.

Keywords: resonant tunneling, semiconductor heterostructures, indirect exchange interaction, spin-dependent tunneling, configuration interaction, RKKY

UDC 621.315.5:539.1:621.382

To my daughter Ann

Acknowledgements

The scientific work and publications have been done in collaboration between Department of Mathematics and Physics of Lappeenranta Unversity of Technology (LUT School of Technology) and A.F. Ioffe Physical Technical Institute, Russian Academy of Sciences, St.Petersburg.

I would like to express my highest appreciation and thanks to my Supervisor at LUT Professor Erkki Lähderanta for his very kind attitude and support throughout the collaboration. With his warm and friendly hospitality he made my stay and work at LUT most pleasant and wonderful.

I would like to express my deepest gratitude to my Supervisor at Ioffe Institute Professor Nikita Averkiev for encouraging my research, for help and guidance throughout the work and for filling the research process with the spirit of true physics and warmth of the human attitude.

I would like to thank my colleagues for very valuable discussions and friendly attitude, especially Boris Aronzon, Petr Arseev, Mikhail Glazov, Vladimir Korenev, Igor Krainov, Vladimir Kulakovskii, Andrey Monakhov, Victor Sapega, Sergey Tarasenko, Valerii Valkov, Sergei Zaitsev.

I wish to thank Professor Alexander Tagantsev and Professor Magnus Willander who took the work of reading and reviewing the thesis.

My sincere gratitude to Professor Martti Puska as opponent.

I would like to express my gratitude to the Lappeenranta University of Technology for financial support and possibility to complete this thesis.

I wish to thank my parents Irina and Vladimir for their care and support and, especially, my Dad for introducing me to the science. I'm most warmly thankful to my wife Maria for her support, patience and love. And I'm extremely thankful to my wonderful daughter Ann for her kind love and happiness.

Lappeenranta, 2014

Igor Rozhansky

List of publications

This thesis consists of an introduction (Chapter I), an explanation of the key theoretical models used throughout the dissertation (Chapter II), a review and discussion of the subject (Chapters III-VI), and Summary (Chapter VII). The original subject of the thesis discussed in the chapters III-VI has been published in the following eight publications:

1 **I. V. ROZHANSKY and N. S. AVERKIEV**, Manifestation of spin-orbit interaction in tunneling between two-dimensional electron layers, *Physical Review B*, **77**, 115309, 2008.

2 **I. V. ROZHANSKY and N. S. AVERKIEV**, Spin-dependent tunneling conductance in two-dimensional structures at zero magnetic field, *Low Temperature Physics*, **35**, 15, 2009.

3 **N. S. AVERKIEV, V. A. ZAKREVSKII, I. V. ROZHANSKY, and N. T. SUDAR**, Peculiarities of holes injection into organic molecular solids, *Applied Physics Letters*, **94**, 233308, 2009.

4 **I. V. ROZHANSKY, N. S. AVERKIEV, and E. LÄHDERANTA**, Tunneling magnetic effect in heterostructures with paramagnetic impurities, *Physical Review B*, **85**, 075315, 2012.

5 **I. V. ROZHANSKY, N. S. AVERKIEV, and E. LÄHDERANTA**, Fano-type coupling of a bound paramagnetic state with 2D continuum, *AIP Conference Proceedings*, **1566**, 335, 2013.

6 **I. V. ROZHANSKY, N. S. AVERKIEV, and E. LÄHDERANTA**, Configuration interaction in delta-doped heterostructures, *Low Temperature Physics*, **39**, 40, 2013.

7 **I. V. ROZHANSKY, I. V. KRAINOV, N. S. AVERKIEV, and E. LÄHDERANTA**, Resonant exchange interaction in semiconductors, *Physical Review B*, **88**, 155326, 2013.

8 **I. V. ROZHANSKY, N. S. AVERKIEV, I. V. KRAINOV, and E. LÄHDERANTA**, Resonant enhancement of indirect exchange interaction in semiconductor heterostructures, *physica status solidi (a)*, **211**, 1048-1054, 2014.

PART I: OVERVIEW OF THE THESIS

CHAPTER I

INTRODUCTION

1.1 Motivation for the research

Research in the field of semiconductor physics has been going on for over a hundred years. A constant progress in the field has been driven both by novel concepts and theoretical achievements and advances in technology, experimental set-ups and tools. Since the invention of the solid state transistor in 1947 the semiconductors have been extensively used in electronics. Semiconductor heterostructures have emerged on the scene of semiconductor physics in 1970s and immediately brought up new physics and new applications in the field of semiconductor electronics and laser optics. At the end of the 20th century experimental and theoretical efforts have permitted to clearly establish quantum confinement and tunnel coupling as key concepts in the field. A semiconductor heterostructure can have a quantum confinement in one dimension (quantum well), two dimensions (quantum wire), or three dimensions (quantum dot) [Harrison (2006)]. Recent advances in fabrication of various semiconductor nanostructures have pushed forward the research which is focused nowadays on the low-dimensional electronic systems. Due to the fundamental limits for further miniaturization of transistors in microprocessors and memory cells the new physical principles are searched to be realized in electronic devices. One of the most actively growing research field here is spintronics, which unites efforts to exploit the spin degree of freedom, i.e. to transfer and process information not only by the charge but also via the electrons spins. In this context, Diluted Magnetic Semiconductors (DMS), mostly based on $A_{III}B_V$-type semiconductors, are considered as mostly promising. Yet, at present, the low-dimensional structures are still far from being well-studied in the frame of spintronics requiring both theoretical and experimental efforts.

An important feature characteristic of nanostructures is that the spatial scale of potential energy profile matches the characteristic length of the quantum tunneling. This leads to the fact that many optical, electrical and spin phenomena are related to the charge carriers passing through classically inaccessible regions. In particular, the non-trivial effects occur in the case where the resonant tunneling takes place. The present work considers a number of phenomena essentially based on the quantum tunneling and especially resonant tunneling, that are attractive for modern semiconductor physics of nanostructures.

1.1.1 Resonant tunneling between two-dimensional electron layers

The tunnelling between 2D electron layers separated by a weakly transparent tunnel barrier is a prime example of resonant tunneling in semiconductor nanostructures. In such a structure unlike the tunneling phenomena in bulk samples, the energy and in-plane momentum conservation put tight restrictions on the tunneling so that the conductance exhibits delta function-like maximum at zero bias broadened by elastic scattering in the layers [Zheng and MacDonald (1993)] and fluctuations of the layers width [Vasko et al. (2000)]. Such a behavior has been observed in a number of experiments [Murphy et al. (1995); Turner et al. (1996); Popov et al. (1998)]. The picture becomes far more complicated when the spin-orbit interaction in the layers is taken into account. Spin-orbit interaction splits the electron spectra into two subbands in each layer. It was suggested that energy and momentum conservation can be fulfilled for the tunneling between opposite subbands of the layers at a finite voltage corresponding to the subbands splitting [Raichev and Debray (2003)], [Zyuzin et al. (2006)]. The key issue remains how the spin-orbit interaction, in particular Rashba and Dresselhaus contributions, would affect the experimentally observed conductivity vs voltage characetistics.

1.1.2 Tunnel injection in molecular solids

All the electronic devices have contacts which are of great importance for their operation. The physics underlying the proper functioning of the contacts is often far from trivial. In fact, tunnel injection more often than it seems is the main mechanism of charge transfer through the contacts. This thesis considers the metal contact to the organic molecular solid material. The organic molecular solids (OMS) are widely used in modern micro and optoelectronics. Light emitting diodes and field effect transistors have been fabricated on the basis of these materials [Forrest (2004)]. The tendency of further expansion of the potential applications for the OMS demands complete understanding of the underlying physics. However, some issues still remain unclear, one of them, addressed in the present work, is the conductivity of the OMS films in a high electric field. This part of the work diverges from the semiconductor heterostuctures by the object considered, however the non-trivial case of the tunnel injection studied might be of importance beyond this particular case.

1.1.3 Tunneling configuration interaction

Another type of quantum resonance phenomena, relevant for semiconductor heterostructures is so-called configuration interaction of a single bound state with a continuum of states. The problem goes back to the famous paper by U. Fano [Fano (1961)] rated as one of the most relevant works of 20th century [Miroshnichenko et al. (2010)]. The suggested theoretical approach often regarded as Fano-Anderson model or configuration interaction succeeded in explaining puzzling asymmetric resonances observed in various experiments in atomic and nuclear physics, condensed matter physics and optics [Miroshnichenko et al. (2010)]. The co-existence of the discrete energy level and the continuum states within the same energy range is rather common in low-dimensional semiconductor structures. Of particular interest here are the structures having a quantum well (QW) and a ferromagnetic or paramagnetic layer located in the vicinity of the QW, but not penetrating into the QW region. In such structures high mobility of the carriers along the QW is combined with the magnetic properties provided by the magnetic layer. A number of recent experiments show that the Mn δ–layer gives rise to circular polarization of the photoluminescence (PL) from the QW in

an external magnetic field applied perpendicular to the QW plane [Dorokhin et al. (2010); Zaitsev et al. (2010)]. It was questioned whether the spin polarization of the carries in the QW is due to the electrons tunneling to Mn site or the tunnel coupling of the holes at Mn with those in the QW. The latter mechanism seemed to lack the proper theoretical description [Miroshnichenko et al. (2010); Blom et al. (2002); Okulov et al. (2011); Aleshkin et al. (2008)]. The study included in this thesis tries to fill the gap.

1.1.4 Indirect exchange interaction via spatially separated channel

Ferromagnetic diluted magnetic semiconductors (DMS) have been in the focus of the extensively developing spintronics for quite a while. However, the particular mechanism responsible for the ferromagnetic properties of GaAs doped with Mn is still unclear [Jungwirth et al. (2006)]. The two-dimensional structures are even less studied in the context of spintronics, and only recently some papers appeared [Rupprecht et al. (2010); Nishitani et al. (2010); Aronzon et al. (2010, 2013)]. It was discovered that the dependence of the Curie temperature on the QW depth shows the non-monotonic behavior [Aronzon et al. (2013)]. Analysis of the parameters of these GaAs/InGaAs/Mn heterostructures shows that the non-monotonic behavior originates from falling of the hole bound state at Mn ion into the energy range of occupied 2D heavy holes subband of the first QW size quantization level. In this case the resonant tunneling is allowed between the bound state and the continuum of the delocalized 2D states in the QW so that much stronger coupling of the hole localized at Mn with the 2D holes gas in the QW is expected. Both too shallow or too deep QW would break the resonant condition and decrease the mutual influence of the QW and the Mn ions. The main goal of the present research was to introduce a proper theory describing the indirect pair exchange interaction between two ions mediated by a 2D free carriers gas located at a tunnel distance with account for the resonant tunnel coupling with the Mn bound states. It will be shown that when the condition for the resonant tunneling is met the interaction strength appears to be strongly enhanced.

1.2 Outline of the work

The dissertation is a theoretical study of resonant tunneling phenomena in semiconductor heterostructures and molecular organic solids. It considers several problems relevant in modern solid state physics. Namely these are tunneling between 2D electron layers with spin-orbit interaction, charge tunnel injection into organic molecular solid material, resonant tunnel coupling of a bound state with continuum of delocalized states in a heterostructure and resonant indirect exchange interaction mediated by spatially separated conducting channel. The quantum tunneling in all cases is approached via the tunnel Hamiltonian method [Bardeen (1961)]. The thesis consists of a summary section and the original papers. The summary section consists of seven chapters as follows:

Chapter 1 is an Introduction.

Chapter 2 includes the description of basic theoretical methods used throughout the work. These are the method of tunneling Hamiltonian, Fano-Anderson model and application of the standing wave scattering problem to the interaction energy calculations.

Chapter 3 concerns the tunneling between two 2D electron layers with account for the spin-orbit interaction. To different contributions to the spin-orbit interaction are considered, namely the Rashba term, resulting from the external electric field and Dresselhaus term originating from the internal

crystal electric field present in semiconductors without inversion assymetry. It is shown that the tunneling conductance can either exhibit resonances at certain voltage values or be substantially suppressed over the whole voltage range. The dependence of the conductance on voltage turns out to be very sensitive to the relation between Rashba and Dresselhaus contributions even in the absence of external magnetic field. The elastic scattering in the layers broadens the resonances or restores the conductance to a larger magnitude in the case of suppression.

The subject of **Chapter 4** lies a bit aside of the semiconductor heterostructures, however it gives another fruitful application of the tunneling Hamiltonian approach to the tunneling phenomena in the solid state. The chapter considers hole injection from metallic electrode into organic molecular solid (OMS) in high electric field when the ionization energy of the molecules exceeds the work function of the metal. It is shown that the main contribution to the injection current comes from direct isoenergetic transitions (without interaction with phonons) from localized states in OMS to empty states in the metal. Strong dependence of the injection current on applied voltage originates from variation of the number of empty states available in the metal rather than by modification of the interface barrier shape.

Chapter 5 presents the theory of tunnel coupling between an impurity bound state and the 2D delocalized states in the quantum well (QW). The study is focused on the resonance case when the bound state energy lies within the continuum of the QW states.The problem is formulated in terms of Anderson-Fano model as configuration interaction between the charge carrier bound state at the impurity and the continuum of delocalized states in the QW. An effect of this interaction on the interband optical transitions in the QW is analyzed. The results are discussed regarding the series of experiments on the GaAs structures with a δ-Mn layer.

Chapter 6 discusses a new mechanism of ferromagnetism in diluted magnetic semiconductor heterosructures, namely the resonant enhancement of indirect exchange interaction between paramagnetic centers via a spatially separated conducting channel. The underlying physical model is similar to the Ruderman-Kittel-Kasuya-Yosida (RKKY) interaction; however, an important difference relevant to the low-dimensional structures is a resonant hybridization of a bound state at the paramagnetic ion with the continuum of delocalized states in the conducting channel. An approach is developed, which unlike RKKY is not based on the perturbation theory and demonstrates that the resonant hybridization leads to a strong enhancement of the indirect exchange. This finding is discussed in the context of the known experimental data supporting the phenomenon.

Chapter 7 contains conclusions summarizing the main topics and results of the thesis.

1.3 Summary of the publications

Publication 1. I. V. ROZHANSKY and N. S. AVERKIEV, Manifestation of spin-orbit interaction in tunneling between two-dimensional electron layers, *Physical Review B*, **77**, 115309, 2008.

An influence of spin-orbit interaction on the tunneling between two 2D electron layers is considered. Particular attention is addressed to the relation between the contribution of Rashba and Dresselhaus types. It is shown that without scattering of the electrons, the tunneling conductance can either exhibit resonances at certain voltage values or be substantially suppressed over the whole voltage range. The dependence of the conductance on voltage turns out to be very sensitive to the relation between Rashba and Dresselhaus contributions even in the absence of magnetic field. The elastic

scattering broadens the resonances in the first case and restores the conductance to a larger magnitude in the latter one. These effects open possibility to determine the parameters of spin-orbit interaction and electrons scattering time in tunneling experiments with no necessity of external magnetic field.

The author of this dissertation carried out the theoretical calculations, numerical calculations, presented the work at the International Conference on Physics of Semiconductors (ICPS-2008) and others, wrote the paper and was the principal author of the publication.

Publication 2. I. V. ROZHANSKY and N. S. AVERKIEV, Spin-dependent tunneling conductance in two-dimensional structures at zero magnetic field, *Low Temperature Physics*, **35**, 15, 2009.

The influence of the spin-orbit interaction on the tunneling between 2D electron layers is considered. A general expression for the tunneling current is obtained with the Rashba and Dresselhaus effects and also elastic scattering of charge carriers on impurities taken into account. It is shown that the particular form of the tunneling conductance as a function of the voltage between layers is extremely sensitive to the relationship between the Rashba and Dresselhaus parameters. This makes it possible to determine the parameters of the spin-orbit interaction and the quantum scattering time directly from measurements of the tunneling conductance in the absence of magnetic field.

The author of this dissertation carried out the theoretical calculations, numerical calculations, wrote the paper and was the principal author of the publication.

Publication 3. N. S. AVERKIEV, V. A. ZAKREVSKII, I. V. ROZHANSKY, and N. T. SUDAR, Peculiarities of holes injection into organic molecular solids, *Applied Physics Letters*, **94**, 233308, 2009.

A microscopic mechanism of hole injection from metallic electrode into organic molecular solid (OMS) in high electric field is proposed. The consideration is focused on the case when the molecules ionization energy exceeds work function of the metal. It is shown that the main contribution to the injection current comes from direct isoenergetic transitions (without interaction with phonons) from localized states in OMS to empty states in the metal. Strong dependence of the injection current on applied voltage originates from variation of the number of empty states available in the metal rather than by modification of the interface barrier shape.

The author of this dissertation carried out the theoretical calculations and wrote the paper.

Publication 4. I. V. ROZHANSKY, N. S. AVERKIEV, and E. LÄHDERANTA, Tunneling magnetic effect in heterostructures with paramagnetic impurities, *Physical Review B*, **85**, 075315, 2012.

An effect of paramagnetic impurity located in a vicinity of a quantum well (QW) on spin polarization of the carriers in the QW is analyzed theoretically. Within approach of Bardeen's tunneling Hamiltonian the problem is formulated in terms of Anderson-Fano model of configuration interaction between a localized hole state at Mn and continuum of heavy hole states in the InGaAs-based QW. The hybridization between the localized state and the QW leads to resonant enhancement of interband radiative recombination. The splitting of the configuration resonances induced by splitting of the localized state in magnetic field results in circular polarization of light emitted from the

QW. The developed theory is capable of explaining known experimental results and allows for calculation of the photoluminescence spectra and dependence of integral polarization on temperature and other parameters.

The author of this dissertation carried out the theoretical calculations, numerical calculations, wrote the paper and was the principal author of the publication.

Publication 5. I. V. ROZHANSKY, N. S. AVERKIEV, and E. LÄHDERANTA, Fano-type coupling of a bound paramagnetic state with 2D continuum, *AIP Conference Proceedings*, **1566**, 335, 2013.

We analyze an effect of a bound impurity state located at a tunnel distance from a quantum well (QW). The study is focused on the resonance case when the bound state energy lies within the continuum of the QW states. Using the developed theory we calculate spin polarization of 2D holes induced by paramagnetic (Mn) delta-layer in the vicinity of the QW and indirect exchange interaction between two impurities located at a tunnel distance from electron gas.

The author of this dissertation carried out the theoretical calculations, numerical calculations, presented the work at the corresponding International Conference on Physics of Semiconductors (ICPS-2012), wrote the paper and was the principal author of the publication.

Publication 6. I. V. ROZHANSKY, N. S. AVERKIEV, and E. LÄHDERANTA, Configuration interaction in delta-doped heterostructures, *Low Temperature Physics*, **39**, 40, 2013.

We analyze the tunnel coupling between an impurity state located in a δ-layer and the 2D delocalized states in the quantum well (QW) located at a few nanometers from the δ – layer. The problem is formulated in terms of Anderson-Fano model as configuration interaction between the carrier bound state at the impurity and the continuum of delocalized states in the QW. An effect of this interaction on the interband optical transitions in the QW is analyzed. The results are discussed regarding the series of experiments on the GaAs structures with a δ-Mn layer.

The author of this dissertation carried out the theoretical calculations, numerical calculations, wrote the paper and was the principal author of the publication.

Publication 7. I. V. ROZHANSKY, I. V. KRAINOV, N. S. AVERKIEV, and E. LÄHDERANTA, Resonant exchange interaction in semiconductors, *Physical Review B*, **88**, 155326, 2013.

We present a non-perturbative calculation of indirect exchange interaction between two paramagnetic impurities via 2D free carriers gas separated by a tunnel barrier. The method accounts for the impurity attractive potential producing a bound state. The calculations show that if the bound impurity state energy lies within the energy range occupied by the free 2D carriers the indirect exchange interaction is strongly enhanced due to resonant tunneling and exceeds by a few orders of magnitude what one would expect from the conventional RKKY approach.

The author of this dissertation carried out the theoretical calculations, numerical calculations, wrote the paper and was the principal author of the publication.

Publication 8. I. V. ROZHANSKY, N. S. AVERKIEV, I. V. KRAINOV, and E. LÄHDERANTA, Resonant enhancement of indirect exchange interaction in semiconductor heterostructures, *physica status solidi (a)*, **211**, 1048-1054 (2014).

We present an approach to calculate indirect exchange interaction between paramagnetic ions via free carriers in heterostructures. Unlike well-known Ruderman-Kittel-Kasuya-Yosida (RKKY) theory the suggested method is not a perturbation theory and thus can be used in the wider variety of cases, especially when resonant effects are important. The method is applied to standard 1D and 2D indirect exchange problems. We further focus on calculation of indirect exchange interaction between two ions mediated by 2D free carriers gas separated by a tunnel barrier. The calculations show that if the ion bound state energy lies within the energy range occupied by the free 2D carriers, the indirect exchange interaction is strongly enhanced due to resonant tunneling and far exceeds what one would expect from the conventional RKKY approach.

The author of this dissertation carried out the theoretical calculations, numerical calculations, presented the work at the International Conference on Nanoscaled Magnetism and Applications (DICNMA-2013), wrote the paper and was the principal author of the publication.

CHAPTER II

BASIC THEORY

2.1 Tunneling Hamiltonian

The tunnel effect is one of the most striking phenomena in quantum mechanics. Most commonly a textbook on quantum mechanics considers tunneling through a potential barrier by solving a single particle stationary Schrödinger equation given the asymptotic behaviour of the solutions, i.e. only outgoing wave behind the barrier. The formulation is that of the scattering problem, the probability for the tunneling is given by ratio of outgoing and incident fluxes. The approach, however, fails if one considers the problem as weak tunneling between two many-particle systems. The occupancy of the final states as well as the density of states behind the barrier does not enter the expression for the transmission coefficient derived from single-particle problem. The issue was resolved by J. Bardeen [Bardeen (1961)], who suggested a different approach, known as the method of tunneling (or transfer) Hamiltonian (TH), which plays an important role, and is widely used to describe tunneling in superconductors and ferromagnets, effects in small tunnel junctions, etc. The main idea is to represent the Hamiltonian as a sum of three parts:

$$\hat{H} = \hat{H}_0^L + \hat{H}_0^R + \hat{H}_T, \tag{2.1}$$

where L and R determine "left" and "right" partial Hamiltonians, describing the systems on the left side and on the right side of the barrier. Basically (2.1) is not a true Hamiltonian, but some formal combination of independent Hamiltonians describing left and right states with tunneling Hamiltonian H_T, which describes the transfer of electrons in the way consistent with the perturbation theory. Let the potential barrier be characterized by the function $U(z)$ such that

$$U(z) = \begin{cases} 0, z < -a \\ U_0(z), -a < z < a \\ 0, z > a \end{cases} \tag{2.2}$$

The left and right Hamiltonians are defined as having two different potentials:

$$U_L(z) = \begin{cases} 0, z < -a \\ U_0(z), -a < z < a \\ U_0(a), z > a \end{cases} \tag{2.3}$$

$$U_R(z) = \begin{cases} U_0(-a), z < -a \\ U_0(z), -a < z < a \\ 0, z > a \end{cases} . \tag{2.4}$$

The $\hat{H}_0^L$ and $\hat{H}_0^R$ have the eigenstates, which without loss of generality we assume to be characterized by the momentum values k and q respectively:

$$\begin{aligned} \hat{H}_0^L |k\rangle &= E_k |k\rangle \\ \hat{H}_0^R |q\rangle &= E_q |q\rangle \end{aligned} \tag{2.5}$$

The states themselves are assumed orthogonal so that

$$\langle q|k\rangle = 0, \tag{2.6}$$

thus the method of tunneling Hamiltonian is not rigorous but rather considered as a phenomenological microscopic approach which, however, proved to give reasonable results in many cases. H_T determines tunneling between $|k\rangle$ and $|q\rangle$ states and is defined through its matrix elements :

$$T_{kq} = \langle k| \hat{H}_T |q\rangle \tag{2.7}$$

The Hamiltonian then becomes:

$$\hat{H} = \sum_k E_k |k\rangle \langle k| + \sum_q E_q |q\rangle \langle q| + \sum_{kq} \left[T_{qk} |q\rangle \langle k| + T_{qk}^* |k\rangle \langle q| \right]. \tag{2.8}$$

The $\hat{H}_T$ is assumed to have such a form that $\hat{H}$ coincides with $\hat{H}_0^R$ in the region $z > -a$ and $\hat{H} = \hat{H}_0^L$ in the region $z < a$. There is no way to write the appropriate interaction term $\hat{H}_T$ explicitly, however it's matrix elements (2.7) can be derived via conventional time-dependent perturbation theory. From the above said about the Haniltonian $\hat{H}$ follows that its eigenstates coincide with the eigenstates $|k\rangle$ of $\hat{H}_0^L$ in the region $z < a$ and the eigenstates $|q\rangle$ of $\hat{H}_0^R$ in the region $z > a$. They form two independent complete systems, which describe the left and right states.

The tunneling is considered as a transition from the left $|k\rangle$ state into the right states $|q\rangle$. Using the time dependent perturbation theory we write:

$$i\hbar \frac{\partial |\Psi\rangle}{\partial t} = \widehat{H} |\Psi\rangle \tag{2.9}$$

$$|\Psi\rangle = |k\rangle e^{-iE_k t/\hbar} + \sum_{q'} a_{q'}(t) e^{-iE_{q'} t/\hbar} |q'\rangle \tag{2.10}$$

with

$$a_{q'}(0) = 0, \quad |a_{q'}(t)| \ll 1$$

Plugging (2.10) into (2.9) we get

$$\begin{aligned} &i\hbar \left[E_k |k\rangle e^{-iE_k t/\hbar} + \sum_{q'} a_{q'}(t) E_q e^{-iE_{q'} t/\hbar} |q'\rangle + \sum_{q'} e^{-iE_{q'} t/\hbar} \frac{\partial}{\partial t} a_{q'}(t) |q'\rangle \right] = \\ &= \widehat{H}_0^L \left[|k\rangle e^{-iE_k t/\hbar} + \sum_{q'} a_{q'}(t) e^{-iE_{q'} t/\hbar} |q'\rangle \right] + \left(\widehat{H} - \widehat{H}_0^L \right) \left[|k\rangle e^{-iE_k t/\hbar} + \sum_{q'} a_{q'}(t) e^{-iE_{q'} t/\hbar} |q'\rangle \right] \end{aligned} \tag{2.11}$$

And further:

$$i\hbar\left[\sum_{q'} e^{-iE_{q'}t/\hbar}\frac{\partial}{\partial t}a_{q'}(t)\,|q'\rangle\right] = \left(\widehat{H}-\widehat{H}_0^L\right)|k\rangle\, e^{-iE_kt/\hbar} + \sum_{q'} a_{q'}(t)\, e^{-iE_{q'}t/\hbar}\widehat{H}\,|q'\rangle$$

Projecting on the $\langle q|$ state:

$$i\hbar\frac{\partial}{\partial t}a_q(t) = \langle q|\,\widehat{H}-\widehat{H}_0^L\,|k\rangle\, e^{-iE_kt/\hbar} + \sum_{q'} a_{q'}(t)\, e^{-iE_{q'}t/\hbar}\,\langle q|\,\widehat{H}\,|q'\rangle \tag{2.12}$$

In the first order of the perturbation theory the last term in (2.12) should be neglected and we arrive at:

$$i\hbar\frac{\partial}{\partial t}a_q(t) = \langle q|\,\widehat{H}-\widehat{H}_0^L\,|k\rangle\, e^{-iE_kt/\hbar}.$$

For the $|a_q(t)|^2$:

$$|a_q(t)|^2 = \left|\langle q|\,\widehat{H}-\widehat{H}_0^L\,|k\rangle\right|^2 4\frac{\sin^2\frac{(E_k-E_q)t}{2\hbar}}{(E_k-E_q)^2},$$

which in the limit $t\to\infty$ (it is assumed, however, that t is not too large and $a_q(t)\ll 1$) results in :

$$|a_q(t)|^2 = \frac{2\pi}{\hbar}t\left|\langle q|\,\widehat{H}-\widehat{H}_0^L\,|k\rangle\right|^2\delta(E_k-E_q).$$

Finally the tunneling rate is expressed via the standard Fermi's Golden Rule expression:

$$w = \frac{2\pi}{\hbar}\,|T_{qk}|^2\,\delta(E_k-E_q), \tag{2.13}$$

where (taking into account 2.6):

$$\langle q|\hat{H}-E_k\,|k\rangle = \langle q|\hat{H}-E_k\,|k\rangle - E_q\,\langle q|k\rangle = \langle q|\hat{H}_T\,|k\rangle = T_{qk}.$$

The matrix element T_{qk} can be rewritten in a more convenient form. Let z_0 be a point inside the barrier: $-a<z_0<a$. Then because at $z<z_0$ $\widehat{H}=\widehat{H}_0^L$

$$T_{qk} = \int\limits_{z>z_0} d\mathbf{r}\,\langle q|\mathbf{r}\rangle\,\langle\mathbf{r}|\hat{H}-E_k\,|k\rangle\,.$$

Also taking into account that for $z>z_0$ $\widehat{H}=\widehat{H}_0^R$ we can add the term which is identically zero:

$$T_{qk} = \int\limits_{z>z_0} d\mathbf{r}\,\langle q|\mathbf{r}\rangle\,\langle\mathbf{r}|\widehat{H}_0^R-E_k\,|k\rangle - \langle q|\,\widehat{H}_0^R-E_q\,|\mathbf{r}\rangle\,\langle\mathbf{r}|k\rangle\,.$$

From (2.13) it follows than for the nonzero tunneling we should consider only the case of $E_q=E_k$:

$$T_{qk} = \int\limits_{z>z_0} d\mathbf{r}\,\langle q|\mathbf{r}\rangle\,\langle\mathbf{r}|\widehat{H}_0^R\,|k\rangle - \langle\mathbf{r}|\,\widehat{H}_0^R\,|q\rangle^*\,\langle\mathbf{r}|k\rangle$$

The potential energy or any other multiplicative operators entering $\widehat{H}_0^R$ cancel each other and what remains is:

$$T_{qk} = \int\limits_{z>z_0} d\mathbf{r} \left[\Psi_q^* (\mathbf{r}) \, \widehat{K} \Psi_k (\mathbf{r}) - \Psi_k (\mathbf{r}) \, \widehat{K} \Psi_q^* (\mathbf{r}) \right] \tag{2.14}$$

where $\widehat{K}$ is the kinetic energy operator. Assuming that $\widehat{K} = -\frac{\hbar^2}{2m}$ we proceed:

$$T_{qk} = -\frac{\hbar^2}{2m} \int\limits_{z>z_0} d\mathbf{r} \nabla \left[\Psi_q^* (\mathbf{r}) \, \nabla \Psi_k (\mathbf{r}) - \Psi_k (\mathbf{r}) \, \nabla \Psi_q^* (\mathbf{r}) \right].$$

Implying the Gauss's theorem from the volume integration we finally arrive at:

$$T_{qk} = -\frac{\hbar^2}{2m} \int\limits_{\Omega} d\mathbf{S} \left[\Psi_q^* (\mathbf{r}) \, \frac{d}{dz} \Psi_k (\mathbf{r}) - \Psi_k (\mathbf{r}) \, \frac{d}{dz} \Psi_q^* (\mathbf{r}) \right], \tag{2.15}$$

where integration is performed over any cross-section $\Omega \perp z$ of the barrier. The Hamiltonain (2.8) can be straightforwardly formulated in the second quantization representation:

$$\hat{H} = \sum_k E_k c_k^{L+} c_k^L + \sum_q E_q c_q^{R+} c_q^R + \sum_{kq} \left[T_{qk} c_q^{R+} c_k^L + T_{kq} c_k^{L+} c_q^R \right]. \tag{2.16}$$

The tunneling current operator can then be defined as the time derivative of the number of particles operator in the left:

$$\widehat{I} = -e \frac{d\hat{N}^L}{dt} = -\frac{ie}{\hbar} \left[\widehat{H}_T, \hat{N}^L \right] \tag{2.17}$$

Using the commutation relations for the creation and annihilation fermion operators we obtain:

$$\widehat{I} = \frac{ie}{\hbar} \sum_{kq} \left[T_{qk} c_q^{R+} c_k^L - T_{kq} c_k^{L+} c_q^R \right] \tag{2.18}$$

From where follows the convenient way to express the mean value of the current operator directly through the unperturbed Green's functions of the left and right systems. That is the main advantage of the tunneling Hamiltonian method – it is easily combined with the many-body theory and allows to construct the characteristics of the coupled system given those of left and right parts separately.

The method of the tunneling Hamiltonian is exploited throughout the whole work presented in this thesis.

2.2 Tunnel coupling of a bound state with a continuum

The problem addressed in this section is the interaction of a bound localized quantum state with the continuum of the delocalized continuum states. It was initially formulated and solved by Fano [Fano (1961)] and Anderson [Anderson (1961)] in the field of atomic spectroscopy. In this section the approach is applied to a single impurity bound state separated by a potential barrier from a continuum of delocalized states. This very case occurs if we consider a quantum well (QW) or a

quantum wire and an impurity bound state, located at a distance of the few nanometers from any of those. The most important case is the resonant one, when the impurity bound state energy lies within the range of the occupied states of the quantum well or the quantum wire. In this case the tunneling substantially modifies the one-particle wavefunctions of the system which leads to a few interesting phenomena discussed in this thesis below. The aim of this section is to develop the proper theory for this case based on the well established Fano-Anderson approach. Let us consider an impurity bound state characterized by the energy ε_0 and the wave function ψ, the continuum wave functions will be denoted by $\varphi(\lambda)$, where λ is any quantum number describing the state. It is assumed now that the continuum states are non-degenerate, i.e. each λ corresponds to a different energy value $\varepsilon(\lambda)$. In the framework of the tunneling Hamiltonian method (see Ch. 2, Sec 2.1) the system can be described by the following Hamiltonian:

$$H = \varepsilon_0 a^+ a + \int \varepsilon_\lambda c_\lambda^+ c_\lambda d\lambda + \int \left(t_\lambda c_\lambda^+ a + t_\lambda^* a^+ c_\lambda \right) d\lambda, \tag{2.19}$$

where a^+, a – the creation and annihilation operators for the bound state c_λ^+, c_λ – the creation and annihilation operators for a continuum state. t_λ is the tunneling matrix element (see Sec. 2.1). The energy here and below is measured from the level of size quantization of the carriers in the QW so that ε_λ is simply their kinetic energy. We seek the eigenstates Ψ of (2.19) expanding them over the known bound state and the continuum states:

$$\Psi(E) = \nu_0(E)\,\psi + \int \nu_\lambda(E)\varphi_\lambda d\lambda, \tag{2.20}$$

E denotes the energy of the state Ψ. In terms of the second quantization we should turn to the field operators $\widehat{\psi} = a\psi, \widehat{\psi}^+ = a^+\psi$, $\widehat{\varphi}_\lambda = c\varphi_\lambda, \widehat{\varphi}_\lambda^+ = c^+\varphi_\lambda$. The creation of a particle in a hybridized state would be described by the field operator:

$$\widehat{\Psi}^+(E) = \nu_0(E)\,\widehat{\psi}^+ + \int \nu_\lambda(E)\widehat{\varphi}_\lambda^+ d\lambda. \tag{2.21}$$

The hybridized state to be found is the eigenstate of the Hamiltonian (2.19) thus the stationary Schrödinger equation

$$\widehat{H}\widehat{\Psi}^+ = E\widehat{\Psi}^+$$

can be written in the form:

$$\begin{aligned} &\left[\varepsilon_0 a^+ a + \int \varepsilon_\lambda c_\lambda^+ c_\lambda d\lambda + \int \left(t_\lambda c_\lambda^+ a + t_\lambda^* a^+ c_\lambda \right) d\lambda\right] \left[\nu_0(E)\,a^+ + \int \nu_\lambda(E) c_\lambda^+ d\lambda\right] = \\ &= E\left[\nu_0(E)\,a^+ + \int \nu_\lambda(E) c_\lambda^+ d\lambda\right]. \end{aligned} \tag{2.22}$$

To project it on the bound state $\widehat{\psi}^+$ we act with operator $\hat{a}$ from the left and take the vacuum expectation value (VEV):

$$\varepsilon_0\nu_0 + \int t_\lambda^*\nu_\lambda d\lambda = E\nu_0.$$

Projecting on the continuum state $\widehat{\varphi}^+$, i.e. applying c_λ from the left and taking VEV reads:

$$\nu_\lambda\varepsilon_\lambda + \nu_0 t_\lambda = E\nu_\lambda$$

Finally we arrive at the following system of equations:

$$\begin{aligned}
&\nu_0(E)\,\varepsilon_0 + \int t_\lambda^* \nu_\lambda(E)\,d\lambda = E\nu_0(E)\,,\\
&\nu_\lambda(E)\,\varepsilon_\lambda + t_\lambda \nu_0(E) = E\nu_\lambda(E)\,.
\end{aligned} \tag{2.23}$$

We will consider the most important case of the bound level energy lying within the range of the continuum: $\varepsilon_0 >> t^2$. For the case of discrete spectrum ε_λ the system (2.23) can be solved in principle, straightforwardly by expressing ν_λ from the second equation and substitute it into the first. However, for the continuous spectrum this procedure inevitably involves a division by zero. This obstacle can be circumvented by introducing the formal solution of the second equation in (2.23) as [Fano (1961)]:

$$\nu_\lambda = \nu_0\left(P\frac{t_\lambda}{E-\varepsilon} + Z(E)\,t_\lambda \delta(E-\varepsilon)\right), \tag{2.24}$$

where P denotes the principal value. That is whenever the integration should occur the principal value must be taken. Substituting (2.24) into the first equation of (2.23) results in (for $\nu_0 \neq 0$) :

$$Z(E) = \frac{E-\varepsilon_0 - F(E)}{|t_{\lambda_E}|^2 D(E)}, \tag{2.25}$$

where

$$\begin{aligned}
F(E) &= P\int \frac{|t_\lambda|^2}{E-\varepsilon}d\lambda\\
D(E) &= \int \delta(E-\varepsilon)\,d\lambda = \left(\frac{d\lambda}{d\varepsilon}\right)_E
\end{aligned} \tag{2.26}$$

Plugging (2.24) into the expansion (2.20) we obtain:

$$\Psi(E) = \nu_0\left[\psi + P\int \frac{t_\lambda}{E-\varepsilon}\phi_\lambda d\lambda + \frac{E-\varepsilon_0-F(E)}{t_{\lambda_E}^*}\phi_{\lambda_E}\right]$$

The coefficient ν_0 should be obtained from the normalization of the function $\Psi(E)$. For the hybridized wave function $\Psi(E)$ λ is no more a good quantum number. However, we formally introduced the parameter λ_E which unambiguously corresponds to the energy E. Let us assume normalization for the continuum functions:

$$\langle\phi_\lambda|\phi_{\lambda'}\rangle = \delta(\lambda-\lambda') = \frac{1}{D(\varepsilon)}\delta(\varepsilon-\varepsilon')$$

The same normalization will be introduced for the hybridized functions:

$$\langle\Psi(E)|\,\Psi(E')\rangle = \frac{\delta(E-E')}{D(E)}. \tag{2.27}$$

The bound state wave function is normalized to unity:

$$\langle\psi|\,\psi\rangle = 1$$

Then we have the following expression for the normalization:

$$\langle \Psi(E)|\ \Psi(E')\rangle = |\nu_0(E)|^2 \begin{bmatrix} 1 + P\int \frac{1}{E-\varepsilon}\frac{1}{E'-\varepsilon}|t_\lambda|^2 D(\varepsilon)\,d\varepsilon + \\ P\int \frac{t^*_\lambda}{E-\varepsilon}\delta(\varepsilon - E')\frac{E'-\varepsilon_0 - F(E')}{t^*_{\lambda_{E'}}}d\varepsilon + \\ P\int \frac{t_\lambda}{E'-\varepsilon}\delta(\varepsilon - E)\frac{E-\varepsilon_0 - F(E)}{t_{\lambda_E}}d\varepsilon \\ + \frac{[E-\varepsilon_0 - F(E)]^2}{|t_{\lambda_E}|^2 D(E)}\delta(E-E') \end{bmatrix}$$

The second term in brackets should be carried out with care. But for the principal parts it would have a double pole. It appears that for the principal part it has a singular term. This is what stated in the so-called Poincare theorem:

$$P\int \frac{1}{E-\varepsilon}\frac{1}{E'-\varepsilon} = P\frac{1}{E-E'}\left(\frac{1}{E'-\varepsilon} - \frac{1}{E-\varepsilon}\right) + \pi^2\delta(E-E')\,\delta(\varepsilon - E) \tag{2.28}$$

Applying the Poincare theorem we proceed:

$$\langle \Psi(E)|\ \Psi(E')\rangle = |\nu_0(E)|^2 \begin{bmatrix} 1 + \frac{1}{E-E'}P\int\left[\left(\frac{1}{E'-\varepsilon} - \frac{1}{E-\varepsilon}\right)\right]|t_\lambda|^2 D(\varepsilon)\,d\varepsilon \\ +\pi^2|t_{\lambda_E}|^2 D(E)\,\delta(E-E') \\ \frac{E'-E}{E-E'} + \frac{F(E)-F(E')}{E-E'} + \frac{[E-\varepsilon_0 - F(E)]^2}{|t_{\lambda_E}|^2 D(E)}\delta(E-E') \end{bmatrix}$$

Note, that the first term in brackets (unity) is exactly cancelled by the fourth and also the second one is cancelled by the fifth because of (2.26):

$$\langle \Psi(E)|\ \Psi(E')\rangle = |\nu_0(E)|^2 \left[\frac{\pi^2|t_{\lambda_E}|^4 D^2(E) + [E-\varepsilon_0 - F(E)]^2}{|t_{\lambda_E}|^2}\right]\frac{\delta(E-E')}{D(E)}$$

Finally, the normalization (2.27) factors out and we get:

$$|\nu_0(E)|^2 = \frac{|t_{\lambda_E}|^2}{\pi^2|t_{\lambda_E}|^4 D^2(E) + (E-\widetilde{\varepsilon_0})^2}, \tag{2.29}$$

where

$$\widetilde{\varepsilon_0} = \varepsilon_0 + F(E)$$

The solution (2.29) exhibits a resonance with the center slightly shifted from ε_0.

From the above analysis it follows that the bound state becomes 'diluted' in the continuum so that all the states now are delocalized with the normalization condition (2.27). Let us now put more attention to the part of the wave function associated with the continuum states. Form (2.20) and (2.24) we have:

$$\Phi(E) = \int \nu_\lambda\phi_\lambda d\lambda = \nu_0\int t_\lambda\phi_\lambda\left(P\frac{1}{E-\varepsilon} + Z(E)\,D(E)\,\delta(\lambda-\lambda_E)\right)d\lambda.$$

Let us now consider the continuum wave function having the form $\varphi_k^{\cos} = A\cos(kx)$, $k > 0$ and the dispersion $\varepsilon = \alpha k^2$. Let also the tunneling parameter be a weak function of k. To get rid of the principal value we apply Sokhotski–Plemelj theorem:

$$P\frac{f(x)}{x} = \frac{f(x)}{x+i\delta} + i\pi f(x)\,\delta(x),$$

then for the principal value part:

$$\int P\frac{\cos kx}{k^2-k_E^2}dk = \frac{1}{4k_E}\int dk \left[\begin{array}{l} \dfrac{e^{ikx}+e^{-ikx}}{k-k_E+i\delta} - \dfrac{e^{ikx}+e^{-ikx}}{k+k_E+i\delta} + \\ +2i\pi\cos k_E x\left[\delta(k-k_E)-\delta(k+k_E)\right] \end{array}\right]$$

and

$$\frac{1}{\alpha}\int_0^\infty P\frac{\cos kx}{k_E^2-k^2}dk = \frac{\pi\sin(k_e x)\,\mathrm{sign}(x)}{2\alpha k_E}.$$

Thus, we finally obtain:

$$\Phi^{\cos}(E) = \nu_0 t_k a A\left[Z(E)\,D(E)\cos(k_E x) + \frac{\pi\sin(k_E x)\,\mathrm{sign}(x)}{2\alpha k_E}\right].$$

After substitution of (2.29) this reduces to:

$$\Phi^{cos}(E) = A\cos\left(k_E x + \Delta^{\cos}\mathrm{sign}(x)\right), \tag{2.30}$$

where

$$\Delta^{cos} = -\arctan\frac{\pi\left|t_{k_E}^{\cos}\right|^2}{2\alpha k_E(E-\widetilde{\varepsilon_0})}. \tag{2.31}$$

Analogously for the continuum functions $\varphi_k^{\sin} = A\sin(kx)$ we would obtain:

$$\Phi^{\sin}(E) = A\sin\left(k_E x + \Delta\,\mathrm{sign}(x)\right), \tag{2.32}$$

with

$$\Delta^{sin} = -\arctan\frac{\pi\left|t_{k_E}^{\sin}\right|^2}{2\alpha k_E(E-\widetilde{\varepsilon_0})}. \tag{2.33}$$

Note presence of the signum function which maintains the parity of the wave function. If we consider the 1D continuum with the impurity bound state being localized at $x = 0$, the complete set of the continuum functions would involve both $\varphi_k^{\cos}$ and $\varphi_k^{\sin}$, however $\varphi_k^{\sin}$ will not be affected by the impurity. That is because the appropriate tunneling parameter would be $t_k^{\sin} \approx 0$ due to negligibly small overlap of the continuum function with the bound state.

As follows from (2.30), due to the scattering at the bound state the continuum wave functions experiences the phase shift (2.33) which rapidly changes its sign when passing through the resonant position $\widetilde{\varepsilon}_0$. The above described basic Fano-Anderson method as applied to the tunneling problem appeared to be very fruitful in analysis of the tunnel coupling developed in this thesis. It is further extended on the case of two bound states interacting with 1D and 2D continuum. The latter case, which describes the impurities in the vicinity of a quantum well, is completely new and has not been covered but for this study.

2.3 Connection between the phase shift and the energy

Formulation of the tunnel coupling in terms of the scattering phase shift at the end of Sec. (2.2) is very convenient to use for calculation of the system energy. In order to do this the scattering problem should be connected to the standing wave problem by looking at scattering in a finite size box [Mueller (2002)]. Let us consider the 1D case and put the system in a box of size $2L$, so that $-L < x < L$ and imply zero boundary conditions. Following the notes given in the previous section we assume the wave functions to be $\varphi_k = A\cos kx$. With account for the tunnel coupling with the bound state the modified wave function would be (2.30):

$$\Phi(E) = A\cos\left(k_E x + \Delta\,\mathrm{sign}(x)\right), \tag{2.34}$$

Without the coupling $\Delta = 0$ and the quantizing conditions for $k > 0$ would be:

$$\cos(-kL) = \cos(kL) = 0,$$

that implies:

$$k_0 L = \pi n, \;\; n = 1/2, 3/2, 5/2... \tag{2.35}$$

The n-th energy level is given by (as in the previous section we assume $\varepsilon = \alpha k^2$):

$$\varepsilon_0 = \alpha k_0^2 = \frac{\alpha\pi^2 n^2}{L^2}, \tag{2.36}$$

and for the density of states:

$$g_0(\varepsilon) = \frac{1}{L}\frac{dn}{d\varepsilon} = \frac{1}{2\pi\sqrt{\alpha\varepsilon}} \tag{2.37}$$

Now for (2.34) the zero boundary conditions are met when:

$$\cot(kL) = \tan\Delta,$$

or, using the equality

$$\arctan x + \mathrm{arccot}\, x = \frac{\pi}{2}\,\mathrm{sign}(x),$$

we have:

$$kL = \pi n - \Delta(k) \tag{2.38}$$

and for the energy level:

$$\varepsilon = \frac{\alpha}{L^2}\left[\pi^2 n^2 - 2\pi n\Delta + \Delta^2\right]$$

We proceed with calculating of the density of states:

$$g = \frac{1}{L}\frac{dn}{d\varepsilon} = \frac{L}{\alpha}\left[2\pi^2 n - 2\pi\Delta - 2\pi n\frac{d\Delta}{dn} + 2\Delta\frac{d\Delta}{dn}\right]^{-1}$$

From (2.35) it is clear that n has the order of L thus in the infinite box limit the second and the fourth terms in brackets must be omitted and we get:

$$g = g_0 + \frac{1}{\pi}\frac{1}{L}\frac{d\Delta}{d\varepsilon}, \tag{2.39}$$

where g_0 is given by (2.37). From the analysis of (2.37) and (2.33) it follows that that the effect of a bound state is a Lorentz-shaped increase of the density of states near the energy corresponding to the shifted resonant position $\widetilde{\varepsilon_0}$. Combining (2.38) and (2.35):

$$k = k_0 - \frac{\Delta}{L} \tag{2.40}$$

The shift in the energy would be:

$$\varepsilon = \varepsilon_0 - 2\alpha k_0 \frac{\Delta(k)}{L}, \tag{2.41}$$

where in the limit of infinitely large box we omit the tern $1/L^2$. From (2.40) it follows that $k - k_0 \sim 1/L$, thus

$$\Delta(k) - \Delta(k_0) = \frac{d\Delta}{dk}_{k_0}(k - k_0) + ... \sim \frac{1}{L}$$

and one can replace $\Delta(k)$ by $\Delta(k_0)$. In order to get the total energy one should sum over the occupied levels (2.41):

$$E = E_0 - \frac{2\pi\alpha}{L^2}\sum_n n\Delta(n),$$

where E_0 is the energy with no account for the coupling. We further replace the sum over discrete $n = n_0, n_0 + 1, n_0 + 2...$ by integration over continous parameter n

$$E = E_0 - \frac{2\pi\alpha}{L^2}\int_0^N \Delta(n)\, n dn,$$

here N is the number of the highest occupied level. Now we formally express n from (2.36) and write:

$$E = E_0 - \frac{1}{\pi}\int_0^{E_{F0}} \Delta(\varepsilon)\, d\varepsilon, \tag{2.42}$$

where the integration is performed up to the Fermi level E_{F0} defined as the energy of the highest occupied state in the absence of the tunnel coupling. It is better to refer this quantity by the number of particles present in the system which is fixed. The true position of the Fermi level will slightly vary depending on whether the interaction is present in the system. The equation (2.42) is the key one to analyze the indirect exchange interaction of the magnetic ions mediated by a spatially separated conducting channel. It connects the scattering phase shift to the energy and, thus, the interaction between the two scattering magnetic centers can be interpreted using the phase shifts they create in different mutual spin configurations.

CHAPTER III

TUNNELING BETWEEN 2D ELECTRON LAYERS

3.1 Introductory remarks

The tunnelling between two quantum wells separated by a weakly transparent tunnel barrier is a prime example of resonant tunneling in semiconductor nanostructures. In such a structure unlike the tunneling phenomena in bulk samples, the energy and in-plane momentum conservation put tight restrictions on the tunneling so that the conductance exhibits delta function-like maximum at zero bias broadened by elastic scattering in the layers [Zheng and MacDonald (1993)] and fluctuations of the layers width [Vasko et al. (2000)]. Such a behavior has been observed in a number of experiments [Murphy et al. (1995); Turner et al. (1996); Popov et al. (1998)]. It turns out that this peculiarity is very sensitive to the spin-orbit interaction (SOI) in the layers and therefore opens possibility to determine the parameters of spin-orbit interaction and electron quantum lifetime in experiments on tunneling between low-dimensional electron layers without external magnetic field.

Spin-orbit interaction (SOI) plays an important role in the widely studied spin-related effects and spintronic devices. In the latter it can be either directly utilized to create spatial separation of the spin-polarized charge carries or indirectly influence the device performance through spin-decoherence time. In 2D structures two kinds of SOI are known to be of the most importance, namely Rashba and Dresselhaus mechanisms. The first one, characterized by parameter α, originates from the structure inversion asymmetry (SIA), while the second one characterized by β is due to the bulk inversion asymmetry (BIA). Most brightly both of the contributions reveal themselves when the values of α and β are comparable. The energy spectra splitting due to SOI can be observed in rather well-developed experiments as that based on Shubnikov–de Haas effect. However, these experiments can hardly tell about the partial contributions of the two mechanisms leaving the determination of the relation between α and β to be a more challenging task. At the same time, in some important cases spin relaxation time τ_s and spin polarization strongly depend on the $\frac{\alpha}{\beta}$ ratio. The tunneling between 2D electron layers turns out to be sensitive to the relation between Rashba and Dresselhaus contributions.

Without SOI the tunneling conductance exhibits delta function-like maximum at zero bias broadened by elastic scattering in the layers [Zheng and MacDonald (1993)] and fluctuations of the layers width [Vasko et al. (2000)]. Such a behavior was indeed observed in a number of experiments [Murphy et al. (1995); Turner et al. (1996); Popov et al. (1998)]. Spin-orbit interaction splits the electron spectra into two subbands in each layer. Energy and momentum conservation can be fulfilled for the

tunneling between opposite subbands of the layers at a finite voltage corresponding to the subbands splitting. However, if the parameters of SOI are equal for the left and right layers, the tunneling remains prohibited due to orthogonality of the appropriate spinor eigenstates. In Ref. [Raichev and Debray (2003)] it was pointed out that this restriction can also be eliminated if Rashba parameters are different for the two layers. A structure design was proposed [Zyuzin et al. (2006)] where exactly opposite values of the Rashba parameters result from the built-in electric field in the left layer being opposite to that in the right layer. Because the SOI of Rashba type is proportional to the electric field, this would result in $\alpha^R = -\alpha^L$, where α^L and α^R are the Rashba parameters for the left and right layers respectively. In this case the peak of the conductance is expected at the voltage U_0 corresponding to the energy of SOI: $eU_0 = \pm 2\alpha k_F$, where k_F is Fermi wavevector. In [**Publication 1**] an arbitrary Rashba and Dresselhaus contributions to the tunnelling between 2D layers is considered. It is shown that the parameters α and β can reveal themselves in a tunneling experiment which unlike other spin-related experiments requires neither magnetic field nor polarized light.

3.2 Theoretical approach

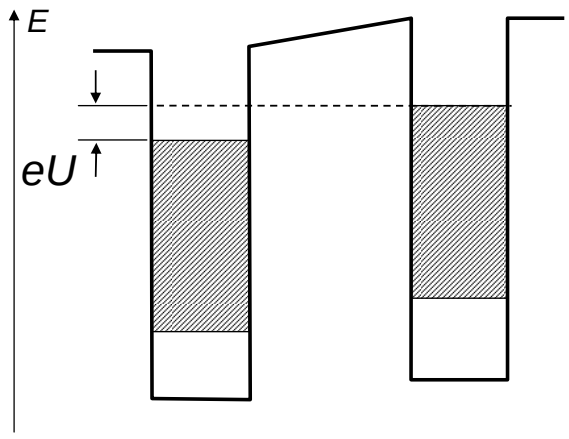

Figure 3.1: Energy diagram of two 2D electron layers.

The system considered in [**Publication 1**] consists of 2D electron layers separated by a potential barrier (see Fig.3.1). We consider zero temperature, only one level of size quantization and not too narrow barrier so that the electrons wavefunctions in the left and right layers overlap weakly. Bardeen's tunneling Hamiltonian (see Sec. 2.1) can be written as:

$$H = H_0^L + H_0^R + H_T, \tag{3.1}$$

where H_0^L, H_0^R are the partial Hamiltonians for the left and right layers respectively, H_T is the tunneling term. The expressions for these terms with the elastic scattering on impurities taken into account have the form:

$$\begin{aligned} H_0^l &= \sum_{k,\sigma} \varepsilon_k^l c_{k\sigma}^{l+} c_{k\sigma}^l + \sum_{k,k',\sigma} V_{kk'}^l c_{k\sigma}^{l+} c_{k'\sigma}^l + H_{SO}^l \\ H_T &= \sum_{k,k',\sigma,\sigma'} T_{kk'\sigma\sigma'} \left(c_{k\sigma}^{L+} c_{k'\sigma'}^R + c_{k'\sigma'}^{R+} c_{k\sigma}^L \right), \end{aligned} \tag{3.2}$$

Here index l is used for the layer designation, $l = R$ for the right layer and $l = L$ for the left layer, k is the wave vector in the plane of the layers, σ is the spin polarization, ε_k^l is the energy of an electron in the layer l having in-plane wavevector k. It can be expressed as:

$$\varepsilon_k^l = \varepsilon + \varepsilon_0^l + \Delta^l, \tag{3.3}$$

where $\varepsilon = \frac{\hbar^2 k^2}{2m}$, m being electron's effective mass, ε_0^l is the size quantization energy and Δ^l is the energy shift due to external voltage applied to the layer l. The second term in the Hamiltonian (6.22) describes elastic scattering on impurities, $V_{kk'}^l$ is the matrix element of the scattering operator. $T_{kk'\sigma\sigma'}$ is the tunneling matrix element discussed in Sec. 2.1 The term H_{SO}^l describes the spin-orbit part of the Hamiltonian, in which there are two terms linear in k, corresponding to interactions of the Rashba type, with the constant α, and Dresselhaus type, with the constant β:

$$H_{SO} = \alpha \left(k_y \sigma_x - k_x \sigma_y\right) + \beta \left(k_x \sigma_x - k_y \sigma_y\right) \tag{3.4}$$

In the second quantization representation this turns to be:

$$\begin{aligned} H_{SO}^l = \alpha^l \sum_k \left(k_y - i k_x\right) c_{k\sigma}^{l+} c_{k\sigma'}^l + \left(k_y + i k_x\right) c_{k\sigma'}^{l+} c_{k,\sigma}^l \\ + \beta^l \sum_k \left(k_x - i k_y\right) c_{k\sigma}^{l+} c_{k\sigma'}^l + \left(k_x + i k_y\right) c_{k\sigma'}^{l+} c_{k\sigma}^l \end{aligned} \tag{3.5}$$

The tunneling current operator is described in Sec. 2.1 and is given by the expression (3.2):

$$\widehat{I} = \frac{ie}{\hbar} \sum_{kq} \left[T_{qk} c_q^{R+} c_k^L - T_{kq} c_k^{L+} c_q^R\right]$$

The current expectation value can therefore be expressed through the density matrix evolution as done in [**Publication 1**] or via the Green's functions method developed in [**Publication 2**]. An expression for the tunneling current in terms of the Green's functions of the individual layers has the form [**Publication 2**]:

$$I = \frac{eT^2 W}{4\pi^3 \hbar^3} \mathrm{Re} \left\{ \mathrm{Tr} \int G_{0V}^R \left(p, \varepsilon - eU\right) G_{0V}^L \left(p, \varepsilon\right) d\mathbf{p} d\varepsilon. \right\}, \tag{3.6}$$

where p is the momentum of the electron in the plane of the layer, G_{0V}^R, G_{0V}^L are the Green's functions for the right and left layers. The subscript V indicates that these Green'z functions take scattering on impurities into account. The further problem consists in expressing the functions G_{0V}^l in terms of the Green's functions G_0^l of the 2D electron gas with spin-orbit interaction in the absence of scattering on impurities. The calculations [**Publication 2**] show that the spin-orbit interaction leads to splitting of the spectrum of eigenstates into two subbands. In a basis of eigenstates of a given layer, the Green's function is a $2x$ diagonal matrix: 2×2:

$$G_{0V} = \begin{bmatrix} G_- & 0 \\ 0 & G_+ \end{bmatrix},$$

where

$$G_\pm \left(\varepsilon, k\right) = \frac{1}{\varepsilon + E_F - \frac{\hbar^2 k^2}{2m} \pm \xi + i \frac{\hbar}{2\tau} sign\ \varepsilon}, \tag{3.7}$$

$$\xi = \sqrt{\left(\alpha^2 + \beta^2\right) k^2 + 4\alpha\beta k_x k_y} \tag{3.8}$$

α and β - are, respectively, the parameters of the Rashba and Dresselhaus spin-orbit interactions in a given layer, and E_F is the Fermi level of the layers in the absence of applied voltage, τ is the scattering time. Passing to the initial spinor basis common to both layers $\sigma = \pm 1/2$, we obtain:

$$G_{0V} = \frac{1}{4}\begin{bmatrix} G_- + G_+ & \gamma^{-1}(G_- - G_+) \\ (\gamma^*)^{-1}(G_- - G_+) & G_- + G_+ \end{bmatrix},$$

where

$$\gamma = \frac{e^{-i\phi}\beta - i\alpha e^{i\phi}}{|e^{-i\phi}\beta - i\alpha e^{i\phi}|},\ \phi = \arctan\frac{k_y}{k_x}$$

Substituting these expressions for each of the layers into Eq. (3.6) and integrating over $|k|$ with allowance for the condition $E_F \gg \alpha k_F$, we arrive at the following expression: :

$$I = \frac{e^2T^2\nu WU}{4\pi\tau}\int\limits_0^{2\pi} d\phi \begin{bmatrix} \left(\frac{1}{(eU+\xi^-)^2+\left(\frac{\hbar}{\tau}\right)^2} + \frac{1}{(eU-\xi^-)^2+\left(\frac{\hbar}{\tau}\right)^2}\right)\left(1 + \mathrm{Re}\gamma^L\gamma^{R*}\right) \\ + \left(\frac{1}{(eU-\xi^+)^2+\left(\frac{\hbar}{\tau}\right)^2} + \frac{1}{(eU+\xi^+)^2+\left(\frac{\hbar}{\tau}\right)^2}\right)\left(1 - \mathrm{Re}\gamma^L\gamma^{R*}\right) \end{bmatrix}, \tag{3.9}$$

where $\xi^{\pm} = \xi^R(k_F) \pm \xi^L(k_F)$.

3.3 Results

The formula (3.9) which gives the tunneling current with account for arbitrary SOI and elastic scattering is the main analytical result of the work. It is obtained via two different techniques as described in [**Publication 1**] and [**Publication 2**]. The general expression (3.9) can be simplified in a few particular cases. It appears that the tunneling conductance can exhibit qualitatively different behavior depending on the relation between Rashba and Dresselhaus contributions. The presence of a different spin-orbit interaction in the layers leads to nontrivial voltage dependence of the interlayer differential conductance $G = dI/dU$. It may contain one or several resonance peaks, the positions of which are related to the energy of the spin-orbit splitting and whose width is related to the impurity scattering time. Here an important role is played by the ratio of these quantities:

$$\eta = \frac{\alpha k_F \tau}{\hbar} \tag{3.10}$$

where α – the characteristic spin-orbit interaction parameter. The value of η shows whether the individual peaks are resolved or if scattering on impurities does not permit one to distinguish the details due to the spin-orbit interaction.

3.3.1 No Spin-Orbit Interaction

In the absence of SOI ($\alpha^R = \alpha^L = 0$, $\beta^R = \beta^L = 0$) the energy spectrum for each of the layers forms a paraboloid:

$$E^l(k^l) = \varepsilon_0 + \frac{\hbar^2(k^l)^2}{2m} \pm \frac{eU}{2}. \tag{3.11}$$

The tunneling requires energy and momentum conservation simultaneously:

$$\begin{aligned} E^R &= E^L \\ k^R &= k^L \end{aligned} \tag{3.12}$$

Both conditions hold simultaneously only for U=0, so that a nonzero voltage will not cause a tunneling current, despite the fact that states occupied by electrons in one layer lie opposite to empty states in the other. The restriction due to momentum conservation can be weakened if the electron scatters at the impurities. Accordingly, one expects a nonzero tunneling current in a certain range of voltages near zero. For this case the general formula (3.9) simplifies considerably, since $\gamma^R = \gamma^L = 1$, $\xi^- = \xi^+ = 0$:

$$I = 2e^2T^2\nu WU\frac{\frac{1}{\tau}}{(eU)^2 + \left(\frac{\hbar}{\tau}\right)^2}. \tag{3.13}$$

This case is represented by curve a in Fig. 3.2.

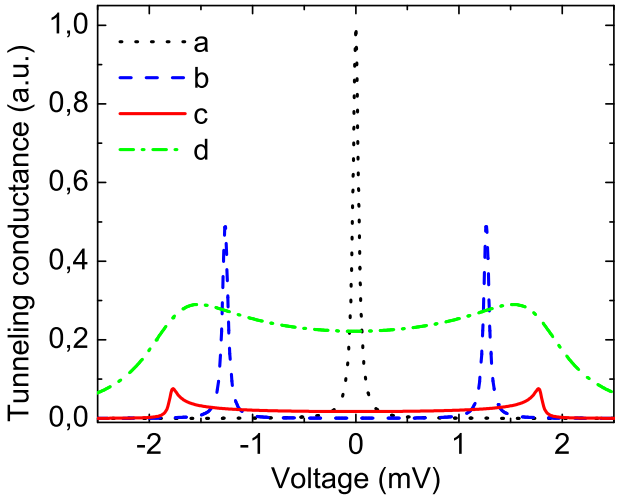

Figure 3.2: Tunneling conductance, a: $\varepsilon_F = 10$ meV, $\alpha = \beta = 0$, $\tau = 2 * 10^{-11}$ s; b: same as a, but $\alpha k_F = 0.6$ meV; c: same as b, but $\beta = \alpha$; d: same as c, but $\tau = 2 * 10^{-12}$ s.

3.3.2 Spin-Orbit Interaction of Rashba type

The spin-orbit interaction gives qualitatively new option for the d.c. conductance to be finite at nonzero voltage. SOI splits the spectra into two subbands. Now an electron from the first subband of the left layer can tunnel to a state in a second subband of the right layer. Let us consider a particular case when only Rashba type of SOI interaction exists in the system, its magnitude being the same in both layers, i.e. $|\alpha^R| = |\alpha^L| \equiv \alpha$, $\beta^R = \beta^L \equiv \beta = 0$. In this case the spectra splits into two paraboloid-like subbands "inserted" into each other. Fig.3.3 shows their cross-sections for both layers, arrows show spin orientation. By applying a certain external voltage $U_0 = \frac{2\alpha k_F}{e}$ the layers

can be shifted on the energy scale in such a way that the cross-section of the "outer" subband of the right layer coincides with the "inner" subband of the left layer (see solid circles in Fig.3.3). At that both conditions (3.12) are satisfied. However, if the spin is taken into account, the interlayer transition can still remain forbidden. It happens if the appropriate spinor eigenstates involved in the transition are orthogonal. This very case occurs if $\alpha^R = \alpha^L$, consequently the conductance behavior remains the same as that without SOI. Contrary, if the Rashba terms are of the opposite signs, i.e. $\alpha^R = -\alpha^L$ the spin orientations in the "outer" subband of the right layer and the "inner" subband of the left layer are the same and the tunneling is allowed at a finite voltage but forbidden at $U = 0$. This situation, pointed out in Ref. [Raichev and Debray (2003); Zyuzin et al. (2006)] should reveal itself in sharp maxima of the conductance at $U = \pm U_0$ as shown in Fig.3.2,b. From this dependence the value of α can be immediately extracted from the position of the peak. For this case from the general expression (3.9) we obtain the following result for the current:

$$I = \frac{2e^2T^2W\nu U\frac{\hbar}{\tau}\left[\delta^2 + e^2U^2 + \left(\frac{\hbar}{\tau}\right)^2\right]}{\left[(eU-\delta)^2 + \left(\frac{\hbar}{\tau}\right)^2\right]\left[(eU+\delta)^2 + \left(\frac{\hbar}{\tau}\right)^2\right]}, \tag{3.14}$$

where $\delta = 2\alpha k_F$. The result is in agreement with that derived in Ref. [Zyuzin et al. (2006)]. It is worth noting that the opposite case when only Dresselhaus type of SOI exists in the system

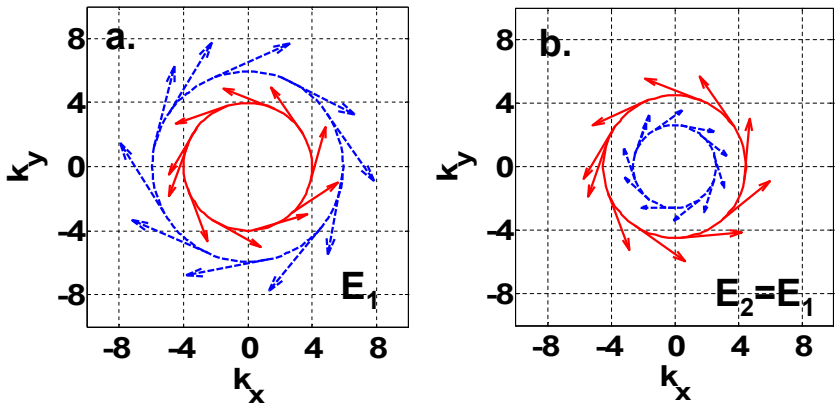

Figure 3.3: Cross-section of electron energy spectra in the left(a) and right (b) layer for the case $\alpha^L = -\alpha^R, \beta^L = \beta^R = 0$.

leads to the same results. However, it is less practical to study the case of the different Dresselhaus parameters in the layers because this type of SOI originates from the crystallographic asymmetry and therefore cannot be varied if the structure composition is fixed. For this case to be realized one needs no make the two layers of different materials.

3.3.3 Both Rashba and Dresselhaus contributions

The presence of Dresselhaus term in addition to the Rashba interaction can further modify the tunneling conductance in a non-trivial way. A special case occurs if the magnitude of the Dresselhaus

term is comparable to that of the Rashba term. Because the Dresselhaus contribution is related to the material crystal structure it is naturally to assume it the same for both layers: $\beta^L = \beta^R \equiv \beta$. Let us add the Dresselhaus contribution to the previously discussed case so that $\alpha^L = -\alpha^R \equiv \alpha,\ \alpha = \beta$. The corresponding energy spectra and spin orientations are shown in Fig.3.4. Note that while the spin orientations in the initial and final states are orthogonal for any transition between the layers, the spinor eigenstates are not, so that the transitions are allowed whenever the momentum and energy conservation requirement (3.12) is fulfilled. It can be also clearly seen from Fig.3.4 that the condition (3.12), meaning overlap of the cross-sections a. and b. occurs only at few points. This is unlike the previously discussed case where the overlapping occurred within the whole circular cross-section shown by solid lines in Fig.3.3. One should naturally expect the conductance for the case presently discussed to be substantially lower. Using (3.9) we arrive at the following expression for the current:

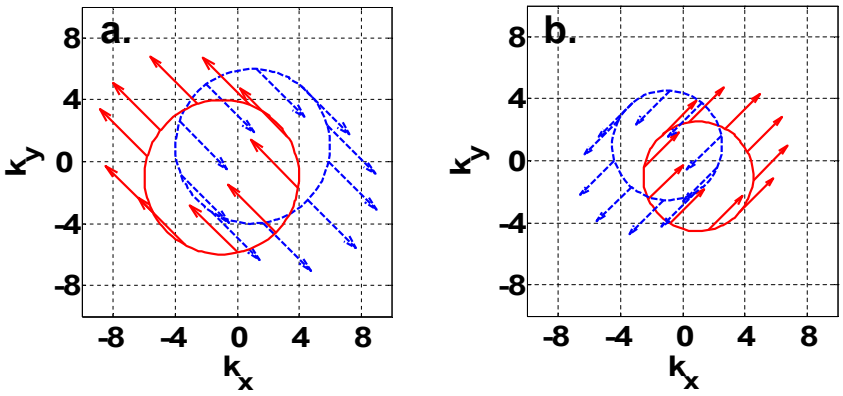

Figure 3.4: Cross-section of electron energy spectra in the left(a) and right (b) layer for the case $\alpha^R = -\alpha^L = \beta$.

$$I = eT^2 W \nu U \left[\frac{G_- \left(G_-^2 - \delta^2\right)}{\sqrt{F_- \left(\delta^4 + F_-\right)}} - \frac{G_+ \left(G_+^2 - \delta^2\right)}{\sqrt{F_+ \left(\delta^4 + F_+\right)}} \right], \tag{3.15}$$

where

$$G_\pm = eU \pm i\frac{\hbar}{\tau}$$
$$F_\pm = G_\pm^2 \left(G_\pm^2 - 2\delta^2\right). \delta = 2\alpha k_F$$

Alternatively, for the case of no interaction with impurities a precise formula for the transition rate between the layers can be obtained by means of Fermi's golden rule. We obtained the following expression for the current:

$$I = \frac{2\pi e T^2 W}{\hbar \alpha^2} \left(\sqrt{K + \frac{8m\alpha^2 eU}{\hbar^2}} - \sqrt{K - \frac{8m\alpha^2 eU}{\hbar^2}} \right), \tag{3.16}$$

where

$$K = 2\delta^2 - e^2U^2 + \frac{16m^2\alpha^4}{\hbar^4}$$

Comparing the results obtained from (3.15) and (3.16) is an additional test for the correctness of (3.15). Both dependencies are presented in Fig.3.5 and show a good match. The same dependence of conductance on voltage is shown in Fig.3.2,c. We see that the tunneling conductance is indeed

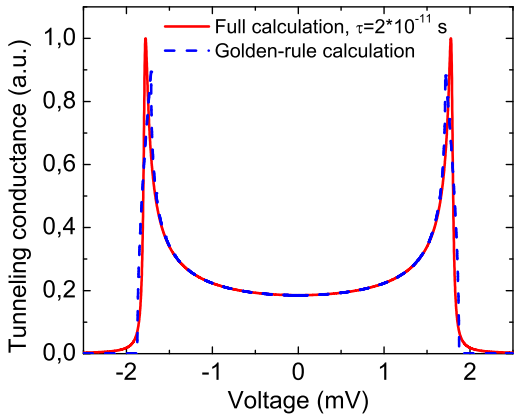

Figure 3.5: Tunneling conductance calculated for the case $\alpha^R = -\alpha^L = \beta$ and very weak scattering compared to the precise result obtained through Fermi's golden rule calculation.

substantially suppressed in the whole voltage range. This situation is qualitatively different from the cases considered previously, in which scattering led to broadening of the resonance peaks. In the present case the weakening of the restrictions on momentum conservation owing to scattering increases the tunneling conductance and restores the spin-orbit features on the current-voltage characteristic. Such an unusual role of the scattering becomes clear from Fig.3.4,a,b. Note that the scattering weakens the requirement of momentum conservation. To account for that one should add a certain thickness to the circles shown in the Figure. This thickness is proportional to τ^{-1}. Consequently, the overlap of the cross-sections now having 'thick' lines occur at larger number of points providing increased tunneling current. Fig.3.2,d shows this dependence for a realistic scattering time $\tau = 2 * 10^{-12}$. In the general case of arbitrary parameters for arbitrary α and β the dependence of conductance on voltage can exhibit various complicated shapes with a number of maxima, being very sensitive to the relation between Rashba and Dresselhaus contributions. The cause of this sensitivity is essentially the "interference" of the angular dependencies of the spinor eigenstates in the layers. A few examples of such interference are shown in Fig.3.6, a–c. All the dependencies shown were calculated for the scattering time $\tau = 2 * 10^{-12}$ s. Fig.3.6,a summarizes the results for all previously discussed cases of SOI parameters, i.e. no SOI (curve 1), the case $\alpha_R = -\alpha_L, \beta = 0$ (curve 2) and $\alpha_R = -\alpha_L = \beta$ (curve 3). Following the magnitude of τ all the resonances are broadener compared to that shown in Fig.3.2. Fig.3.6,b (curve 2) demonstrates the conductance calculated for the case $\alpha_L = -\frac{1}{2}\alpha_R = \beta$, Fig.3.6,c (curve 2) – for the case $\alpha_L = \frac{1}{2}\alpha_R = \beta$. The curve 1 corresponding to the case of no SOI is also shown in all the figures for reference. Despite of the scattering all the patterns shown in Fig.3.6 remain very distinctive. That means that in principle

the relation between the Rashba and Dresselhaus contributions to SOI can be extracted merely from the I-V curve measured in a proper tunneling experiment.

3.3.4 Spin-orbit interaction and scattering time in real structures

Figure 3.7 shows the dependence of the tunneling differential conductance for three different values of the parameter η. The value $\eta = 10$ corresponds to negligibly small scattering in comparison with the spin-orbit splitting, the corresponding tunneling characteristics take on a pronounced resonance character. For $\eta = 0.5$ all three cases are nearly the same, and that value can be regarded as critical from the standpoint of experiment. Let us estimate the value of η for the real experimental situation.

For structures based on AlGaAs one typically has $\varepsilon_F = 10$ meV, $\alpha^l k_F \approx 0.6$ meV, and the scattering time in real structures for tunneling experiments can fully reach $\tau = 10^{-12}$ s. This corresponds to $\eta \approx 1$, i.e., in such structures one would expect to see well resolved features due to the spin-orbit interaction. In structures based on GaSb the spin-orbit splitting is substantially larger, so that one would expect $\eta \approx 8$ at the same value of the scattering time. This means that a well distinguishable picture should be observed in such structures even for $\tau \approx 10^{-13}$ s.

Thus it is possible to determine the values of both types of interaction in a tunneling experiment, provided that a difference between layers in the parameters of one of these interactions can be created. For example, a difference in the Dresselhaus parameters implies the use of different materials for the left and right layers or, more realistically, solid solutions of different composition. Clearly it is much simpler to achieve different values of the Rashba parameters. Since the Rashba mechanism is directly related to the external electric field in the structure, a difference in the parameters α^L and α^R means simply a different electric field in the right and left layers. We have considered above the case of parameters of equal magnitude but opposite sign, $\alpha^L = -\alpha^R$, which corresponds to the presence of an electric field directed along the normal to the plane of the layers in opposite directions in the right and left layers. Just this situation arises if a charged plane is placed at the center of the barrier. Such a plane of ionized impurities can be created by doping in the central part of the barrier or by using two doping delta-layers on the outer sides.

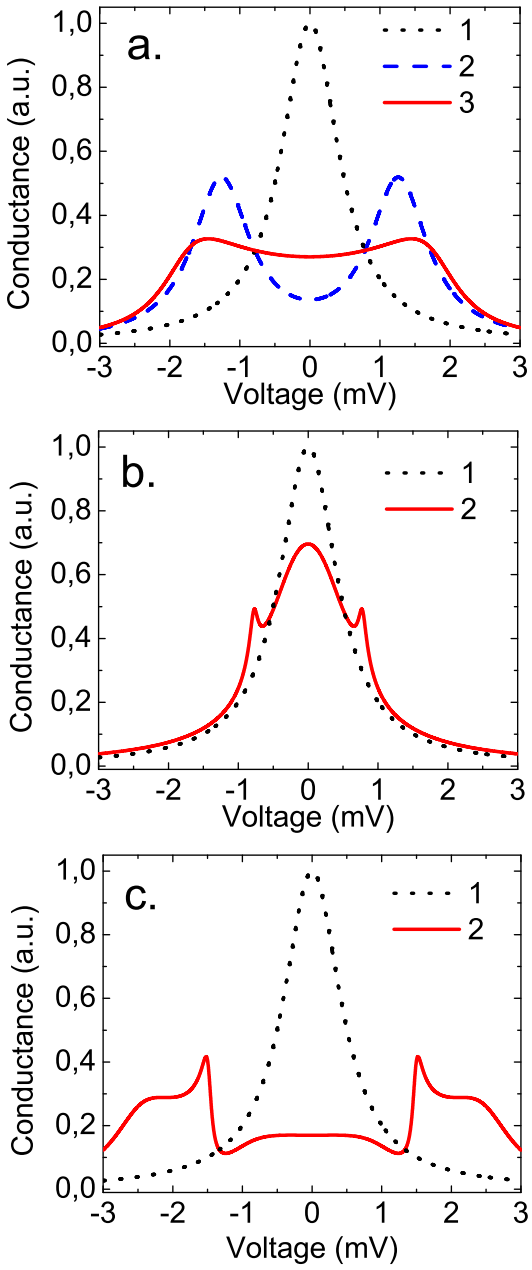

Figure 3.6: Tunneling conductance calculated for various parameters of SOI

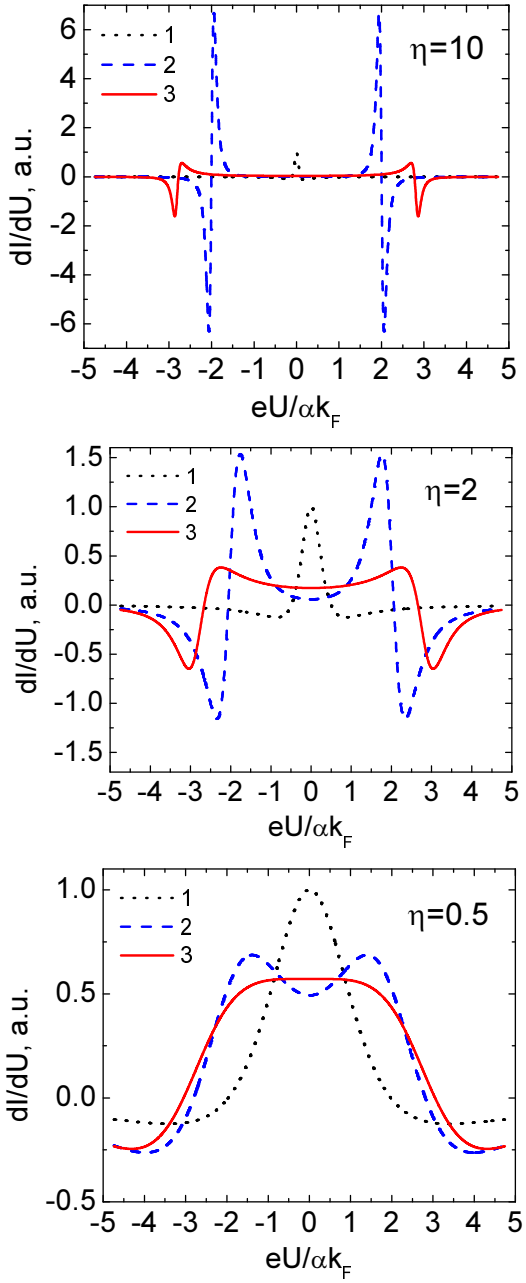

Figure 3.7: Tunneling conductance calculated for different parameters of the spin-orbit interaction and different parameters η 1 – $\alpha^R = \alpha^L$, $\beta = 0$ 2 – $\alpha^R = -\alpha^L$, $\beta = 0$, 3– $\alpha^R = -\alpha^L$, $\beta = |\alpha^R|$.

CHAPTER IV

INJECTION INTO ORGANIC MOLECULAR SOLIDS

4.1 Introductory remarks

The subject of this chapter lies a bit aside of the semiconductor heterostructures, however it gives another fruitful example of applying the tunneling Hamiltonian approach (See Ch. 2, Sec. 2.1) to the tunneling phenomena in the solid state. The organic molecular solids (OMS) are widely used in modern micro and optoelectronics. Light emitting diodes and field effect transistors have been fabricated on the basis of these materials [Forrest (2004)]. The tendency of further expansion of the potential applications for the OMS demands complete understanding of the underlying physics. However, some issues still remain unclear, one of them is the conductivity of the OMS films in a high electric field. The large energy bandgap of $\approx$3 eV for OMS provides rather low concentration of free intrinsic charge carriers. Therefore, these materials are dielectrics in a weak electric field. In a high electric field the charge carriers can be injected from electrodes and produce an electric current. The injection level is determined by the barrier formed at metal-dielectric interface. The injection current (electron and hole) from the metal into appropriate bands of crystal inorganic dielectric or semiconductor is usually obtained by the equations similar to those describing field and thermionic emission from metal to vacuum [Chynoweth (1960)]. The effective potential barrier height at the interface for the electron injection is assumed to be the difference between the work function of the metal electrode and the electron affinity of the OMS. Similar equations are often applied to the description of carriers injection into organic molecular solids [Yan et al. (2000)-Ganzorig et al. (2006)]. However, for these materials band theory of crystalline solids is not applicable due to weak interaction between molecules and their conductivity being of hopping character. Therefore, recently more attention is called to the microscopic mechanism of the injection into OMS, in particular to the tunneling of the charge carriers from metal to OMS with high concentration of the localized states having gaussian energy distribution [Liu and Kao (1991)-Arkhipov et al. (1999)]. The results obtained for injection of electrons are usually directly applied also to the hole injection (see, for example [Bässler (1993),Agrawal et al. (2008)]). This seems to be rather unproved, because the shape of the barrier in the case of electron injection is different from that in the case of hole injection. The specific of the hole injection into organic molecular solids was firstly discussed in [Zakrevskii and Sudar (1992)]. In that paper the hole injection was considered as ionization of molecules close to the surface of metallic anode. The ionization occurred due to tunnel transition of an electron from the upper molecular orbital (HOMO level) to an empty electron level in metal.

Unlike the case of electron injection for the hole injection the potential barrier at the interface in a high electric field has a trapezoidal shape. The effective height of the barrier is determined by the ionization energy of a localized state rather than by the difference between the ionization energy and work function of the metal. In [**Publication 3**] the hole injection in analyzed theoretically, (i.e. the electron transitions from molecular HOMO levels of organic materials into metal) for the case when the molecular levels have substantially lower energy than the Fermi level of the metal.

4.2 Theoretical approach

It is assumed that the potential barrier at metal-OMS interface is narrow and requires a single hop of the electron. For the correct barrier shape one should take into account the Coulomb interaction between electron, hole and their mirror images in metal. The barrier shape in the electric field F is given by [Suvorov and Trebukhovskii (1972)]:

$$U\left(x,x_i,F\right)=E_F+\varphi+exF-\frac{e^2}{16\pi\varepsilon\varepsilon_o x}-\frac{e^2}{4\pi\varepsilon\varepsilon_o\left(x_i-x\right)}+\frac{e^2}{4\pi\varepsilon\varepsilon_o\left(x_i+x\right)}, \tag{4.1}$$

where x_i is the distance of a localized state (denoted by index i) from anode, E_F denotes Fermi energy of the electrode, φ is the work function of the electrode. The first and second terms in (4.1) determine the barrier height at the interface in the absence of the electric field, the third term accounts for the influence of the electric field on the charge energy at the distance x from anode, the fourth term stands for the interaction of electron with its mirror-image in metal, the fifth term - the interaction between the ion and electron, the sixth – interaction of electron with ion's mirror-image. The shape of the barrier at the metal-OMS interface is shown in Fig.4.2. The calculation of the tunnel injection current was carried out in the framework of the tunneling Hamiltonian method (Sec. 2.1):

$$H=H_L+H_R+H_T,$$

The eigenstates $|L\rangle$, $|R\rangle$ of the appropriate partial Hamiltonians have the energies E_L, E_R and wavefunctions ψ_L, ψ_R. The tunneling matrix element T is given by 2.15 and the tunneling current density J is obtained from the single electron tunneling rate derived in Sec. 2.1, see (2.13):

$$J=e\frac{2\pi}{\hbar}V\int_0^\infty dE\int_a^\infty dx|\widetilde{T}(x)|^2Z\left(E\right)g(x,E)\left(1-f\left(E\right)\right)f_{loc}\left(x,E\right), \tag{4.2}$$

where e is the elementary charge, $Z(E)$ - density of states in metal, $f\left(E\right)$ - Fermi distribution in metal, a is the minimal distance from the electrode to the localized state in OMS, $f_{loc}\left(x,E\right)-$ filling factor of the localized states in organic material, $g(x,E)$ - density of localized states in the organic material.

It is worth noting that when the energy states in OMS underlie Fermi level in metal direct isoenergetic tunneling transitions can be substantially suppressed by the factor $\left(1-f\left(E\right)\right)$ (4.2), in other words there can be not enough empty states for the tunneling electrons from OMS. In this case it is important to estimate the contribution of indirect tunneling processes involving phonons. Calculation of indirect transitions rate using second-order perturbation theory with account of electron-phonon interaction and tunneling meets a certain difficulty. The tunneling transitions in the Bardeen's

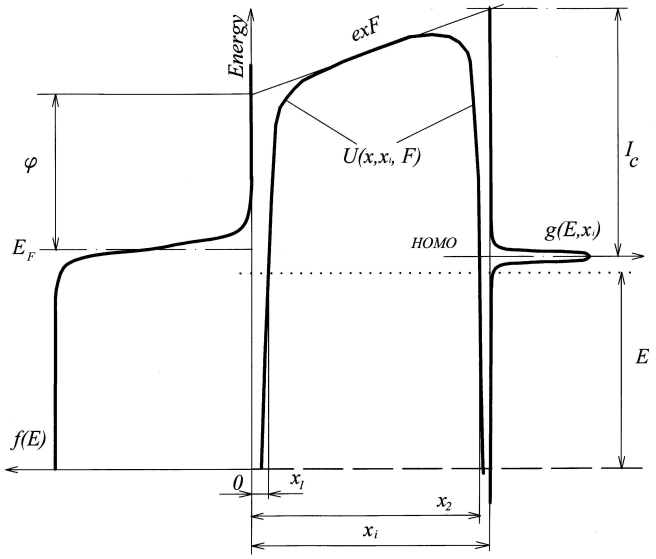

Figure 4.1: The shape of potential barrier controlling the holes injection from metal into OMS.

approach occur between the states of the same energy and in this way differ from the conventional quantum-mechanical transitions. This leads to singularities in energy denominators in the second order perturbation theory. For the calculation of the tunneling rates for acoustic phonons in metal another approach was used as suggested in [**Publication 3**]. The tunneling is treated by energy splitting of the metal-OMS system eigenstates by a value T. Then the electrons tunneling rate is calculated within the first order of the perturbation theory. In this approach The following expression is used for the phonon assisted tunnel current density:

$$J = V\frac{\pi^2 e\Xi^2 m^2}{s\rho\hbar^4}\int\limits_0^\infty dE\int\limits_a^\infty dx|\widetilde{T}(x)|^2 Z\left(E\right)g\left(x,E\right)\frac{1-f\left(E+2s\sqrt{2mE}\right)}{e^{\frac{2s\sqrt{2mE}}{kT}}-1}f_{loc}\left(x,E\right), \quad (4.3)$$

where Ξ stands for deformation potential constant, indicating the efficiency of interaction between electrons and acoustic phonons, s is a sound velocity in the metal, ρ is the metal density, m is a free electron mass, k is the Boltzmann constant, T is the temperature.

4.3 Results

The injection current was calculated for the injection limited case assuming all the holes injected into organic material instantly reach the cathode, in this case $f_{loc}\left(x,E\right)$=1. The calculation of the current density according to (4.2) and (4.3) was performed by means of numerical integration with the following parameters: ε=3, E_F =5 eV, φ =5 eV. The Gaussian spectrum of OMS localized

states (HOMO levels) was assumed, i.e.

$$g(E, x_i) = \frac{N_{loc}}{\sqrt{2\pi}\sigma} \exp\left\{ -\frac{[ex_iF + E_F + \varphi - I_C - E]^2}{2\sigma^2} \right\}, \tag{4.4}$$

where σ is the distribution dispersion, N_{loc} is a concentration of the localized states, I_c is ionization energy of the OMS molecules. The calculations were performed for $N_{loc} = 10^{21}$ cm^{-3} and σ=0.1 eV. E=0 corresponds to the bottom of the conductance band of the metal. Fig.4.3 shows the depen-

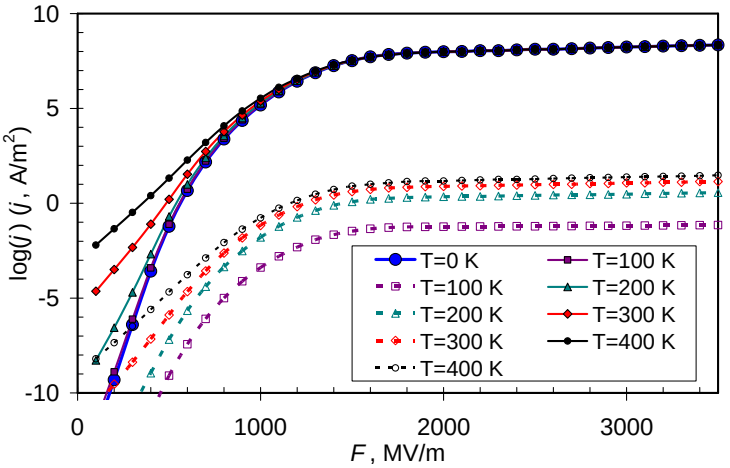

Figure 4.2: Dependence of the current density on electric field for different values of temperature for direct transitions (solid line) and transitions with phonon absorption (dashed line).

dencies of the current density on the electric field calculated for I_c=6 eV and a=0.6 nm for different temperatures. Solid lines correspond to the current calculated using (4.2), which takes into account only direct electron transitions from HOMO levels to the metal, dashed lines correspond to the current calculated using (4.3), accounting for only indirect transitions with phonon absorption. It can be seen that for the temperature being in the range from 0 to 400 K and for any value of the electric field the current of direct transitions substantially exceeds that of indirect transitions. This result allows to conclude that for the processes of hole injection the indirect transitions can be neglected and the current can be calculated using (4.2).

For the dependencies $j(F)$ shown in Fig.4.3 two characteristic regions can be distinguished. At relatively low field $F \leq$1500 MV/m the current density rapidly increases with the field and is significantly affected by the temperature. As the field is increased further the increase of j is slowed down so that in high electric field it weakly depends on the field and almost does not depend on the temperature.

Fig. 4.3 shows $j(F)$ dependencies, calculated for I_c=6.5 eV for different values of the minimal distance from electrode a and the temperature. The figure demonstrates that influence of a on j is different for different ranges of F. Let us recall that in zero field the maximum of localized states density $g(E)$ lies well beyond the Fermi level of the metal. Therefore, at zero temperature and zero

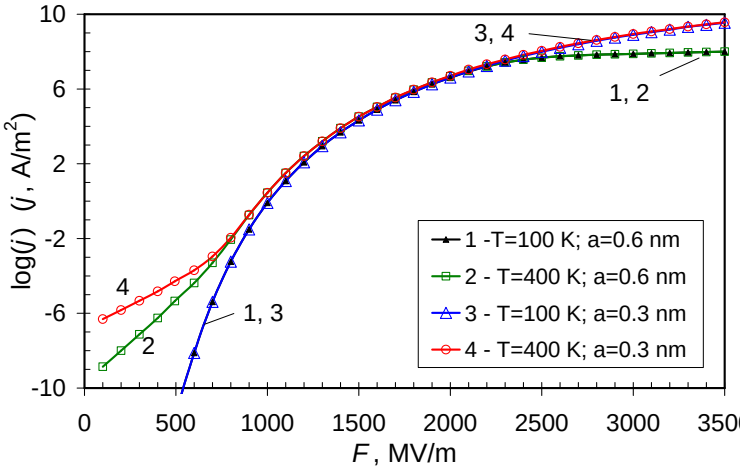

Figure 4.3: Dependence of the current density on electric field for different values of temperature and minimal hopping distance.

electric field the tunneling from OMS states is forbidden because there are no empty states available in metal. The external electric field shifts the OMS localized states up on energy scale towards the Fermi level of the metal while the temperature spreads the Fermi distribution in metal. Both factors provide empty states and in this way enhance the tunneling. At that, the role of the minimal distance a from the OMS states to metal appears to be different. In high electric field ($F > 2500$ MV/m) the electrostatic energy of all the OMS states is high enough being close to or higher than the Fermi level of the anode. Hence, the tunneling from any of them is allowed being obviously most efficient from those closely located to the metal-OMS interface. Thus, in this range of the electric field the current is crucially dependent on the minimal distance a (curves 3 and 4 differ from curves 1 and 2 in Fig.4.3) being insensible to the temperature (curves 1,2 coincide as well as curves 3,4 in Fig.4.3, the direct current shows no dependence on the temperature in high field in Fig.4.3). On the contrary, in the low field ($F < 1500$ MV/m) the current behavior depends on the temperature. If the temperature is low (see curves 1,3 corresponding to $T = 100$ K) the Fermi distribution in metal does not provide enough empty states for the tunneling from the OMS states which are close to the anode. However, the tunneling is allowed from OMS states located farther from the interface because they are higher on the energy scale due to the electric field. Consequently, the minimal distance a doesn't play a role in this regime illustrated by the curves 1 and 3 in Fig.4.3 which coincide in low field. The situation for the high temperature (represented by curves 2,4 corresponding to $T = 400$ K) is different. Despite the energy of the OMS states which are near the interface is still well beyond the Fermi level of the electrode the tunneling to metal is allowed due to spreading of the Fermi distribution by the temperature. Thus, the role of minimal distance a is also important here (see curves 2,4). In the mid field range $2500 > F > 1500$ MV/m the difference between the curves is hardly pronounced in the given scale. In this regime the main contribution to the injection current comes from the tunneling from OMS states located farther then the minimal distance a and having their energy within the band of kT width around the Fermi level. Therefore, both the dependencies on a and on the temperature are much weaker than in the extreme regimes.

The results of the modeling can be compared to the experimental data found in the literature for the hole conductivity in OMS. The comparison shows qualitative agreement in wide range of temperature and electric field values. Our modeling reproduces characteristic features of I-V dependencies, i.e. the effect of the temperature in weak electric field [van Woudenbergh et al. (2001)], the transition to the Fowler-Nordheim like dependence and current saturation in a strong field [Ganzorig et al. (2006), Hsiao et al. (2006)]. The role of the indirect tunneling processes with phonon absorbtion was analyzed for the first time in [**Publication 3**]. It was shown that the injection current is governed mostly by the direct transitions of electrons from molecular HOMO levels to empty states in metal. The contribution of the processes with phonon absorption is negligibly small.

CHAPTER V

CONFIGURATION INTERACTION IN HETEROSTRUCTURES

5.1 Introductory remarks

The mixing of a quantum state belonging to a discrete spectrum with continuum spectrum states has come into focus in the works of U. Fano [Fano (1961)] and Anderson [Anderson (1961)] in the context of atomic spectroscopy and autoionization. Recently, this problem also proved relevant to the physics of nanostructures. The modern physics of low dimensional structures often deals with a quantum well or a quantum wire which posses the charge carriers quantized in one or two dimensions while being free to move in the others interacting with bound states. The latter can be either an impurity or defect or a quantum dot. A striking example of this very case which is of particular interest nowadays is a semiconductor heterostructure containing a quantum well (QW) and a ferromagnetic or paramagnetic layer located in the vicinity of the QW. Such structures are believed to combine high mobility of the carriers in the QW and magnetic properties provided by the magnetic layer. A number of recent experiments with the InGaAs-based quantum wells with a remote Mn layer show that the Mn δ–layer located at a few nanometers from the QW gives rise to circular polarization of the photoluminescence (PL) from the QW in an external magnetic field applied perpendicular to the QW plane [Dorokhin et al. (2010); Zaitsev et al. (2010)]. It was questioned whether the spin polarization of the carries in the QW is due to the electrons tunneling to Mn site or the tunnel coupling of the holes at Mn with those in the QW. The latter mechanism which previously had no proper theoretical description is considered in [**Publication 4**] and [**Publication 6**].

5.2 Tunneling between bound state and a quantum well

The system under study consists of a δ–layer of the impurities (donors or acceptors) and a QW having one level of size quantization for the electrons or holes respectively. The energy level of the impurity bound state lies within the range of the 2D states size quantization subband in the QW. The potential barrier separating the impurity from the QW is assumed to be weakly transparent for the tunneling. The Tunneling Hamiltonian approach is used (see Ch. 2, Sec. 2.1) The total Hamiltonian is expressed as $H = H_i + H_{QW} + H_T$, where H_i is partial Hamiltonian having the bound state at the impurity as its eigenstate. H_{QW} in the same way corresponds to the QW itself, its eigenfunctions φ_λ form non-degenerate continuum of states characterized by the quantum number(s) λ. The term

H_T accounts for the tunneling. In the second quantization representation (2.19)

$$H = \varepsilon_0 a^+ a + \int \varepsilon_\lambda c_\lambda^+ c_\lambda d\lambda + \int \left(t_\lambda c_\lambda^+ a + t_\lambda^* a^+ c_\lambda \right) d\lambda, \tag{5.1}$$

where a^+, a – the creation and annihilation operators for the bound state characterized by its energy ε_0, and c_λ^+, c_λ – the creation and annihilation operators for a continuum state having energy ε_λ. The energy here and below is measured from the level of size quantization of the carriers in the QW so that ε_λ is simply their kinetic energy. The calculation of the tunneling matrix element is carried out in [**Publication 6**] where it is extended to the case of valence band structure. The attraction potential of the impurity is considered spherically symmetric, so the whole system (impurity+QW) has the cylindrical symmetry with z axis directed normally to the QW plane and going through the impurity center. Thus it appears convenient to represent the QW states in cylindrical coordinates rather than as plane waves. In this case each state is characterized by the wavenumber k and the cylindrical harmonic number l:

$$\varphi_{kl} = \eta(z) \sqrt{\frac{m}{2\pi\hbar^2}} J_l(k\rho)\, e^{il\theta} \tag{5.2}$$

where $J_l(k\rho)$ is the Bessel function of order l, ρ and θ are the polar coordinates in the QW plane, m–the in-plane effective mass, $\eta(z)$ is the envelope function of size quantization in z-direction. The wavefunction (5.2) has the normalization:

$$\langle \varphi_{kl} | \varphi_{k'l'} \rangle = \delta(\varepsilon - \varepsilon')\, \delta_{ll'}, \tag{5.3}$$

where $\varepsilon = \hbar^2 k^2 / 2m$. The potential barrier separating the deep impurity level from the QW in the first approximation can be assumed having a rectangular shape. Inside the barrier the function $\eta(z)$ is (z-axis is directed towards the impurity, $z = 0$ corresponds to the QW boundary):

$$\eta(z) \sim \frac{1}{\sqrt{a}} e^{-qz}, \tag{5.4}$$

where $q = \sqrt{\frac{2mE_0}{\hbar^2}}$, a is the QW width, E_0 is the binding energy of the bound state, at the same time E_0 determines the height of the potential barrier. For the bound electrons at donor impurity coupled to the QW conductance band the calculation of the tunneling matrix element is straightforward. The spherical potential of the impurity results in the ground state of the carrier to be angular independent, therefore the efficient tunneling overlap occurs only with the zeroth cylindrical harmonic $\varphi_{k0} \equiv \varphi(\varepsilon)$. For the deep impurity level one can use zero radius potential approximation [Lucovsky (1965)] and express the s-type wavefunction as:

$$\psi = \sqrt{2q} \frac{e^{-qr}}{r}. \tag{5.5}$$

In calculation of the tunneling matrix element (2.15) the integration is done over the surface located anywhere inside the barrier which is more convenient to take at the impurity site. This yields for the electrons tunneling between the donor state and the QW:

$$t_k^e = \sqrt{\frac{2\pi}{aq\left(1 + \frac{k^2}{q^2}\right)}} \sqrt{E_0} e^{-qd} \tag{5.6}$$

It is clearly seen that as long as the case $k << q$ is considered, the tunneling parameter has very weak dependence on k.

In order to apply the same approach to the 2D holes in GaAs interacting with an acceptor state it has to be generalized for the case of the valence band complex structure. This involves two stages: a) account for the proper Bloch states states in the QW and at the acceptor and b) generalizing the tunneling matrix element calculation on the case of a valence band in GaAs. The stage a) is described in [**Publication 4**] while the stage b) is more extensively treated in [**Publication 6**]. The problem is considered for the $In_xGa_{1-x}As$ QW having only one level of size quantization for the heavy holes, the light holes ar assumed split off due to the size quantization. The basis of Bloch amplitudes is formed of the states with certain projection of the total angular momentum $J = 3/2$ on z axis which is perpendicular to the QW plane:

$$\left(e_{3/2},\ e_{1/2}\,,\, e_{-1/2}\,,\, e_{-3/2}\right). \tag{5.7}$$

The wavefunctions $\varphi_{kl,j}$ in this basis have the form:

$$\varphi_{kl,-\frac{3}{2}} = \begin{pmatrix} 0 \\ 0 \\ 0 \\ \varphi_{kl}\left(\rho\right) \end{pmatrix}, \quad \varphi_{kl,+\frac{3}{2}} = \begin{pmatrix} \varphi_{kl}\left(\rho\right) \\ 0 \\ 0 \\ 0 \end{pmatrix}. \tag{5.8}$$

The kinetic energy of the 2D QW state is related to k as

$$\varepsilon = \frac{\hbar^2 k^2}{2m'_{hh}}, \tag{5.9}$$

where m'_{hh} is the in-plane heavy hole mass in the QW.

In order to determine wavefunction ψ of a hole localized at an acceptor one should consider the kinetic part of the Luttinger Hamiltonian and attractive potential of the acceptor $U(r)$. The spherically symmetrical potential preserves the symmetry Γ_8, thus the ground state is 4-fold degenerate and can be classified by angular momentum projection. The eigenfunctions of Luttinger Hamiltonian with spherically symmetric attractive potential can be explicitly found in the model of zero radius potential. [Averkiev and Il'inskii (1994)]. In the basis of the Bloch amplitudes they are expressed as follows:

$$\begin{aligned}
\psi_{+\frac{3}{2}} &= \begin{pmatrix} R_0Y_{00} + \frac{1}{\sqrt{5}}R_2Y_{20} \\ -\frac{2}{\sqrt{10}}R_2Y_{21} \\ \frac{2}{\sqrt{10}}R_2Y_{22} \\ 0 \end{pmatrix}, \ \psi_{+\frac{1}{2}} = \begin{pmatrix} \frac{2}{\sqrt{10}}R_2Y_{2,-1} \\ R_0Y_{00} - \frac{1}{\sqrt{5}}R_2Y_{20} \\ 0 \\ \frac{2}{\sqrt{10}}R_2Y_{22} \end{pmatrix}, \\
\psi_{-\frac{1}{2}} &= \begin{pmatrix} \frac{2}{\sqrt{10}}R_2Y_{2,-2} \\ 0 \\ R_0Y_{00} - \frac{1}{\sqrt{5}}R_2Y_{20} \\ \frac{2}{\sqrt{10}}R_2Y_{21} \end{pmatrix}, \ \psi_{-\frac{3}{2}} = \begin{pmatrix} 0 \\ \frac{1}{\sqrt{5}}R_2Y_{2,-2} \\ -\frac{2}{\sqrt{10}}R_2Y_{2,-1} \\ R_0Y_{00} + \frac{1}{\sqrt{5}}R_2Y_{20} \end{pmatrix}.
\end{aligned} \tag{5.10}$$

Here

$$
\begin{aligned}
R_0 &= C_0 \left(\frac{\beta}{r} e^{-qr\sqrt{\beta}} + \frac{e^{-qr}}{r} \right), \\
R_2 &= C_0 \left(\frac{\beta}{r} e^{-qr\sqrt{\beta}} \left(1 + \frac{3}{qr\sqrt{\beta}} + \frac{3}{q^2 r^2 \beta} \right) - \frac{e^{-qr}}{r} \left(1 + \frac{3}{qr} + \frac{3}{q^2 r^2} \right) \right), \\
C_0 &= \sqrt{\frac{q}{\beta^{3/2}+1}}, \\
q &= \sqrt{\frac{2 m_{hh} E_0}{\hbar^2}}, \\
\beta &= \frac{m_{lh}}{m_{hh}},
\end{aligned}
\tag{5.11}
$$

E_0 is the binding energy of the hole at the acceptor, Y_{lm} are the spherical harmonics. m_{lh}, m_{hh} - respectively are the bulk light hole mass and the heavy hole mass in GaAs. Note, that the radial part of all nonzero components of the wavefunctions (5.10) have two characteristic decay lengths, the largest of the two being always determined by the light hole mass $m_{lh} \approx 0.08\ m_0$, where (m_0 is the free electron mass).

The generalization of the tunneling matrix element starts from treating the kinetic energy operator K entering the (2.14) as the kinetic part of the Luttinger Hamiltonian ($\hbar k_x$,$\hbar k_y$,$\hbar k_z$ are, as usual, the momentum operators along the appropriate axis):

$$
K = \begin{pmatrix} F & H & I & 0 \\ H^* & G & 0 & I \\ I^* & 0 & G & -H \\ 0 & I^* & -H^* & F \end{pmatrix},
\tag{5.12}
$$

$$
\begin{aligned}
F &= -Ak^2 - \frac{B}{2}\left(k^2 - 3k_z^2\right), \\
G &= -Ak^2 + \frac{B}{2}\left(k^2 - 3k_z^2\right), \\
H &= Dk_z\left(k_x - ik_y\right), \\
I &= \frac{\sqrt{3}}{2} B \left(k_x^2 - k_y^2\right) - iDk_x k_y,
\end{aligned}
\tag{5.13}
$$

A and B being the appropriate valence band parameters. The functions ψ_α, $\varphi_{\lambda\beta}$ in (2.14) become now 4-component vector functions (also the spin indices α and β are added here). Analogously to the simple band case the integration (2.14) over the whole space is reduced to the integration over the surface Ω_S inside the barrier, at that, only z–projection of the kinetic energy operator is required. The expression for tunneling parameter simplifies into:

$$
{t_{kl\alpha\beta}}^{(h)} = (B - A) \int_{\Omega_S} dS \left({\varphi_{kl\beta}}^* \frac{d}{dz} \psi_\alpha - \psi_\alpha \frac{d}{dz} {\varphi_{kl\beta}}^* \right),
\tag{5.14}
$$

where φ_{kl} is given by (5.2).

This generalization, however, appears to have some issues. Indeed, the largest decay length of the bound state ψ_α is determined by the light hole mass while the decay length of the QW states is

governed by the heavy hole. Due to this circumstance the result of the surface integration (5.14) becomes dependent on the particular position of the integration surface inside the barrier. However, it can be shown that in the case of two masses the exponential dependence of the tunneling parameter on the barrier thickness is determined by the smallest mass, but the exact value of the tunneling parameter cannot be correctly obtained within the given approach. Now we define $q = \frac{\sqrt{2m_{hh}E_0}}{\hbar^2}$, $\beta = m_{lh}/m_{hh}$. The explicit evaluation of the overlap integrals with account for $k << q$ shows that the tunneling configuration interaction to be accounted for is only between the zeroth cylindrical harmonic $\varphi_{k0,-\frac{3}{2}}$ and the bound state $\psi_{-\frac{3}{2}}$ as well as between $\varphi_{k0,+\frac{3}{2}}$ and $\psi_{+\frac{3}{2}}$. Both are governed by the same tunneling parameter t_k^h:

$$t_k^h = \left(\frac{A-B}{\hbar^2/2m_0}\right)\sqrt{\frac{\pi}{aq}}\sqrt{\frac{m_{hh}m'_{hh}}{m_0^2}}\zeta\left(k/q\right)\beta\sqrt{E_0}\exp\left(-\chi\left(k/q\right)\sqrt{\beta}qd\right), \tag{5.15}$$

where $1 \leq \chi \leq 2$, $\zeta \sim 1$ are weak dimensionless functions of k/q, m'_{hh} is the effective in-plane heavy hole mass. The tunneling parameter t_k^h exponentially depends on the barrier thickness with the light hole mass entering the exponent index. The particular expressions for χ and ζ depend on the particular barrier cross-section one chooses for calculation of the tunneling matrix element.

In both cases for t_k^e, t_k^h it is reasonable to assume that the tunneling parameter does not depend on k as weak tunneling implies $k << q$. However, the particular shape of the barrier becomes important when one is concerned with experimental dependence on the distance d between the impurity and the QW.

5.3 Effect on the photoluminescence

The tunneling Hamiltonian (5.1) with known tunneling parameter $t(\varepsilon)$ allows one to construct the eigenfunctions Ψ of the whole system given those of the bound state ψ and the QW states $\varphi(\varepsilon)$:

$$\Psi\left(E\right) = \nu_0\left(E\right)\psi + \int_0^\infty \nu\left(E,\varepsilon\right)\varphi\left(\varepsilon\right)d\varepsilon, \tag{5.16}$$

E denotes the energy of the state Ψ. Here $\varphi(\varepsilon)$ are the wavefunctions with zeroth cylindrical harmonic, as was shown above the other harmonics are not affected by the tunneling configuration interaction. The approach fully described in Ch. 2, Sec. 2.2 leads to the following solution for the expansion coefficients in 5.16:

$$\begin{aligned}
{\nu_0}^2\left(E\right) &= \frac{t^2\left(E\right)}{\pi^2 t^4\left(E\right) + \left(E-\widetilde{\varepsilon_0}\right)^2}, \\
\nu\left(E,\varepsilon\right) &= \nu_0\left(E\right)\left(P\frac{t\left(\varepsilon\right)}{E-\varepsilon} + Z\left(E\right)t\left(E\right)\delta\left(E-\varepsilon\right)\right),
\end{aligned} \tag{5.17}$$

where

$$\begin{aligned}
Z\left(E\right) &= \frac{E-\varepsilon_0-F\left(E\right)}{t^2\left(E\right)}, \\
F\left(E\right) &= \int_0^\infty P\frac{t^2\left(\varepsilon\right)}{\left(E-\varepsilon\right)}d\varepsilon,
\end{aligned} \tag{5.18}$$

$$\tilde{\varepsilon}_0(E) = \varepsilon_0 + F(E). \tag{5.19}$$

Because of $k << q$ it is reasonable to put t =const everywhere, except for (5.18) where decrease of t at $E \to \infty$ is necessary for convergence of the integral.

In order to analyze the influence of the configuration interaction on the photoluminescence spectra we have to calculate matrix element of operator $\hat{M}$ describing interband radiative transitions between the hybridized wavefunction $\Psi(E)$ and wavefunction of 2D the carrier in the other band of the QW which we denote by $\xi_{k'l'}$, here k' is the magnitude of the wavevector, l' is the number of cylindrical harmonic analogously to (5.2). If, for instance, one considers the acceptor-type impurity then $\Psi(E)$ is the hybridized wavefunction of the 2D holes and $\xi_{k'l'}$ is the wavefunction of the 2D electrons in the QW. We assume that (a) there are no radiative transitions between the bound state wavefunction ψ and the 2D carrier wavefunction $\xi_{k'l'}$ in the other band thus the matrix element for transitions from the bound state:

$$\left\langle \xi_{k'l'} \left| \hat{M} \right| \psi \right\rangle = 0, \tag{5.20}$$

(b) the interband radiative transitions between the free 2D states in the QW are direct. According to (5.2) the wavefunctions $\varphi(\varepsilon)$ and $\xi(\varepsilon')$ corresponding to the zeroth harmonic in the cylindrical basis are:

$$\begin{aligned} \varphi(\varepsilon) &= \eta(z)\sqrt{\frac{m}{2\pi\hbar^2}} J_0\left(k\rho\right) \\ \xi(\varepsilon') &= \zeta(z)\sqrt{\frac{m'}{2\pi\hbar^2}} J_0\left(k'\rho\right), \end{aligned} \tag{5.21}$$

where

$$k = \frac{\sqrt{2m\varepsilon}}{\hbar}, \;\; k' = \frac{\sqrt{2m'\varepsilon'}}{\hbar},$$

$\eta(z), \zeta(z)$ – the appropriate size quantization functions in z–direction, m, m' are the in-plane masses of the electrons and holes respectively if the donor-type impurity is considered and vice versa for the acceptor case. Without the tunnel coupling the matrix element for the direct optical transitions between the states $\varphi(\varepsilon)$ and $\xi(\varepsilon')$ is given by:

$$M_0\left(\varepsilon', \varepsilon\right) = \left\langle \xi(\varepsilon') \left| \hat{M} \right| \varphi(\varepsilon) \right\rangle = \gamma u_k \frac{\sqrt{mm'}}{k\hbar^2} \delta\left(k - k'\right), \tag{5.22}$$

where u_k is the appropriate dipole matrix element for the Bloch amplitudes,

$$\gamma = \int \eta(z)\zeta(z)dz.$$

According to the above mentioned considerations it is only this matrix element that is affected by the tunnel coupling, preserving the matrix elements corresponding to the transitions between other than the zeroth cylindrical harmonic. The problem is now to find the modified matrix element M

for the transitions between the states $\Psi(E)$ and $\xi(\varepsilon')$. Because the wave functions (5.21) are not localized, one can use the asymptotic form of the Bessel function, i.e.:

$$\begin{aligned}\varphi(\varepsilon) &\sim \eta(z)\sqrt{\frac{m}{2\pi\hbar^2}}\sqrt{\frac{2}{\pi\rho}}\cos\left(k\rho-\pi/4\right)\\ \xi(\varepsilon') &= \zeta(z)\sqrt{\frac{m'}{2\pi\hbar^2}}\sqrt{\frac{2}{\pi k'\rho}}\cos\left(k'\rho-\pi/4\right)\end{aligned} \tag{5.23}$$

The modification of such type by the tunnel coupling was discussed in Ch. 2, Sec. 2.2. From (2.30) it follows that asymptotically

$$\Psi(E) \approx \eta(z)\sqrt{\frac{m}{2\pi\hbar^2}}\sqrt{\frac{2}{\pi k_E\rho}}\cos\left(k_E\rho-\pi/4+\Delta\right),$$

so we have:

$$M\left(\varepsilon',E\right) = \left\langle \xi(\varepsilon')\left|\hat{M}\right|\Psi(E)\right\rangle = \cos\Delta * M_0 - \sin\Delta * M_{\sin}, \tag{5.24}$$

where

$$M_{\sin} \sim \int\limits_0^\infty \cos\left(k'\rho-\pi/4\right)\sin\left(k\rho-\pi/4\right)d\rho$$

One could note that

$$\frac{M_{\sin}}{M_0} \sim \frac{\int\limits_0^L \cos\left(k\rho-\pi/4\right)\sin\left(k\rho-\pi/4\right)d\rho}{\int\limits_0^L \cos\left(k\rho-\pi/4\right)\cos\left(k\rho-\pi/4\right)d\rho} \sim \frac{1}{L}, \quad L->\infty,$$

therefore the last term in (5.24) is to be omitted and finally:

$$M = M_0\cos\Delta$$

With use of (2.33) we get:

$$M\left(\varepsilon',E\right)^2 = M_0\left(\varepsilon',E\right)^2\left[1-\frac{\pi^2t^4}{\pi^2t^4+\left(E-\widetilde{\varepsilon_0}\right)^2}\right], \tag{5.25}$$

where the difference in the denominator from the formula (2.33) is due to the fact that now t is calculated via the wave function which are normalized by energy delta-function and thus has different dimensionality than in (2.33). We proceed further with the Fermi's Golden Rule for the transition probability:

$$W(\hbar\omega) = \frac{2\pi}{\hbar}\int_0^\infty\int_0^\infty \left|M\left(\varepsilon',E\right)\right|^2 f'\left(\varepsilon'\right)f^h\left(E\right)\delta\left(E+\varepsilon'+E_g-\hbar\omega\right)dEd\varepsilon', \tag{5.26}$$

where E_g – the QW bandgap, $\hbar\omega$ – the energy of the radiated photon, f^h, f' – the energy distribution functions for the carriers in the hybridized and intact bands respectively. Substituting (5.22) and

(5.25) into (5.26) one should treat correctly the delta-function for the wavenumbers of the zeroth cylindrical harmonic. It can be shown that:

$$\delta^2(k-k') = \frac{\sqrt{S}}{\pi^{3/2}}\delta(k-k'),$$

where S is the area of the QW. Then we arrive at:

$$W\left(\hbar\omega\right) = \frac{u^2 f\left(E_\omega\right)}{\pi^{1/2}\hbar^2}\frac{\sqrt{2\widetilde{m}S}}{\sqrt{\hbar\omega - E_g}}\left(1 - \frac{\pi^2 t^4}{\pi^2 t^4 + \left(E_\omega - \widetilde{\varepsilon_0}\right)^2}\right), \tag{5.27}$$

where

$$\begin{aligned} &f\left(E_\omega\right) = f'\left(\alpha^{-1}E_\omega\right) f^h\left(E_\omega\right), \\ &E_\omega = \frac{\hbar\omega - E_g}{1+\alpha^{-1}}, \\ &\widetilde{m} = \frac{mm'}{m+m'}, \\ &\alpha = m'/m, \end{aligned} \tag{5.28}$$

while for the all cylindrical harmonics altogether the unperturbed optical transition rate yields:

$$W_0\left(\hbar\omega\right) = \frac{2\pi u^2 f\left(E_\omega\right)}{\hbar}\left(\frac{\widetilde{m}}{\hbar^2}S\right). \tag{5.29}$$

The result (5.27) obtained for a single impurity can be applied to an ensemble of impurities provided their interaction between each other is weak compared to the tunnel coupling with the QW. In this case the sample area S should be replaced with n^{-1}, n being the sheet concentration of the impurities in the delta-layer. After normalization by the area of the QW from (5.27),(5.29) we finally get the spectral density of the luminescence intensity:

$$I\left(\hbar\omega, \widetilde{\varepsilon_0}\right) = I_0\left(\hbar\omega\right)\left(1 - a\left(\widetilde{\varepsilon_0}\right)\sqrt{n}\frac{\pi^2 t^4}{\pi^2 t^4 + \left(E_\omega - \widetilde{\varepsilon_0}\right)^2}\right), \tag{5.30}$$

where

$$\begin{aligned} &a(\widetilde{\varepsilon_0}) = \frac{\hbar}{\pi^{3/2}\sqrt{2\widetilde{m}\widetilde{\varepsilon_0}\left(1+\alpha^{-1}\right)}}, \\ &I_0\left(\hbar\omega\right) = \frac{2\pi u^2\widetilde{m}}{\hbar^3} f\left(E_\omega\right). \end{aligned}$$

5.4 Polarization of the spectra

It follows from (5.30) that the bound state lying within the energy range of the continuum causes a dip in the luminescence spectra emitted from the QW. If then for any reason the bound state is split the luminescence spectra will show the appropriate number of the dips shifted by the splitting energy Δ. If one considers the splitting in the magnetic field applied along z each of the split

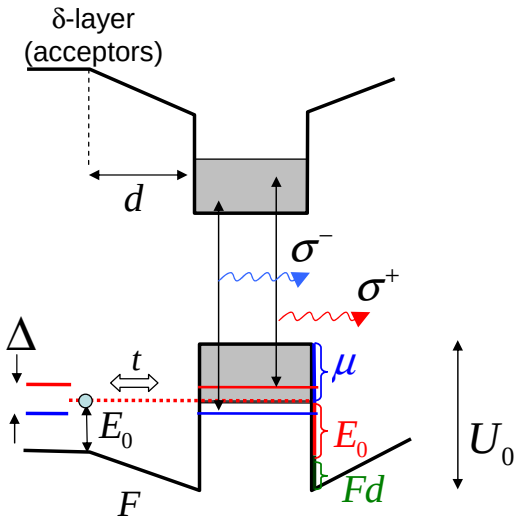

Figure 5.1: Mechanism of polarization of the luminescence for the acceptor type impurity. The localized hole levels split in magnetic field. Each of them effectively couples with the 2D holes having certain projection of angular momentum. Shifted positions of the resonances with account for temperature distribution of the holes cause the difference in intensities of circular polarizations σ^+, σ^-. The scheme also shows the simple electrostatic model described in the text.

sublevels is characterized by certain projection of spin and interacts with only one of the 2D carriers spin subbands characterized by the same projection of spin. Thus, for each of the two circular polarizations σ^+, σ^- of the light emitted from the QW one would expect one dip, its spectral position being different for σ^+ and σ^- in accordance with the splitting energy Δ. As an example let us consider the GaAs-based QW and 2D heavy holes interacting via the tunneling configuration interaction with the bound state at an acceptor. This case is shown schematically in Fig.5.1. The 2D holes with the projections of total angular momentum $j = +3/2$ and $j = -3/2$ recombine emitting respectively right- (σ^+) and left- (σ^-) circularly polarized light. In Sec. 5.2 it was shown that the heavy holes with $j = -3/2 (j = +3/2)$ interact basically with the bound states $\psi_{-\frac{3}{2}} (\psi_{+\frac{3}{2}})$. An external magnetic field applied along z would cause Zeeman splitting of the bound state energy level ε_0 into $\varepsilon_0^+ = \varepsilon_0 + \Delta/2$ and $\varepsilon_0^- = \varepsilon_0 - \Delta/2$. The splitting $\Delta = \varepsilon_0^+ - \varepsilon_0^-$ may also originate from exchange interaction of the holes with spin-polarized acceptor ions. Let us refer to the case of Mn ions having positive g-factor ($g \approx 3$, see [Schneider et al. (1987)]. The hole is coupled to Mn in antiferromagnetic way thus the level ε_0^+ corresponds to $j = -3/2$ and ε_0^- to $j = +3/2$. As follows from (5.19),(5.28) the difference in the positions of the resonances (dips) E_ω^+ and E_ω^- corresponding to the bound state sublevels ε_0^+ and ε_0^- is given by:

$$\widetilde{\Delta} = E_\omega^+ - E_\omega^- = \Delta + t^2 \ln\left(1 + \frac{\widetilde{\Delta}}{E_\omega^-}\right). \tag{5.31}$$

Unless the positions of the resonances are too close to the band edge the last term in (5.31) can be neglected and $\widetilde{\Delta} = \Delta = \varepsilon_0^+ - \varepsilon_0^-$. With account for the energy distribution functions for the

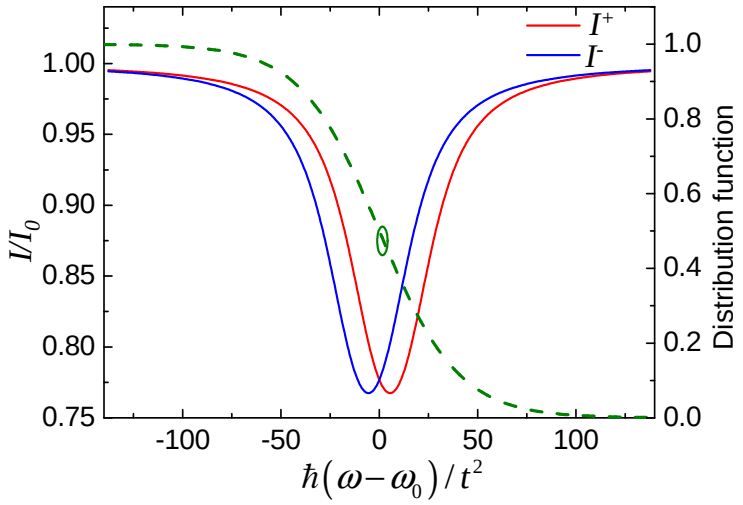

Figure 5.2: Modification of the luminescence spectrum by tunneling configuration interaction. The integral polarization occurs when the carriers distribution function (dashed line) strongly varies in the vicinity of the configuration resonances, ω_0 is the position of the resonance without bound level splitting.

holes and electrons the shifted positions of the resonances lead to the difference in the luminescence intensity for the opposite circular polarizations. In the discussed example of the antiferromagnetic alignment of the hole the luminescence spectra $I^+(\hbar\omega, \widetilde{\varepsilon_0}^+)$, $I^-(\hbar\omega, \widetilde{\varepsilon_0}^-)$ having the resonance positions at ε_0^+ and ε_0^- correspond to the circular polarizations σ^- and σ^+ respectively. As can be seen from (5.30) the difference in the resonance positions $\Delta = \widetilde{\varepsilon_0}^+ - \widetilde{\varepsilon_0}^-$ leads to the integral polarization of the spectra if the distribution function $f(E)$ significantly varies in the vicinity of ε_0. This is illustrated in Fig.5.2. The functions I^- and I^+ are shown by blue and red solid lines respectively. The integral polarization is naturally defined as:

$$P = \frac{P(\sigma^+) - P(\sigma^-)}{P(\sigma^+) + P(\sigma^-)} \approx \frac{\int\limits_{E_g}^{\infty} I^-(\hbar\omega)\, d(\hbar\omega) - \int\limits_{E_g}^{\infty} I^+(\hbar\omega)\, d(\hbar\omega)}{2\int\limits_{E_g}^{\infty} I_0(\hbar\omega)\, d(\hbar\omega)}$$

With use of (5.30) this yields:

$$P = -\sqrt{n}\frac{\int\limits_0^{\infty} \pi t^2(E) \left[\frac{a\left(\widetilde{\varepsilon_0}^+\right)\pi t^2(E)}{\pi^2 t^4(E) + \left(E - \widetilde{\varepsilon_0}^+\right)^2} - \frac{a\left(\widetilde{\varepsilon_0}^-\right)\pi t^2(E)}{\pi^2 t^4(E) + \left(E - \widetilde{\varepsilon_0}^-\right)^2}\right] f(E)\, dE}{2\int\limits_0^{\infty} f(E)\, dE}. \tag{5.32}$$

The slow varying functions $f(E)$ and $\widetilde{\varepsilon}_0(E)$ in the integral may be assumed as constants taken at $\widetilde{\varepsilon_0}^-, \widetilde{\varepsilon_0}^+$, the tunneling parameter will be treated as a constant in the whole range of interest $t^2(E) \equiv t^2$.

Then treating the expression in brackets as delta-functions we obtain:

$$P = -\frac{\sqrt{\pi}\hbar t^2\sqrt{n}}{2^{3/2}\sqrt{m}} \frac{f\left(\varepsilon_0^+\right)\left(\varepsilon_0^+\right)^{-1/2} - f\left(\varepsilon_0^-\right)\left(\varepsilon_0^-\right)^{-1/2}}{\int\limits_0^\infty f\left(E\right) dE}. \tag{5.33}$$

For the considered case the polarization degree appears to be negative. The positive sign would have appeared if the ferromagnetic coupling between the acceptor ion and the hole had been assumed.

In [**Publication 4**] the dependence of the circular polarization degree is analyzed as a function of the temperature and the QW Fermi level position with regard to the bound state energy. Let us consider the hybridization of the holes and the intact wave function of the electrons in the conductance band. Then $f' \equiv F_e(E)$, $f^h \equiv F_h(E)$ are two arbitrary Fermi distributions of the electrons and holes respectively. They are characterized by the chemical potentials μ_e, μ_h and the temperatures T_e and T respectively. Let us analyze a few particular cases, for all of them it is implied $\widetilde{\varepsilon_0} > \Delta$. Firstly, let the holes be fully degenerate and both energies $\widetilde{\varepsilon_0^-}$ and $\widetilde{\varepsilon_0}^+$ lying well beyond the quasi Fermi level of the holes so that: $\mu_h - \widetilde{\varepsilon_0^+} >> \Delta$. In this case the distribution function of the holes can be considered as $F_h(E) = 1$ in the range $E \in \left(\widetilde{\varepsilon_0^-}, \widetilde{\varepsilon_0^+}\right)$ Assuming further the electrons to be non-degenerate we obtain the dependence shown in Fig.5.3 (the effective temperature is defined here as $T^* = \alpha T_e$) for different values of the parameter $\gamma \equiv \Delta/\widetilde{\varepsilon_0}$. The polarization shows nonmonotonous behavior

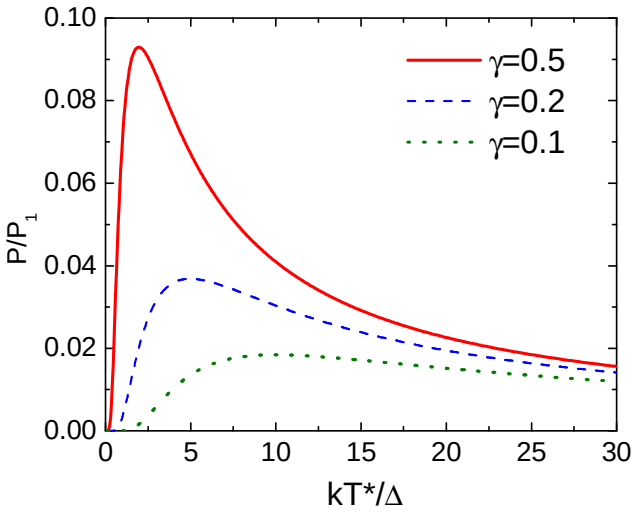

Figure 5.3: Temperature dependence of integral polarization. Electrons are non-degenerate, holes are either non-degenerate or have the constant distribution function for different values of parameter $\gamma \equiv \Delta/\widetilde{\varepsilon_0}$. P_1 is the normalization constant.

with increasing the temperature. In the discussed theory the polarization arises from splitting of the configuration resonances positions for σ^+ and σ^- spectra. The configuration resonance itself causes the redistribution of the transitions rate in the vicinity of the resonance energy conserving the total rate, thus the net polarization is subject to the difference in occupation numbers for $\widetilde{\varepsilon_0^-}$ and $\widetilde{\varepsilon_0}^+$. The maximum integral polarization is therefore naturally expected when the derivative of the combined

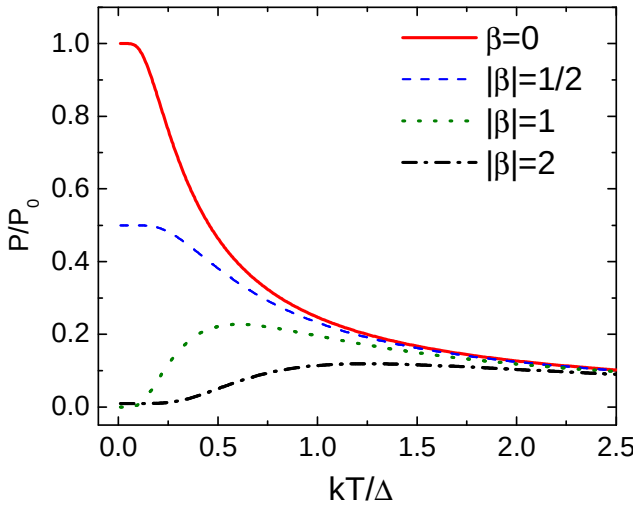

Figure 5.4: Temperature dependence of polarization for the case of electrons distribution function being constant within the configuration resonances. The parameter $\beta \equiv \frac{\widetilde{\varepsilon}_0 - \mu_h}{\Delta}$ denotes deviation of the holes Fermi level from the configuration resonance, $\gamma = 0.1$. P_0 is the normalization constant.

distribution function $f(E)$ reaches its maximum within the range $E \in \left(\widetilde{\varepsilon_0}^-, \widetilde{\varepsilon_0}^+\right)$. For the considered non-degenerate energy distribution function the maximum of the derivative is at $\widetilde{\varepsilon}_0$ when $\widetilde{\varepsilon}_0 = kT^*$ and the value of the derivative decreases with increase of $\widetilde{\varepsilon}_0$. This explains the overall decrease of the maximum polarization with decrease of γ in Fig.5.3. Exactly the same dependence is valid for the case when both electrons and holes are non-degenerate. The only difference from the previously considered case is that now the effective temperature T^* is given by

$$\frac{1}{T^*} = \left(\frac{1}{\alpha T_e} + \frac{1}{T}\right).$$

Now let us consider the electrons distribution function F_e being nearly constant within the configuration resonances. This can be due to the electrons non-equilibrium distribution with a high quasi Fermi level or high electrons temperature T_e. The holes are now considered to have Fermi distribution function characterized by the chemical potential μ_h and the temperature T. We also assume $kT << \widetilde{\varepsilon}_0$. The dependence of the polarization degree on the temperature derived from (5.33) for this case is plotted in Fig.5.4 for different values of the parameter β (the value of γ was taken 0.1). In this case the maximum of the distribution function derivative is at the holes Fermi level μ_h, therefore the largest integral polarization corresponds to $\beta = 0$.

5.5 The electrostatic effect

Because of the tunneling involved in the polarization of the luminescence one might reasonably expect very strong dependence of the polarization degree on the distance d between the δ–layer

and the QW (i.e. the thickness of the spacer). However, the purely exponential dependence of the polarization on the barrier thickness appears to be weakened due to the electrostatic effect shown in Fig.5.1 and explained below. Let us for simplicity consider the electrons distribution function being nearly constant within the configuration resonances. The holes are considered to have Fermi distribution function characterized by the chemical potential μ and the temperature T. In the absence of an external optical pumping the holes in the QW are in thermodynamic equilibrium with the acceptors in the δ–layer, therefore they have the same chemical potential. Under low pumping conditions the already large concentration of the holes in the QW is not strongly violated, so it is reasonably to assume that the quasi Fermi levels of the holes at the acceptors and in the QW coincide, it means that $\varepsilon_0 = \mu$. Strictly speaking, this is valid for a single bound level, if the level is split so that $\varepsilon_0^+ - \varepsilon_0^- = \Delta$, one should probably assume $\varepsilon_0^- = \mu$. From (5.33) we get the following simplified expression:

$$P = -\frac{\sqrt{\pi}\hbar t^2\sqrt{n}}{2^{5/2}\sqrt{m'_{hh}}\mu^{3/2}}\tanh\frac{\Delta}{2kT} \tag{5.34}$$

As we will show below both t and μ contribute to the dependence of the integral polarization P on the spacer thickness d and the QW depth U_0. The holes in the QW provide an electrical charge density estimated as $\sigma = eN\mu$, where e is the elementary charge, N is the 2D density of states. The positively charged plane of the QW and negatively charged δ–layer of partly ionized acceptors separated by a distance d produce an electric field

$$F = \frac{4\pi eN\mu}{\varepsilon}, \tag{5.35}$$

ε being dielectric constant of the material. Due to the electric field F the valence band edge at position of Mn layer appears to be shifted from the valence band edge just outside of the QW by $F \cdot d$. Because the quasi Fermi level of the acceptors exceeds the local position of the valence band edge by the binding energy E_0, the equality of the quasi Fermi levels leads to a simple equation (see Fig.5.1) :

$$U_0 = \mu + E_0 + eFd, \tag{5.36}$$

where U_0 is the QW depth and μ is the chemical potential of the holes in the QW. With (5.35) one gets :

$$\mu = \frac{U_0 - E_0}{1 + \frac{4\pi Ned}{\varepsilon}} \approx \frac{(U_0 - E_0)\,\varepsilon}{4\pi Ned}. \tag{5.37}$$

In order to estimate the dependence of the tunneling parameter t on the QW and spacer parameters we consider the WKB tunneling through trapezoid barrier as seen in Fig.5.1. With taking into account (6.25) and (5.37) this leads to the following expression (we assume $\mu \ll U_0$):

$$t^2 \sim \exp\left(-\kappa d\right), \tag{5.38}$$

where

$$\kappa = \frac{4\sqrt{2m_{lh}}}{3\hbar\left(U_0 - E_0\right)}\left(U_0^{3/2} - E_0^{3/2}\right) \tag{5.39}$$

From (5.34), (5.38), (5.39), (5.37) follows the dependence of integral polarization on the spacer thickness:

$$P \sim d^{3/2} \exp(-\kappa d), \tag{5.40}$$

Note that electrostatic effect results in the dependence of μ on d which leads to the dependence of P on d being not purely exponential but weakened by the pre-exponential factor $d^{3/2}$. While the correction is pre-exponential it appears to be significant enough up to $\kappa d \approx 2-3$ which is typical for the experimental situation.

5.6 Comparison with experimental data

In the proposed theory the polarization of light emitted from the QW originates from the splitting of the impurity bound state and therefore may exceed the polarization degree expected from an intrinsic g-factor of the 2D carriers located in the QW. An external magnetic field is assumed non-quantizing. An estimate for the energy of Landau levels separation gives:

$$\hbar\omega_c = \frac{e\hbar B}{m'_{hh}c} \approx 0.3 \text{ meV}$$

for the magnetic field $B = 0.5$ T. This value is substantially less than the typical kinetic energy of the holes estimated as $\varepsilon \approx 1-10$ meV. However, this value might be comparable to the tunneling parameter. Therefore for the experimental data the validity of the developed theory is well justified for $B \lesssim 0.5$ T. The tunnel coupling causes a dip in the luminescence spectra. This means that in the considered scheme the polarization of the luminescence from the QW is expected to be of the opposite sign than that due to the optical transitions between the bound state and the free carriers inside the barrier. In particular, the configuration interaction between the 2D heavy holes and Mn δ-layer considered in Sec.5.4 leads to the negative sign of the polarization. Such result contradicts the known experimental data [Zaitsev (2012),Korenev et al. (2012)], where the polarization is shown to be positive. This might suggest that regarding these particular experiments the polarization is not due to the holes configuration interaction but rather due to polarization of the electrons as suggested in [Korenev et al. (2012)]. The other possibility might be that the relevant bound state of the hole at Mn is more complex and does not resemble the simple antiferromagnetic exchange coupling with Mn ion.

Let us estimate the expected magnitude of the circular polarization degree due to the tunneling configuration interaction. We assume the deep impurity level $E_0 = 100$ meV, the barrier thickness $d = 5$ nm, the QW width $a = 10$ nm. Taking the effective mass as that of the electrons in GaAs $m = 0.06\, m_0$ for the simple band case described by (5.6) one gets for the tunneling parameter $\left(t^e\right)^2 \approx 2$ meV. The estimation for the holes tunneling parameter appears to be far less, taking $m_{hh} = 0.5\ m_0$, $m'_{hh} = 0.15\ m_0$ from (6.25) one gets $\left(t^h\right)^2 \sim 0.01$ meV. The polarization degree is to be estimated using (5.33). We take $\Delta = 1$ meV, $T_e = T_h = 20$ K, the sheet concentration of the impurities $n = 10^{13}$ cm^{-2}. Then for the case of the donor impurity $t = t^e$, $\varepsilon_0 = 4$ meV, $\mu_h = -1$ meV, $\mu_e = \varepsilon_0^-$, one gets $|P| \approx 40\%$, for the acceptor impurity $t = t^h$, $\mu_e = -1$ meV, $\varepsilon_0 = 2$ meV, $\mu_h = \varepsilon_0^-$ gives $|P| \approx 0.5\%$. An illustration of the luminescence spectra for the two circular polarizations is presented Fig.5.5. For this we used an intermediate value for the tunneling parameter $t^2 = 0.3$ meV ($|P| \approx 0.15\%$) and accounted for inhomogeneous broadening of the spectra by normal distribution of the bandgap E_g with the dispersion $\sigma = 3$ meV (corresponds to

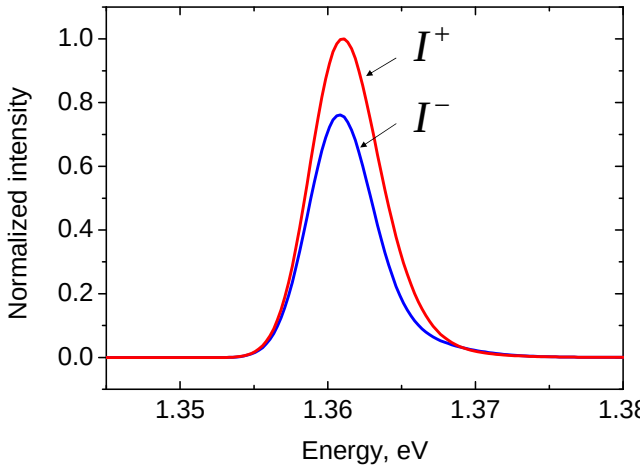

Figure 5.5: (An example of calculated luminescence spectra for the two circular polarizations. The case of antiferromagnetic coupling implies I^- corresponds to (σ^+) polarization while I^+ to (σ^-) polarization. The parameters used in calculations are given in the text.

the fluctuation of the QW width by half a monolayer). Fig. 5.6 shows a fit using the developed theory and the parameters mentioned above to the experimental data obtained in the group of [Zaitsev et al. (2010)]. The same set of parameters allowed for the fit of spectra for different width of the spacing, i.e. the distance between Mn δ-layer and the QW. The weak dependence on the spacer width is due to the electrostatic effect described in Sec. 5.5. While the fit shows indeed a good agreement with the experiment the issue regarding the polarization sign is still a demand for the new experiments to be carried out for such structures.

5.7 Summary of the results

The theory covered by this chapter describes the tunnel coupling between a continuum of states in the QW and an impurity bound state located outside of the QW. It succeeded in combining the tunneling Hamiltonian method (Sec. 2.1) with the Fano-Anderson exactly solvable model (Sec. 2.2) The calculation of the matrix elements for the direct interband optical transitions in the QW was carried out. It was found that for such transitions the tunnel coupling of the 2D QW states with the impurity states leads to the drop of the luminescence spectral density at the frequency corresponding to the configuration resonance. If the bound hole state is split in the projection of the hole angular momentum this modification of the spectra leads to an integral circular polarization of the light emitted from the QW. The key advantage of the approach used in the present study is that the unknown eigenfunctions of the system are expressed through those of the uncoupled states. It was also discovered that the electrostatic effect leads to the weakening of the polarization dependence on the tunnel barrier which is observed experimentally. While the theory developed in this chapter is capable for describing interaction of a bound state with continuum both for the electrons and for the holes, one still has to know which of these prevail in an experimentally studied structure in order to properly apply the theory. An example of applying the theory to the experimental data is discussed.

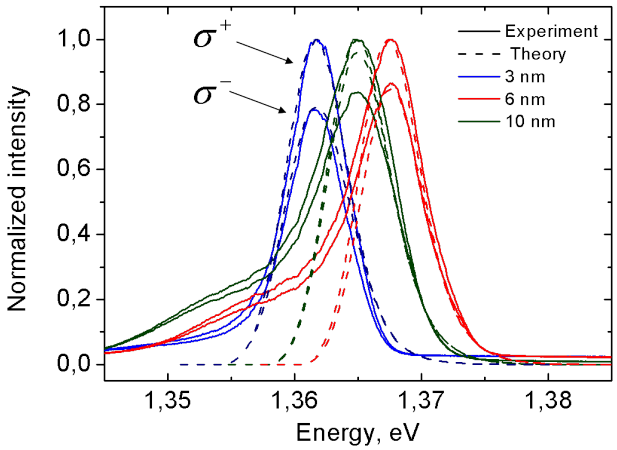

Figure 5.6: The fit of a theory to the experimental photoluminescence spectra for the samples having different thickness of the barrier separating the Mn δ-layer from the QW. This thickness varies from 3 nm (blue) to 10 nm (green). The external magnetic field $B = 0.3T$ is applied.

It is clear that the proposed theory is able to provide a good match to the photoluminescence data available, however there is still a demand for a clarification of the experiments in order to resolve whether issue with the polarization sign is indeed coming from a bound state structure or from domination of the electrons contribution to the tunnel coupling discussed in this section. Finally, the dependence of the circular polarization degree is analyzed as a function of the temperature and the QW Fermi level position with regard to the bound state energy.

CHAPTER VI

RESONANT INDIRECT EXCHANGE INTERACTION

6.1 Introductory remarks

In this chapter the theory of tunnel coupling between a paramagnetic impurity layer with a continuum of delocalized states is further developed to describe the indirect exchange interaction between the paramagnetic ions mediated by the free carriers in a quantum well or a quantum wire. A semiconductor doped with a paramagnetic impurity such as Mn belongs to so-called diluted magnetic semiconductors (DMS) which are nowadays under a particular attention of the semiconductor physics community. A lot of efforts are put forward to combine the numerous advantages of semiconductors with the spin-related phenomena introduced by the magnetic impurities. In this field, however, still much remains unclear. For instance, the mechanism responsible for the ferromagnetic properties of GaAs doped with small amount of Mn has not yet been understood [Jungwirth et al. (2006)]. The low-dimensional structures are considered as most promising for the semiconductor spintronics, however their magnetic properties are even less studied and experiments are few. These InGaAs heterostructures containing a QW and a remote Mn δ-layer show ferromagnetic behavior similar to that of the bulk Mn-doped InGaAs DMS [Rupprecht et al. (2010); Nishitani et al. (2010); Aronzon et al. (2010)]. It was discovered, however, that the dependence of the Curie temperature on the QW depth shows the non-monotonic behavior [Aronzon et al. (2013)]. Analysis of the parameters of these GaAs/InGaAs/Mn heterostructures shows that the non-monotonic behavior originates from falling of the hole bound state at Mn ion into the energy range of occupied 2D heavy holes subband of the first QW size quantization level. This situation is the one discussed in Ch. 5. The non-monotonous behaviour of the Curie temperature suggests that there is a contribution to the Mn-induced ferromagnetism which is related to the QW. The ferromagnetism mediated by a free carriers is well known as Ruderman-Kittel-Kasuya-Yosida (RKKY) interaction. However, the ferromagnetic interaction mediated by a remote conducting channel which involves the tunneling has not been studied so far. The non-monotonous behavior of the ferromagnetic interaction on the QW depth supports the resonant tunneling to be of importance here. Both too shallow or too deep QW would break the resonant condition and decrease the mutual influence of the QW and the Mn ions. The goal of the present work was to establish a proper theory describing the indirect pair exchange interaction between two ions mediated by a 2D free carriers gas located at a tunnel distance with account for the resonant tunnel coupling with the Mn bound states. It is shown that when the condition for the resonant tunneling is met the interaction strength appears to be strongly enhanced.

The classical RKKY theory deals with the delocalized carriers described by plane waves. A straightforward way to get a solution for the problem would be an improvement of the RKKY results by replacing the plane waves by the hybridized wave functions obtained in Sec. 2.2. This way is considered in [**Publication 5**]. However, in general the approach fails due to the resonant character of the hybridization. When the wavefunctions are strongly modified i.e. in the case of the resonant tunneling RKKY theory (which is a perturbation theory) fails. It would deliver a divergent result when the resonant tunneling occurs near the Fermi level. The other approach well developed for the 1D case of magnetic multilayers is to solve one-particle electron problem exactly for the potential which takes the magnetic moments of the magnetic ions as parameters. The exchange interaction energy between the ions is then interpreted as the difference in the total system energy calculated for the different potentials [Erickson et al. (1993); Stiles (1993); Lang et al. (1993)]. The developed theory follows the latter approach and applies it to the indirect exchange between the two magnetic ions mediated by the plane waves in 1D and 2D cases in [**Publication 8**] as well as to the target case of resonant tunneling in [**Publication 7**] and [**Publication 8**]. In the theoretical approach used below energy is extracted from the scattering phase shift. This is done following the method which is fully described in Ch. 2, Sec. 2.3 of this dissertation.

6.2 Indirect exchange interaction. Non-perturbative approach

The conventional RKKY theory describes pair interaction between two magnetic ions mediated by free carriers gas. The ions do not interact directly so the explicit exchange interaction is only between a magnetic ion spin and a free carrier spin. It is written in the form [Ruderman and Kittel (1954)]:

$$H_J = J\delta\left(\mathbf{r}-\mathbf{R}_1\right)\widehat{\mathbf{I}}_1\widehat{\mathbf{S}} + J\delta\left(\mathbf{r}-\mathbf{R}_2\right)\widehat{\mathbf{I}}_2\widehat{\mathbf{S}}. \tag{6.1}$$

where $\mathbf{R_{1,2}}$ – the ions positions, $\widehat{\mathbf{I}}_{1,2}, \widehat{\mathbf{S}}$ – the spin operators for the ion and the free carrier respectively, J – the exchange constant. According the RKKY approach the H_J is treated as perturbation and in the second-order one obtains the energy correction which is proportional to $J^2\mathbf{I_1}\mathbf{I_2}$ and depends on R in oscillating way. Here $\mathbf{I_1}, \mathbf{I_2}$ are the ions spins which are well defined for the non-perturbed state basis. If we try to discard the perturbation theory limitation and consider exact solution for the Hamiltonian containing (6.1) the problem becomes far more complicated. Each of the free carriers spins is coupled with both ions and the only quantity that is conserved is the total spin of the two ions and all the electrons. The exact solution for this many-body problem is hard to find. However, there is a certain room to improve the perturbative RKKY approach for the case when the direct exchange interaction determined by the constant J is still small compared to the free carriers Fermy energy E_F, but the modification of the coordinate parts of the wavefunctions is not small. In this case the total spin of the free carriers in the ground state would be small (otherwise due to the Pauli exclusion principle it would provide the energy correction of the order of E_F), thus one can assume that the total spin of the ions $\mathbf{I_1} + \mathbf{I_2}$ is nearly conserved. Thus, the eigenstates can be classified by the total spin of the two impurities in the range $0..2I$. The interaction energy can then be calculated by treating the ion spins classically as the energy difference between the states with zero total spin and with the total spin $2I$, corresponding to the antiparallel and parallel configuration of the ions spins respectively. As H_J (6.1) does not mix the free carrier spin projections we can further replace $\widehat{\mathbf{S}}$ with a parameter $s = \pm|s|$. Finally, the interaction energy is calculated as:

$$\Delta E = E_{\uparrow\uparrow} - E_{\uparrow\downarrow}, \tag{6.2}$$

where $E_{\uparrow\uparrow}, E_{\uparrow\downarrow}$ is the energy of the system with parallel and antiparallel configurations with single-particle Hamiltonians being respectively:

$$\begin{aligned} H_{\uparrow\uparrow} =& H_0 + JIs\left[\delta\left(\mathbf{r}-\mathbf{R}_1\right)+\delta\left(\mathbf{r}-\mathbf{R}_2\right)\right], \\ H_{\uparrow\downarrow} =& H_0 + JIs\left[\delta\left(\mathbf{r}-\mathbf{R}_1\right)-\delta\left(\mathbf{r}-\mathbf{R}_2\right)\right], \end{aligned} \tag{6.3}$$

where $H_0 = -(\hbar^2/2m)\Delta$ is the unperturbed Hamiltonian for the free carrier of the mass m. Once the single-particle Hamiltonian is fixed in the form (6.3) the appropriate solutions of the stationary Schrödinger equation can be found exactly. The appropriate difference in the total energy of an ensemble of electrons can be obtained by analyzing the solutions of $H_{\uparrow\uparrow}, H_{\uparrow\downarrow}$ in a finite-size box of size L with zero boundary conditions [Stiles (1993); Mueller (2002)]. The obtained spectra of single-particle states is filled with a fixed number of particles with account for Pauli exclusion principle and the total energy is calculated by summing the filled states energies. The total energy difference between parallel and antiparallel ions spin configurations is interpreted as the indirect interaction energy between the ions.

6.3 Indirect exchange interaction in 1D

For the 1D case it appears of particular importance to take into account the localized states $E<0$ whenever they occur in the spectra, i.e. when the contact interaction is represented by an attractive delta-function potential. Analysis of the 1D finite-box descrete spectra of double delta potential (6.3) is similar to standard university level problems. Taking the continuous limit $L\to\infty$ we obtain:

$$\Delta E = \frac{1}{2\pi}\int_0^{E_F} f\left(E,R\right)dE + \Delta E_{loc}, \tag{6.4}$$

where

$$\begin{aligned} f =& 2\arctan\frac{j^2\sin 2kR}{4k^2+2j^2\sin^2 kR}+ \\ &+\arctan\frac{4kj+j^2\sin 2kR}{4k^2-2j^2\sin^2 kR}-\arctan\frac{4kj-j^2\sin 2kR}{4k^2-2j^2\sin^2 kR}, \\ j =& JI\left|s\right|\frac{m}{\hbar^2},\ k=\frac{\sqrt{2mE}}{\hbar},\ R=\left|\mathbf{R_1}-\mathbf{R_2}\right| \end{aligned} \tag{6.5}$$

E_F is the Fermi energy of the unperturbed free carriers gas. ΔE_{loc} stands for the difference in the bound states energy for the parallel and antiparallel configurations. The bound state energy is determined from the following equation:

$$\begin{aligned} &\left(\kappa\tanh\left(\kappa R/2\right)+\kappa+2j\right)\left(\kappa\coth\left(\kappa R/2\right)+\kappa\pm 2j\right) \\ &=-\left(\kappa\tanh\left(\kappa R/2\right)+\kappa\pm 2j\right)\left(\kappa\coth\left(\kappa R/2\right)+\kappa+2j\right), \end{aligned}$$

where $\kappa=\sqrt{2m\left|E_{loc}\right|}/\hbar$, "+","-" correspond to parallel and antiparallel ion spin configurations respectively. For the large distance between the ions $\kappa R >> 1$:

$$E_{loc}\left(\kappa R -> \infty\right) = -\frac{\left(JIs\right)^2 m}{2\hbar^2}.$$

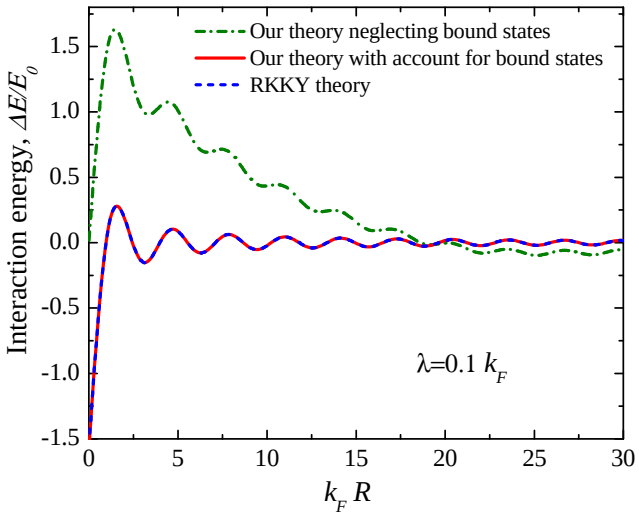

Figure 6.1: Indirect exchange energy in 1D case. The exact calculation with and without account of the bound states compared to the RKKY theory

Always one such level exists for antiparallel ions spins configuration, for the parallel configuration there are no solutions for the repulsive double-delta potential and two bound states for the attractive double-delta potential. Fig.6.1 shows the indirect interaction energy calculated according to (6.4) and the result of the RKKY theory in 1D [Aristov (1997)]:

$$E_{RKKY} = E_0 \,\mathrm{si}(2k_F R),$$

where $E_0 = 4j^2\hbar^2/\pi m$, $\mathrm{si}(x)$ is the sine integral. The exchange constant is taken such as $j/k_F = 0.1$. In order to show the role of the localized states we also plotted the part of interaction energy associated with delocalized states, i.e. neglecting ΔE_{loc} (Fig.6.1). As clearly seen from the figure at $R < 1/j$ it is of key importance to take into account the overlapping of the localized states which strongly contribute to the indirect exchange. At large distance between the ions the interaction is only due to the plane waves and one gets the result of the RKKY theory. Interestingly, if we do take into account the localized states the exact solution perfectly matches the RKKY perturbation theory. This agreement remains very good up to $j/k_F = 1$ which is actually beyond the perturbation theory criteria.

6.4 Indirect exchange interaction in 2D

To solve the 2D case it is more convenient to write (6.3) in the momentum representation:

$$\left(k^2 - {k_E}^2\right)\Psi\left(\mathbf{k}\right) + \\ + 2\lambda_1 e^{-i\mathbf{k}\mathbf{R_1}}\Psi\left(\mathbf{R_1}\right) + 2\lambda_2 e^{-i\mathbf{k}\mathbf{R}_2}\Psi\left(\mathbf{R}_2\right) = 0, \tag{6.6}$$

where

$$\lambda_{1,2} = JI_{1,2}s\frac{m}{\hbar^2},\ k_E = \frac{\sqrt{2mE}}{\hbar^2}. \tag{6.7}$$

Equation (6.6) gives $\Psi(\mathbf{k})$ only for $k \neq k_E$. In order to get the solution for arbitrary it is fruitful to apply the very same technique as described in Sec. 2.2 (see formula (2.24)):

$$\Psi(\mathbf{k}) = \left(2\lambda_1 e^{-i\mathbf{k}\mathbf{R_1}}\Psi(\mathbf{R_1}) + 2\lambda_2 e^{-i\mathbf{k}\mathbf{R}_2}\Psi(\mathbf{R}_2)\right) \times \left[P\frac{1}{k_E^2 - k^2} + Z\delta\left(k_E^2 - k^2\right)\right], \tag{6.8}$$

where P denotes the principal value, $\varepsilon \equiv \varepsilon_\lambda$, Z is an unknown function of k_E to be determined later. After inverse Fourier transformation and integration over the polar angle φ in k–space we obtain:

$$\Psi(\mathbf{r}) = \frac{1}{2}\lambda_1\left[\frac{Z}{\pi}J_0(k_E\rho_1) + Y_0(k_E\rho_1)\right]\Psi(\mathbf{R_1}) + \frac{1}{2}\lambda_2\left[\frac{Z}{\pi}J_0(k_E\rho_2) + Y_0(k_E\rho_2)\right]\Psi(\mathbf{R}_2), \tag{6.9}$$

where J_0, Y_0 – Bessel and Neumann functions of zeroth order, $\rho_{1,2} = |\mathbf{r} - \mathbf{R_{1,2}}|$. Substituting $\mathbf{r} = \mathbf{R_{1,2}}$ yields:

$$\begin{aligned}\Psi(\mathbf{R_1}) &= \lambda_1\Psi(\mathbf{R_1})(F + ZT) + \lambda_2(f + Zt)\Psi(\mathbf{R}_2)\\ \Psi(\mathbf{R}_2) &= \lambda_1\Psi(\mathbf{R_1})(f + Zt) + \lambda_2(F + ZT)\Psi(\mathbf{R}_2),\end{aligned} \tag{6.10}$$

where

$$\begin{aligned}F &= \frac{1}{\pi}P\int_0^\infty \frac{1}{k_E^2 - k^2}kdk \quad T = \frac{1}{2\pi}\\ f &= \frac{1}{\pi}P\int_0^\infty \frac{J_0(kR)}{k_E^2 - k^2}kdk \quad t = \frac{1}{2\pi}J_0(k_E R)\\ R &= |\mathbf{R_1} - \mathbf{R_2}|.\end{aligned} \tag{6.11}$$

The quantity F diverges logarithmically resembling the known issue of dimension deficiency for the delta-potential in 2D [Nyeo (2000); Cavalcanti (1999)]. The issue is resolved by renormalization:

$$\frac{1}{\lambda_{1,2}} \to \frac{1}{\lambda_{1,2}} + F. \tag{6.12}$$

From (6.10) with (6.12) requiring $\Psi(\mathbf{R}_{1,2}) \neq 0$ we get the equation for Z:

$$(\lambda_1 ZT - 1)(\lambda_2 ZT - 1) = \lambda_1\lambda_2(f + Zt)^2. \tag{6.13}$$

Each of the two roots $Z_{1,2}$ determines the solutions $\Psi_{Z_{1,2}}(\mathbf{r}$ and the general solution is a linear combination of the two:

$$\Psi(\mathbf{r}) = A\Psi_{Z_1}(\mathbf{r}) + B\Psi_{Z_2}(\mathbf{r}) \tag{6.14}$$

Let us put the system in a big cylindrical box of radius L and apply the boundary conditions $\Psi(L, \varphi) = 0$. Using the asymptotic of $\Psi(\mathbf{r})$ from (6.9)-(6.14) we obtain:

$$\Psi(L,\varphi) = \begin{bmatrix} AC_1^+\cos(k_E L + \delta_1) \\ +BC_2^+\cos(k_E L + \delta_2)\end{bmatrix}\cos(k_E R\cos\varphi) + \begin{bmatrix} AC_1^-\sin(k_E L + \delta_1) \\ +BC_2^-\sin(k_E L + \delta_2)\end{bmatrix}\sin(k_E R\cos\varphi), \tag{6.15}$$

where

$$\tan\delta_{1,2} = -\frac{\pi}{Z_{1,2}},$$
$$C^{\pm}_{1,2} = \frac{\lambda_1\Psi_{Z_{1,2}}(\mathbf{R_1}) \pm \lambda_2\Psi_{Z_{1,2}}(\mathbf{R}_2)}{2\sin\delta_{1,2}}. \tag{6.16}$$

Imposing the zero boundary condition yields:

$$\left[\begin{array}{l} k_E = \dfrac{\pi n}{L} + \dfrac{\Delta_1}{L} \\ k_E = \dfrac{\pi n}{L} + \dfrac{\Delta_2}{L} \end{array}\right.$$

Here $\Delta_{1,2}$ are functions of $\lambda_{1,2}, f, T, t$ Assuming zero temperature and Fermi distribution of the electrons the total energy shift for the system is obtained as described in Sec. 2.3 (see (2.42):

$$\Delta E = \frac{1}{\pi}\int_0^{E_F}\left[\Delta_1(E) + \Delta_2(E)\right]dE, \tag{6.17}$$

where E_F is the Fermi level. The phase shifts $\Delta_{1,2}$ depend on $\lambda_{1,2}$, thus ΔE is different for different configurations of the ions and electrons spins. The exchange energy is given by:

$$E_{ex} = \left(\Delta E_{\uparrow\uparrow -} + \Delta E_{\uparrow\uparrow +}\right) - \left(\Delta E_{\uparrow\downarrow -} + \Delta E_{\uparrow\downarrow +}\right). \tag{6.18}$$

Here in the indices the arrows denote ion spin projection and the signs stand for the electron spin projection. Substituting (6.17) into (6.18) we finally arrive at:

$$E_{ex} = \frac{1}{\pi}\int_0^{E_F}\arctan\left[2\zeta(j)\,Y_0(k_E R)\,J_0(k_E R)\right]dE, \tag{6.19}$$

where $\zeta(j)$ is known function,

$$\zeta(j) = j^2 - \frac{j^4}{2} + O\left(j^6\right)$$
$$j = JI|s|\frac{m}{\hbar^2}. \tag{6.20}$$

For $j \ll 1$ from (6.19) follows the known result of $2D$ RKKY theory [Aristov (1997)]:

$$E_{RKKY} = \frac{{k_F}^2(JIs)^2}{\pi m\hbar^2}\chi(R),$$
$$\chi(R) = J_0(k_F R)\,Y_0(k_F R) + J_1(k_F R)\,Y_1(k_F R). \tag{6.21}$$

6.5 Resonant indirect exchange interaction

Let us now address the problem of indirect exchange interaction mediated by a free carriers gas separated by a tunnel barrier from the paramagnetic ions. Because the spin-spin interaction operator

contains the delta-function (6.1), its matrix elements are proportional to the product of basis wave functions amplitudes at the ions site. For a wavefunction amplitude decaying inside the tunnel barrier one would simply expect a suppression of the indirect exchange interaction by a factor of $exp(-4\kappa d)$, where $\kappa = \sqrt{2mU_0}/\hbar$, U_0 and d are the barrier height and width respectively. However, if the ion has its own spin-independent attracting potential forming a bound state, the particle form the conducting layer with the same energy can effectively tunnel to the ions bound state. In terms of quantum mechanics it means that for the energy coinciding with that of the bound state the single-particle stationary wave function has an enhanced amplitude at the ion site due to the resonant tunneling. Let us consider two magnetic ions located at the same distance d from the the quantum well and coupled with the 2D electron gas of the QW through a tunnel barrier. The distance R between the ions is assumed to be large enough so that they do not interact directly. The ions are assumed to have a bound state which may lie within the energy range of the occupied states of the 2D gas. In this case the resonant tunneling can occur between the delocalized state of the QW 2D subband and the ion bound state. The hybridization of these is treated as fully discussed in Ch. 2, Sec. 2.2 and Ch. 5, Sec. 5.2, Sec. 5.4. However, in this chapter it needs to be extended for the case of two bound states being hybridized with the continuum. We consider the total Hamiltonian consisting of three terms:

$$H = H_0 + H_T + H_J, \tag{6.22}$$

where H_0 – the Hamiltonian of the system without tunnel coupling and spin-spin interaction, H_T – the tunnelling term, H_J – the exchange interaction term (6.1). In the second quantization representation:

$$\begin{aligned} H_0 &= \varepsilon_0 a_1^+ a_1 + \varepsilon_0 a_2^+ a_2 + \int \varepsilon_\lambda c_\lambda^+ c_\lambda d\lambda, \\ H_T &= \int \left(t_{1\lambda} a_1^+ c_\lambda + t_{2\lambda} a_2^+ c_\lambda + h.c. \right) d\lambda, \\ H_J &= JA \left(I_1 s a_1^+ a_1 + I_2 s a_2^+ a_2 \right), \end{aligned} \tag{6.23}$$

where $a_{1,2}^+, a_{1,2}$ – the creation and annihilation operators for the bound states at the impurity ions $1, 2$, characterized by the same energy ε_0 and localized wavefunctions ψ_1, ψ_2. c_λ^+, c_λ – the creation and annihilation operators for a continuum state characterized by the quantum number(s) λ, having the energy ε_λ and the wavefunction φ_λ, energy is measured from the QW size quantization level,

$$A = |\psi_1(\mathbf{R_1})|^2 = |\psi_2(\mathbf{R}_2)|^2. \tag{6.24}$$

The tunneling matrix element further referred as tunneling parameters are given by (2.15):

$$t_{(1,2),\lambda} = -\frac{\hbar^2}{2m_\perp} \int_{\Omega_S} dS \left(\varphi_\lambda \frac{d}{dz} \psi_{1,2}^* - \psi_{1,2}^* \frac{d}{dz} \varphi_\lambda \right), \tag{6.25}$$

where integration is over the plane Ω_S, parallel to the QW plane and passing through the ions centers, $m_\perp$ is the effective mass in the direction perpendicular to the QW plane. Let z-axis be normal to the QW plane ($z = 0$ corresponds to the QW boundary), x-axis passes through the ions centers so that their coordinates are:

$$\mathbf{R}_1 = (-R/2, 0, d); \;\; \mathbf{R}_2 = (R/2, 0, d).$$

We assume that the localized wavefunctions ψ_1, ψ_2 do not overlap, thus their particular form is not important. It is convenient to take them in the form:

$$\psi_{1,2} = \left(\frac{2}{\pi r_0^2}\right)^{3/4} e^{-\left(\frac{x \pm R/2}{r_0}\right)^2} e^{-\left(\frac{y}{r_0}\right)^2} e^{-\left(\frac{z-d}{r_0}\right)^2}, \tag{6.26}$$

where r_0 is the localization radius. The continuum wavefunctions are taken as follows:

$$\varphi_{\mathbf{k}} = \eta(z)\, e^{i\mathbf{k}\rho} \tag{6.27}$$

Here $\mathbf{k}$ is the in-plane wavevector, ρ – 2D in-plane radius-vector, $\eta(z)$ is the envelope function of size quantization along z. Outside of the QW:

$$\eta(z) = \zeta a^{-1/2} e^{-qz}, \tag{6.28}$$

where $q = \sqrt{2m_\perp U_0}/\hbar^2$, U_0 is the binding energy of the bound state, which at the same time determines the height of the potential barrier between impurities and the QW [**Publication 6**], a is the QW width, ζ is a dimensionless parameter weakly depending on q and a. For a realistic rectangular QW $\zeta \approx 0.5$. The calculation of (6.25) using (6.26) (assuming $r_0 \ll k^{-1}$) and (6.27) yields :

$$t_{1,2}(k) = \sqrt{\frac{\hbar^2 T}{2\pi m}} e^{i\mathbf{k}\mathbf{R_{1,2}}}, \tag{6.29}$$

where T – the energy parameter for the tunneling:

$$T = (2\pi)^{3/2} \zeta^2 \frac{r_0 m}{a m_\perp} U_0 e^{-2qd}, \tag{6.30}$$

m – the effective mass along the QW plane.

The hybridized eigenfunctions Ψ of the whole system are expanded over the bound states and the delocalized states in the form (see Sec. 2.2):

$$\Psi = \nu_1\psi_1 + \nu_2\psi_2 + \Phi, \quad \Phi = \int \nu_{\mathbf{k}} \varphi_{\mathbf{k}} d\mathbf{k} \tag{6.31}$$

Plugging (6.31) into the stationary Schrödinger equation $H\Psi = E\Psi$ with Hamiltonian (6.22) analogously to (2.23) we get:

$$\begin{aligned}
&\nu_1(\varepsilon_0 - E + \lambda_1) + \int t_{1\mathbf{k}}\nu_{\mathbf{k}} d\mathbf{k} = 0 \\
&\nu_2(\varepsilon_0 - E + \lambda_2) + \int t_{2\mathbf{k}}\nu_{\mathbf{k}} d\mathbf{k} = 0 \\
&\nu_{\mathbf{k}}(\varepsilon - E) + \nu_1 t^*_{1\mathbf{k}} + \nu_2 t^*_{2\mathbf{k}} = 0,
\end{aligned} \tag{6.32}$$

where

$$\lambda_{1,2} = JAI_{1,2}s, \qquad \varepsilon = \frac{\hbar^2 k^2}{2m}$$

$\nu_{\mathbf{k}}$ is expressed from the last equation of (6.32) as follows:

$$\nu_{\mathbf{k}} = P\frac{\nu_1 t^*_{1\mathbf{k}} + \nu_2 t^*_{2\mathbf{k}}}{E - \varepsilon} + Z\left(\nu_1 t^*_{1\mathbf{k}} + \nu_2 t^*_{2\mathbf{k}}\right)\delta(E - \varepsilon), \tag{6.33}$$

where P denotes principal value and $Z(E)$ is to be determined. Plugging (6.33) into (6.32) yields:

$$\begin{aligned}&\nu_1\left(\lambda_1+F_{11}+ZT_{11}-E'\right)+\nu_2\left(F_{21}+ZT_{21}\right)=0\\&\nu_1\left(F_{12}+ZT_{12}\right)+\nu_2\left(\lambda_2+F_{22}+ZT_{22}-E'\right)=0,\end{aligned}\tag{6.34}$$

where

$$\begin{aligned}&F_{\alpha\beta}=P\int\frac{t^*_{\alpha\lambda}t_{\beta\lambda}}{E-\varepsilon}d\lambda,\quad T_{\alpha\beta}=\int t^*_{\alpha\lambda}t_{\beta\lambda}\delta\left(\varepsilon-E\right)d\lambda,\\&E'=E-\varepsilon_0,\quad \alpha,\beta=1,2.\end{aligned}\tag{6.35}$$

Plugging (6.29) into (6.35) we get:

$$\begin{aligned}&T_{11}=T_{12}=T,\ \ T_{12}=T_{21}\equiv t=TJ_0\left(k_ER\right),\\&F_{11}=F_{22}\equiv F,\ \ F_{12}=F_{21}\equiv f=\pi TY_0\left(k_ER\right),\end{aligned}\tag{6.36}$$

where $k_E=\sqrt{2mE}/\hbar$. F represents the shift of the resonance position with respect to ε_0 and plays the same role as in (6.11). It can be explicitly evaluated given more accurate expression than (6.29) taking into account $k\sim r_0^{-1}$ to avoid the divergence. This is, in fact, the same as the renormalization procedure (6.12) for the true delta-potential. The finite F still contains extra degree of the tunneling parameter T, does not depend on R and can be neglected in the lowest order in T. From (6.34) follows the equation for Z:

$$\left(ZT-E'+\lambda_1\right)\left(ZT-E'+\lambda_2\right)=\left(f+Zt\right)^2.\tag{6.37}$$

With use of (6.31) and (6.33) the delocalized part of the hybridized wavefunction is given by:

$$\Phi\left(E\right)=\pi\sqrt{\frac{2\pi mT}{\hbar^2}}\left[\begin{array}{c}\nu_1\left(\dfrac{Z}{\pi}J_0\left(k\rho_1\right)+Y_0\left(k\rho_1\right)\right)\\+\nu_2\left(\dfrac{Z}{\pi}J_0\left(k\rho_2\right)+Y_0\left(k\rho_2\right)\right)\end{array}\right]\tag{6.38}$$

Proceeding analogously to (6.14)-(6.19) we, however, keep only the leading order in the tunneling parameter which appears to be T^2. Then we end up with the exhcnage energy for the tunneling case:

$$E_{ex}=\frac{1}{\pi}\int\limits_0^{E_F}\arctan\left[\frac{8\pi^2T^2j^2J_0\left(kR\right)Y_0\left(kR\right)}{\left(\left(\varepsilon-\varepsilon_0\right)^2-j^2\right)^2}\right]d\varepsilon,\tag{6.39}$$

where $j=|JAIs|$. The expression (6.39) is somewhat similar to (6.19), but now the argument of arctangent in (6.39) has poles at $\varepsilon=\varepsilon_0\pm j$ and the result strongly depends on whether these resonances are within the range of integration $\varepsilon\in[0,E_F]$. If they are, from the width of the resonances the amplitude of the exchange interaction energy is estimated as:

$$E_{res}\sim\sqrt{Tj},\tag{6.40}$$

while the period of the oscillations is $\hbar/\sqrt{2m\varepsilon_0}$. The limiting non-resonant case occurs if $\varepsilon_0\gg E_F$, $j\ll E_F$. The integration (6.39) then results in:

$$\begin{aligned}&E_{nr}=\frac{8\pi T^2j^2E_F}{\varepsilon_0^4}\chi\left(R\right),\\&\chi\left(R\right)=J_0\left(k_FR\right)Y_0\left(k_FR\right)+J_1\left(k_FR\right)Y_1\left(k_FR\right).\end{aligned}\tag{6.41}$$

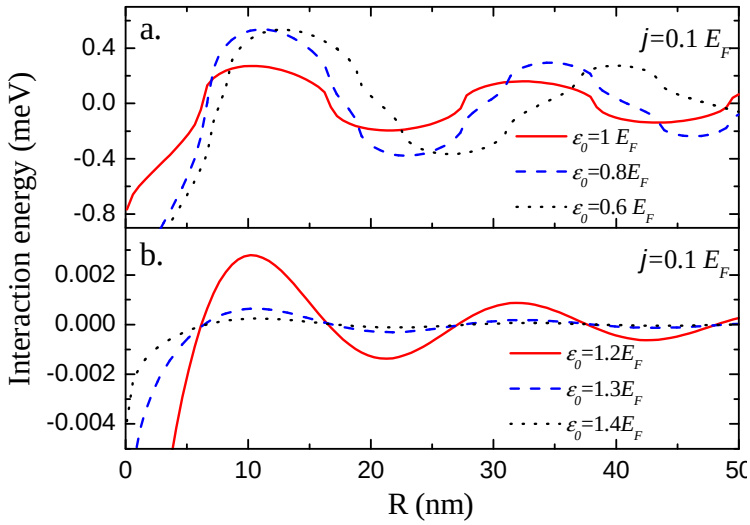

Figure 6.2: Indirect exchange interaction energy vs distance between ions in the resonant (a) and non-resonant (b) case

The condition $j \ll E_F$ allows for the perturbation theory thus the expression (6.41) is what one would expect from the conventional RKKY approach. The functional dependence on R is exactly the same as for 2D RKKY interaction without tunneling [Aristov (1997)] and the prefactor accounts for the particular model we have used to describe the tunneling and the bound impurity state. The interaction energy amplitude for the resonance case appears to be substantially higher than for the non-resonant one. Assuming for both cases $\varepsilon_0 \sim E_F$ we can roughly estimate the amplification:

$$\gamma \equiv \frac{E_{res}}{E_{nr}} \sim \frac{\varepsilon_0^4}{8\pi T^{3/2} j^{3/2} E_F}. \tag{6.42}$$

For an estimate we take the parameters based on InGaAs-based heterostructures studied in [Zaitsev et al. (2010); Korenev et al. (2012); Tripathi et al. (2011)]. For $T \sim 0.01E_F$, $j \sim 0.1E_F$ γ can be as high as 3 orders of magnitude. Fig.6.2 shows the results of the numerical calculation according to (6.39) for different positions of the bound state energy ε_0 related to the Fermi level E_F. The domain of applicability starts from $R > r_0$ (for real structures $r_0 \sim 1$ nm). We take $m = 0.1m_0$ (m_0 – free electron mass), $E_F = 10$ meV, $j = 0.1E_F$. The upper panel (Fig.6.2a) represents the resonant case. For all the curves the resonances are within the integration range. In the case of $\varepsilon_0 = E_F$ one of the two resonances goes outside of the range and the exchange energy is somewhat decreased. For the nonresonant case shown in (Fig.6.2b) the argument of arctangent in (6.39) has no poles and the amplitude of the oscillations is dramatically decreased by two orders of magnitude. Fig.6.3 shows the dependence of the exchange energy on j. While for the non-resonant case it resembles the expected dependence $E_{ex} \sim j^2$, for the resonant case the interaction energy may even decrease with increase of j when one of the resonances leaves the range $[0, E_F]$. This very case occurs for $j = 0.3E_F$ in Fig.6.3a. The formula (6.39) has another non-resonant limiting case for $j \gg E_F, j \gg \varepsilon_0$. However, its applicability in this case remains questionable because with $j >> E_F$ the ions spins dynamics (neglected in our model) may be essential. It seems, however,

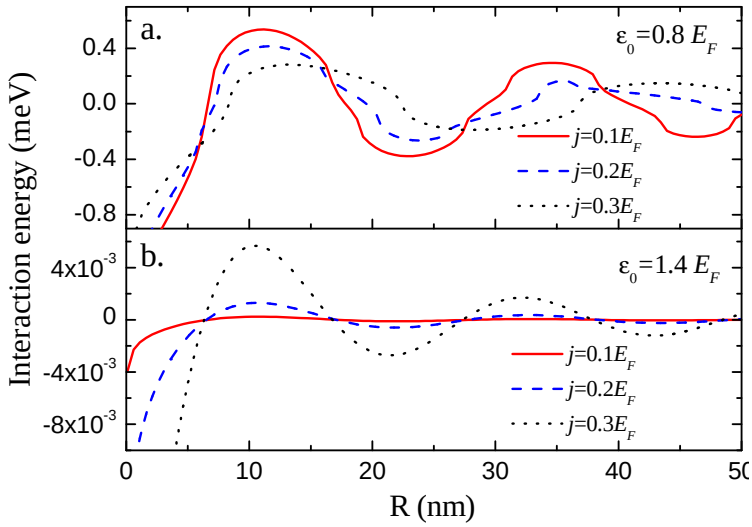

Figure 6.3: Indirect exchange energy vs distance between ions for various j in the resonant (a) non-resonant (b) case.

the small tunneling parameter T allows for the case when the exchange constant is of the order of E_F while the ions spins dynamics yet does not play a role. This issue requires further investigation.

6.6 Summary of the results

We performed indirect exchange energy calculation following the method described in Sec. (2.3), i.e. by analyzing the quantized spectra of the free carriers interacting with spin-dependent impurity potential. This approach applied to the standard indirect exchange problem in 1D and 2D is in agreement with the RKKY theory in the weak interaction limit and shows the role of the localized states. The method was further applied to the case of the indirect exchange interaction mediated by a 2D free carriers gas separated by a tunnel barrier from the magnetic ions. This allowed for taking into account the attracting potential of the impurity and analyzing the case when it possesses a bound state. If the bound state energy lies within the free carriers energy range they get effectively hybridized. Due to the resonance tunneling phenomenon this hybridizations remains effective even when the free carriers gas is separated from the impurity ions by a tunnel barrier. In this case the indirect exchange interaction appears to be much stronger than expected from the RKKY approach. A number of experimental observations [Aronzon et al. (2013)] indicate that this new mechanism of ferromagnetism in diluted magnetic semiconductor heterosructures is comparable or exceeds that of the Mn delta-layer itself.

CHAPTER VII

Conclusions

The main purpose of this work was to advance the theory and to improve the knowledge and understanding of the physics of a number of resonant tunneling effects in semiconductor nanostructures. The main achievements of the studies included in this thesis are listed below.

A manifestation of spin-orbit interaction in the tunneling between two 2D electron layers is considered. General expression is obtained for the tunneling current with account of Rashba and Dresselhaus types of spin-orbit interaction and elastic scattering. It is demonstrated that the tunneling conductance is very sensitive to relation between Rashba and Dresselhaus contributions and opens possibility to determine the spin-orbit interaction parameters and electron quantum lifetime in direct tunneling experiments with no external magnetic field applied.

A microscopic mechanism of hole injection from metallic electrode into organic molecular solid (OMS) in high electric field is proposed. The consideration is focused on the case when the molecules ionization energy exceeds work function of the metal. It is shown that the main contribution to the injection current comes from direct isoenergetic transitions from localized states in OMS to empty states in the metal. Strong dependence of the injection current on applied voltage originates from variation of the number of empty states available in the metal, while the distortion of the interface barrier does not play the key role.

The theory of tunnel coupling between an impurity bound state and the 2D delocalized states in the quantum well (QW) is developed. An effect of this interaction on the interband optical transitions in the QW is analyzed. For such transitions the tunnel coupling leads to the drop of the luminescence spectral density at the frequency corresponding to the bound state energy level. This modification of the spectra leads to an integral circular polarization of the light emitted from the QW provided the bound hole state is split in the projection of the hole angular momentum. The results are discussed regarding the series of experiments on the GaAs structures with a δ-Mn layer.

A new mechanism of ferromagnetism in diluted magnetic semiconductor heterosructures is considered, namely the resonant enhancement of indirect exchange interaction between paramagnetic centers via a spatially separated conducting channel. The underlying physical model is similar to the Ruderman-Kittel-Kasuya-Yosida (RKKY) interaction; however, an important difference relevant to the low-dimensional structures is a resonant hybridization of a bound state at the paramagnetic ion with the continuum of delocalized states in the conducting channel. An approach is developed, which unlike RKKY is not based on the perturbation theory and demonstrates that the resonant hy-

bridization leads to a strong enhancement of the indirect exchange. This finding is discussed in the context of the known experimental data supporting the phenomenon.

The contents of the thesis has been published in 8 publications in the journals Physical Review B, Applied Physics Letters, Low Temperature Physics and Physica Status Solidi (a), it has been presented at various international conferences including International Conferences on Physics of Semiconductors, European Physical Society Conference, International Conference on Nanoscale Magnetism and Applications, International Conference on Physics and Applications of Spin-related Phenomena in Semiconductors, All-Russian Conferences on Physics of Semiconduuctors, and others.

BIBLIOGRAPHY

Agrawal, R., Kumar, P., Ghosh, S., Mahapatro, A. K., 2008. Thickness dependence of space charge limited current and injection limited current in organic molecular semiconductors. Appl. Phys. Lett. 93, 073311.

Aleshkin, V. Y., Gavrilenko, L. V., Odnoblyudov, M. A., Yassievich, I. N., 2008. Impurity resonance states in semiconductors. Semiconductors 42, 880–904.

Anderson, P. W., 1961. Localized magnetic states in metals. Phys. Rev. 124, 41.

Aristov, D. N., 1997. Indirect RKKY interaction in any dimensionality. Phys. Rev. B 55, 8064–8066.

Arkhipov, V. I., Wolf, U., Bässler, H., 1999. Current injection from a metal to a disordered hopping system. ii. comparison between analytic theory and simulation. Phys. Rev. B. 59, 7514.

Aronzon, B., Davydov, A., Goiran, M., Raquet, B., Lashkul, A., Lähderanta, E., 2013. Quantum, normal and anomalous hall effect in 2d ferromagnetic structures: GaAs/InGaAs/GaAs quantum well with remote Mn delta-layer. Journal of Physics: Conference Series 456, 012001.

Aronzon, B. A., Pankov, M. A., Rylkov, V. V., Meilikhov, E. Z., Lagutin, A. S., Pashaev, E. M., Chuev, M. A., Kvardakov, V. V., Likhachev, I. A., Vihrova, O. V., Lashkul, A. V., Lähderanta, E., Vedeneev, A. S., Kervalishvili, P., 2010. Ferromagnetism of low-dimensional Mn-doped III-V semiconductor structures in the vicinity of the insulator-metal transition. J. Appl. Phys. 107 (2), 023905.

Averkiev, N. S., Il'inskii, S. Y., 1994. Spin ordering of carriers localized at two deep centers in cubic semiconductors. Phys. Solid. State 36, 278.

Bardeen, J., 1961. Tunnelling from a many-particle point of view. Phys. Rev. Lett. 6, 57–59.

Bässler, H., 1993. Charge transport in disordered organic photoconductors a monte carlo simulation study. Phys. Stat. Sol. (b) 175, 15.

Blom, A., Odnoblyudov, M. A., Yassievich, I. N., Chao, K. A., 2002. Resonant states induced by impurities in heterostructures. Phys. Rev. B 65 (15), 155302.

Cavalcanti, R. M., 1999. Exact Green's functions for delta-function potentials and renormalization in quantum mechanics. Rev.Bras.Ens.Fis. 21, 336.

Chynoweth, A. G., 1960. Internal field emission. in Gibson, A. F. (Ed.), Progress in Semiconductors 4, 95.

Dorokhin, M. V., Zaitsev, S. V., Brichkin, A. S., Vikhrova, O. V., Danilov, Y. A., Zvonkov, B. N., Kulakovskii, V. D., Prokof'eva, M. M., Sholina, A. E., 2010. Influence of delta Mn doping parameters of the GaAs barrier on circularly polarized luminescence of GaAs/InGaAs heterostructures. Physics of the Solid State 52, 2291–2296.

Erickson, R. P., Hathaway, K. B., Cullen, J. R., 1993. Mechanism for non-Heisenberg exchange coupling between ferromagnetic layers. Phys. Rev. B 47, 2626–2635.

Fano, U., 1961. Effects of configuration interaction on intensities and phase shifts. Phys. Rev. 124 (6), 1866–1878.

Forrest, S. R., 2004. The path to ubiquitous and low-cost organic electronic appliances on plastic. Nature 428, 911.

Ganzorig, C., Sakomura, M., Ueda, K., Fujihira, M., 2006. Current-voltage behavior in hole-only single-carrier devices with self-assembling dipole molecules on indium tin oxide anodes. Appl. Phys. Let. 89, 263501.

Harrison, P., 2006. Quantum Wells, Wires and Dots: Theoretical and Computational Physics of Semiconductor Nanostructures, Second Edition. John Wiley and Sons, New York.

Hsiao, C.-C., Chang, C.-H., Jen, T.-H., Hung, M.-C., Chen, S.-A., 2006. High-efficiency polymer light-emitting diodes based on poly[2-methoxy-5-(2-ethylhexyloxy)-1,4-phenylene vinylene] with plasma-polymerized CHF3-modified indium tin oxide as an anode. Appl. Phys. Let. 88, 033512.

Jungwirth, T., Sinova, J., Masek, J., Kucera, J., MacDonald, A. H., 2006. Theory of ferromagnetic (III, Mn) V semiconductors. Rev. Mod. Phys. 78, 809–864.

Korenev, V. A., Akimov, I. A., Zaitsev, S. V., Sapega, V. F., Langer, L., Yakovlev, D. R., Danilov, Y. A., Bayer, M., 2012. Dynamic spin polarization by orientation-dependent separation in a ferromagnet-semiconductor hybrid. Nat. Commun. 3, 959.

Lang, P., Nordström, L., Zeller, R., Dederichs, P. H., 1993. *Ab initio* calculations of the exchange coupling of Fe and Co monolayers in Cu. Phys. Rev. Lett. 71, 1927–1930.

Liu, D., Kao, K. C., 1991. High-field hole injection, conduction, and breakdown in polyethylene films fabricated by plasma polymerization. J. Appl. Phys. 69, 2489.

Lucovsky, G., 1965. On the photoionization of deep impurity centers in semiconductors. Sol.St.Comm 3, 299–302.

Miroshnichenko, A. E., Flach, S., Kivshar, Y. S., 2010. Fano resonances in nanoscale structures. Rev. Mod. Phys. 82 (3), 2257–2298.

Mueller, E., 2002. Scattering tutorial.
URL `http://people.ccmr.cornell.edu/~emueller/scatter.pdf`

Murphy, S. Q., Eisenstein, J. P., Pfeiffer, L. N., West, K. W., 1995. Lifetime of two-dimensional electrons measured by tunneling spectroscopy. Phys. Rev. B 52, 14825.

Nishitani, Y., Chiba, D., Endo, M., Sawicki, M., Matsukara, F., Dietl, T., Ohno, H., 2010. Curie temperature versus hole concentration in field-effect structures of $Ga_{1-x}Mn_xAs$. Phys. Rev. B 81, 045208.

Nyeo, S.-L., 2000. Regularization methods for delta-function potential in two-dimensional quantum mechanics. American Journal of Physics 68 (6), 571–575.

Okulov, V. I., Lonchakov, A. T., Govorkova, T. E., Okulova, K. A., Podgornykh, S. M., Paranchich, L. D., Paranchich, S. Y., 2011. Anomalous low-temperature contribution to the heat capacity from hybridized electronic states on transition element impurities. Low Temperature Physics 37 (3), 220–225.

Popov, V. G., Dubrovskii, Y. V., Khanin, Y. N., Vdovin, E. E., Maude, D. K., Portal, J.-C., Andersson, T. G., Thordson, J., 1998. Semiconductors 35, 539.

Raichev, O. E., Debray, P., 2003. Tunneling spectroscopy of spin-split states in quantum wells. Phys. Rev. B 67, 155304.

Ruderman, M. A., Kittel, C., 1954. Indirect exchange coupling of nuclear magnetic moments by conduction electrons. Phys. Rev. 96, 99–102.

Rupprecht, B., Krenner, W., Wurstbauer, U., Heyn, C., T., T. W., Wilde, M. A., Wegscheider, W., Grundler, D., 2010. Magnetism in a Mn modulation-doped InAs/InGaAs heterostructure with a two-dimensional hole system. J. Appl. Phys. 107, 093711.

Schneider, J., Kaufmann, U., Wilkening, W., Baeumler, M., Köhl, F., 1987. Electronic structure of the neutral manganese acceptor in gallium arsenide. Phys. Rev. Lett. 59, 240–243.

Stiles, M. D., 1993. Exchange coupling in magnetic heterostructures. Phys. Rev. B 48, 7238–7258.

Suvorov, A. L., Trebukhovskii, V. V., 1972. Usp. Fiz. Nauk 107, 657, in Russian.

Tripathi, V., Dhochak, K., Aronzon, B. A., Rylkov, V. V., Davydov, A. B., Raquet, B., Goiran, M., Kugel, K. I., Aug 2011. Charge inhomogeneities and transport in semiconductor heterostructures with a Mn delta-layer. Phys. Rev. B 84, 075305.

Turner, N., Nicholls, J. T., Linfield, E. H., Brown, K. M., Jones, G. A. C., Ritchie, D. A., 1996. Tunneling between parallel two-dimensional electron gases. Phys. Rev. B 54, 10614.

van Woudenbergh, T., Blom, P. W. M., Vissenberg, M. C. J. M., Huiberts, J. N., 2001. Temperature dependence of the charge injection in poly-dialkoxy-p-phenylene vinylene. Appl. Phys. Let. 79, 1697.

Vasko, F. T., Balev, O. G., Studart, N., 2000. Inhomogeneous broadening of tunneling conductance in double quantum wells. Phys. Rev. B 62, 12940.

Yan, P., Zhou, Y., Yoshimura, N., 2000. DC conduction in polyethylene films under high electric field after annealing. Jpn. J. Appl. Phys., Part 1 39, 3492.

Zaitsev, S. V., 2012. Magneto-optics of heterostructures with an InGaAs/GaAs quantum well and a ferromagnetic delta-layer of Mn. Low Temperature Physics 38 (5), 399–412.

Zaitsev, S. V., Dorokhin, M. V., Brichkin, A. S., Vikhrova, O. V., Danilov, Y. A., Zvonkov, B. N., Kulakovskii, V. D., 2010. Ferromagnetic effect of a Mn delta layer in the GaAs barrier on the spin polarization of carriers in an InGaAs/GaAs quantum well. JETP Letters 90, 658–662.

Zakrevskii, V. A., Sudar, N. T., 1992. Sov. Phys. Solid State 34, 1727.

Zheng, L., MacDonald, A. H., 1993. Tunneling conductance between parallel two-dimensional electron systems. Phys. Rev. B 47, 10619.

Zyuzin, V. A., Mishchenko, E. G., Raikh, M. E., 2006. Tunneling between two-dimensional electron layers with correlated disorder: Anomalous sensitivity to spin-orbit coupling. Phys. Rev. B 74, 205322.

PART II: PUBLICATIONS

PUBL. 1

I. V. ROZHANSKY and N. S. AVERKIEV, MANIFESTATION OF SPIN-ORBIT INTERACTION IN TUNNELING BETWEEN TWO-DIMENSIONAL ELECTRON LAYERS, *Physical Review B*, **77**, 115309, 2008.

PHYSICAL REVIEW B **77**, 115309 (2008)

Manifestation of spin-orbit interaction in tunneling between two-dimensional electron layers

I. V. Rozhansky* and N. S. Averkiev
A. F. Ioffe Physico-Technical Institute, Russian Academy of Sciences, 194021 St. Petersburg, Russia
(Received 16 October 2007; revised manuscript received 29 December 2007; published 10 March 2008)

An influence of spin-orbit interaction on the tunneling between two two-dimensional electron layers is considered. Particular attention is addressed to the relation between the contribution of Rashba and Dresselhaus types. It is shown that without scattering of the electrons, the tunneling conductance can either exhibit resonances at certain voltage values or be substantially suppressed over the whole voltage range. The dependence of the conductance on voltage turns out to be very sensitive to the relation between Rashba and Dresselhaus contributions even in the absence of magnetic field. The elastic scattering broadens the resonances in the first case and restores the conductance to a larger magnitude in the latter one. These effects open the possibility to determine the parameters of spin-orbit interaction and electron scattering time in tunneling experiments with no necessity of external magnetic field.

DOI: 10.1103/PhysRevB.77.115309 PACS number(s): 73.40.Gk, 73.63.Hs, 71.70.Ej

I. INTRODUCTION

Spin-orbit interaction (SOI) plays an important role in the widely studied spin-related effects and spintronic devices. In the latter, it can be either directly utilized to create spatial separation of the spin-polarized charge carriers or indirectly influence the device performance through spin-decoherence time. In two-dimensional (2D) structures, two kinds of SOI are known to be of the most importance, namely, Rashba and Dresselhaus mechanisms. The first one, characterized by parameter α, originates from the structure inversion asymmetry, while the second one characterized by β is due to the bulk inversion asymmetry. Most importantly, both of the contributions reveal themselves when the values of α and β are comparable. In this case, a number of interesting effects occur: The electron energy spectrum becomes strongly anisotropic,[1] the electron spin relaxation rate becomes dependent on the spin orientation in the plane of the quantum well,[2] a magnetic breakdown should be observed in the Shubnikov–de Haas effect.[3] The energy spectra splitting due to SOI can be observed in rather well-developed experiments as that based on Shubnikov–de Haas effect. However, these experiments can hardly tell about the partial contributions of the two mechanisms, leaving the determination of the relation between α and β to be a more challenging task. At the same time, in some important cases spin relaxation time τ_s and spin polarization strongly depend on the $\frac{\alpha}{\beta}$ ratio. In this paper, we consider the tunneling between 2D electron layers, which turns out to be sensitive to the relation between Rashba and Dresselhaus contributions. The specific feature of the tunneling in the system under consideration is that the energy and in-plane momentum conservation put tight restrictions on the tunneling. Without SOI, the tunneling conductance exhibits a delta-function-like maximum at zero bias broadened by elastic scattering in the layers[4] and fluctuations of the layer width.[5] Such a behavior was indeed observed in a number of experiments.[6–8] Spin-orbit interaction splits the electron spectra into two subbands in each layer. Energy and momentum conservation can be fulfilled for the tunneling between opposite subbands of the layers at a finite voltage corresponding to the subbands splitting. However, if the parameters of SOI are equal for the left and right layers, the tunneling remains prohibited due to orthogonality of the appropriate spinor eigenstates. In Ref. 9, it was pointed out that this restriction can also be eliminated if Rashba parameters are different for the two layers. A structure design was proposed[10] where exactly opposite values of the Rashba parameters result from the builtin electric field in the left layer being opposite to that in the right layer. Because the SOI of Rashba type is proportional to the electric field, this would result in $\alpha^R=-\alpha^L$, where α^L and α^R are the Rashba parameters for the left and right layers, respectively. In this case, the peak of the conductance is expected at the voltage U_0 corresponding to the energy of SOI: $eU_0=\pm 2\alpha k_F$, where k_F is the Fermi wave vector. In this paper, we consider arbitrary Rashba and Dresselhaus contributions in the 2D layers and obtain a general expression for dc tunneling current. We show that different relations between Rashba and Dresselhaus contributions correspond to different shapes of current-voltage characteristic. Special attention is focused on particular but the most typical case of both contributions with the same order of magnitude.[11,12] In this case, the structure of the electron eigenstates should even suppress the tunneling at any voltage. At that, the scattering at impurities becomes very important because it restores the features of current-voltage characteristic containing information about SOI parameters. Finally, we show that the parameters α and β can reveal themselves in a tunneling experiment which, unlike other spin-related experiments, requires neither magnetic field nor polarized light.

II. CALCULATIONS

The system under study consists of 2D electron layers separated by a potential barrier (see Fig. 1). We consider zero temperature, only one level of size quantization, and a not too narrow barrier so that the electron wave functions in the left and right layers overlap weakly. Bardeen's tunneling Hamiltonian[4,5,13] can be written as

$$H = H_0^L + H_0^R + H_T, \tag{1}$$

where H_0^L and H_0^R are the partial Hamiltonians for the left and right layers, respectively, and H_T is the tunneling term. Tak-

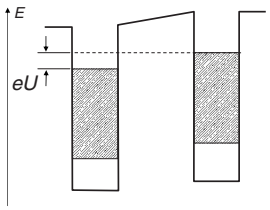

FIG. 1. Energy diagram of two 2D electron layers.

ing account of the elastic scattering and SOI in the layers, these terms have the following form:

$$H_0^l = \sum_{k,\sigma} \varepsilon_k^l c_{k\sigma}^{l+} c_{k\sigma}^l + \sum_{k,k',\sigma} V_{kk'}^l c_{k\sigma}^{l+} c_{k'\sigma}^l + H_{SO}^l,$$

$$H_T = \sum_{k,k',\sigma,\sigma'} T_{kk'\sigma\sigma'} (c_{k\sigma}^{L+} c_{k'\sigma'}^R + c_{k'\sigma'}^{R+} c_{k\sigma}^L), \tag{2}$$

Here, index l is used for the layer designation, $l=R$ for the right layer and $l=L$ for the left layer. k here and further throughout the paper denotes the wave vector parallel to the layer planes, σ is the spin polarization taking the values $\sigma = \pm 1/2$ and ε_k^l is the energy of an electron in the layer l having in-plane wave vector k. It can be expressed as

$$\varepsilon_k^l = \varepsilon + \varepsilon_0^l + \Delta^l, \tag{3}$$

where $\varepsilon = \frac{\hbar^2 k^2}{2m}$, m being the electron's effective mass, ε_0^l is the size quantization energy, and Δ^l is the energy shift due to the external voltage applied to the layer l. We shall also use the value $\Delta^{ll'}$ defined as $\Delta^{ll'} = (\Delta^l - \Delta^{l'}) + (\varepsilon_0^l - \varepsilon_0^{l'})$. The second term in the Hamiltonian [Eq. (2)] $V_{kk'}^l$ is the matrix element of the scattering operator. We consider only elastic scattering. The tunneling constant $T_{kk'\sigma\sigma'}$ in Eq. (2) denotes size quantization level splitting caused by the wave function overlap. By lowercase t, we shall denote the overlap integral itself. Parametrically, $T \sim t\varepsilon_F$, where ε_F is the electron Fermi energy. The term H_{SO}^l describes the spin-orbit part of the Hamiltonian,

$$\hat{H}_{SO}^l = \alpha^l \sum_k (k_y - ik_x) c_{k\sigma}^{l+} c_{k\sigma'}^l + (k_y + ik_x) c_{k\sigma'}^{l+} c_{k,\sigma}^l + \beta^l \sum_k (k_x - ik_y) c_{k\sigma}^{l+} c_{k\sigma'}^l + (k_x + ik_y) c_{k\sigma'}^{l+} c_{k\sigma}^l. \tag{4}$$

The tunneling current is given by[4]

$$I = \frac{ie}{\hbar} T \int dk \, \mathrm{Tr}(\langle \hat{\rho}_{kk'\sigma\sigma'}^{RL} \rangle - \langle \hat{\rho}_{kk'\sigma\sigma'}^{LR} \rangle) \delta_{kk'}, \tag{5}$$

where $\hat{\rho}_{kk'\sigma\sigma'}^{ll'} = c_{k,\sigma}^{l+} c_{k',\sigma'}^{l'}$, $\langle\,\rangle$ denotes the expectation value in the quantum-mechanical sense, δ is the Kronecker symbol, and trace refers to the spin indices. For further calculations, it is convenient to introduce four-dimensional vector operator $\hat{S}_{kk'}^{ll'}$, whose components are given by

$$(\hat{S}_{kk'}^{ll'})_{\nu=0,1,2,3} = \mathrm{Tr}(\sigma_\nu \hat{\rho}_{kk'\sigma\sigma'}^{ll'}),$$

where σ_ν are the Pauli matrices, including identity matrix σ_0. This vector operator fully determines the current. Its time evolution is governed by

$$\frac{d\hat{S}_{kk'}^{ll'}}{dt} = \frac{i}{\hbar}[H, \hat{S}_{kk'}^{ll'}]. \tag{6}$$

In the standard way of reasoning,[14] Eq. (6) turns into

$$(\hat{S}_{kk'}^{ll'} - \hat{S}_{kk'}^{(0)ll'}) w = \frac{i}{\hbar}[H, \hat{S}_{kk'}^{ll'}]. \tag{7}$$

Here, $\hat{S}_{kk'}^{(0)ll'}$ represents the stationary solution of Eq. (6) without interaction (i.e., tunneling and scattering by impurities) and w^{-1} is the time of adiabatic turn-on of the interaction. $\hat{S}_{kk'}^{(0)ll'}$ has the diagonal form

$$\hat{S}_{kk'}^{(0)ll'} = \hat{S}_k^{(0)l} \delta_{kk'} \delta_{ll'}. \tag{8}$$

Here and further, we avoid duplications of the indices, i.e., use l instead of ll and k instead of kk. The calculations performed in a way similar to Ref. 14 bring us to the following system of equations with respect to $\hat{S}_k^{ll'}$:

$$0 = (\Delta^{ll'} + i\hbar w)\hat{S}_k^{ll'} + T(\hat{S}_k^{l'} - \hat{S}_k^l) + \boldsymbol{M}(k)\hat{S}_k^{ll'} - \sum_{k'} \left(\frac{A_{kk'}^l \hat{S}_k^{ll'} - B_{kk'}^{ll'} \hat{S}_{k'}^{ll'}}{\varepsilon' - \varepsilon - \Delta^{ll'} + i\hbar w} + \frac{B_{kk'}^{ll'} \hat{S}_k^{ll'} - A_{kk'}^{l'} \hat{S}_{k'}^{ll'}}{\varepsilon - \varepsilon' - \Delta^{ll'} + i\hbar w} \right), \tag{9}$$

$$i\hbar w(\hat{S}_k^{(0)l} - \hat{S}_k^l) = T(\hat{S}_k^{l'l} - \hat{S}_k^{ll'}) + \boldsymbol{M}(k)\hat{S}_k^l + \sum_{k'} \frac{2i\hbar w A_{kk'}^l (\hat{S}_k^l - \hat{S}_{k'}^{l'})}{(\varepsilon' - \varepsilon)^2 + (\hbar w)^2}, \tag{10}$$

where $\boldsymbol{M}$ is a known matrix, depending on k and parameters of SOI. Here, the quadratic forms of the impurities potential matrix elements are

$$A_{kk'}^l \equiv |V_{k'k}^l|^2,$$

$$B_{kk'}^{ll'} \equiv V_{k'k}^l V_{kk'}^{l'}. \tag{11}$$

As Eqs. (9) and (10) comprise system of linear integral equations, $A_{kk'}^l$ and $B_{kk'}^{ll'}$ enter Eq. (5) linearly and can be themselves averaged over a spatial distribution of the impurities. We assume a short range potential of impurities and introduce $A \equiv \langle A_{kk'}^l \rangle$ and $B \equiv \langle B_{kk'}^{ll'} \rangle$ averaged over their spatial distribution. Here, we took $\langle A^l \rangle = \langle A^{l'} \rangle$ for brevity and omitted the index l. (As for B, the index is omitted because $B_{kk'}^{ll'} = B_{kk'}^{l'l}$.) According to Eq. (11), A denotes inverse electron's scattering time,

$$\frac{1}{\tau} = \frac{2\pi}{\hbar}\nu\langle|V_{kk'}|^2\rangle = \frac{2\pi}{\hbar}\nu A, \tag{12}$$

where ν is the 2D density of states. We note that the averaged correlators A and B have different parametrical dependences on the tunneling transparency t,

$$\frac{B}{A} \sim t^2 \sim T^2. \tag{13}$$

This result holds both for noncorrelated and strongly correlated arrangements of the impurities. Unlike Ref. 10 and according to Eq. (13), we conclude that the correlator B has to be neglected in the calculation of the current within the order of T^2. In the method used here, this result appears quite naturally; however, it can be similarly traced in the diagrammatic technique used in Ref. 10. For the same reason, the tunneling term is to be dropped from Eq. (10). By means of Fourier transformation on energy variable, the system of Eqs. (9) and (10) can be reduced to the system of linear algebraic equations. Finally, $\hat{S}_k^{ll'}$ can be expressed as a function of $\hat{S}_k^{(0)l}$. Finally, the current [Eq. (5)] is expressed through $\langle\hat{\rho}_{k\sigma}^{(0)R}\rangle$ and $\langle\hat{\rho}_{k\sigma}^{(0)L}\rangle$. For the considered case of zero temperature,

$$\langle\rho_{k\sigma}^{(0)l}\rangle = \frac{1}{2W}\theta(\varepsilon_F^l + \Delta^l - \varepsilon - \varepsilon_\sigma),$$

where W is the lateral area of the layers,

$$\varepsilon_\sigma = \pm|\alpha^l(k_x - ik_y) - \beta^l(ik_x - k_y)|.$$

Without loss of generality, we consider the case of identical layers and external voltage applied, as shown in Fig. 1,

$$\varepsilon_0^R = \varepsilon_0^L,$$

$$\Delta^L = -\frac{eU}{2}, \quad \Delta^R = +\frac{eU}{2},$$

$$\Delta^{RL} = -\Delta^{LR} = eU.$$

We obtain the following expression for the current:

$$I = \frac{ie}{2\pi\hbar}T^2\nu\int_0^{2\pi}\int_0^{\infty}(\zeta^L + \zeta^R)\mathrm{Tr}(\rho_\sigma^{(0)R} - \rho_\sigma^{(0)L})d\varepsilon d\varphi, \tag{14}$$

where

$$\zeta^l = \frac{C^l[(C^l)^2 - 2bk^2\sin 2\varphi - gk^2]}{(f + 2d\sin 2\varphi)^2k^4 - 2(C^l)^2(c + 2a\sin 2\varphi)k^2 + (C^l)^4},$$

$$C^l(U) = \Delta^l + i\frac{\hbar}{\tau},$$

$$a = \alpha^L\beta^L + \alpha^R\beta^R,$$

$$b = (\beta^L + \beta^R)(\alpha^L + \alpha^R),$$

$$c = (\beta^L)^2 + (\beta^R)^2 + (\alpha^L)^2 + (\alpha^R)^2,$$

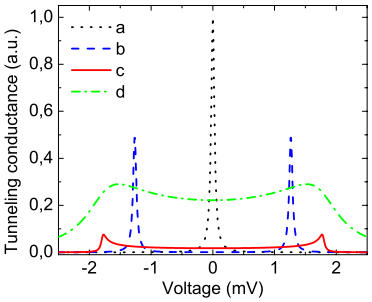

FIG. 2. (Color online) Tunneling conductance. (a) ε_F=10 meV, α=β=0, τ=2×10^{-11} s; (b) same as (a), but αk_F=0.6 meV; (c) same as (b), but β=α; (d) same as (c), but τ=2×10^{-12} s.

$$d = \alpha^L\beta^L - \alpha^R\beta^R,$$

$$f = (\beta^L)^2 - (\beta^R)^2 + (\alpha^L)^2 - (\alpha^R)^2,$$

$$g = (\beta^L + \beta^R)^2 + (\alpha^L + \alpha^R)^2. \tag{15}$$

Parameters a–g are various combinations of the Rashba and Dresselhaus parameters. Both types of SOI are known to be small in real structures so that $\alpha k_F \ll \varepsilon_F$ and $\beta k_F \ll \varepsilon_F$. We also use the assumptions: $\frac{\varepsilon_F\tau}{\hbar} \gg 1$ and $eU \ll \varepsilon_F$. This allows us to reduce Eq. (14) to

$$I = \frac{ie^2}{2\pi\hbar}T^2\nu WU\int_0^{2\pi}[\zeta^L(\varepsilon_F) + \zeta^R(\varepsilon_F)]d\varphi. \tag{16}$$

The integral over φ in Eq. (16) can be calculated analytically by means of a complex variable integration. The result for arbitrary α^l and β^l is not given here for it is rather cumbersome. Instead, we will discuss most important limit cases and plot a few examples for the arbitrary case.

III. RESULTS AND DISCUSSION

The general expression of Eq. (16) can be simplified in a few particular cases. It appears that the tunneling conductance can exhibit qualitatively different behaviors depending on the relation between Rashba and Dresselhaus contributions. We shall start from the case when SOI is completely absent, then consider situations when one type of SOI, say, Rashba mechanism, dominates, and, finally, turn to the case when both Rashba and Dresselhaus contributions are present and have comparable strengths. The analytical results for each of these cases are illustrated with conductance vs voltage characteristics for the following parameters taken to resemble typical GaAs structures: ε_F=10 meV and $\alpha^l k_F$ =0.6 meV. The plots shown in Figs. 2(a)–2(c) and 5 were calculated for negligibly small scattering (still not strictly zero to avoid delta peaks in the plots). The plots presented in Figs. 2(d) and 6 were calculated with electron's scattering time being of the order of picosecond. This was proven to be quite achievable in real structures prepared for tunneling experiments.[7]

In the absence of SOI, the tunneling conductance has a Lorentz-type dependence centered at zero voltage.[4,6] The width of the peak corresponds to the electron's scattering time τ. As will be shown below, the same behavior is expected when the parameters of SOI are equal for both layers. In this case, the tunneling current does not possess any footprints of SOI. However, if any of the SOI parameters in the one 2D layer differs from that in the other layer, they immediately affect the dependence of the tunneling conductance on voltage. Moreover, it appears that the particular shape of this dependence is determined not merely by the difference in one SOI parameter (say, Rashba term $\alpha^L \neq \alpha^R$) but also by the absolute values of both Rashba and Dresselhaus parameters even if one of them remains equal for both layers (in our example, $\beta^L = \beta^R$). Therefore, theoretically, it becomes possible to determine the magnitude and, particulary, the relation between both types of SOI from a plain tunneling experiment whenever one manages to obtain electron layers with different values of either type of SOI. The difference in Dresselhaus contributions can be achieved by using different materials for the layers. While this at first seems to be questionable from the technological point of view, the idea of using a solid solution with varied composition does not seem that exotic. Obviously, the difference in Rashba terms seems to be much easier to achieve. The Rashba mechanism originates from the structure inversion asymmetry caused by the builtin electrical field. Thus, if the electric fields are not equal in the two layers, the Rashba parameters α^L and α^R will be different also. A most vivid manifestation of SOI in the tunneling conductance is expected if these parameters are made of the same magnitude but opposite signs. This case corresponds to the electric field directed normally to the layer planes and in opposite directions in the left and right layers. Hypothetically, this will be the case if a charged plane is placed in the middle of the barrier. Such a plane can be created by a delta layer of ionized impurities.[9,10] The experimental realization of this has some uncertainty as such a layer might significantly affect the tunneling barrier. Nevertheless, the doping regions positioned at both outer sides of the system rather than in the barrier can also produce the electrical field having opposite directions for both layers.

Now, we shall turn to the consideration of each of the different possible cases and obtain the analytical expressions for the tunneling current. In each case, the behavior of the conductivity is explained, considering the structure of the electron eigenstates in the layers and with account of the conservation of energy, in-plane momentum, and spin polarization (if accounted for). In fact, with no accounting of the scattering, the results can be obtained in a simpler way, by means of Fermi's golden rule (FGR). This gives an opportunity to verify our general result in the limit of infinite scattering time by comparison with those obtained via FGR calculation. Such a comparison is shown below for the case of equal magnitudes of Rashba and Dresselhaus terms.

A. No spin-orbit interaction

In the absence of SOI ($\alpha^R = \alpha^L = 0$, $\beta^R = \beta^L = 0$) the energy spectrum for each of the layers forms a paraboloid,

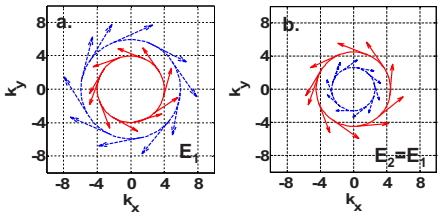

FIG. 3. (Color online) Cross section of electron energy spectra in the left (a) and right (b) layers for the cases $\alpha^L = -\alpha^R$ and $\beta^L = \beta^R = 0$.

$$E^l(k^l) = \varepsilon_0 + \frac{\hbar^2 (k^l)^2}{2m} \pm \frac{eU}{2}. \tag{17}$$

The tunneling requires energy and momentum conservation simultaneously,

$$E^R = E^L,$$

$$k^R = k^L. \tag{18}$$

Both conditions are satisfied only at $U=0$ so that a nonzero external voltage does not produce any current despite the fact that it produces empty states in one layer aligned to the filled states in the other layer (Fig. 1). The momentum conservation restriction in Eq. (18) is weakened if the electrons scatter at the impurities. Accordingly, one should expect a nonzero tunneling current within a finite voltage range in the vicinity of zero. For the considered case, the general formula [Eq. (16)] is simplified radically as all the parameters [Eq. (15)] reduce to zero. Finally, we get the well-known result,[4]

$$I = 2e^2 T^2 \nu W U \frac{\frac{1}{\tau}}{(eU)^2 + \left(\frac{\hbar}{\tau}\right)^2}. \tag{19}$$

The conductance defined as $G(U) = I/U$ has a Lorentz-shaped peak at $U=0$ turning into a delta function at $\tau \to \infty$. This case is shown in Fig. 2(a).

B. Spin-orbit interaction of Rashba type

The spin-orbit interaction gives qualitatively new option for the dc conductance to be finite at nonzero voltage. SOI splits the spectra into two subbands. Now, an electron from the first subband of the left layer can tunnel to a state in a second subband of the right layer. Let us consider a particular case when only Rashba type of SOI interaction exists in the system, its magnitude being the same in both layers, i.e., $|\alpha^R| = |\alpha^L| \equiv \alpha$ and $\beta^R = \beta^L \equiv \beta = 0$. In this case, the spectra splits into two paraboloidlike subbands "inserted" into each other. Figure 3 shows their cross sections for both layers; arrows show spin orientation. By applying a certain external voltage $U_0 = \frac{2\alpha k_F}{e}$, the layers can be shifted on the energy scale in such a way that the cross section of the "outer" subband of the right layer coincides with the "inner" subband

of the left layer (see solid circles in Fig. 3). At that, both conditions [Eq. (18)] are satisfied. However, if the spin is taken into account, the interlayer transition can still remain forbidden. It happens if the appropriate spinor eigenstates involved in the transition are orthogonal. This very case occurs if $\alpha^R=\alpha^L$. Consequently, the conductance behavior remains the same as that without SOI. In contrast, if the Rashba terms are of opposite signs, i.e., $\alpha^R=-\alpha^L$ the spin orientations in the outer subband of the right layer and the inner subband of the left layer are the same, and tunneling is allowed at a finite voltage but forbidden at $U=0$. This situation, pointed out in Refs. 9 and 10, should reveal itself in sharp maxima of the conductance at $U=\pm U_0$, as shown in Fig. 2(b). From this dependence, the value of α can be immediately extracted from the position of the peak. Evaluating Eq. (15) for this case and, further, expression (16), we obtain the following result for the current:

$$I=\frac{2e^2T^2W\nu U\frac{\hbar}{\tau}\left[\delta^2+e^2U^2+\left(\frac{\hbar}{\tau}\right)^2\right]}{\left[(eU-\delta)^2+\left(\frac{\hbar}{\tau}\right)^2\right]\left[(eU+\delta)^2+\left(\frac{\hbar}{\tau}\right)^2\right]}, \quad (20)$$

where $\delta=2\alpha k_F$. The result is in agreement with that derived in Ref. 10, taken for an uncorrelated spatial arrangement of the impurities. As we have already noted, the interlayer correlator B should be neglected because parametrically it has higher order of tunneling overlap integral t than the intralayer correlator A [Eq. (13)]. Therefore, we conclude that the result [Eq. (20)] is valid for an arbitrary degree of correlation in the spatial distribution of the impurities in the system. It is worth noting that the opposite case when only the Dresselhaus type of SOI exists in the system leads to the same results. However, it is less practical to study the case of the different Dresselhaus parameters in the layers because this type of SOI originates from the crystallographic asymmetry and, therefore, cannot be varied if the structure composition is fixed. For this case to be realized, one needs to make the two layers of different materials.

C. Both Rashba and Dresselhaus contributions

The presence of the Dresselhaus term in addition to the Rashba interaction can further modify the tunneling conductance in a nontrivial way. A special case occurs if the magnitude of the Dresselhaus term is comparable to that of the Rashba term. We shall always assume the Dresselhaus contribution to be the same in both layers: $\beta^L=\beta^R\equiv\beta$. Let us add the Dresselhaus contribution to the previously discussed case so that $\alpha^L=-\alpha^R\equiv\alpha$ and $\alpha=\beta$. The corresponding energy spectra and spin orientations are shown in Fig. 4. Note that while the spin orientations in the initial and final states are orthogonal for any transition between the layers, the spinor eigenstates are not, so that the transitions are allowed whenever the momentum and energy conservation requirement [Eq. (18)] is fulfilled. It can also be clearly seen from Fig. 4 that the condition [Eq. (18)], meaning overlap of the cross sections (a) and (b), occurs only at a few points. This is unlike the previously discussed case where the overlapping

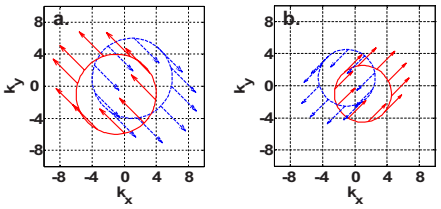

FIG. 4. (Color online) Cross section of electron energy spectra in the left (a) and right (b) layers for the case $\alpha^R=-\alpha^L=\beta$.

occurred within the whole circular cross section shown by solid lines in Fig. 3. One should naturally expect the conductance for the case presently discussed to be substantially lower. Using Eq. (16), we arrive at a rather cumbersome expression for the current,

$$I=eT^2W\nu U\left[\frac{G_-(G_-^2-\delta^2)}{\sqrt{F_-(\delta^4+F_-)}}-\frac{G_+(G_+^2-\delta^2)}{\sqrt{F_+(\delta^4+F_+)}}\right], \quad (21)$$

where

$$G_\pm=eU\pm i\frac{\hbar}{\tau},$$

$$F_\pm=G_\pm^2(G_\pm^2-2\delta^2).$$

Alternatively, for the case of no interaction with impurities, a precise formula for the transition rate between the layers can be obtained by means of Fermi's golden rule. We obtained the following expression for the current:

$$I=\frac{2\pi eT^2W}{\hbar\alpha^2}\left(\sqrt{K+\frac{8m\alpha^2eU}{\hbar^2}}-\sqrt{K-\frac{8m\alpha^2eU}{\hbar^2}}\right), \quad (22)$$

where

$$K=2\delta^2-e^2U^2+\frac{16m^2\alpha^4}{\hbar^4}.$$

Comparing the results obtained from Eqs. (21) and (22) is an additional test for the correctness of Eq. (21). Both dependencies are presented in Fig. 5 and show a good match. The same dependence of conductance on voltage is shown in Fig. 2(c). As can be clearly seen in the figure, the conductance is indeed substantially suppressed in the whole voltage range. This is qualitatively different from all previously mentioned cases. Furthermore, the role of the scattering at impurities appears to be different as well. The previously considered cases were characterized by the resonance behavior of the conductance. The scattering broadened the resonances into Lorentz-shaped peaks with the characteristic width $\delta=\hbar/(e\tau)$. On the contrary, for the last case, the weakening of momentum conservation due to the scattering increases the tunneling conductance and restores the manifestation of SOI in its dependence on voltage.

To understand such an unusual role of the scattering, let us again consider the overlap of the spectra cross sections in

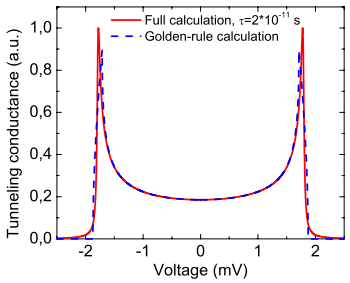

FIG. 5. (Color online) Tunneling conductance calculated for the case $\alpha^R=-\alpha^L=\beta$ and very weak scattering compared to the precise result obtained through Fermi's golden rule calculation.

Figs. 4(a) and 4(b). Note that the scattering weakens the requirement of momentum conservation. To account for that, one should add a certain thickness to the circles shown in the figure. This thickness is proportional to τ^{-1}. Consequently, the overlap of the cross sections now having "thick" lines occurs at a larger number of points, providing increased tunneling current. Figure 2(d) shows this dependence for a realistic scattering time $\tau=2\times10^{-12}$ s.

In general, for arbitrary α and β, the dependence of conductance on voltage can exhibit various complicated shapes, with a number of maxima being very sensitive to the relation between Rashba and Dresselhaus contributions. The origin of such sensitivity is the interference of the angular dependencies of the spinor eigenstates in the layers. A few examples of such interference are shown in Figs. 6(a)–6(c). All the dependencies shown were calculated for the scattering time $\tau=2\times10^{-12}$ s. Figure 6(a) summarizes the results for all previously discussed cases of SOI parameters, i.e., no SOI (curve 1), the case $\alpha_R=-\alpha_L$, $\beta=0$ (curve 2), and $\alpha_R=-\alpha_L=\beta$ (curve 3). Following the magnitude of τ, all the reasonances are broadenered compared to that shown in Fig. 2. Figure 6(b) (curve 2) demonstrates the conductance calculated for the case $\alpha_L=-\frac{1}{2}\alpha_R=\beta$, and Fig. 6(c) (curve 2) for the case $\alpha_L=\frac{1}{2}\alpha_R=\beta$. Curve 1 corresponding to the case of no SOI is also shown in all the figures for reference. Despite the scattering, all the patterns shown in Fig. 6 remain very distinctive. That means that, in principle, the relation between the Rashba and Dresselhaus contributions to SOI can be extracted merely from the *I-V* curve measured in a proper tunneling experiment.

IV. SUMMARY

As we have shown, in the system of two 2D electron layers separated by a potential barrier, SOI can reveal itself in the tunneling current. The difference in spin structure of eigenstates in the layers results in a sort of interference and affects the tunneling rate. Consequently, the dependence of tunneling conductance on voltage appears to be very sensitive to the parameters of SOI. Thus, we propose a way to extract the parameters of SOI and, in particular, the relation between Rashba and Dresselhaus contributions in the tunneling experiment. We emphasize that unlike many other spin-related experiments, the manifestation of SOI studied in this paper should be observed without external magnetic field. Our calculations show that the interference picture may be well resolved for GaAs samples with the scattering times down to $\sim10^{-12}$ s; in some special cases the scattering even restores the traces of SOI otherwise not seen due to destructive interference.

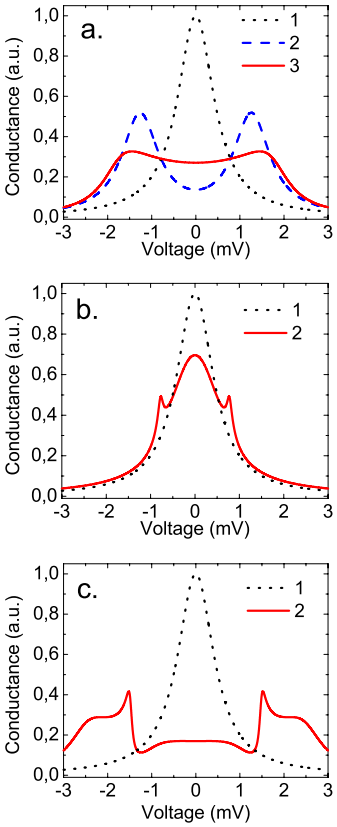

FIG. 6. (Color online) Tunneling conductance calculated for various parameters of SOI.

ACKNOWLEDGMENTS

This work has been supported in part by RFBR, President of RF support (Grant No. MK-8224.2006.2), and by Scientific Programs of RAS.

*igor@quantum.ioffe.ru

[1] B. Jusserand, D. Richards, G. Allan, C. Priester, and B. Etienne, Phys. Rev. B **51**, 4707 (1995).
[2] N. S. Averkiev, L. E. Golub, A. S. Gurevich, V. P. Evtikhiev, V. P. Kochereshko, A. V. Platonov, A. S. Shkolnik, and Yu. P. Efimov, Phys. Rev. B **74**, 033305 (2006).
[3] N. S. Averkiev, M. M. Glazov, and S. A. Tarasenko, Solid State Commun. **133**, 543 (2007).
[4] L. Zheng and A. H. MacDonald, Phys. Rev. B **47**, 10619 (1993).
[5] F. T. Vasko, O. G. Balev, and N. Studart, Phys. Rev. B **62**, 12940 (2000).
[6] S. Q. Murphy, J. P. Eisenstein, L. N. Pfeiffer, and K. W. West, Phys. Rev. B **52**, 14825 (1995).
[7] N. Turner, J. T. Nicholls, E. H. Linfield, K. M. Brown, G. A. C. Jones, and D. A. Ritchie, Phys. Rev. B **54**, 10614 (1996).
[8] V. G. Popov, Yu. V. Dubrovskii, Yu. N. Khanin, E. E. Vdovin, D. K. Maude, J.-C. Portal, T. G. Andersson, and J. Thordson, Semiconductors **35**, 539 (1998).
[9] O. E. Raichev and P. Debray, Phys. Rev. B **67**, 155304 (2003).
[10] V. A. Zyuzin, E. G. Mishchenko, and M. E. Raikh, Phys. Rev. B **74**, 205322 (2006).
[11] S. D. Ganichev, V. V. Bel'kov, L. E. Golub, E. L. Ivchenko, P. Schneider, S. Giglberger, J. Eroms, J. De Boeck, G. Borghs, W. Wegscheider, D. Weiss, and W. Prettl, Phys. Rev. Lett. **92**, 256601 (2004).
[12] S. Giglberger, L. E. Golub, V. V. Bel'kov, S. N. Danilov, D. Schuh, C. Gerl, F. Rohlfing, J. Stahl, W. Wegscheider, D. Weiss, W. Prettl, and S. D. Ganichev, Phys. Rev. B **75**, 035327 (2007).
[13] T. Jungwirth and A. H. MacDonald, Phys. Rev. B **53**, 7403 (1996).
[14] W. Kohn and J. M. Luttinger, Phys. Rev. **108**, 590 (1957).

PUBL. 2

I. V. ROZHANSKY and N. S. AVERKIEV, SPIN-DEPENDENT TUNNELING CONDUCTANCE IN TWO-DIMENSIONAL STRUCTURES AT ZERO MAGNETIC FIELD, *Low Temperature Physics*, **35**, 15, 2009.

Spin-dependent tunneling conductance in two-dimensional structures at zero magnetic field

I. V. Rozhansky[a)] and N. S. Averkiev

A. F. Ioffe Physical Technical Institute of the Russian Academy of Sciences, ul. Politekhnicheskaya 26, St. Petersburg 194021, Russia
(Submitted July 23, 2008)
Fiz. Nizk. Temp. **35**, 21–28 (January 2009)

The influence of the spin-orbit interaction on the tunneling between two-dimensional electron layers is considered. A general expression for the tunneling current is obtained with the Rashba and Dresselhaus effects and also elastic scattering of charge carriers on impurities taken into account. It is shown that the particular form of the tunneling conductance as a function of the voltage between layers is extremely sensitive to the relationship between the Rashba and Dresselhaus parameters. This makes it possible to determine the parameters of the spin-orbit interaction and the quantum scattering time directly from measurements of the tunneling conductance in the absence of magnetic field. © *2009 American Institute of Physics*. [DOI: 10.1063/1.3064872]

I. INTRODUCTION

In the spin-orbit interaction a particle spin can be manifested directly in the absence of external magnetic field, and this effect is therefore extremely attractive from the standpoint of spintronic applications. The spin-orbit interaction can be used to create spatially separate spin-polarized charge carriers; it can indirectly influence the operation of devices, e.g., by affecting the spin coherence time. In two-dimensional (2D) systems two types of spin-orbit interaction are the most important, giving terms in the Hamiltonian which are linear in the wave vector of the particle: the Rashba and Dresselhaus effects. Essentially both types of interaction are due to the absence of inversion symmetry of a system. The first, characterized by a parameter α, is a consequence of the absence of a center of inversion of the structure design (Rashba effect), and the second, characterized by a parameter β, is a consequence of the absence of a center of inversion in the symmetry point group of the material (Dresselhaus effect). The two types of interaction are manifested with particular clarity when α and β are comparable in value. In this case a number of interesting effects appear: the energy spectrum becomes strongly anisotropic,[1,2] the spin relaxation time begins to depend on the orientation of the spin in the plane of the quantum well,[3] and magnetic breakdown should be observed in the Shubnikov-de Haas effect.[4] The splitting of the energy spectrum due to the spin-orbit interaction can be observed experimentally. However, in the majority of cases it is rather hard to establish the relative contributions of the Rashba and Dresselhaus mechanisms. At the same time, in several important cases the spin relaxation time and spin polarization time depend substantially on the relationship between α and β. In this paper we consider the tunneling between two 2D electron layers, and will show that this tunneling is very sensitive to the relationship between α and β. In such a system the tunneling is of a resonant character on account of the restrictions imposed by the energy and momentum conservation laws. Without the spin-orbit interaction, the tunneling conductance is nonzero in a narrow region of interlayer voltages close to zero, the width of this region being determined by the impurity scattering time[5] and fluctuations of the layer widths.[6] Such behavior of the tunneling conductance has been observed repeatedly in experiments.[7–9] The spin-orbit interaction causes splitting of the energy spectra of electrons in the layers into two subbands. Here tunneling with conservation of energy and momentum in the plane of the layers can occur between different subbands at a finite voltage corresponding to the energy of the spin-orbit splitting. However, if the parameters of the spin-orbit interaction are the same for the left and right layers, then transitions between different subbands are forbidden because of the orthogonality of the corresponding spinor states. It has been pointed out[10] that tunneling between different subbands becomes possible if the Rashba parameters in the left and right layers are different. A scheme for such a structure was proposed in Ref. 11, where Rashba parameters of the same absolute value but of opposite sign arise as a result of delta doping of the tunneling barrier at the center. A charged plane of ionized impurity should give rise to an electric field of different sign for the left and right layers. Since the Rashba type of spin-orbit interaction is proportional to the external electric field, this leads to the relation $\alpha^R=-\alpha^L$, where α^L and α^R are the Rashba interaction parameters for the left and right layers. In this case the resonance peak of the tunneling conductance should arise at an interlayer voltage U_0 corresponding to the energy $eU_0=\pm 2\alpha k_F$, where k_F is the magnitude of the wave vector at the Fermi surface. In the present paper we consider the general case of arbitrary contributions of the Rashba and Dresselhaus interactions and obtain the corresponding expression for the tunneling current. It is shown that different relationships between the Rashba and Dresselhaus contributions correspond to different voltage dependence of the tunneling conductance. In particular, we consider the most common case when the two contributions are comparable in magnitude.[12,13] In this case the features of the spectrum of eigenstates in the layers lead to significant suppression of the tunneling in the whole range of voltages. Here scattering on impurities begins to play a key role—it restores the features of the current-voltage characteristic which carry information about the parameters of

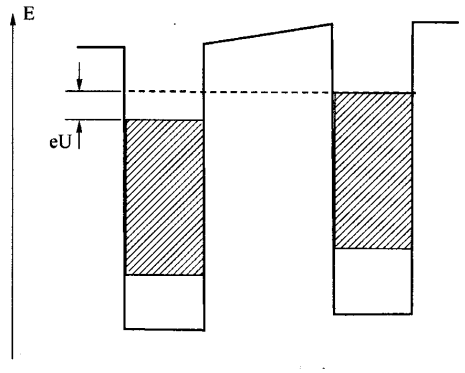

FIG. 1. Energy diagram of the 2D electron layers.

the spin-orbit interaction. Thus we shall show that the parameters α and β can be manifested clearly in a tunneling experiment, which, unlike other spin experiments, does not require an external magnetic field or polarized light.

II. THEORY

We consider a system of two 2D electron layers (quantum wells) separated by a potential barrier (see Fig. 1). We shall assume that there is only one size-quantization level, that the temperature is zero, and that the width of the barrier is large enough that the wave functions of the electrons in different layers are weakly overlapping. In a Bardeen approach[5,6,14] the tunneling Hamiltonian has the form

$$H = H_0^L + H_0^R + H_T, \tag{1}$$

where H_0^L and H_0^R are the "partial" Hamiltonians of the left and right layers and H_T is the tunneling term. The expressions for these terms with the elastic scattering on impurities taken into account have the form

$$H_0^l = \sum_{k,\sigma} \varepsilon_k^l c_{k\sigma}^{l+} c_{k\sigma}^l + \sum_{k,k',\sigma} V_{kk'}^l c_{k\sigma}^{l+} c_{k'\sigma}^l + H_{SO}^l,$$

$$H_T = \sum_{k,k',\sigma,\sigma'} T_{kk'\sigma\sigma'} (c_{k\sigma}^{L+} c_{k'\sigma'}^R + c_{k'\sigma'}^{R+} c_{k\sigma}^L). \tag{2}$$

Here c^+ and c are the creation and annihilation operators, the index l denotes the layer ($l=R$ for the right layer and $l=L$ for the left), $\mathbf{k}$ is the wave vector in the plane of the layers, σ is the spin polarization, which takes the values $\sigma_+ = 1/2$, $\sigma_- = -1/2$, and ε_k^l is the energy of an electron with wave vector $\mathbf{k}$ in the plane in layer l. The expression for ε_k^l has the form

$$\varepsilon_k^l = \varepsilon + \varepsilon_0^l + \Delta^l, \tag{3}$$

where $\varepsilon = \hbar^2 k^2/2m$, m is the effective mass of the electron, ε_0^l is the size quantization energy, and Δ^l is the shift due to an applied voltage U, $\Delta^l = \pm eU/2$. We shall assume that the two potential wells are identical, so that $\varepsilon_0^L = \varepsilon_0^R$. This simplification is not fundamental, since inequivalence of the wells leads to a shift of the voltage scale without qualitatively affecting the results. The second term in Hamiltonian (2) describes elastic scattering on impurities, where $V_{kk'}^l$ is the matrix element of the scattering operator. The constant $T_{kk'\sigma\sigma'}$ in Eq. (2) has the meaning of the tunneling splitting of the energy levels due to overlap of the wave functions of the particles of the left and right layers. It is assumed below that the tunneling occurs for $\mathbf{k}=\mathbf{k}'$ and $\sigma=\sigma'$, so that $T_{kk'\sigma\sigma'} = T\delta_{kk'}\delta_{\sigma\sigma'}$, where δ is the Kronecker delta. We denote the overlap integral by t and assume that the external voltage applied to the system is small compared to the electron Fermi energy ε_F. Then $T \sim t\varepsilon_F$. The term H_{SO}^l describes the spin-orbit part of the Hamiltonian, in which there are two terms linear in k, corresponding to interactions of the Rashba type, with the constant α, and Dresselhaus type, with the constant β:

$$H_{SO} = \alpha(k_y\sigma_x - k_x\sigma_y) + \beta(k_x\sigma_x - k_y\sigma_y), \tag{4}$$

where k_x and k_y are the projections of the wave vector on the mutually perpendicular axes x and y in the plane of the layers, σ_x and σ_y are Pauli matrices. Passing to a description in the second-quantization representation, we get

$$H_{SO}^l = \alpha^l \sum_k (k_y - ik_x) c_{k\sigma_+}^{l+} c_{k\sigma_-}^l + (k_y + ik_x) c_{k\sigma_-}^{l+} c_{k,\sigma_-}^l + \beta^l \sum_k (k_x - ik_y) c_{k\sigma_+}^{l+} c_{k\sigma_-}^l + (k_x + ik_y) c_{k\sigma_+}^{l+} c_{k\sigma_-}^l. \tag{5}$$

We note that Hamiltonian (1) does not contain matrix elements of the scattering operator which couple different layers, i.e., quantities of the type $V_{kk'}^{LR}$, $V_{kk'}^{RL}$. At the same time, as a result of the second quantization of impurity fields of the form (short-range potential)

$$V(\mathbf{r}) = \sum_a V_0 \delta(\mathbf{r} - \mathbf{r}_a), \tag{6}$$

where the index a denotes summation over impurities with centers at the coordinates $\mathbf{r}_a$ and δ is the delta function, quantities off-diagonal in the layer indices appear together with the diagonal quantities V^L and V^R. We shall show, however, that the matrix elements $V^{ll'}$ containing different layer indices are parametrically small in comparison both to the intralayer matrix elements V^L and V^R and to the tunneling term H_T. We introduce the quadratic forms of the matrix elements of the impurity scattering operator:

$$A_{kk'}^l \equiv |V_{k'k}^l|^2 \quad B_{kk'}^{ll'} \equiv V_{k'k}^l V_{kk'}^{l'}. \tag{7}$$

Since $A_{kk'}^l$ and $B_{kk'}^{ll'}$ appear linearly in the final expression for the current, their averaging over the spatial positions of the impurities can be done separately. Indeed, let us introduce the impurity-averaged quantities $A \equiv \langle A_{kk'}^l \rangle$ and $B \equiv \langle B_{kk'}^{ll'} \rangle$. Since we are considering a parabolic spectrum, scattering on a short-range potential, and identical layers, A and B are independent of k, k', and l. One can see from Eqs. (6) and (7) that A has the meaning of the inverse scattering time of the electrons in each layer:

$$\frac{1}{\tau} = \frac{2\pi}{\hbar} \nu \langle |V_{kk'}^l|^2 \rangle = \frac{2\pi}{\hbar} \nu A, \tag{8}$$

where ν is the 2D density of states. Importantly, the correlators A and B have different parametric dependence on the tunneling transparency t. Indeed, the matrix elements calculated on the wave functions of different layers contain addi-

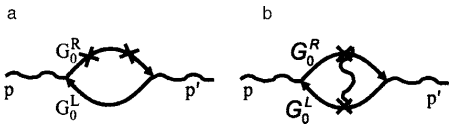

FIG. 2. Two types of diagrams for calculating the tunneling current.

tional smallness due to the smallness of the overlap of these wave functions. Averaging of the two types of correlators over the positions of the impurities gives

$$\frac{B}{A} \sim t^2 \sim T^2. \tag{9}$$

Since the matrix elements $V^{ll'} \sim \sqrt{B}$ and $V^l \sim \sqrt{A}$, using Eq. (9) we get

$$\frac{V^{ll'}}{V^l} \sim t \ll 1.$$

The interlayer matrix elements $V^{ll'}$ are also parametrically small in comparison with the tunneling term in the Hamiltonian (1), since it follows from Eqs. (8) and (9) that $V^{ll'} \sim t(\hbar/\tau)$ $(l \neq l')$, while $T \sim t\varepsilon_F$, and therefore

$$\frac{V^{ll'}}{T} \sim \frac{\hbar}{\varepsilon_F \tau} \ll 1.$$

Thus in a first-order perturbation theory we need to include in the Hamiltonian (2) only the layer-diagonal matrix elements of the interaction with impurities, V^L and V^R.

For the tunneling conductance, in analogy with the case of ordinary conductance, one can obtain the Kubo formula.[15] The Kubo formula takes tunneling into account as a perturbation, and the tunneling current to leading order is proportional to T^2. To calculate the tunneling current we use the Green function method. An expression for the tunneling current in terms of the Green functions of the individual layers has the form

$$l = \frac{eT^2 W}{4\pi^3 \hbar^3} \mathrm{Re}\left\{ \mathrm{Tr} \int G_{0V}^R(\mathbf{p}, \varepsilon - eU) G_{0V}^L(\mathbf{p}, \varepsilon) d\mathbf{p} d\varepsilon \right\}, \tag{10}$$

where p is the momentum of the electron in the plane of the layer, G_{0V}^R and G_{0V}^L are the Green functions for the right and left layers. The subscript V indicates that these Green functions take scattering on impurities into account. The problem consists in expressing the functions G_{0V}^l in terms of the Green functions G_0^l of the 2D electron gas with spin-orbit interaction in the absence of scattering on impurities. This calculation reduces to summation of the two types of diagrams shown in Fig. 2. The branches correspond to the unperturbed Green functions G_0^l and the crosses to the matrix elements $V_{kk'}^l$. The ladder diagrams of type "b" give the vertex corrections.[5,11] However, the ladder diagrams do not give a substantial contribution to the tunneling current. It can be shown that for Hamiltonian (2) the upper branches of the diagrams in Fig. 2 (corresponding to G_0^R) will contain only $V_{kk'}^R$ and the lower diagrams only $V_{kk'}^L$. Therefore, diagrams of type "a" contain only quadratic forms of the intralayer correlator $A_{kk'}$ (7), while diagrams of type "b" contain only the intralayer correlator $B_{kk'}$. However, it follows from Eq. (9) that when the averaging over impurities is taken into account (for an arbitrary degree of their spatial correlation) the interlayer correlator is of higher order in smallness in the tunneling parameter T and therefore should be dropped in calculations to leading order. Thus the expression for the tunneling current with scattering on impurities taken into account is obtained as a result of a summation of diagrams of type "a" only, and it therefore contains only the scattering time on impurities in the same layer and, unlike the case of Ref. 11, does not contain the time corresponding to scattering on impurities found in different layers.

The spin-orbit interaction leads to splitting of the spectrum of eigenstates into two subbands. In a basis of eigenstates of a given layer, the Green function is a 2×2 diagonal matrix:

$$G_{0V} = \begin{bmatrix} G_- & 0 \\ 0 & G_+ \end{bmatrix},$$

where

$$G_\pm(\varepsilon, k) = \frac{1}{\varepsilon + \varepsilon_F - \dfrac{\hbar^2 k^2}{2m} \pm \xi + i\dfrac{\hbar}{2\tau}\,\mathrm{sgn}\,\varepsilon}, \tag{11}$$

$$\xi = \sqrt{(\alpha^2 + \beta^2)k^2 + 4\alpha\beta k_x k_y}. \tag{12}$$

α and β are, respectively, the parameters of the Rashba and Dresselhaus spin-orbit interactions in a given layer, and ε_F is the Fermi level of the layers in the absence of applied voltage. The scattering time τ is given by expression (8). Passing to the initial spinor basis common to both layers, $\sigma = \pm 1/2$, we obtain

$$G_{0V} = \frac{1}{4}\begin{bmatrix} G_- + G_+ & \gamma^{-1}(G_- - G_+) \\ (\gamma^*)^{-1}(G_- - G_+) & G_- + G_+ \end{bmatrix}, \tag{13}$$

where

$$\gamma = \frac{\mathrm{e}^{-i\phi}\beta - i\alpha \mathrm{e}^{i\phi}}{|\mathrm{e}^{-i\phi}\beta - i\alpha \mathrm{e}^{i\phi}|}, \quad \phi = \arctan\frac{k_y}{k_x}.$$

Substituting these expressions for each of the layers into Eq. (10) and integrating over $|k|$ with allowance for the condition $\varepsilon_F \gg \alpha k_F$, we arrive at the following expression:

$$I = \frac{e^2 T^2 \nu W U}{4\pi\tau} \int_0^{2\pi} d\phi \left[\left(\frac{1}{(eU + \xi^-)^2 + (\hbar/\tau)^2} + \frac{1}{(eU - \xi^-)^2 + (\hbar/\tau)^2} \right)(1 + \mathrm{Re}\,\gamma^L \gamma^{R*}) \right.$$
$$\left. + \left(\frac{1}{(eU - \xi^+)^2 + (\hbar/\tau)^2} + \frac{1}{(eU + \xi^+)^2 + (\hbar/\tau)^2} \right)(1 - \mathrm{Re}\,\gamma^L \gamma^{R*}) \right],$$

where $\xi^{\pm}=\xi^{R}(k_F)\pm\xi^{L}(k_F)$. The integral over ϕ in Eq. (13) can be done analytically by the methods of complex analysis. However, the general expression for arbitrary Rashba and Dresselhaus parameters α^l and β^l turns out to be rather awkward and will not be written out here. Instead we shall discuss the most important limiting cases and give some examples for the arbitrary case. We note that the final expression for the tunneling current can also be obtained by another technique that gives precisely the same answer but which is more awkward in the intermediate calculations.[16] The results of the calculations can be checked in the limiting case when scattering on impurities is absent. In that case a simple calculation with the use of Fermi's golden rule is possible. An example of such a comparison is presented in Ref. 16.

III. RESULTS AND DISCUSSION

The general expression (13) can be simplified in a number of particular cases. It turns out that the dependence of the tunneling conductance on the voltage applied to the layers can have qualitatively different form depending on the relationship between the Rashba and Dresselhaus parameters. Let us first consider the case when the spin-orbit interaction is completely absent. This case is equivalent to the presence of a strictly identical spin-orbit interaction in the layers. We shall then consider cases when the spin-orbit interaction is different in the left and right layers, in particular, when one type of spin-orbit interaction (e.g., Rashba) is predominant, and, finally, the case when both types of interaction are present and comparable in magnitude. As will be shown below, the presence of a different spin-orbit interaction in the layers leads to nontrivial voltage dependence of the interlayer differential conductance $G=dI/dU$. That dependence may contain one or several resonance peaks, the positions of which are related to the energy of the spin-orbit splitting and whose width is related to the impurity scattering time. Here an important role is played by the ratio of these quantities:

$$\eta=\frac{\mu k_F\tau}{\hbar}, \tag{14}$$

where μ is the characteristic spin-orbit interaction parameter. The value of η shows whether the individual peaks are resolved or if scattering on impurities does not permit one to distinguish the details due to the spin-orbit interaction. All of the results of the calculations discussed above are presented in Fig. 3 for three values of the parameter η. Below we shall discuss what values of this parameter correspond to the real experimental situation.

A. With no spin-orbit interaction

In the absence of spin-orbit interaction ($\alpha^R=\alpha^L=0$, $\beta^R=\beta^L=0$) the energy spectrum of each layer is a paraboloid:

$$\varepsilon^l(k^l)=\varepsilon_0+\frac{\hbar^2(k^l)^2}{2m}\pm\frac{eU}{2}. \tag{15}$$

A necessary condition for tunneling is that energy and momentum in the plane of the layers be conserved simultaneously:

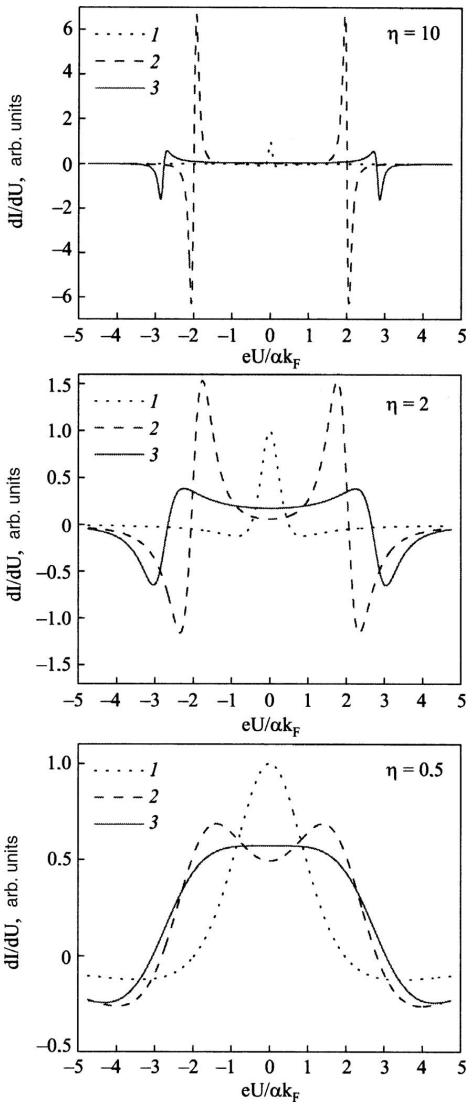

FIG. 3. Tunneling conductance calculated for different parameters of the spin-orbit interaction and different parameters η.

$$\varepsilon^R=\varepsilon^L \quad k^R=k^L. \tag{16}$$

Both conditions hold simultaneously only for $U=0$, so that a nonzero voltage will not cause a tunneling current, despite the fact that states occupied by electrons in one layer lie opposite to empty states in the other. The restriction due to momentum conservation in Eq. (16) can be weakened if the electron scatters on impurities. Accordingly, one expects a nonzero tunneling current in a certain range of voltages near zero. For this case the general formula (13) simplifies considerably, since $\gamma^R=\gamma^L=1$ and $\xi^-=\xi^+=0$. We then have the known result[5]

$$I = 2e^2T^2\nu WU\frac{1/\tau}{(eU)^2+(\hbar/\tau)^2}. \quad (17)$$

The differential tunneling conductance G has a resonance peak at $U=0$, broadened in accordance with $\hbar/\tau$. Such a dependence has been observed experimentally.[7,8]

B. Identical spin-orbit interaction in the layers

If the spin-orbit interaction is the same in both layers, then $\xi^-=0$ and the last term in square brackets in expression (13) is zero, so that $\gamma^L\gamma^{R^*}=1$. Thus the result is no different from the case with no spin-orbit interaction. Physically this means that, although the spin-orbit interaction leads to splitting of the size-quantization subbands, transitions between different subbands are forbidden by virtue of the orthogonality of the states. Then, since the interaction is exactly the same in the left and right layers, it doesn't matter whether one is talking about the subbands in the same layer or in different layers. This case is represented by curve *1* in Fig. 3. For comparison with the other cases here it is assumed that the interaction in the layers is the same, characterized by a parameter $\mu=\alpha$, so that the splitting of the subbands at the Fermi level is $\Delta\varepsilon=\alpha k_F$.

C. Spin-orbit interaction of one type

For the sake of definiteness we consider the case when only the Rashba type of interaction is present. If the Rashba parameters in the two layers are equal, $\alpha^R=\alpha^L\equiv\alpha$, then the spinor states in these subbands are orthogonal, and transitions between layers are forbidden in exactly the same way as in the case with no spin-orbit interaction. However, if the Rashba parameters are of opposite sign, i.e., $\alpha^R=-\alpha^L$, $\alpha=|\alpha^R|$, then the spin polarization in the first subband of the right layer and the second subband of the left layer are identical, and tunneling is allowed between these subbands, while it is forbidden between the first subbands and between the second subbands, including in the case of zero bias $U=0$. This situation, which was mentioned in Refs. 10 and 11, gives rise to peaks of the conductance at nonzero voltage. The value of the spin-orbit splitting can be determined from the position of the peak. For the case under discussion we should set $\gamma^L\gamma^{R^*}=-1$, $\xi^-=0$; $\xi^+=2\alpha k$ in formula (13), which leads to the following formula for the tunneling current:

$$I=\frac{2e^2T^2W\nu U\hbar\tau^{-1}[\delta^2+e^2U^2+(\hbar/\tau)^2]}{[(eU+\delta)^2+(\hbar/\tau)^2][(eU+\delta)^2+(\hbar/\tau)^2]}, \quad (18)$$

where $\delta=2\alpha k_F$. This result, shown by curve *2* in Fig. 3, agrees with that obtained in Ref. 11 for uncorrelated positions of the impurities. However, according to Eq. (9), the interlayer correlator B has a higher order of smallness in the tunneling t than does the intralayer correlator A. Therefore, in our view, the result (18) is valid for arbitrary degree of spatial correlation of the impurities. The case when only the Dresselhaus interaction is present in the system leads to exactly the same result. However, the case of Dresselhaus interaction parameters of different magnitude is apparently more complicated to realize in practice, as it requires preparation of layers of different materials.

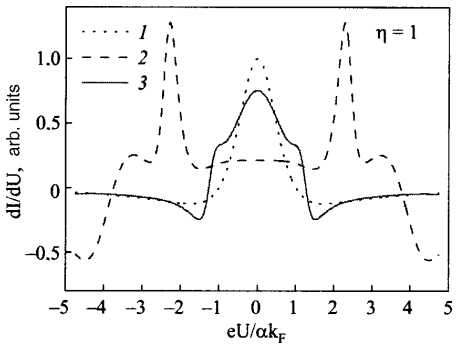

FIG. 4. Tunneling conductance for different parameters of the spin-orbit interaction: $\alpha^R=\alpha^L=\beta$ (curve *1*), $\alpha^R=-2\alpha^L=\beta$ (curve *2*), $\alpha^R=2\alpha^L=\beta$ (curve *3*).

D. Interference of the spin-orbit interactions

The presence of the Dresselhaus term in addition to the Rashba term in the spin-orbit part of the Hamiltonian leads to nontrivial changes in the conductance. We shall assume that the Dresselhaus term is the same for the left and right layers: $\beta^L=\beta^R\equiv\beta$, and the Rashba terms, as in the previous case, are of opposite sign: $\alpha^L=-\alpha^R\equiv\alpha$. We start with the case when both types of interaction are equal in absolute value, i.e., $\alpha=\beta$. The corresponding energy spectra and orientations of the spin in all the subbands are different, the spinor states of the subband of the left and right layers are not orthogonal,[16] and therefore transitions are always allowed, provided, of course, that conditions (16) are satisfied. Satisfaction of the second of those conditions, however, is extremely sensitive to the value of the scattering time,[16] so that for weak scattering, i.e., large values of the parameter η, tunneling is substantially suppressed in the whole voltage range, while for small η the tunneling conductance increases. The general formula (13) in this case has the form:

$$I=eT^2W\nu U\left[\frac{G_-(G_-^2-\delta^2)}{\sqrt{F_-(\delta^4+F_-)}}-\frac{G_+(G_+^2-\delta^2)}{\sqrt{F_+(\delta^4+F_+)}}\right], \quad (19)$$

where

$$G_\pm=eU\pm i\frac{\hbar}{\tau}\quad F_\pm=G_\pm^2(G_\pm^2-2\delta^2),\quad \delta=2\alpha k_F.$$

The corresponding dependence is shown by curve *3* in Fig. 3. We see that the tunneling conductance is indeed substantially suppressed in the whole voltage range. This situation is qualitatively different from the cases considered previously, in which scattering led to broadening of the resonance peaks. In the present case the weakening of the restrictions on momentum conservation owing to scattering increases the tunneling conductance and restores the spin-orbit features on the current-voltage characteristic.

In the general case of arbitrary parameters α and β the particular shape of the voltage dependence of the tunneling conductance is very sensitive to their values. The cause of this sensitivity is essentially the "interference" of the angular dependences of the spinor eigenstates in the layers. Some examples of such "interference" are shown in Fig. 4.

E. Spin-orbit interaction and scattering time in real structures

Figure 3 shows the dependence of the tunneling differential conductance for three different values of the parameter η. The value $\eta=10$ corresponds to negligibly small scattering in comparison with the spin-orbit splitting, the corresponding tunneling characteristics take on a pronounced resonance character. For $\eta=0.5$ all three cases are nearly the same, and that value can be regarded as critical from the standpoint of experiment. Let us estimate the value of η for the real experimental situation. For structures based on AlGaAs one typically has $\varepsilon_F=10$ meV, $\alpha' k_F \approx 0.6$ meV, and the scattering time in real structures for tunneling experiments can fully reach $\tau=10^{-12}$ s.[8] This corresponds to $\eta \approx 1$, i.e., in such structures one would expect to see well-distinguishable features due to the spin-orbit interaction. In structures based on GaSb the spin-orbit splitting is substantially larger, so that one would expect $\eta \approx 8$ at the same value of the scattering time. This means that a well-distinguishable picture should be observed in such structures even for $\tau \approx 10^{-13}$ s.

Thus it is possible to determine the values of both types of interaction in a tunneling experiment, provided that a difference between layers in the parameters of one of these interactions can be created. For example, a difference in the Dresselhaus parameters implies the use of different materials for the left and right layers or, more realistically, solid solutions of different composition. Clearly it is much simpler to achieve different values of the Rashba parameters. Since the Rashba mechanism is directly related to the external electric field in the structure, a difference of the parameters α^L and α^R means simply a different electric field in the right and left layers. We have considered above the case of parameters of equal magnitude but opposite sign, $\alpha^L=-\alpha^R$, which corresponds to the presence of an electric field directed along the normal to the plane of the layers in opposite directions in the right and left layers. Just this situation arises if a charged plane is placed at the center of the barrier. Such a plane of ionized impurities can be created by δ doping in the central part of the barrier, as was proposed in Refs. 10 and 11. A possible drawback of that arrangement is the influence of the δ layer on the tunneling. If that is a problem one could create an electric field of opposite sign in the two layers by using two δ layers on the outer sides of the layer instead of one δ layer in the central part.

IV. CONCLUSION

We have shown that in a system of two 2D electron layers separated by a potential barrier the spin-orbit interaction can be manifested directly in the tunneling conductance. The difference of the spin structure of the eigenstates in the layers leads to a kind of "interference" and affects the rate of tunneling transitions. The particular form of the voltage dependence of the tunneling conductance turns out to be sensitive to the parameters of the spin-orbit interaction. These parameters and, in particular, the ratio of the Rashba and Dresselhaus contributions can be extracted directly from the tunneling current-voltage characteristic. It should be emphasized that, in contrast to numerous other spin experiments, the given manifestation of the spin-orbit interaction does not rely on an external magnetic field or orientation of the charge carriers by polarized light. Calculations show that the interference pattern is well resolved for GaAs-based structures with a characteristic scattering time of $\sim 10^{-12}$ s. A necessary condition for the appearance of the spin-orbit features in the tunneling conductance is a difference of the parameters of the spin-orbit interaction of one type (Rashba or Dresselhaus) in the two layers.

This study was supported in part by the Russian Foundation for Basic Research (RFBR Grant Nos. 08-02-00069, 07-02-00449), programs of the Presidium and Physical Science Division of the Russian Academy of Sciences, and the government of St. Petersburg.

[a]E-mail: igor@quantum.ioffe.ru

[1]E. A. de Andrada e Silva, Phys. Rev. B **46**, 1921 (1992).
[2]B. Jusserand, D. Richards, G. Allan, C. Priester, and B. Etienne, Phys. Rev. B **51**, 4707 (1995).
[3]N. S. Averkiev, L. E. Golub, A. S. Gurevich, V. P. Evtikhiev, V. P. Kochereshko, A. V. Platonov, A. S. Shkolnik, and Yu. P. Efimov, Phys. Rev. B **74**, 033305 (2006).
[4]N. S. Averkiev, M. M. Glazov, and S. A. Tarasenko, Solid State Commun. **133**, 543 (2007).
[5]L. Zheng and A. H. MacDonald, Phys. Rev. B **47**, 10619 (1993).
[6]F. T. Vasko, O. G. Balev, and N. Studart, Phys. Rev. B **62**, 12940 (2000).
[7]S. Q. Murphy, J. P. Eisenstein, L. N. Pfeiffer, and K. W. West, Phys. Rev. B **52**, 14825 (1995).
[8]N. Turner, J. T. Nicholls, E. H. Linfield, K. M. Brown, G. A. C. Jones, and D. A. Ritchie, Phys. Rev. B **54**, 10614 (1996).
[9]V. G. Popov, Yu. V. Dubrovskiĭ, Yu. N. Khanin, E. E. Vdovin, D. K. Maud, J.-C. Portal, T. G. Andersson, and J. Tordson, Fiz. Tekh. Poluprovodn. **32**, 602 (1998) [Semiconductors **32**, 539 (1998)].
[10]O. E. Raichev and P. Debray, Phys. Rev. B **67**, 155304 (2003).
[11]V. A. Zyuzin, E. G. Mishchenko, and M. E. Raikh, Phys. Rev. B **74**, 205322 (2006).
[12]S. D. Ganichev, V. V. Bel'kov, L. E. Golub, E. L. Ivchenko, P. Schneider, S. Giglberger, J. Eroms, J. De Boeck, G. Borghs, W. Wegscheider, D. Weiss, and W. Prettl, Phys. Rev. Lett. **92**, 256601 (2004).
[13]S. Giglberger, L. E. Golub, V. V. Bel'kov, S. N. Danilov, D. Schuh, C. Gerl, F. Rohlfing, J. Stahl, W. Wegscheider, D. Weiss, W. Prettl, and S. D. Ganichev, Phys. Rev. B **75**, 035327 (2007).
[14]T. Jungwirth and A. H. MacDonald, Phys. Rev. B **53**, 7403 (1996).
[15]G. D. Mahan, *Many-Particle Physics*, Plenum, New York (1981).
[16]I. V. Rozhansky and N. S. Averkiev, Phys. Rev. B **77**, 115309 (2008).

Translated by Steve Torstveit

PUBL. 3

N. S. AVERKIEV, V. A. ZAKREVSKII, I. V. ROZHANSKY, and N. T. SUDAR, PECULIARITIES OF HOLES INJECTION INTO ORGANIC MOLECULAR SOLIDS, *Applied Physics Letters*, **94**, 233308, 2009.

Peculiarities of holes injection into organic molecular solids

N. S. Averkiev,[1] V. A. Zakrevskii,[1] I. V. Rozhansky,[1,a)] and N. T. Sudar[2]
[1]*A.F. Ioffe Physical Technical Institute, Russian Academy of Sciences, 194021 St. Petersburg, Russia*
[2]*St. Petersburg State Polytechnical University, 195251 St. Petersburg, Russia*

(Received 18 February 2009; accepted 4 May 2009; published online 11 June 2009)

A microscopic mechanism of holes injection from metallic electrode into organic molecular solids (OMSs) in high electric field is proposed. A case is considered of ionization energy of the molecules exceeding work function of the metal. It is shown that the main contribution to the injection current comes from direct isoenergetic transitions (without interaction with phonons) from localized states in OMS to empty states in the metal. Strong dependence of the injection current on applied voltage originates from variation of the number of empty states available in the metal rather than by modification of the interface barrier shape. © *2009 American Institute of Physics*.
[DOI: 10.1063/1.3147858]

The organic molecular solids (OMSs) are widely used in modern micro- and optoelectronics. Light-emitting diodes and field effect transistors have been fabricated on the basis of these materials.[1] The tendency of further expansion of the potential applications for the OMS demands complete understanding of the underlying physics. However, some issues still remain unclear. One of them addressed by the present paper is the conductivity of the OMS films in a high electric field. The large energy band gap of ≈ 3 eV for OMS provides rather low concentration of free intrinsic charge carriers. Therefore, these materials are dielectrics in a weak electric field. In a high electric field, the charge carriers can be injected from electrodes and produce an electric current. The injection level is determined by the barrier formed at metal-dielectric interface. The injection current (electron and hole) from the metal into appropriate bands of crystal inorganic dielectric or semiconductor is usually obtained by the equations similar to those describing field and thermionic emission from metal to vacuum.[2] The effective potential barrier height at the interface for the electron injection is assumed to be the difference between the work function of the metal electrode and the electron affinity of the OMS.[3,4] Similar equations are often applied to the description of carriers injection into OMSs.[5–8] However, for these materials band theory of crystalline solids is not applicable due to weak interaction between molecules and their conductivity being of hopping character. Therefore, recently more attention is called to the microscopic mechanism of the injection into OMS, in particular to the tunneling of the charge carriers from metal to OMS with high concentration of the localized states having Gaussian energy distribution.[6–12] The results obtained for injection of electrons are usually directly applied also to the holes injection (see, for example, Refs. 10 and 11). This seems to be rather unproved because the shape of the barrier in the case of electron injection is different from that in the case of hole injection. The specific of the hole injection into OMS was first discussed in Ref. 13. In that paper, the holes injection was considered as ionization of molecules close to the surface of metallic anode. The ionization occurred due to tunnel transition of an electron from the upper molecular orbital [highest occupied molecular (HOMO) level] to an empty electron level in metal. Unlike the case of electron injection for the hole injection, the potential barrier at the interface in a high electric field has a trapezoidal shape. The effective height of the barrier is determined by the ionization energy of a localized state rather than by the difference between the ionization energy and work function of the metal. Calculation within this approach was performed in Ref. 14. The dependence of the injection current on the applied electric field obtained in Ref. 14 appeared to be of somewhat modified Fowler–Nordheim type. It should be noted that in Ref. 14, the tunnel transitions considered are from monoenergetic states of the OMS to the Fermi level of the metal, i.e., both energy distribution of the OMS localized states and the temperature-dependent Fermi distribution in metal are neglected. This simplification does not allow obtaining proper dependence of the injection current on temperature and also modifies the dependence on the electric field. In present work, we consider electron transitions from molecular HOMO levels of organic materials into metal (i.e., the holes injection) for the case when the molecular levels have substantially lower energy than the Fermi level of the metal. It is assumed that the potential barrier at metal-OMS interface is narrow and requires a single jump of the electron. For the barrier, we also take account of the Coulomb interaction between electron, hole, and their mirror images in metal. The barrier shape in the electric field F is given by[15]

$$U(x,x_i,F) = E_F + \varphi + exF - \frac{e^2}{16\pi\varepsilon\varepsilon_o x} - \frac{e^2}{4\pi\varepsilon\varepsilon_o(x_i - x)} + \frac{e^2}{4\pi\varepsilon\varepsilon_o(x_i + x)}, \quad (1)$$

where x_i is the distance of a localized state (denoted by index i) from anode, E_F denotes Fermi energy of the electrode, and φ is the work function of the electrode. The first and second terms in Eq. (1) determine the barrier height at the interface in the absence of the electric field, the third term accounts for the influence of the electric field on the charge energy at the distance x from anode, the fourth term stands for the interaction of electron with its mirror image in metal, the fifth term is the interaction between the ion and electron, and the sixth is the interaction of electron with ion's mirror image.

a)Electronic mail: igor@quantum.ioffe.ru.

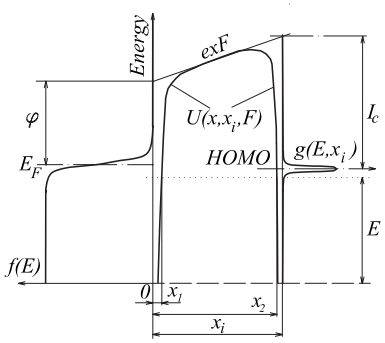

FIG. 1. The shape of potential barrier controlling the holes injection from metal into OMS.

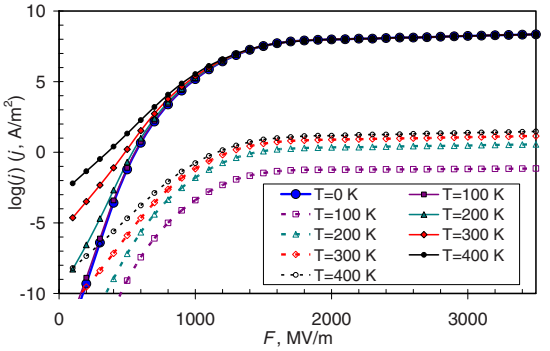

FIG. 2. (Color online) Dependence of the current density on electric field for different values of temperature for direct transitions (solid line) and transitions with phonon absorption (dashed line).

The shape of the barrier at the metal-OMS interface is shown in Fig. 1. In this work, we calculate the field and temperature dependence of injection current density in high electric field conditions. It will be shown that for the case under study, the strong dependence of injection current on applied voltage is not caused by the distortion of the barrier shape but rather originates from the tradeoff between the tunneling distance and the number of the empty states available in metal for the isoenergetic tunneling. The calculation of the tunneling injection current was carried out in the framework of Bardeen's theory.[16] For the tunneling current density of the electron transitions from organic material into metal electrode we then obtain

$$J = e\frac{2\pi}{\hbar}V\int_0^\infty dE\int_a^\infty dx|\tilde{T}(x)|^2 Z(E)g(x,E) \times[1-f(E)]f_{\mathrm{loc}}(x,E), \quad (2)$$

where e is the elementary charge, $\tilde{T}(x)$ is the Bardeen's tunneling matrix element describing tunneling from a localized state at a distance x into the metal electrode, $Z(E)$ is the density of states in metal, $f(E)$ is Fermi distribution in metal, a is the minimal distance from the electrode to the localized state in OMS, $f_{\mathrm{loc}}(x,E)$ is the filling factor of the localized states in organic material, and $g(x,E)$ is the density of localized states in the organic material.

It is worth noting that when the energy states in OMS underlie Fermi level in metal, direct isoenergetic tunneling transitions can be substantially suppressed by the factor $[1-f(E)]$ [Eq. (2)]. In other words, there can be not enough empty states for the tunneling electrons from OMS. As soon as we consider this very case, it is important to estimate the contribution of indirect tunneling processes mostly those involving phonons. We give an example of such estimation for acoustic phonons in metal. Calculation of indirect transitions rate using second-order perturbation theory with account of electron-phonon interaction and tunneling meets a certain difficulty. The tunneling transitions in the Bardeen's approach occur between the states of the same energy and in this way differ from the conventional quantum-mechanical transitions. This leads to singularities in energy denominators in the second order perturbation theory. For the calculation of the tunneling rates, we used another approach. The tunneling is treated by energy splitting of the metal-OMS system eigenstates by a value $\tilde{T}$. Then the electrons tunneling rate is calculated within the first order of the perturbation theory. Finally we obtained the following expression for the phonon assisted tunnel current density,

$$J = V\frac{\pi^2 e\Xi^2 m^2}{s\rho\hbar^4}\int_0^\infty dE\int_a^\infty dx|\tilde{T}(x)|^2 Z(E)g(x,E) \times\frac{1-f(E+2s\sqrt{2mE})}{e^{(2s\sqrt{2mE})/(kT)}-1}f_{\mathrm{loc}}(x,E), \quad (3)$$

where Ξ stands for deformation potential constant, indicating the efficiency of interaction between electrons and acoustic phonons, s is a sound velocity in the metal, ρ is the metal density, m is a free electron mass, k is the Boltzmann constant, and T is the temperature.

Below we shall consider particular case of Eqs. (2) and (3) assuming all the holes injected into organic material instantly reach the cathode, in this case $f_{\mathrm{loc}}(x,E)=1$ (injection limited current). The calculation of the current density according to Eqs. (2) and (3) was performed by means of numerical integration with the following parameters: $\varepsilon=3$, $E_F=5$ eV, and $\varphi=5$ eV. The Gaussian spectrum of OMS localized states (HOMO levels) was assumed, i.e.,

$$g(E,x_i) = \frac{N_{\mathrm{loc}}}{\sqrt{2\pi}\sigma}\exp\left\{-\frac{[ex_iF+E_F+\varphi-I_C-E]^2}{2\sigma^2}\right\}, \quad (4)$$

where σ is the distribution dispersion, N_{loc} is a concentration of the localized states, I_c is ionization energy of the OMS molecules. The calculations were performed for $N_{\mathrm{loc}}=10^{21}$ cm^{-3} and $\sigma=0.1$ eV. $E=0$ corresponds to the bottom of the conductance band of the metal.

Figure 2 shows the dependencies of the current density on the electric field calculated for $I_c=6$ eV and $a=0.6$ nm for different temperatures. Solid lines correspond to the current calculated using Eq. (2), which takes into account only direct electron transitions from HOMO levels to the metal and dashed lines correspond to the current calculated using Eq. (3) accounting for only indirect transitions with phonon absorption. It can be seen that for the temperature being in the range from 0 to 400 K and for any value of the electric field the current of direct transitions substantially exceeds that of indirect transitions. This result allows to conclude that for the processes of hole injection, the indirect transitions can be neglected and the current can be calculated using Eq. (2).

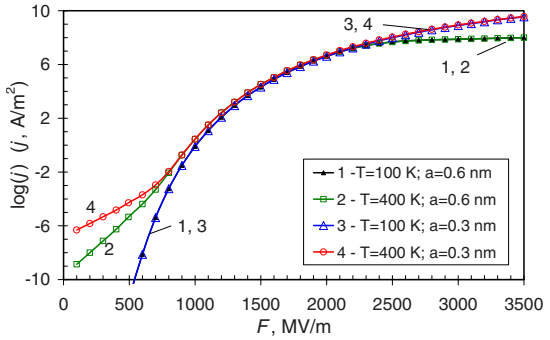

FIG. 3. (Color online) Dependence of the current density on electric field for different values of temperature and minimal hopping distance.

For the dependencies $j(F)$ shown in Fig. 2, two characteristic regions can be distinguished. At relatively low field $F \leq 1500$ MV/m, the current density rapidly increases with the field and is significantly affected by the temperature. As the field is increased further, the increase of j is slowed down so that in high electric field it weakly depends on the field and almost does not depend on the temperature.

Figure 3 shows $j(F)$ dependencies calculated for $I_c = 6.5$ eV for different values of the minimal distance from electrode a and the temperature. The figure demonstrates that influence of a on j is different for different ranges of F.

Let us recall that in zero field, the maximum of localized states density $g(E)$ lies well beyond the Fermi level of the metal. Therefore at zero temperature and zero electric field, the tunneling from OMS states is forbidden because there are no empty states available in metal. The external electric field shifts the OMS localized states up on energy scale toward the Fermi level of the metal while the temperature spreads the Fermi distribution in metal. Both factors provide empty states and in this way enhance the tunneling. At that, the role of the minimal distance a from the OMS states to metal appears to be different. In high electric field ($F > 2500$ MV/m), the electrostatic energy of all the OMS states is high enough being close to or higher than the Fermi level of the anode. Hence, the tunneling from any of them is allowed being obviously most efficient from those closely located to the metal-OMS interface. Thus, in this range of the electric field the current is crucially dependent on the minimal distance a (curves 3 and 4 differ from curves 1 and 2 in Fig. 3) being insensible to the temperature (curves 1 and 2 coincide as well as curves 3 and 4 in Fig. 3. The direct current shows no dependence on the temperature in high field in Fig. 2). On the contrary, in the low field ($F < 1500$ MV/m), the current behavior depends on the temperature. If the temperature is low (see curves 1 and 3 corresponding to $T = 100$ K) the Fermi distribution in metal does not provide enough empty states for the tunneling from the OMS states, which are close to the anode. However, the tunneling is allowed from OMS states located farther from the interface because they are higher on the energy scale due to the electric field. Consequently, the minimal distance a doesn't play a role in this regime illustrated by the curves 1 and 3 in Fig. 3, which coincide in low field. The situation for the high temperature (represented by curves 2 and 4 corresponding to $T = 400$ K) is different. The energy of the OMS states which are near the interface is still well beyond the Fermi level of the electrode. Despite that the tunneling is allowed due to spreading of the Fermi distribution by the temperature. Thus, the role of minimal distance a is also important here (see curves 2 and 4). In the mid field range $2500 \text{ MV/m} > F > 1500 \text{ MV/m}$, the difference between the curves is hardly pronounced in the given scale. In this regime the main contribution to the injection current comes from the tunneling from OMS states located farther then the minimal distance a and having their energy within the band of kT width around the Fermi level. Therefore, both the dependencies on a and on the temperature are much weaker than in the extreme regimes.

The results of the modeling can be compared to the experimental data found in the literature for the hole conductivity in OMS. The comparison shows qualitative agreement in wide range of temperature and electric field values. Our modeling reproduces characteristic features of I-V dependencies, i.e., the effect of the temperature in weak electric field,[17] the transition to the Fowler–Nordheim-like dependence and current saturation in a strong field.[8,18]

In the present work, we have theoretically considered hole injection from the metal into OMS with account of real shape and height of the potential barrier at metal-OMS interface. The obtained equation allows us to describe the hole injection in a wide temperature range and electric field values. The role of the indirect tunneling processes with phonon absorption was analyzed for the first time. It was shown that the injection current is governed mostly by the direct transitions of electrons from molecular HOMO levels to empty states in metal. The contribution of the processes with phonon absorption is negligibly small.

The work has been supported in part by Leading Scientific Schools (Grant No. N 1972.2008.2), Russian Foundation for Basic Research, scientific programs of RAS.

[1] S. R. Forrest, Nature (London) **428**, 911 (2004).
[2] A. G. Chynoweth, Prog. Semicond. **4**, 95 (1960).
[3] I. D. Parker, J. Appl. Phys. **75**, 1656 (1994).
[4] J. H. Burroughes, D. D. C. Bradley, A. R. Brown, R. N. Marks, K. Mackay, R. H. Friend, P. L. Burns, and A. B. Holmes, Nature (London) **347**, 539 (1990).
[5] P. Yan, Y. Zhou, and N. Yoshimura, Jpn. J. Appl. Phys., Part 1 **39**, 3492 (2000).
[6] D. Liu and K. C. Kao, J. Appl. Phys. **69**, 2489 (1991).
[7] N. R. Tu and K. C. Kao, J. Appl. Phys. **85**, 7267 (1999).
[8] C. Ganzorig, M. Sakomura, K. Ueda, and M. Fujihira, Appl. Phys. Lett. **89**, 263501 (2006).
[9] M. A. Abkowitz, H. A. Mizes, and J. S. Facci, Appl. Phys. Lett. **66**, 1288 (1995).
[10] H. Bässler, Phys. Status Solidi B **175**, 15 (2006).
[11] R. Agrawal, P. Kumar, S. Ghosh, and A. K. Mahapatro, Appl. Phys. Lett. **93**, 073311 (2008).
[12] V. I. Arkhipov, U. Wolf, and H. Bässler, Phys. Rev. B **59**, 7514 (1999); V. I. Arkhipov, E. V. Emelianova, Y. H. Tak, and H. Bässler, J. Appl. Phys. **84**, 848 (1998); V. I. Arkhipov, H. von Seggern, and E. V. Emelianova, Appl. Phys. Lett. **83**, 5074 (2003).
[13] V. A. Zakrevskii and N. T. Sudar, Sov. Phys. Solid State **34**, 1727 (1992).
[14] T. Ouisse, Eur. Phys. J. B **22**, 415 (2001).
[15] A. L. Suvorov and V. V. Trebukhovskii, Usp. Fiz. Nauk **107**, 657 (1972) [in Russian].
[16] J. Bardeen, Phys. Rev. Lett. **6**, 57 (1961).
[17] T. van Woudenbergh, P. W. M. Blom, M. C. J. M. Vissenberg, and J. N. Huiberts, Appl. Phys. Lett. **79**, 1697 (2001).
[18] C. C. Hsiao, C. H. Chang, T.-H. Jen, M.-C. Hung, and S.-A. Chen, Appl. Phys. Lett. **88**, 033512 (2006).

PUBL. 4

I. V. ROZHANSKY, N. S. AVERKIEV, and E. LÄHDERANTA, TUNNELING MAGNETIC EFFECT IN HETEROSTRUCTURES WITH PARAMAGNETIC IMPURITIES, *Physical Review B*, **85**, 075315, 2012.

PHYSICAL REVIEW B **85**, 075315 (2012)

Tunneling magnetic effect in heterostructures with paramagnetic impurities

I. V. Rozhansky,[1,2,*] N. S. Averkiev,[1] and E. Lähderanta[2]
[1]*A.F. Ioffe Physical Technical Institute, Russian Academy of Sciences, 194021 St. Petersburg, Russia*
[2]*Lappeenranta University of Technology, P.O. Box 20, FI-53851, Lappeenranta, Finland*
(Received 1 November 2011; published 21 February 2012)

An effect of paramagnetic impurity located in a vicinity of a quantum well (QW) on spin polarization of the carriers in the QW is analyzed theoretically. Within the approach of Bardeen's tunneling Hamiltonian the problem is formulated in terms of the Anderson-Fano model of configuration interaction between a localized hole state at Mn and continuum of heavy hole states in the InGaAs-based QW. The hybridization between the localized state and the QW leads to resonant enhancement of interband radiative recombination. The splitting of the configuration resonances induced by splitting of the localized state in magnetic field results in circular polarization of light emitted from the QW. The developed theory is capable of explaining known experimental results and allows for calculation of the photoluminescence spectra and dependence of integral polarization on temperature and other parameters.

DOI: 10.1103/PhysRevB.85.075315 PACS number(s): 75.75.−c, 78.55.Cr, 78.67.De

I. INTRODUCTION

Various phenomena based on the interference of a bound quantum-mechanical state and continuum states have been intensively studied since the famous paper by Fano[1] rated among the most relevant works of 20th century.[2] He suggested a theoretical approach often regarded as the Fano-Anderson model or Fano configuration interaction which succeeded in explaining asymmetric resonances observed in atomic spectroscopy experiments. It further appeared that numerous examples of Fano resonances existed in atomic and nuclear physics, condensed matter physics, and optics.[2] The coexistence of the discrete energy level and the continuum states within the same energy range is also quite common in low-dimensional semiconductor structures.[2–5] Of particular interest nowadays are the structures having a quantum well (QW) and a ferromagnetic or paramagnetic layer located in the vicinity of the QW. Such structures are believed to combine high mobility of the carriers in the QW and magnetic properties provided by the magnetic layer. In particular, an exchange interaction with ferromagnetic layer leads to spin polarization of holes.[6] For GaAs-based structures with an Mn δ layer the holes probably play an important role in promoting a ferromagnetic state of the Mn layer.[7,8] The system considered in the present work consists of a GaAs-based heterostructure with $In_xGa_{1-x}As$ QW ($x = 0.1 - 0.2$) and a δ layer of paramagnetic acceptors (Mn) located at a distance of several nanometers from the QW. A number of recent experiments show that the Mn δ layer gives rise to circular polarization of the photoluminescence (PL) from the QW in an external magnetic field applied perpendicular to the QW plane.[9,10] It was found that the PL intensities at wavelength corresponding to interband direct transitions in the QW differ for opposite circular polarizations. If Mn is replaced by a nonmagnetic acceptor (carbon) the polarization decreases dramatically. Thus the polarization is not due to the intrinsic g factor of the two-dimensional (2D) carriers in the QW which in this way is proved to be small. On the contrary, the holes localized at Mn do have $g \approx 3$ (see Ref. 11) and possibly can penetrate into the QW by means of the quantum-mechanical tunneling which is expected to be of a resonant type if the energy of the localized state coincides with that of the free 2D hole in the QW. The purpose of our work is to establish a proper theory capable of describing the polarization of the PL emitted from the QW induced by paramagnetic impurity by means of weak tunnel coupling. Figure 1 shows schematically a band diagram of the considered system. To study tunnel hybridization between the localized hole state at Mn and the 2D continuum states in the QW we utilize the Fano configuration interaction approach[1] and show how this hybridization reveals itself in the photoluminescence at the QW wavelength. In our theory the circular polarization in the external magnetic field appears in the following manner. An external magnetic field splits the localized level of the hole sitting at Mn. The splitting Δ could be either due to a conventional Zeeman effect or caused by the p-d exchange interaction with Mn electrons. For each of the split levels the tunnel coupling occurs with only one (of the two having opposite spin projections) 2D heavy hole subbands in the QW. As a result the distribution of holes appears to be different in the two subbands resulting in different intensities of σ^+ and σ^- polarized light emitted from the QW.

We have to mention here that while the considered mechanism based on the holes tunneling is quite naturally expected in the p-type system, there are other mechanisms that might contribute to the experimentally observed polarization. One of those is nonresonant tunneling of electrons from QW to Mn followed by recombination with the holes localized at Mn. Up to now it still remains unclear which of the mechanisms has larger contribution to the polarization in experiments on photoluminescence.[9,10] In our paper we focus only on the mechanism related to the holes' resonant tunneling and therefore for making things more clear we assume that the 2D electrons are localized in the QW and do not penetrate to the impurity site (e.g., due to the high offset of the conductance band).

The paper is organized as follows. In Sec. II we consider one bound hole state at the acceptor and the 2D states in the QW being decoupled from each other. In Sec. III we study hybridization of the bound state with the 2D continuum states by means of tunnel configuration interaction. Finally, the effect

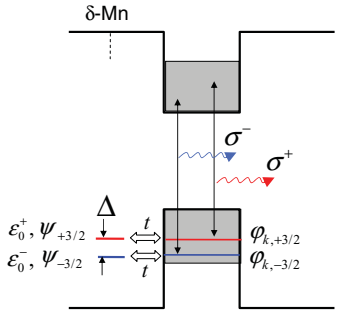

FIG. 1. (Color online) Mechanism of polarization of the luminescence. The localized hole levels split in magnetic field. Each of them effectively couples with the 2D holes having certain projection of angular momentum. Shifted positions of the resonances with account for temperature distribution of the holes cause the difference in intensities of circular polarizations σ^+, σ^-.

of the hybridization on the PL polarization in the magnetic field is discussed in Secs. IV and V.

II. HOLE STATES AT ACCEPTOR AND IN QUANTUM WELL

In this section we consider the bound state of a hole at an acceptor and the 2D QW states independently as if they were separated by an infinitely wide potential barrier. Nevertheless, it is worth remembering that the whole system under study (impurity + QW) has cylindrical symmetry with the cylindrical axis z directed normally to the QW plane and going through the impurity center. Thus for further calculations it will be most convenient to represent the QW states in cylindrical coordinates rather than as plane waves. In this case each state is characterized by the wave number k and the cylindrical harmonic number l. The corresponding wave function normalized by a circle of an area S is given by

$$\varphi_{kl}(\rho,\theta,z) = \eta(z)\frac{\pi^{1/4}}{\sqrt{2}}\frac{\sqrt{k}}{S^{1/4}}J_l(k\rho)e^{il\theta}, \tag{1}$$

where $J_l(k\rho)$ is the Bessel function of order l, ρ and θ are the polar coordinates in the QW plane, $\eta(z)$ is the envelope function of size quantization in the z direction. The wave function is normalized to unity. Firstly, let us treat this continuum as a set of discrete states, each characterized by its energy ε_k and its wave function φ_{kl}. Considering the 2D carriers as free implies that the magnetic field applied to the QW is nonquantizing. The validity of this assumption is discussed in Sec. V. Below we consider $In_xGa_{1-x}As$ QW having only one level of size quantization for the heavy holes; we neglect the light holes being split off due to the size quantization. The basis of Bloch amplitudes to be used is formed of the states with certain projection of the total angular momentum $J = 3/2$ on the z axis which is perpendicular to the QW plane:

$$(e_{3/2},\ e_{1/2}\ ,e_{-1/2}\ ,e_{-3/2}). \tag{2}$$

The wave functions describing the heavy holes in this basis have the form,

$$\varphi_{kl,-\frac{3}{2}} = \begin{pmatrix} 0 \\ 0 \\ 0 \\ \varphi_{kl}(\rho) \end{pmatrix}, \quad \varphi_{kl,+\frac{3}{2}} = \begin{pmatrix} \varphi_{kl}(\rho) \\ 0 \\ 0 \\ 0 \end{pmatrix}. \tag{3}$$

The kinetic energy of the 2D QW state is related to k as

$$\varepsilon = \frac{\hbar^2 k^2}{2m'_{hh}}, \tag{4}$$

where m'_{hh} is the in-plane heavy hole mass in the QW.

In order to determine wave function ψ of a hole localized at an acceptor one should consider the kinetic part of the Luttinger Hamiltonian and attractive potential of the acceptor $U(r)$. The spherically symmetrical potential preserves the symmetry Γ_8, thus the ground state is fourfold degenerate and can be classified by angular momentum projection. The eigenfunctions of Luttinger Hamiltonian with spherically symmetric attractive potential can be explicitly found in the model of zero radius potential.[12] In the basis of the Bloch amplitudes they are expressed as follows:

$$\begin{aligned}
\psi_{+\frac{3}{2}} &= \begin{pmatrix} R_0Y_{00} + \frac{1}{\sqrt{5}}R_2Y_{20} \\ -\frac{2}{\sqrt{10}}R_2Y_{21} \\ \frac{2}{\sqrt{10}}R_2Y_{22} \\ 0 \end{pmatrix}, \\
\psi_{+\frac{1}{2}} &= \begin{pmatrix} \frac{2}{\sqrt{10}}R_2Y_{2,-1} \\ R_0Y_{00} - \frac{1}{\sqrt{5}}R_2Y_{20} \\ 0 \\ \frac{2}{\sqrt{10}}R_2Y_{22} \end{pmatrix}, \\
\psi_{-\frac{1}{2}} &= \begin{pmatrix} \frac{2}{\sqrt{10}}R_2Y_{2,-2} \\ 0 \\ R_0Y_{00} - \frac{1}{\sqrt{5}}R_2Y_{20} \\ \frac{2}{\sqrt{10}}R_2Y_{21} \end{pmatrix}, \\
\psi_{-\frac{3}{2}} &= \begin{pmatrix} 0 \\ \frac{1}{\sqrt{5}}R_2Y_{2,-2} \\ -\frac{2}{\sqrt{10}}R_2Y_{2,-1} \\ R_0Y_{00} + \frac{1}{\sqrt{5}}R_2Y_{20} \end{pmatrix}.
\end{aligned} \tag{5}$$

Here

$$\begin{aligned}
R_0 &= C_0\left(\frac{\beta}{r}e^{-qr\sqrt{\beta}} + \frac{e^{-qr}}{r}\right), \\
R_2 &= C_0\left(\frac{\beta}{r}e^{-qr\sqrt{\beta}}\left(1 + \frac{3}{qr\sqrt{\beta}} + \frac{3}{q^2r^2\beta}\right)\right. \\
&\quad \left. - \frac{e^{-qr}}{r}\left(1 + \frac{3}{qr} + \frac{3}{q^2r^2}\right)\right), \\
C_0 &= \sqrt{\frac{q}{\beta^{3/2}+1}}, \quad q = \sqrt{\frac{2m_{hh}E_0}{\hbar^2}}, \quad \beta = \frac{m_{lh}}{m_{hh}}.
\end{aligned} \tag{6}$$

E_0 is the binding energy of the hole at the acceptor; Y_{lm} are the spherical harmonics. m_{lh},m_{hh}, respectively, are the bulk light hole mass and the heavy hole mass in GaAs. Note that the radial part of all nonzero components of the wave functions (5) have two characteristic decay lengths, the largest of the

two being always determined by the light hole mass $m_{lh} \approx 0.08\, m_0$, where ($m_0$ is the free electron mass).

III. TUNNELING BETWEEN ACCEPTOR AND QUANTUM WELL

With ionization energy of Mn being of the order of $E_0 \sim 100$ meV and the width of the potential barrier separating the Mn δ layer from the QW of the order of $d \sim 3$ nm one can estimate the tunneling transparency of the barrier for the light hole as $\exp(-2\frac{\sqrt{2m_{lh}E_0}}{\hbar}d) \approx 0.05$. With that, the barrier appears to be weakly transparent and one can get use of the so-called tunneling Hamiltonian (or transfer Hamiltonian) formalism originally proposed by Bardeen.[13] In this approach the total Hamiltonian of the system is expressed as follows:

$$H = \varepsilon_0 a^+ a + \sum_{k,l} \varepsilon_k c_{kl}^+ c_{kl} + \sum_{k,l} (T_{kl} c_{kl}^+ a + T_{kl}^* a^+ c_{kl}), \qquad (7)$$

where a^+, a are the creation and annihilation operators for the localized state characterized by its energy ε_0, and c_{kl}^+, c_{kl} are the creation and annihilation operators for the 2D QW state characterized by its wave number k and the cylindrical harmonic number l. The energy here and below is measured from the 2D hole size quantization level, therefore ε_k is given by (4). The tunneling parameter T_{kl} describes the tunnel coupling between the localized state and the QW state. Our analysis will be focused on the case of the hole's kinetic energy being substantially less then the binding energy E_0 (i.e., $k \ll q$). From Eqs. (1), (3), and (5) it follows that for this case the overlap integrals involving φ_{kl} with $l \neq 0$ are suppressed by a small parameter k/q. It means that for the studied case only the zeroth cylindrical harmonic should be taken into account. For $k \ll q$ it is also reasonable to assume that $T_k \equiv T_{k0}$ does not depend on k. Still, its rapidly decreasing behavior for $k \gg q$ has to be kept in mind when it provides convergence for integration over k. Interaction with only the zeroth harmonic means that the continuum spectrum modified by tunneling is nondegenerate. This fact is not essential for the qualitative results obtained below, but simplifies the calculations. Finally, we conclude that the tunneling configuration interaction to be accounted for is only between $\varphi_{k0,-\frac{3}{2}}$ and $\psi_{-\frac{3}{2}}$, and between $\varphi_{k0,+\frac{3}{2}}$ and $\psi_{+\frac{3}{2}}$. Both are governed by the same tunneling parameter T_k which in the framework of the Bardeen's approach can be estimated as

$$T_k \sim \frac{\hbar^2}{2m_0} \frac{q\sqrt{k}}{S^{1/4}} \exp(-qd\sqrt{\beta}). \qquad (8)$$

The tunneling parameter T_k exponentially depends on the barrier thickness with the light hole mass entering the exponent index.

The transfer Hamiltonian (7) with known tunneling parameter (8) allows one to apply the Fano-Anderson model[13] and construct eigenfunctions Ψ of the whole system from those of the localized state ψ and the QW states φ_k:

$$\Psi(E) = \nu_0(E)\psi + \sum_k \nu_k(E)\varphi_k, \qquad (9)$$

where E denotes the energy of the state Ψ. Here φ_k are the QW wave functions of the zeroth cylindrical harmonic $\varphi_k = \varphi_{k0}$.

Plugging (9) into the stationary Schrodinger equation,

$$H\Psi = E\Psi,$$

with H being the effective Hamiltonian (7) one gets the following system of linear equations:

$$\nu_0\varepsilon_0 + \sum_k \nu_k T_k^* = E\nu_0, \qquad \nu_k\varepsilon_k + T_k\nu_0 = E\nu_k. \qquad (10)$$

Solving the eigenvalue problem for (10) one can get the spectrum and the coefficients ν_0, ν_k (i.e., the eigenfunctions of the system). Transition from the discrete set of states $\nu_k(E)$ to the continuous function $\nu(\varepsilon, E)$ is straightforward (as the continuum states are nondegenerate we can use the energy ε instead of k as the quantum number). Instead of (9) and (10) we write

$$\Psi(E) = \nu_0(E)\psi + \int_0^\infty \nu(E,\varepsilon)\varphi(\varepsilon)d\varepsilon, \qquad (11)$$

$$\begin{aligned} \nu_0(E)\varepsilon_0 + \int_0^\infty t(\varepsilon)\nu(E,\varepsilon)d\varepsilon &= E\nu_0(E), \\ \nu(E,\varepsilon)\varepsilon + t(\varepsilon)\nu_0(E) &= E\nu(E,\varepsilon). \end{aligned} \qquad (12)$$

The normalizations for ψ and $\varphi(\varepsilon)$ are

$$\langle\psi(\varepsilon_0)|\psi(\varepsilon_0)\rangle = 1, \quad \langle\varphi(\varepsilon)|\varphi(\varepsilon')\rangle = \delta(\varepsilon - \varepsilon'). \qquad (13)$$

With the chosen normalization, the discrete tunneling parameter T_k and the one entering (12) are related as follows:

$$T_k^2 N_0(\varepsilon) = t^2(\varepsilon), \qquad (14)$$

where

$$N_0(\varepsilon) = \sqrt{\frac{m'_{hh}S}{2\pi^3\varepsilon\hbar^2}} \qquad (15)$$

is the density of states with the zeroth cylindrical harmonic. The discrete system (10) is an eigenvalue problem, but the continuous problem (12) is not. In the present work we consider the case of the localized energy level lying within the range of the continuum states: $\varepsilon_0 \gg t^2$. For this case the solution of (12) can be obtained in the form,[1]

$$\begin{aligned} \nu_0{}^2(E) &= \frac{t^2(E)}{\pi^2 t^4(E) + (E - \widetilde{\varepsilon}_0)^2}, \\ \nu(E,\varepsilon) &= \nu_0(E)\left(P\frac{t(\varepsilon)}{E-\varepsilon} + Z(E)t(E)\delta(E-\varepsilon)\right), \end{aligned} \qquad (16)$$

where

$$Z(E) = \frac{E - \varepsilon_0 - F(E)}{t^2(E)}, \quad F(E) = P\int_0^\infty \frac{t^2(\varepsilon)}{E-\varepsilon}d\varepsilon. \qquad (17)$$

P stands for the principal value and $\widetilde{\varepsilon}_0$ is the center of configuration resonance, which appears to be slightly shifted from ε_0:

$$\widetilde{\varepsilon}_0(E) = \varepsilon_0 + F(E). \qquad (18)$$

Because of $k \ll q$ it is reasonable to treat $t = \text{const}$ everywhere, except for (17) where decrease of t at $E \to \infty$ is necessary for the integral convergence. In order to analyze the influence of the configuration interaction on the luminescence spectra we have to calculate matrix element of the operator

$\hat{M}$ describing interband radiative transitions between the hybridized hole wave function $\Psi(E)$ and the wave function of an electron in the QW of the conductance band $\xi_{k_e l_e}$; here k_e is the electron wave number, and l_e is the cylindrical harmonic number analogously to (1). As was already discussed in Sec. I we assume that (a) there are no radiative transitions between the localized hole wave function ψ and the 2D electron wave function $\xi_{k_e l_e}$, (b) the interband radiative transitions between the free 2D states in the QW are direct. The appropriate matrix elements are therefore given by

$$\langle \xi_{k_e l_e} | \hat{M} | \psi \rangle = 0, \tag{19}$$

$$M_0 = \langle \xi_{k_e l_e} | \hat{M} | \varphi_{kl} \rangle = u_k \delta(k - k_e) \delta_{l,l_e}, \tag{20}$$

where u_k is the appropriate dipole matrix element. With use of Eqs. (11), (16), (19), and (20) we arrive at the matrix element for the transitions between the states $\Psi(E)$ and $\xi_{k_e 0}$ (according to previous notes this matrix element differs from M_0 only for the zeroth cylindrical harmonic):

$$M = \langle \xi_{k_e 0} | \hat{M} | \Psi(E) \rangle = \nu(E, \alpha\varepsilon_e) u(\alpha\varepsilon_e), \tag{21}$$

$\alpha = m_e/m'_{hh}$, where m_e is the effective in-plane electron mass, $\varepsilon_e = \hbar^2 k_e^2/2m_e$. The particular form of M (21) prevents from calculation of the ratio M^2/M_0^2 as done in the classical Fano resonance calculations.[1] The latter assume unperturbed matrix element M_0 to be constant. This is obviously not the case for the direct optical transitions demanding momentum conservation (20). In our case the ratio M^2/M_0^2 doesn't readily give a physically meaningful result due to the delta function in Eq. (16); one rather has to proceed to calculation of an observable. With the Fermi's Golden Rule for the transition probability we write

$$W(\hbar\omega) = \frac{2\pi}{\hbar} \int_0^\infty \int_0^\infty |M(E', \varepsilon_e)|^2 f_e(\varepsilon_e) f_h(E') \times \delta(E' + \varepsilon_e + E_g - \hbar\omega) dE' d\varepsilon_e, \tag{22}$$

where E_g is the bandgap, $\hbar\omega$ is the energy of the radiated photon, and f_e, f_h are the energy distribution functions for the electrons and holes, respectively. To deal properly with the delta function entering M^2 in Eq. (21) and emerging in Eq. (22) we pass on to averaging $W(\hbar\omega)$ over a small spectral interval of the width Ω centered at ω_0:

$$\widetilde{W}(\hbar\omega_0) = \frac{1}{\Omega} \int_{\omega_0 - \Omega/2}^{\omega_0 + \Omega/2} W(\hbar\omega) d\omega.$$

Using Eqs. (21) and (16) we obtain

$$\widetilde{W}(\hbar\omega_0) = \frac{2\pi}{\hbar} \frac{1}{\hbar\Omega} \int_{\frac{\hbar\omega_0 - E_g - \hbar\Omega/2}{1+\alpha^{-1}}}^{\frac{\hbar\omega_0 - E_g + \hbar\Omega/2}{1+\alpha^{-1}}} \times \left[N(E') - \frac{1}{t^2(E')(\pi^2 + Z^2(E'))} \right] \times u^2(\alpha^{-1} E') f(E') dE', \tag{23}$$

where

$$f(E') = f_e(\alpha^{-1} E') f_h(E'). \tag{24}$$

The first term in brackets describes the transition rate for radiative recombination in the QW with no account for the tunneling, therefore $N(E')$ here is the total density of states (including not only the zeroth but all cylindrical harmonics):

$$N(E') = \frac{m'_{hh} S}{2\pi\hbar^2}. \tag{25}$$

Integration assuming the functions $\widetilde{\varepsilon}_0, t, u, f$ being constant within the range of integration [$t(E) \equiv t$, $u(E) \equiv u$ are assumed constant everywhere] yields

$$\widetilde{W}(\hbar\omega_0) = \frac{2\pi}{\hbar} u^2 f(E) \left[\frac{m'_{hh} S}{2\pi\hbar^2} - \frac{1}{\hbar\Omega\pi} \left[\arctan \frac{\Delta E + w}{\pi t^2} - \arctan \frac{\Delta E - w}{\pi t^2} \right] \right], \tag{26}$$

where

$$E = \frac{\hbar\omega_0 - E_g}{1 + \alpha^{-1}}, \quad \Delta E = E - \widetilde{\varepsilon}_0(E), \quad w = \frac{\hbar\Omega}{2(1 + \alpha^{-1})}. \tag{27}$$

As we consider the weak tunneling, t^2 is the smallest energy scale. In the vicinity of resonance,

$$\Delta E \in (-w + t^2, w - t^2), \tag{28}$$

expansion of Eq. (26) to the first order in t^2 gives

$$\widetilde{W}(\hbar\omega_0) = \frac{2\pi}{\hbar} u^2 f(E) \times \left[\frac{m'_{hh} S}{2\pi\hbar^2} - \frac{1}{\hbar\Omega} + \frac{1}{1 + \alpha^{-1}} \frac{t^2}{w^2 - (\Delta E)^2} \right]. \tag{29}$$

Note that Eq. (29) has term $-1/\hbar\Omega$ which does not depend on the tunneling. Its appearance is due to a peculiarity of the mathematics of the Fano model reflected in Eq. (16). When a noninteracting state with energy ε_0 is appended to the system so that ε_0 lies within its spectrum, one of the energy levels of the whole system becomes doubly degenerate. This fact is not properly accounted for in Eq. (16) and one state is lost. It should be added back manually to the spectral density by canceling the second term in Eq. (29). Treating the same issue in a different way, one should examine $\Delta\widetilde{W} = \widetilde{W} - \widetilde{W}_0$ instead of W itself, $\widetilde{W}_0$ being the unperturbed transition rate [Eq. (26) evaluated for $t = 0$]. In a similar way studying the ratio of matrix elements in the original Fano work[1] circumvents the disappearance of one level.

The results obtained for a single impurity can also be applied to an ensemble of impurities provided their interaction between each other is weak compared to the tunnel coupling with the QW. If the concentration of the impurities is low enough to produce only weak perturbation of the luminescence spectra, we can simply multiply the tunneling term by the number of impurities. After normalization by the area of the QW we finally get the spectral density of the luminescence intensity:

$$I(\hbar\omega_0) = \frac{2\pi}{\hbar} u^2 f(E) \left[\frac{m'_{hh}}{2\pi\hbar^2} + \frac{n}{\pi\hbar\Omega} \left[\arctan \frac{\Delta E - w}{\pi t^2} - \arctan \frac{\Delta E + w}{\pi t^2} - \pi \frac{\operatorname{sgn}(\Delta E - w) - \operatorname{sgn}(\Delta E + w)}{2} \right] \right], \tag{30}$$

where n is the surface concentration of the impurities. The last term in brackets corrects the lost level issue to provide exact canceling of the perturbation of the spectra at $t = 0$. For high concentration of the impurities the formula (30) may give a meaningless result (the intensity may become negative at some points). Indeed for high concentration the real physical picture becomes slightly different—interaction between the impurities splits their energy levels forming a small range of discrete levels, accordingly, the configuration resonances become slightly shifted. Taking this effect into account eliminates the puzzling behavior of (30) at high concentration but does not affect the answer for the polarization degree given in the next section.

The obtained analytical result (30) was verified by numerical simulation performed for the discrete system (10). The system was solved for 500 discrete levels with interlevel separation 10^{-5} eV, and the discrete tunneling parameter was taken as $T_k = 3.3 \times 10^{-5}$ eV; this corresponds to the continuous tunneling parameter being $t^2 = 10^{-4}$ eV. The other relevant parameters were as follows: $w = 5 \times 10^{-4}$ eV, $n = 10^{10}$ cm^{-2}, $m_e = 0.03\ m_0$, $m_{hh} = 0.5\ m_0$, $m'_{hh} = 0.15\ m_0$. In both calculations all the states were assumed fully occupied [i.e., the energy distribution function was kept $f(E) = 1$]. Analogously to (20) the matrix element for the discrete system was taken: $M_k(\varepsilon,\varepsilon_e) = u_k \delta_{k,k_e}\delta_{l,l_e}$. The calculation result presented in Fig. 2 demonstrates perfect agreement with the analytical expression (30) and confirms the validity of the latter. Both approaches demonstrate that the tunnel configuration interaction gives rise to the luminescence intensity within a certain spectral range (28) near ω_0. This increase is compensated by the decrease outside of this range as can be seen in Fig. 2. The width of the resonance is determined by Ω which has the meaning of spectral resolution of the measurement setup. However, for comparison with experimental spectra the inhomogeneous broadening should be accounted for as it usually exceeds the instrumental spectral resolution. An expression for the integral intensity

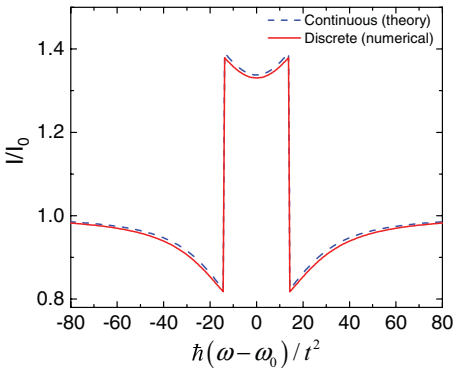

FIG. 2. (Color online) Modification of the luminescence spectrum by tunneling configuration interaction: numerical calculation for the discrete levels (solid line) and analytical formula (30) (dashed line).

over the whole spectra reads

$$I = \frac{2\pi}{\hbar}\int_0^\infty u^2 f(E)\left[\frac{m'_{hh}}{2\pi\hbar^2} - \frac{nt^2(E)}{\pi^2 t^4(E) + (E-\widetilde{\varepsilon}_0)^2} + n\delta(E-\widetilde{\varepsilon}_0)\right]dE. \tag{31}$$

This formula follows from (22) in the same way as (26) and (29) were obtained. The delta function here is added manually to treat the lost level issue—it provides canceling of the second term in the limit $t \to 0$ and thus gives the correct expression in the absence of the tunneling:

$$I_0 = \frac{2\pi}{\hbar}\int_0^\infty u^2 f(E)\frac{m'_{hh}}{2\pi\hbar^2}dE. \tag{32}$$

Note that the spectral width of the resonance Ω does not enter the expression for the integral intensity (31).

IV. POLARIZATION OF THE SPECTRA

The redistribution of the PL intensity near the energy corresponding to the bound level does not change the integral intensity but it causes the polarization in the magnetic field as illustrated by Fig. 1. The 2D holes with the projections of total angular momentum $j = +3/2$ and $j = -3/2$ recombine emitting, respectively, right- (σ^+) and left- (σ^-) hand circularly polarized light. In Sec. III it was shown that the heavy holes with $j = -3/2$ interact basically with the bound state $\psi_{-\frac{3}{2}}$. Let us denote the energy of this state as ε_0^-. The 2D holes with $j = +3/2$ interact in turn with $\psi_{+\frac{3}{2}}$ having the energy ε_0^+. An external magnetic field applied perpendicular to the QW plane would cause Zeeman splitting between ε_0^+ and ε_0^-. The splitting $\Delta = \varepsilon_0^+ - \varepsilon_0^-$ may also originate from the exchange interaction of the holes with spin-polarized Mn ions. The value of Δ in this case is determined by the exchange constant and depend on the degree of Mn spin polarization. The splitting of the localized energy level leads, in turn, to the splitting of the configuration resonance. Indeed, it follows from (17) that the splitting of the configuration resonances $\widetilde{\varepsilon}_0{}^+$ and $\widetilde{\varepsilon}_0{}^-$ corresponding to the localized levels ε_0^+ and ε_0^- is given by

$$\widetilde{\Delta} = \widetilde{\varepsilon}_0{}^+ - \widetilde{\varepsilon}_0{}^- = \Delta + t^2 \ln\left(1 + \frac{\widetilde{\Delta}}{\widetilde{\varepsilon}_0{}^-}\right). \tag{33}$$

Unless $\widetilde{\varepsilon}_0{}^-$ is too close to the valence band edge the last term in Eq. (33) can be neglected and $\widetilde{\Delta} \approx \Delta = \varepsilon_0^+ - \varepsilon_0^-$. The applicability of this result is limited to the case $\varepsilon_0 > \Delta$. This condition, in fact, means that neither of the split bound state levels go beyond the energy range of the 2D continuum. Our consideration will be always limited to this case. The difference in the resonances positions for the two 2D holes subbands leads to the difference in the luminescence intensity for σ^+ and σ^- polarizations if one takes into account the energy distribution functions for the holes and electrons (24).

Let I^+, I^- be the integral luminescence intensities for the circular polarizations σ^+ and σ^-, respectively. Assuming $|I^\pm - I_0| \ll I_0$ the integral polarization degree is given by

$$P = \frac{I^+ - I^-}{2I_0}.$$

With use of Eq. (31) this yields

$$P = \frac{n\pi\hbar^2}{m_{hh'}} \frac{f(\widetilde{\varepsilon}_0^-) - f(\widetilde{\varepsilon}_0^+) + \int_0^\infty \left[\frac{t^2(E)f(E)}{\pi^2 t^4(E) + (E-\widetilde{\varepsilon}_0^+)^2} - \frac{t^2(E)f(E)}{\pi^2 t^4(E) + (E-\widetilde{\varepsilon}_0^-)^2} \right] dE}{\int_0^\infty f(E)dE}. \tag{34}$$

The slow varying functions in the upper integrals can be replaced by their values taken at $\widetilde{\varepsilon}_0^-, \widetilde{\varepsilon}_0^+$, the tunneling parameter will be treated as a constant in the whole range of interest $t^2(E) \equiv t^2$.

Then expanding over t^2 gives for the first-order term:

$$P = \frac{n\pi\hbar^2 t^2}{m'_{hh}} \frac{f(\widetilde{\varepsilon}_0^-)(\widetilde{\varepsilon}_0^-)^{-1} - f(\widetilde{\varepsilon}_0^+)(\widetilde{\varepsilon}_0^+)^{-1}}{\int_0^\infty f(E)dE}. \tag{35}$$

The formula (35) leaves not much room for further simplification for the general case of $f_e(E), f_h(E)$ being two arbitrary Fermi distributions characterized by the chemical potentials μ_e, μ_h and the temperatures T_e and T_h, respectively. Let us analyze a few particular cases leading to compact analytical expressions for P. All the cases imply $\widetilde{\varepsilon}_0 > \Delta$. Firstly, let the holes be fully degenerate and both energies $\widetilde{\varepsilon}_0^-$ and $\widetilde{\varepsilon}_0^+$ lying well beyond the quasi-Fermi level of the holes so that $\mu_h - \widetilde{\varepsilon}_0^+ \gg \Delta$. In this case the distribution function of the holes can be considered as $F_h(E) = 1$ in the range $E \in (\widetilde{\varepsilon}_0^-, \widetilde{\varepsilon}_0^+)$ Assuming further the electrons to be nondegenerate the formula (35) is reduced to

$$P = P_1 e^{-\frac{\widetilde{\varepsilon}_0}{kT^*}} \sinh\frac{\Delta}{2kT^*}, \tag{36}$$

where

$$P_1 = \frac{2\pi n\hbar^2 t^2}{m'_{hh}\widetilde{\varepsilon}_0 kT^*}.$$

Here $T^* = \alpha T_e$. Exactly the same expression is valid for the case when both electrons and holes are nondegenerate. The only difference from the previously considered case is that now the effective temperature T^* is given by

$$\frac{1}{T^*} = \left(\frac{1}{\alpha T_e} + \frac{1}{T}\right).$$

The expression (36) is plotted in Fig. 3 for different values of the parameter $\gamma \equiv \Delta/\widetilde{\varepsilon}_0$. The polarization shows nonmonotonous behavior with increasing the temperature. In the discussed theory the polarization arises from splitting of the configuration resonance positions for σ^+ and σ^- spectra. The configuration resonance itself causes the redistribution of the transition rate in the vicinity of the resonance energy conserving the total rate, thus the net polarization is subject to the difference in occupation numbers for $\widetilde{\varepsilon}_0^-$ and $\widetilde{\varepsilon}_0^+$. The maximum integral polarization is therefore naturally expected when the derivative of the combined distribution function $f(E)$ reaches its maximum within the range $E \in (\widetilde{\varepsilon}_0^-, \widetilde{\varepsilon}_0^+)$. For the considered nondegenerate energy distribution function the maximum of the derivative is at $\widetilde{\varepsilon}_0$ when $\widetilde{\varepsilon}_0 = kT^*$ and the value of the derivative decreases with increase of $\widetilde{\varepsilon}_0$. This explains the overall decrease of the maximum polarization with decrease of γ in Fig. 3.

For another case we consider the electron distribution function f_e being nearly constant within the configuration resonances. This can be due to the electron nonequilibrium distribution with a high quasi-Fermi level or high electron temperature T_e. The holes are now considered to have a Fermi distribution function characterized by the chemical potential μ_h and the temperature T. We also assume $kT \ll \widetilde{\varepsilon}_0$. In this case from (35) we get

$$P = P_0 \left(\frac{2\exp(\beta\xi)\sinh(\xi/2) + \gamma}{\exp(2\beta\xi) + 2\exp(\beta\xi)\cosh(\xi/2) + 1} \right), \tag{37}$$

where

$$\beta = \frac{\widetilde{\varepsilon}_0 - \mu_h}{\Delta}, \quad \xi = \Delta/kT, \quad P_0 = \frac{n\pi\hbar^2 t^2}{m'_{hh}\mu_h^2}. \tag{38}$$

The dependence (37) of P/P_0 on $1/\xi$ is plotted in Fig. 4 for different values of the parameter β (the value of γ was taken 0.1). In this case the maximum of the distribution function derivative is at the holes' Fermi level μ_h, therefore the largest integral polarization corresponds to $\beta = 0$. For this particular case (37) simplifies into

$$P = P_0 \left(\tanh(\xi) + \frac{\gamma}{2\cosh^2(\xi)} \right). \tag{39}$$

The calculated integral polarization can be alternatively expressed through an effective g factor of the holes g_{eff}. Let us consider the Zeeman term in the Hamiltonian of the 2D holes:

$$H_B = \mu_0 g_{\text{eff}} J_z B,$$

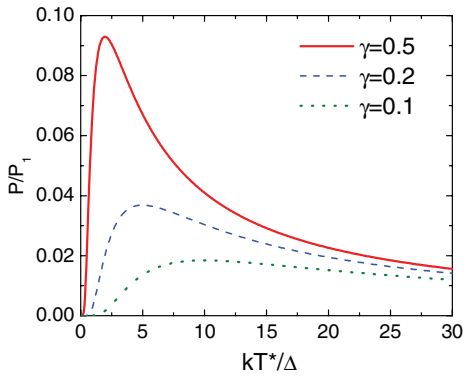

FIG. 3. (Color online) Temperature dependence of integral polarization. Electrons are nondegenerate; holes are either nondegenerate or have the constant distribution function for different values of parameter $\gamma \equiv \Delta/\widetilde{\varepsilon}_0$.

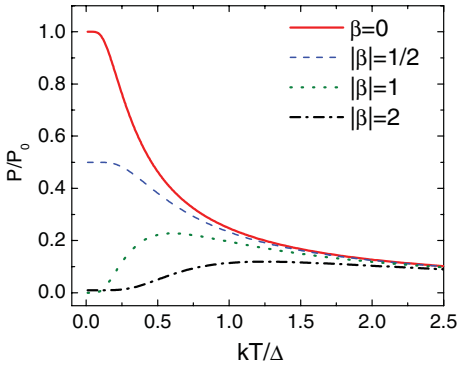

FIG. 4. (Color online) Temperature dependence of polarization for the case of electron distribution function being constant within the configuration resonances. The parameter $\beta \equiv \frac{\tilde{\varepsilon}_0 - \mu_h}{\Delta}$ denotes deviation of the holes Fermi level from the configuration resonance $\gamma = 0.1$.

where J_z is the angular momentum projection operator, μ_0 is the Bohr magneton, and B is the magnetic field applied along the z direction. The polarization of 2D holes due to the splitting between the two subbands with $j = +3/2$ and $j = -3/2$ is given by

$$P_B = \frac{\int_0^\infty (f(E - \Delta_B/2) - f(E + \Delta_B/2))dE}{\int_0^\infty (f(E - \Delta_B/2) + f(E + \Delta_B/2))dE}, \quad (40)$$

where $\Delta_B = 3\mu_0 g_{\text{eff}} B$. For the nondegenerate case one gets

$$P_B = \tanh \frac{\Delta_B}{2kT^*}. \quad (41)$$

Comparing Eq. (41) with Eq. (36) gives

$$g_{\text{eff}} = \frac{2kT^*}{3\mu_0 B} \tanh^{-1} \left[\left(\frac{2\pi n \hbar^2 t^2}{m_{hh'} \tilde{\varepsilon}_0 kT^*} \right) e^{-\frac{\tilde{\varepsilon}_0}{kT^*}} \sinh \frac{\Delta_B}{2kT^*} \right]. \quad (42)$$

In the same way an expression for the degenerate case can be easily obtained.

V. DISCUSSION

The key advantage of the Fano approach used in the present study is that the unknown eigenfunctions of the complex system are expressed through the known ones of the uncoupled states; in our case these are the hole localized at Mn and the free 2D hole in the QW. Given the expansion (9) any effects on the localized state can be translated into effects for the whole coupled system. The binding energy for a hole at a single Mn in GaAs is known to be $E_0 \approx 110$ meV.[14] For the enhanced Mn concentrations in the delta layer up to 10^{13} cm^{-2} the impurity band is established with the binding energy lowering down to 50 meV or even less.[15–17] In this case for the valence band QW depth starting from 50 meV the considered resonance tunneling effects are expected. Estimations for the splitting energy Δ subject to both exchange interaction between the hole and Mn and the external magnetic field. For small concentration of Mn the Zeeman splitting can be simply estimated as $\Delta = \mu_0 g B$ with B being an external magnetic field and $g \approx 3$ is the g factor for the hole at Mn. This makes $\Delta \sim 0.1$ meV for $B \sim 1$ T. Samples with higher Mn concentrations up to a few percent are known to exhibit ferromagnetic properties;[16] in this case the levels splitting Δ is to be considered with account for p-d exchange interaction.[16] The particular value of Δ for typical experimental samples still remains questionable; in the ferromagnetic regime the splitting is believed to be in the range $\Delta \sim 1 - 10$ meV by the order of magnitude. The magnitude of the tunnel coupling is, of course, the key parameter determining the polarization. From Eqs. (8) and (14) it follows that the tunneling parameter can be estimated as

$$t^2 = \left(\frac{\hbar^2}{2m_0} \right)^2 \frac{2m_{hh} m'_{hh} E_0}{\hbar^4} e^{-\frac{2\sqrt{2m_{lh} E_0}}{\hbar} d}. \quad (43)$$

Substituting $E_0 = 100$ meV, $d = 4$ nm one obtains the characteristic value $t^2 \sim 0.1$ meV. We then take the Mn concentration $n \sim 10^{12}$ cm^{-2}, $\xi = 1$, $\varepsilon_0 \sim 3$ meV, $\beta = 0$. This set of parameters gives an estimate for the integral polarization degree $P_0 \approx 0.2$, $P_1 \approx 0.6$. The experimental temperature dependence of polarization obtained in Ref. 10 qualitatively agrees with (39). Beside the analytical expressions for the general case (35) and particular cases (36) and (39), a numerical simulation of the PL spectra can be performed based on (30) with account for the inhomogeneous broadening. An example of such calculation is shown in Fig. 5. For the calculation the following parameters were taken: $\Delta = 1$ meV, $n = 10^{11}$ cm^{-2}, $T = T_e = 20$ K, and $\varepsilon_0 = \mu_h = 1$ meV; the inhomogeneous broadening of the spectra was accounted for by normal distribution of E_g with the dispersion $\sigma = 3$ meV (corresponds to the fluctuation of the QW width by half a monolayer). The calculated spectra presented in Fig. 5 seem to be in good agreement with the experimental results obtained in Refs. 9 and 10. The energy shift of the spectra peaks appears to be ≈ 0.2 meV being substantially less than Δ. It is worth noting that in our theory the polarization originates from the splitting of the bound hole state at Mn and therefore may exceed the polarization degree expected from an intrinsic g factor of the 2D holes located in the QW

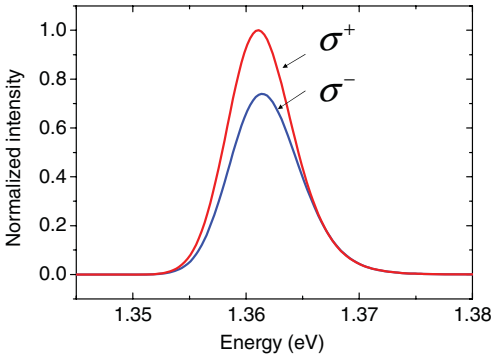

FIG. 5. (Color online) An example of calculated luminescence spectra for right (σ^+) and left (σ^-) circular polarizations with account of inhomogeneous broadening. The parameters used in calculations are given in the text. The energy shift of the peaks is $\approx$0.2 meV.

(this polarization is also of the opposite sign). However, it clearly reveals itself in the photoluminescence spectra in the wavelength range corresponding to the QW bandgap. As seen from (35) the degree of such polarization is governed by the concentration of the impurities and the value of localized level splitting which can be caused either by Zeeman effect or by exchange interaction of the localized hole with Mn d-electron states.

As mentioned in Sec. II the external magnetic field was assumed nonquantizing. Indeed an estimate for the energy of Landau levels separation gives

$$\hbar\omega_c = \frac{e\hbar B}{m'_{hh}c} \approx 0.3 \text{ meV}$$

for the magnetic field $B = 0.5$ T. This value is substantially less than the typical kinetic energy of the holes estimated as $\varepsilon \approx 1$–10 meV. However, this value is comparable with the tunneling parameter t^2. Therefore for the experimental data the validity of the developed theory is well justified for $B \lesssim 0.5$ T.

VI. SUMMARY

The presented theory treats the configuration interaction between a continuum of states in the QW and a paramagnetic impurity located outside of the QW. We utilized the well-known Fano approach for calculation of the matrix elements for the direct interband optical transitions in the QW. For such transitions the tunnel coupling of the 2D QW states with the bound impurity states always leads to the enhancement of the luminescence spectral density at the configuration resonance. This new result is not covered by the conventional Fano formula.[1,2] The redistribution of the PL spectral density in the vicinity of the resonance does not affect the integral intensity but it causes an integral circular polarization of the light emitted from the QW provided the bound hole state is split in the projection of the hole angular momentum. The presented theory expresses the eigenstates of the system with weak tunnel coupling through the wave functions of the hole localized at the paramagnetic center and the 2D states of the continuum. For this reason it seems to be capable of describing other effects expected in such systems like anisotropy of the holes' g factor in the QW induced by the paramagnetic impurity or the indirect exchange interaction between the localized hole states provided by the free 2D carriers located at a tunnel distance.

ACKNOWLEDGMENTS

We thank V. D. Kulakovskii for very fruitful discussions and also express our thanks to B. A. Aronzon, P. I. Arseev, V. L. Korenev, V. F. Sapega, and S. V. Zaitsev for useful and helpful comments. The work has been supported by RFBR (Grants No. 09-02-00469, No. 11-02-00348, No. 11-02-00146, No. 12-02-00815, and No. 12-02-00141), Russian Ministry of Education and Science (Contracts No. 14.740.11.0892 and No. 11.G34.31.0001 with SPbSPU and leading scientist G.G. Pavlov).

*rozhansky@gmail.com

[1] U. Fano, Phys. Rev. **124**, 1866 (1961).
[2] A. E. Miroshnichenko, S. Flach, and Y. S. Kivshar, Rev. Mod. Phys. **82**, 2257 (2010).
[3] A. Blom, M. A. Odnoblyudov, I. N. Yassievich, and K. A. Chao, Phys. Rev. B **65**, 155302 (2002).
[4] V. I. Okulov, A. T. Lonchakov, T. E. Govorkova, K. A. Okulova, S. M. Podgornykh, L. D. Paranchich, and S. Y. Paranchich, Low Temp. Phys. **37**, 220 (2011).
[5] V. Aleshkin, L. Gavrilenko, M. Odnoblyudov, and I. Yassievich, Semiconductors **42**, 880 (2008).
[6] V. Korenev, JETP Letters **78**, 564 (2003).
[7] B. A. Aronzon, M. V. Kovalchuk, E. M. Pashaev, M. A. Chuev, V. V. Kvardakov, I. A. Subbotin, V. V. Rylkov, M. A. Pankov, I. A. Likhachev, B. N. Zvonkov, Yu. A. Danilov, O. V. Vihrova, A. V. Lashkul, and R. Laiho, J. Phys. Condens. Matter **20**, 145207 (2008).
[8] B. A. Aronzon, M. A. Pankov, V. V. Rylkov, E. Z. Meilikhov, A. S. Lagutin, E. M. Pashaev, M. A. Chuev, V. V. Kvardakov, I. A. Likhachev, O. V. Vihrova, A. V. Lashkul, E. Lahderanta, A. S. Vedeneev, and P. Kervalishvili, J. Appl. Phys. **107**, 023905 (2010).
[9] M. Dorokhin, S. Zaitsev, A. Brichkin, O. Vikhrova, Y. Danilov, B. Zvonkov, V. Kulakovskii, M. Prokofeva, and A. Sholina, Phys. Solid State **52**, 2291 (2010).
[10] S. Zaitsev, M. Dorokhin, A. Brichkin, O. Vikhrova, Y. Danilov, B. Zvonkov, and V. Kulakovskii, JETP Lett. **90**, 658 (2010).
[11] J. Schneider, U. Kaufmann, W. Wilkening, M. Baeumler, and F. Köhl, Phys. Rev. Lett. **59**, 240 (1987).
[12] N. S. Averkiev and S. Y. Il'inskii, Phys. Solid State **36**, 278 (1994).
[13] J. Bardeen, Phys. Rev. Lett. **6**, 57 (1961).
[14] W. Schairer and M. Schmidt, Phys. Rev. B **10**, 2501 (1974).
[15] V. F. Sapega, M. Ramsteiner, O. Brandt, L. Däweritz, and K. H. Ploog, Phys. Rev. B **73**, 235208 (2006).
[16] T. Jungwirth, J. Sinova, J. Mašek, J. Kučera, and A. H. MacDonald, Rev. Mod. Phys. **78**, 809 (2006).
[17] D. A. Woodbury and J. S. Blakemore, Phys. Rev. B **8**, 3803 (1973).

PUBL. 5

I. V. ROZHANSKY, N. S. AVERKIEV, and E. LÄHDERANTA, FANO-TYPE COUPLING OF A BOUND PARAMAGNETIC STATE WITH 2D CONTINUUM, *AIP Conference Proceedings*, **1566**, 335, 2013.

Fano-type coupling of a bound paramagnetic state with 2D continuum

I. V. Rozhansky[*,†], N. S. Averkiev[*] and E. Lähderanta[†]

[*]*A.F. Ioffe Physical Technical Institute, 194021 St.Petersburg, Russia*
[†]*Lappeenranta University of Technology, P.O. Box 20, FI-53851, Lappeenranta, Finland*

Abstract. We analyze an effect of a bound impurity state located at a tunnel distance from a quantum well (QW). The study is focused on the resonance case when the bound state energy lies within the continuum of the QW states. Using the developed theory we calculate spin polarization of 2D holes induced by paramagnetic (Mn) delta-layer in the vicinity of the QW and indirect exchange interaction between two impurities located at a tunnel distance from electron gas.

Keywords: configuration interaction, Fano resonance
PACS: 75.75.-c, 78.55.Cr, 78.67.De

INTRODUCTION

Heterostructures with paramagnetic impurities spatially separated from the free charge carriers are gaining much interest within the semiconductor spintronics studies. The spatial separation at a tunnel distance preserves high mobility of the free carriers while their spin polarization induced by the impurities can be substantial [1].

We consider nanostructures based on GaAs/InGaAs, containing a quantum well (QW) and Mn δ-layer, separated from the QW by 3-6 nm. We present a theory capable of describing the spin polarization of 2D holes in the QW due to resonant tunnel coupling with the bound hole state at Mn. The developed approach is further implemented for describing indirect exchange interaction between two impurities located at a tunnel distance from the free electron gas.

THEORETICAL MODEL

The hybridization of the bound hole state with the continuum of 2D free carriers states is described on the basis of the Fano model of configuration interaction and the Bardeen's tunneling Hamiltonian. In the secondary quantization representation the total Hamiltonian can be written as follows:

$$H = \varepsilon_0 a^+ a + \sum_\lambda \varepsilon_\lambda c_\lambda^+ c_\lambda + \sum_\lambda t_\lambda c_\lambda^+ a + t_\lambda^* a^+ c_\lambda, \qquad (1)$$

where a^+, a – the creation and annihilation operators for the bound state characterized by its energy ε_0, and c_λ^+, c_λ – the creation and annihilation operators for the continuum state having energy ε_λ, t_λ – the tunneling parameter. The Hamiltonian (1) allows one to construct the eigenfunctions Ψ of the whole system from those of the bound state ψ and the QW states φ_λ

$$\Psi(E) = v_0(E)\,\psi + \int_0^\infty v(E,\varepsilon)\varphi(\varepsilon)\,d\varepsilon, \qquad (2)$$

With account for the valence band structure all the wavefunctions here are 4-component vectors in the basis of Bloch amplitudes with certain projection of the total angular momentum $J = 3/2$ on z axis which is perpendicular to the QW plane. The envelope function for the bound state is obtained within zero radius potential model and its decay length is determined by both light hole and heavy hole mass. Due to the cylindrical symmetry it is convenient to represent the QW states in cylindrical coordinates. For the considered set of reasonable parameters for Mn impurity and the QW an effective tunnel coupling occurs with only the zeroth cylindrical harmonic. Using the Fano model [2] one straightforwardly obtains the solution for $v_0(E)$ and $v(E,\varepsilon)$. The tunnel coupling of a hole at Mn with the 2D holes states in the QW can manifest itself in different ways depending on the relevant observable [3].

SPIN POLARIZATION OF 2D HOLES

For the optical transitions in the QW the presence of an optically inactive bound state results in symmetrical drop of the photoluminescence intensity near the bound state energy level:

$$I(\omega) = \frac{2\pi u^2 f}{\hbar}\left[\frac{m_h}{2\pi\hbar^2} - \frac{n\pi^2 t^4}{\pi^2 t^4 + \alpha^2\hbar^2(\omega-\omega_0)^2}\right], \qquad (3)$$

where n – 2D concentration of impurities, f – the thermal distribution function, ω_0 – the resonant frequency, $\alpha = m_e/(m_e+m_h)$, u – dipole matrix element, t – the

The Physics of Semiconductors
AIP Conf. Proc. 1566, 335-336 (2013); doi: 10.1063/1.4848422

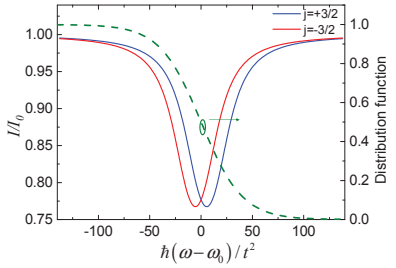

FIGURE 1. Intensity of optical transitions for the holes with opposite projections of the angular momentum.

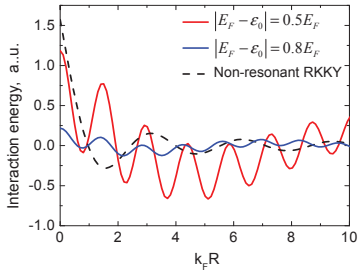

FIGURE 2. Interaction energy for non-resonant part (dashed line) and resonant part (solid line) of RKKY interaction.

tunneling parameter. It was shown experimentally that the 2D holes g-factor is not responsible for the observed circular polarization of light emitted at QW wavelength under external magnetic field applied along z. The magnetic field, however, effectively splits the bound state of the hole at Mn. For each of the split levels the tunnel coupling occurs with only one of the two spin subbands of the 2D holes. As a result the redistribution of the photoluminescence intensity for σ^+ and σ^- polarizations occur at different spectral positions. With account for the thermal distribution of the holes the integral intensity becomes different for the two polarizations (Fig. 1). This theory can explain the observed degree of circular polarization and its dependence on the distance between the Mn δ-layer and the QW.

INDIRECT EXCHANGE

With the wavefunction (2) of the hybridized state we address the topical problem of resonant indirect exchange interaction in the considered structures. Being yet still on the way of solving the true 2D problem we report the results for 1D case. We consider two paramagnetic impurities located far from each other but both close to the 1D electron gas allowing the tunnel coupling. The wavefunction of the coupled state is found analogously to the single impurity case. According to the RKKY theory the energy of indirect exchange interaction between nuclei 1,2 located at positions R_1 and R_2 is given by:

$$\varepsilon \sim J^2 \mathbf{I}_1 \mathbf{I}_2 \int_0^{E_F} dE \int_{E_F}^{\infty} dE' \frac{\Psi^*(E',R_1)\Psi(E,R_1)\Psi^*(E,R_2)\Psi(E',R_2)}{E-E'}, \quad (4)$$

where $\mathbf{I}_1, \mathbf{I}_2$ – spin operators for the nuclei $1,2$ respectively, J – exchange coupling constant, E_F – Fermi level of the electron gas. After plugging (2) into (4) two main contributions can be distinguished. The first one is the non-resonant contribution originating from the second term of (2). This contribution is exactly the conventional 1D RKKY interaction suppressed by the factor t^4. The second one is the resonant part originating from the first term in (2). This part has naturally the same order in tunneling parameter but also strongly depends on the position of the bound state energy ε_0 with regard to the Fermi level of the electron gas E_F. Fig. 2 illustrates the dependence of the two contributions on the distance between impurities $R = |R_1 - R_2|$. Depending on the ratio $|E_F - \varepsilon_0|/E_F$ the resonant RKKY part can be either negligibly small or dominating. One can also note that while the period of the oscillations for the non-resonant part is $2k_F R$, the resonant part oscillates with the two periods $2(k_F - k_0)R$, $2(k_F + k_0)R$,where $k_0 = \sqrt{2m\varepsilon_0}/\hbar$.

ACKNOWLEDGMENTS

We thank V. D. Kulakovskii, B. A. Aronzon, P. I. Arseev, V. L. Korenev, V. F. Sapega, S. V. Zaitsev for useful discussions. The work has been supported by RFBR (grants no 11-02-00348, 11-02-00146, 12-02-00815,12-02-00141), Russian Ministry of Education and Science (contract N 14.740.11.0892, contract N 11.G34.31.0001 with SPbSPU and leading scientist G.G. Pavlov), RF President Grant NSh-5442.2012.2.

REFERENCES

1. S. Zaitsev, M. Dorokhin, A. Brichkin, O. Vikhrova, Y. Danilov, B. Zvonkov, and V. Kulakovskii, *JETP Letters* **90**, 658–662 (2010).
2. U. Fano, *Phys. Rev.* **124**, 1866–1878 (1961).
3. I. V. Rozhansky, N. S. Averkiev, and E. Lähderanta, *Phys. Rev. B* **85**, 075315 (2012).

PUBL. 6

I. V. ROZHANSKY, N. S. AVERKIEV, and E. LÄHDERANTA, CONFIGURATION INTERACTION IN DELTA-DOPED HETEROSTRUCTURES, *Low Temperature Physics*, **39**, 40, 2013.

Low Temperature Physics/Fizika Nizkikh Temperatur, 2013, v. 39, No. 1, pp. 40–47

Configuration interaction in delta-doped heterostructures

I.V. Rozhansky[1,2], N.S. Averkiev[1], and E. Lähderanta[2]

[1] *A.F. Ioffe Physical Technical Institute, Russian Academy of Sciences, St.Petersburg 194021, Russia*
E-mail: rozhansky@gmail.com

[2] *Lappeenranta University of Technology, P.O. Box 20, Lappeenranta FI-53851, Finland*

Received September 13, 2012

We analyze the tunnel coupling between an impurity state located in a δ-layer and the 2D delocalized states in the quantum well (QW) located at a few nanometers from the δ-layer. The problem is formulated in terms of Anderson–Fano model as configuration interaction between the carrier bound state at the impurity and the continuum of delocalized states in the QW. An effect of this interaction on the interband optical transitions in the QW is analyzed. The results are discussed regarding the series of experiments on the GaAs structures with a δ-Mn layer.

PACS: **75.75.–c** Magnetic properties of nanostructures;
78.55.Cr III–V semiconductors;
78.67.De Quantum wells.

Keywords: quantum wells, configuration interaction, paramagnetic impurities, delta-doping.

1. Introduction

The problem of so-called configuration interaction of a single bound state with a continuum of states goes back to the famous paper by U. Fano [1] rated as one of the most relevant works of 20th century [2]. The suggested theoretical approach often regarded as Fano–Anderson model or configuration interaction succeeded in explaining puzzling asymmetric resonances observed in various experiments in atomic and nuclear physics, condensed matter physics and optics [2]. The co-existence of the discrete energy level and the continuum states within the same energy range is also quite common in low-dimensional semiconductor structures [2–5]. Of particular interest nowadays are the structures having a quantum well (QW) and a ferromagnetic or paramagnetic layer located in the vicinity of the QW, but not penetrating into the QW region. In such structures high mobility of the carriers along the QW is combined with the magnetic properties provided by the magnetic layer. A number of recent experiments show that the Mn δ-layer gives rise to circular polarization of the photoluminescence (PL) from the QW in an external magnetic field applied perpendicular to the QW plane [6,7]. It was questioned whether the spin polarization of the carries in the QW is due to the electrons tunneling to Mn site or the tunnel coupling of the holes at Mn with those in the QW. The latter mechanism seemed to lack the proper theoretical description. In this paper we try to fill this gap. We show that the simple scheme of the holes configuration interaction leads to the opposite sign of the circular polarization than that observed in the experiment. The model system considered in the present paper consists of a δ-layer of the impurities (donors or acceptors) and a QW having one level of size quantization for the electrons or holes, respectively. The energy level of the impurity bound state lies within the range of the 2D states size quantization subband in the QW. We will be considering the case of rather deep impurity level in the sense that the impurity activation energy substantially exceeds the kinetic energy of the 2D carriers in the QW. The attracting potential of the impurity is assumed spherically symmetric and since it is a deep level we treat it with zero radius potential approximation [8]. At that we consider both the simple band structure and the one of the GaAs valence band type.

2. Tunneling between impurity and quantum well

In this section we consider the configuration interaction between a single impurity bound state and the continuum of 2D states in the QW. The potential barrier separating the impurity from the QW is assumed to be weakly transparent for the tunneling. Rigorous calculation of the eigenfunctions is rather hard to perform as it requires solving stationary Schrödinger equation in the complicated 3D potential. In order to circumvent the explicit solving of the Schrödinger equation for tunneling problems the so-called tunneling or transfer Hamiltonian formalism is commonly used as originally proposed by Bardeen [9]. The total Hamiltonian

is expressed as $H = H_i + H_{QW} + H_T$, where H_i is partial Hamiltonian having the bound state at the impurity as its eigen state. H_{QW} in the same way corresponds to the QW itself, its eigenfunctions φ_λ form nondegenerate continuum of states characterized by the quantum number(s) λ. The term H_T accounts for the tunneling. In the secondary quantization representation the total Hamiltonian can be written as follows:

$$H = \varepsilon_0 a^+ a + \int \varepsilon_\lambda c_\lambda^+ c_\lambda d\lambda + \int (t_\lambda c_\lambda^+ a + t_\lambda^* a^+ c_\lambda) d\lambda, \quad (1)$$

where a^+, a are the creation and annihilation operators for the bound state characterized by its energy ε_0, and c_λ^+, c_λ are the creation and annihilation operators for a continuum state having energy ε_λ. The energy here and below is measured from the level of size quantization of the carriers in the QW so that ε_λ is simply their kinetic energy. The expression (1) is rather general, in fact it can be regarded as introducing the coupling between two systems into the Hamiltonian in the most simple phenomenological way. From this viewpoint the coupling parameter t_λ is still to be determined through exact solving of the eigenvalue problem for the whole system. Bardeen's approach suggests a simple recipe for calculation of the tunneling parameter for the case of weak tunneling through a potential barrier:

$$t_\lambda = \int_\Omega (\varphi_\lambda^* K\psi - \psi K \varphi_\lambda^*) d\mathbf{r}, \quad (2)$$

where integration is performed over the region Ω to the one side of the barrier. Here K is the kinetic energy operator:

$$K = -\frac{\hbar^2}{2m}\Delta. \quad (3)$$

The attraction potential of the impurity is considered spherically symmetric, so the whole system (impurity+QW) has the cylindrical symmetry with z axis directed normally to the QW plane and going through the impurity center. Thus for further calculations it will be most convenient to represent the QW states in cylindrical coordinates rather than as plane waves. In this case each state is characterized by the wavenumber k and the cylindrical harmonic number l:

$$\varphi_{kl} = \eta(z)\sqrt{\frac{m}{2\pi\hbar^2}} J_l(k\rho) e^{il\theta}, \quad (4)$$

where $J_l(k\rho)$ is the Bessel function of order l, ρ and θ are the polar coordinates in the QW plane, m is the in-plane effective mass, $\eta(z)$ is the envelope function of size quantization in z direction. The wavefunction (4) has the normalization:

$$\langle \varphi_{kl} \mid \varphi_{k'l'} \rangle = \delta(\varepsilon - \varepsilon')\delta_{ll'}, \quad (5)$$

where $\varepsilon = \hbar^2 k^2 / 2m$. The potential barrier separating the deep impurity level from the QW in the first approximation can be assumed having a rectangular shape. Inside the barrier the function $\eta(z)$ is (z axis is directed towards the impurity, $z = 0$ corresponds to the QW boundary)

$$\eta(z) \sim \frac{1}{\sqrt{a}} e^{-qz}, \quad (6)$$

where $q = \sqrt{2mE_0/\hbar^2}$, a is the QW width, E_0 is the binding energy of the bound state, at the same time E_0 determines the height of the potential barrier. Let us firstly consider the simple band case valid for the bound electrons at donor impurity coupled to the QW conductance band. The spherical potential of the impurity results in the ground state of the carrier to be angular independent, therefore the efficient tunneling overlap occurs only with the zeroth cylindrical harmonic $\varphi_{k0} \equiv \varphi(\varepsilon)$. For the deep impurity level one can use zero radius potential approximation [8] and express the *s*-type wavefunction as

$$\psi = \sqrt{2q}\frac{e^{-qr}}{r}. \quad (7)$$

The volume integral (2) is reduced to the surface integral over the surface Ω_S inside the barrier which is more convenient to take at the impurity site. This yields for the electrons tunneling between the donor state and the QW:

$$t_k^e = \sqrt{\frac{2\pi}{aq(1+k^2/q^2)}}\sqrt{E_0} e^{-qd}. \quad (8)$$

It is clearly seen that as long as the case $k << q$ is considered, the tunneling parameter has very weak dependence on k.

In order to apply the same approach to the holes tunneling in GaAs it has to be generalized for the case of the valence band complex structure. Let us consider $In_xGa_{1-x}As$ QW having only one level of size quantization for the heavy holes and neglect the light holes being split off due to the size quantization. The basis of Bloch amplitudes to be used is formed of the states with certain projection of the total angular momentum $J = 3/2$ on z axis. It would be tempting to generalize (2) by treating K as the kinetic part of the Luttinger Hamiltonian ($\hbar k_x$, $\hbar k_y$, $\hbar k_z$ are, as usual, the momentum operators along the appropriate axis):

$$K = \begin{pmatrix} F & H & I & 0 \\ H^* & G & 0 & I \\ I^* & 0 & G & -H \\ 0 & I^* & -H^* & F \end{pmatrix}, \quad (9)$$

$$F = -Ak^2 - \frac{B}{2}(k^2 - 3k_z^2),$$

$$G = -Ak^2 + \frac{B}{2}(k^2 - 3k_z^2),$$

$$H = Dk_z(k_x - ik_y),$$

$$I = \frac{\sqrt{3}}{2}B(k_x^2 - k_y^2) - iDk_xk_y. \quad (10)$$

The functions ψ_α, $\varphi_{\lambda\beta}$ in (2) become now 4-component vector functions (also the spin indices α and β are added here). The explicit expression for the bound hole state functions ψ_α and the 2D hole states $\varphi_{\lambda\beta}$ can be found in Ref. 10. The important thing about those is while the decay length in z direction of the 2D wavefunctions $\varphi_{\lambda\beta}$ is controlled by the heavy hole mass $m_{hh} \approx 0.5\, m_0$ (m_0 is the free electron mass), the decay length of radial part of the bound state wavefunction ψ_α is characterized by both heavy hole mass m_{hh} and the light hole mass $m_{lh} \approx 0.08\, m_0$ [10]. Analogously to the simple band case the integration (2) over the whole space is reduced to the integration over the surface Ω_S inside the barrier, at that, only z projection of the kinetic energy operator is required. The expression for tunneling parameter simplifies into

$$t_{kl\alpha\beta}^{(h)} = (B-A)\int\limits_{\Omega_S} dS\left(\varphi_{kl\beta}^{*}\frac{d}{dz}\psi_\alpha - \psi_\alpha\frac{d}{dz}\varphi_{kl\beta}^{*}\right), \quad (11)$$

where φ_{kl} is given by (4).

Regrettably, the above given straightforward generalization of (2) fails to be fully correct. Indeed, the largest decay length of the bound state ψ_α is determined by the light hole mass while the decay length of the QW states is governed by the heavy hole. Due to this circumstance the result of the surface integration (11) becomes dependent on the particular position of the integration surface inside the barrier. However, it can be shown that in the case of two different masses the exponential dependence of the tunneling parameter on the barrier thickness is determined by the smallest mass, but the exact value of the tunneling parameter cannot be correctly obtained within the given approach. Now we define $q = \sqrt{2m_{hh}E_0}/\hbar^2$, $\beta = m_{lh}/m_{hh}$. The explicit evaluation of the overlap integrals with account for $k << q$ shows that the tunneling configuration interaction to be accounted for is only between the zeroth cylindrical harmonic $\varphi_{k0,-3/2}$ and the bound state $\psi_{-3/2}$ as well as between $\varphi_{k0,+3/2}$ and $\psi_{+3/2}$. Both are governed by the same tunneling parameter t_k^h:

$$t_k^h = \left(\frac{A-B}{\hbar^2/2m_0}\right)\sqrt{\frac{\pi}{aq}}\sqrt{\frac{m_{hh}m'_{hh}}{m_0^2}}\zeta(k/q)\beta\sqrt{E_0}\times$$

$$\times\exp\left(-\chi(k/q)\sqrt{\beta}qd\right), \quad (12)$$

where $1 \le \chi \le 2$, $\zeta \sim 1$ are weak dimensionless functions of k/q, m'_{hh} is the effective in-plane heavy hole mass. The tunneling parameter t_k^h exponentially depends on the barrier thickness with the light hole mass entering the exponent index. The particular expressions for χ and ζ depend on the surface one chooses for the integration in (2).

In both cases for t_k^e, t_k^h it is reasonable to assume that the tunneling parameter does not depend on k as weak tunneling implies $k << q$. Still, its rapidly decreasing behavior for $k >> q$ has to be kept in mind when it provides convergence for integration over k. In our estimations the shape of the potential barrier separating the QW was assumed rectangular. This is quite reasonable for the estimation at $k << q$. However, the particular shape of the barrier becomes important when one is concerned with experimental dependence on the distance d between the impurity and the QW.

3. Effect on the luminescence spectrum

The transfer Hamiltonian (1) with known tunneling parameter $t(\varepsilon)$ allows one to construct the eigenfunctions Ψ of the whole system given those of the bound state ψ and the QW states $\varphi(\varepsilon)$:

$$\Psi(E) = \nu_0(E)\psi + \int\limits_0^\infty \nu(E,\varepsilon)\varphi(\varepsilon)d\varepsilon, \quad (13)$$

E denotes the energy of the state Ψ. Here $\varphi(\varepsilon)$ are the wavefunctions with zeroth cylindrical harmonic, as was shown above the other harmonics are not affected by the tunneling configuration interaction. Plugging (13) into the stationary Schrödinger equation

$$H\Psi = E\Psi$$

with H being the effective Hamiltonian (1) one gets the following system of equations:

$$\begin{aligned} &\nu_0(E)\varepsilon_0 + \int\limits_0^\infty t(\varepsilon)\nu(E,\varepsilon)d\varepsilon = E\nu_0(E), \\ &\nu(E,\varepsilon)\varepsilon + t(\varepsilon)\nu_0(E) = E\nu(E,\varepsilon). \end{aligned} \quad (14)$$

In the present work we consider the case of the bound level energy lying within the range of the continuum: $\varepsilon_0 >> t^2$. For this case the solution is obtained as shown in Ref. 1:

$$\nu_0{}^2(E) = \frac{t^2(E)}{\pi^2 t^4(E) + (E-\tilde{\varepsilon}_0)^2},$$

$$\nu(E,\varepsilon) = \nu_0(E)\left(P\frac{t(\varepsilon)}{E-\varepsilon} + Z(E)t(E)\delta(E-\varepsilon)\right), \quad (15)$$

where

$$Z(E) = \frac{E-\varepsilon_0-F(E)}{t^2(E)},$$

$$F(E) = \int\limits_0^\infty P\frac{t^2(\varepsilon)}{(E-\varepsilon)}d\varepsilon, \quad (16)$$

P stands for the principal value and $\tilde{\varepsilon}_0$ is the center of configuration resonance, which appears to be slightly shifted from ε_0:

$$\tilde{\varepsilon}_0(E) = \varepsilon_0 + F(E). \quad (17)$$

Because of $k << q$ it is reasonable to put $t =$ const everywhere, except for (16) where decrease of t at $E \to \infty$ is necessary for convergence of the integral.

In order to analyze the influence of the configuration interaction on the luminescence spectra we have to calculate matrix element of operator $\hat{M}$ describing interband radiative transitions between the hybridized wavefunction $\Psi(E)$ and wavefunction of 2D the carrier in the other band of the QW which we denote by $\xi_{k'l'}$, here k' is the magnitude of the wavevector, l' is the number of cylindrical harmonic analogously to (4). If, for instance, one considers the acceptor-type impurity then $\Psi(E)$ is the hybridized wavefunction of the 2D holes and $\xi_{k'l'}$ is the wavefunction of the 2D electrons in the QW. We assume that (a) there are no radiative transitions between the bound state wavefunction ψ and the 2D carrier wavefunction $\xi_{k'l'}$ in the other band thus the matrix element for transitions from the bound state:

$$\left\langle \xi_{k'l'} \middle| \hat{M} \middle| \psi \right\rangle = 0, \tag{18}$$

(b) the interband radiative transitions between the free 2D states in the QW are direct. According to (4) the wavefunctions $\varphi(\varepsilon)$ and $\xi(\varepsilon')$ corresponding to the zeroth harmonic in the cylindrical basis are

$$\varphi(\varepsilon) = \eta(z)\sqrt{\frac{m}{2\pi\hbar^2}}J_0(k\rho),$$

$$\xi(\varepsilon') = \zeta(z)\sqrt{\frac{m'}{2\pi\hbar^2}}J_0(k'\rho), \tag{19}$$

where

$$k = \frac{\sqrt{2m\varepsilon}}{\hbar}, \qquad k' = \frac{\sqrt{2m'\varepsilon'}}{\hbar},$$

$\eta(z), \zeta(z)$ are the appropriate size quantization functions in z direction, m, m' are the in-plane masses of the electrons and holes, respectively, if the donor-type impurity is considered and vice versa for the acceptor case. Without the tunnel coupling the matrix element for the direct optical transitions between the states $\varphi(\varepsilon)$ and $\xi(\varepsilon')$ is given by

$$M_0(\varepsilon,\varepsilon') = \left\langle \xi(\varepsilon') \middle| \hat{M} \middle| \varphi(\varepsilon) \right\rangle = u_k \frac{\sqrt{mm'}}{k\hbar^2}\delta(k-k'), \tag{20}$$

where u_k is the appropriate dipole matrix element for the Bloch amplitudes. According to the above mentioned considerations it is only this matrix element that is affected by the tunnel coupling, while the matrix elements for the transitions between higher cylindrical harmonic are preserved. Denoting by M the modified matrix element for transitions between the states $\Psi(E)$ and $\xi(\varepsilon')$ with the further use of the Fano theory [1] one obtains

$$M(E,\varepsilon')^2 = M_0(E,\varepsilon')^2\left[1 - \frac{\pi^2 t^4}{\pi^2 t^4 + (E-\tilde{\varepsilon}_0)^2}\right]. \tag{21}$$

We proceed further with the Fermi's Golden Rule for the transition probability:

$$W(\hbar\omega) = \frac{2\pi}{\hbar}\times$$

$$\times\int_0^\infty\int_0^\infty |M(E,\varepsilon')|^2 f'(\varepsilon')f(E)\delta(E+\varepsilon'+E_g-\hbar\omega)\,dEd\varepsilon', \tag{22}$$

where E_g is the QW bandgap, $\hbar\omega$ is the energy of the radiated photon, f, f' are the energy distribution functions for the carriers in the hybridized and intact bands, respectively. Substituting (20) and (21) into (22) one should treat correctly the delta-function for the wavenumbers of the zeroth cylindrical harmonic. It can be shown that

$$\delta^2(k-k') = \frac{\sqrt{S}}{\pi^{3/2}}\delta(k-k'),$$

where S is the area of the QW. Then we arrive at

$$W(\hbar\omega) = \frac{u^2 f(E_\omega)}{\pi^{1/2}\hbar^2}\frac{\sqrt{2\tilde{m}S}}{\sqrt{\hbar\omega - E_g}}\left(1 - \frac{\pi^2 t^4}{\pi^2 t^4 + (E_\omega - \tilde{\varepsilon}_0)^2}\right), \tag{23}$$

where

$$f(E_\omega) = f'(\alpha^{-1}E_\omega)f(E_\omega), \qquad E_\omega = \frac{\hbar\omega - E_g}{1+\alpha^{-1}},$$

$$\tilde{m} = \frac{mm'}{m+m'}, \qquad \alpha = \frac{m'}{m}, \tag{24}$$

while for the all cylindrical harmonics altogether the unperturbed optical transition rate yields:

$$W_0(\hbar\omega) = \frac{2\pi u^2 f(E_\omega)}{\hbar}\left(\frac{\tilde{m}}{\hbar^2}S\right). \tag{25}$$

The result (23) obtained for a single impurity can be applied to an ensemble of impurities provided their interaction is weak compared to the tunnel coupling with the QW. In this case the sample area S should be replaced with the inverse sheet concentration of the impurities in the delta-layer n^{-1}. After normalization by the area of the QW from (23), (25) we finally get the spectral density of the luminescence intensity:

$$I(\hbar\omega,\tilde{\varepsilon}_0) = I_0(\hbar\omega)\left(1 - a(\tilde{\varepsilon}_0)\sqrt{n}\frac{\pi^2 t^4}{\pi^2 t^4 + (E_\omega - \tilde{\varepsilon}_0)^2}\right), \tag{26}$$

where

$$a(\tilde{\varepsilon}_0) = \frac{\hbar}{\pi^{3/2}\sqrt{2\tilde{m}\tilde{\varepsilon}_0(1+\alpha^{-1})}},$$

$$I_0(\hbar\omega) = \frac{2\pi u^2 \tilde{m}}{\hbar^3} f(E_\omega).$$

4. Polarization of the spectra

It follows from (26) that the bound state lying within the energy range of the continuum causes a dip in the luminescence spectra emitted from the QW. If then for any reason the bound state is split the luminescence spectra will show the appropriate number of the dips shifted by the splitting energy Δ. If one considers the splitting in the magnetic field applied along z each of the split sublevels is characterized by certain projection of spin and interacts with only one of the 2D carriers spin subbands characterized by the same projection of spin. Thus, for each of the two circular polarizations σ^+, σ^- of the light emitted from the QW one would expect one dip, its spectral position being different for σ^+ and σ^- in accordance with the splitting energy Δ. As an example let us consider the GaAs-based QW and 2D heavy holes interacting via the tunneling configuration interaction with the bound state at an acceptor. This case is shown schematically in Fig. 1. The 2D holes with the projections of total angular momentum $j = +3/2$ and $j = -3/2$ recombine emitting, respectively, right- (σ^+) and left- (σ^-) circularly polarized light. In Sec. 2 it was shown that the heavy holes

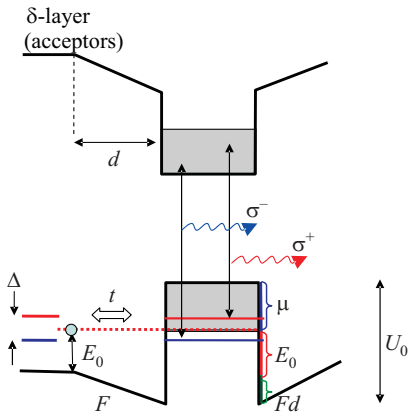

Fig. 1. (Color online) Mechanism of polarization of the luminescence for the acceptor type impurity. The localized hole levels split in magnetic field. Each of them effectively couples with the 2D holes having certain projection of angular momentum. Shifted positions of the resonances with account for temperature distribution of the holes cause the difference in intensities of circular polarizations σ^+, σ^-. The scheme also shows the simple electrostatic model described in the text.

with $j = -3/2$ ($j = +3/2$) interact basically with the bound states $\psi_{-3/2}$ ($\psi_{+3/2}$). An external magnetic field applied along z would cause Zeeman splitting of the bound state energy level ε_0 into $\varepsilon_0^+ = \varepsilon_0 + \Delta/2$ and $\varepsilon_0^- = \varepsilon_0 - \Delta/2$. The splitting $\Delta = \varepsilon_0^+ - \varepsilon_0^-$ may also originate from exchange interaction of the holes with spin-polarized acceptor ions. Let us refer to the case of Mn ions having positive g-factor ($g \approx 3$, see Ref. 11). The hole is coupled to Mn in antiferromagnetic way thus the level ε_0^+ corresponds to $j = -3/2$ and ε_0^- to $j = +3/2$. As follows from (17), (24) the difference in the positions of the resonances (dips) E_ω^+ and E_ω^- corresponding to the bound state sublevels ε_0^+ and ε_0^- is given by

$$\tilde{\Delta} = E_\omega^+ - E_\omega^- = \Delta + t^2 \ln\left(1 + \frac{\tilde{\Delta}}{E_\omega^-}\right). \qquad (27)$$

Unless the positions of the resonances are too close to the band edge the last term in (26) can be neglected and $\tilde{\Delta} = \Delta = \varepsilon_0^+ - \varepsilon_0^-$. With account for the energy distribution functions for the holes and electrons the shifted positions of the resonances lead to the difference in the luminescence intensity for the opposite circular polarizations. In the discussed example of the antiferromagnetic alignment of the hole the luminescence spectra $I^+(\hbar\omega, \tilde{\varepsilon}_0^+)$, $I^-(\hbar\omega, \tilde{\varepsilon}_0^-)$ having the resonance positions at ε_0^+ and ε_0^- correspond to the circular polarizations σ^- and σ^+, respectively. As can be seen from (26) the difference in the resonance positions $\Delta = \tilde{\varepsilon}_0^+ - \tilde{\varepsilon}_0^-$ leads to the integral polarization of the spectra if the distribution function $f(E)$ significantly varies in the vicinity of ε_0. This is illustrated in Fig. 2. The functions I^- and I^+ are shown by blue and red solid lines, respectively. The integral polarization is naturally defined as

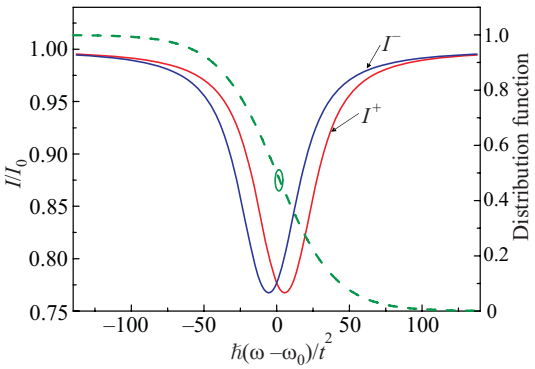

Fig. 2. (Color online) Modification of the luminescence spectrum by tunneling configuration interaction. The integral polarization occurs when the carriers distribution function (dashed line) strongly varies in the vicinity of the configuration resonances. ω_0 is the position of the resonance without bound level splitting.

$$P = \frac{P(\sigma^+) - P(\sigma^-)}{P(\sigma^+) + P(\sigma^-)} \approx \frac{\int\limits_{E_g}^{\infty} I^-(\hbar\omega)\, d(\hbar\omega) - \int\limits_{E_g}^{\infty} I^+(\hbar\omega)\, d(\hbar\omega)}{2\int\limits_{E_g}^{\infty} I_0(\hbar\omega)\, d(\hbar\omega)}.$$

With use of (26) this yields:

$$P = -\sqrt{n}\,\frac{\int\limits_0^{\infty} \pi t^2(E)\left[\dfrac{a(\tilde{\varepsilon}_0^+)\pi t^2(E)}{\pi^2 t^4(E) + (E-\tilde{\varepsilon}_0^+)^2} - \dfrac{a(\tilde{\varepsilon}_0^-)\pi t^2(E)}{\pi^2 t^4(E) + (E-\tilde{\varepsilon}_0^-)^2}\right] f(E)dE}{2\int\limits_0^{\infty} f(E)dE}. \tag{28}$$

The slow varying functions $f(E)$ and $\tilde{\varepsilon}_0(E)$ in the integral may be assumed as constants taken at $\tilde{\varepsilon}_0^-$, $\tilde{\varepsilon}_0^+$, the tunneling parameter will be treated as a constant in the whole range of interest $t^2(E) \equiv t^2$.

Then treating the expression in brackets as delta-functions we obtain

$$P = -\frac{\sqrt{\pi}\hbar t^2\sqrt{n}}{2^{3/2}\sqrt{m}}\,\frac{f(\varepsilon_0^+)(\varepsilon_0^+)^{-1/2} - f(\varepsilon_0^-)(\varepsilon_0^-)^{-1/2}}{\int\limits_0^{\infty} f(E)dE}. \tag{29}$$

Note that for the considered example the polarization degree appears to be negative. The positive sign would have appeared if the ferromagnetic coupling between the acceptor ion and the hole had been assumed.

5. The electrostatic effect

Because of the tunneling involved in the polarization of the luminescence one might reasonably expect very strong dependence of the polarization degree on the distance d between the δ-layer and the QW (i.e., the thickness of the spacer). However, the purely exponential dependence of the polarization on the barrier thickness appears to be weakened due to the electrostatic effect shown in Fig. 1 and explained below. Let us for simplicity consider the electrons distribution function being nearly constant within the configuration resonances. The holes are considered to have Fermi distribution function characterized by the chemical potential μ and the temperature T. In the absence of external optical pumping the holes in the QW are in thermodynamic equilibrium with the acceptors in the δ-layer, therefore they have the same chemical potential. Under low-pumping conditions the already large concentration of the holes in the QW is not strongly violated, so it is reasonably to assume that the quasi-Fermi levels of the holes at the acceptors and in the QW coincide, it means that $\varepsilon_0 = \mu$. Strictly speaking, this is valid for a single bound level, if the level is split so that $\varepsilon_0^+ - \varepsilon_0^- = \Delta$, one should probably assume $\varepsilon_0^- = \mu$. From (29) we get the following simplified expression:

$$P = -\frac{\sqrt{\pi}\hbar t^2\sqrt{n}}{2^{5/2}\sqrt{m'_{hh}}\,\mu^{3/2}} \tanh\frac{\Delta}{2kT}. \tag{30}$$

As we will show below both t and μ contribute to the dependence of the integral polarization P on the spacer thickness d and the QW depth U_0. The holes in the QW provide an electrical charge density estimated as $\sigma = eN\mu$, where e is the elementary charge, N is the 2D density of states. The positively charged plane of the QW and negatively charged δ-layer of partly ionized acceptors separated by a distance d produce an electric field

$$F = \frac{4\pi eN\mu}{\varepsilon}, \tag{31}$$

ε being dielectric constant of the material. Due to the electric field F the valence band edge at position of the impurities delta-layer appears to be shifted from the valence band edge just outside of the QW by $F \cdot d$. Because the quasi-Fermi level of the acceptors exceeds the local position of the valence band edge by the binding energy E_0, the equality of the quasi-Fermi levels leads to a simple equation (see Fig. 1):

$$U_0 = \mu + E_0 + eFd, \tag{32}$$

where U_0 is the QW depth and μ is the chemical potential of the holes in the QW. With (31) one gets

$$\mu = \frac{U_0 - E_0}{1 + 4\pi Ned/\varepsilon} \approx \frac{(U_0 - E_0)\varepsilon}{4\pi Ned}. \tag{33}$$

In order to estimate the dependence of the tunneling parameter t on the QW and spacer parameters we consider the WKB tunneling through trapezoid barrier as seen in Fig. 1. With taking into account (12) and (33) this leads to the following expression (we assume $\mu \ll U_0$):

$$t^2 \sim \exp(-\kappa d), \tag{34}$$

where

$$\kappa = \frac{4\sqrt{2m_{lh}}}{3\hbar(U_0 - E_0)}(U_0^{3/2} - E_0^{3/2}). \qquad (35)$$

From (20), (33)–(35) follows the dependence of integral polarization on the spacer thickness:

$$P \sim d^{3/2} \exp(-\kappa d). \qquad (36)$$

Note that electrostatic effect results in the dependence of μ on d which leads to the dependence of P on d being not purely exponential but weakened by the pre-exponential factor $d^{3/2}$. While the correction is pre-exponential, it appears to be quite impotant up to $\kappa d \approx 2$–3 which is typical for the experimental situation.

6. Discussion

In the proposed theory the polarization of light emitted from the QW originates from the splitting of the impurity bound state and therefore may exceed the polarization degree expected from an intrinsic g-factor of the 2D carriers located in the QW. The sign of the polarization deserves special discussion. As was shown above, the tunnel coupling causes a dip in the luminescence spectra. This means that in the considered scheme the polarization of the luminescence from the QW is expected to be of the opposite sign than that due to the optical transitions between the bound state and the free carriers inside the barrier. In particular, the configuration interaction between the 2D heavy holes and Mn δ-layer considered in Sec. 4 leads to the negative sign of the polarization (a mistake made in Ref. 10 has mislead to the positive sign). Such result contradicts the known experimental data [12,13], where the polarization is shown to be positive. This might suggest that regarding these particular experiments the polarization is not due to the holes configuration interaction but rather due to polarization of the electrons as suggested in Ref. 13. The other possibility might be that the relevant bound state of the hole at Mn is more complex and does not resemble the simple antiferromagnetic exchange coupling with Mn ion.

Let us estimate the expected magnitude of the circular polarization degree due to the tunnel configuration interaction. We assume the deep impurity level $E_0 =$ 100 meV, the barrier thickness $d =$ 5 nm, the QW width $a =$ 10 nm. Taking the effective mass as that of the electrons in GaAs $m = 0.06\, m_0$ for the simple band case described by (8) one gets for the tunneling parameter $(t^e)^2 \approx$ 2 meV. The estimation for the holes tunneling parameter appears to be far less, taking $m_{hh} = 0.5\, m_0$, $m'_{hh} = 0.15\, m_0$ from (12) one gets $(t^h)^2 \sim 0.01$ meV. The polarization degree is to be estimated using (29). We take $\Delta =$ 1 meV, $T_e = T_h =$ 20 K, the sheet concentration of the impurities $n = 10^{13}$ cm^{-2}. Then for the case of the donor impurity $t = t^e$, $\varepsilon_0 =$ $= 4$ meV, $\mu_h =$ –1 meV, $\mu_e = \varepsilon_0^-$, one gets $|P| \approx 40\%$, for the acceptor impurity $t = t^h$, $\mu_e =$ –1 meV, $\varepsilon_0 =$ $= 2$ meV, $\mu_h = \varepsilon_0^-$ gives $|P| \approx 0.5\%$. An illustration of the luminescence spectra for the two circular polarizations is presented Fig. 3. For this we used an intermediate value for the tunneling parameter $t^2 = 0.3$ meV ($|P| \approx 0.15\%$) and accounted for inhomogeneous broadening of the spectra by normal distribution of the bandgap E_g with the dispersion $\sigma = 3$ meV (corresponds to the fluctuation of the QW width by half a monolayer).

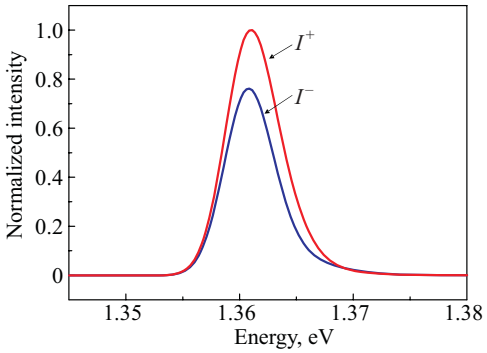

Fig. 3. (Color online) An example of calculated luminescence spectra for the two circular polarizations. The case of antiferromagnetic coupling implies I^- corresponds to σ^+ polarization while I^+ to σ^- polarization. The parameters used in calculations are given in the text.

7. Summary

The presented theory describes the tunnel coupling between a continuum of states in the QW and an impurity bound state located outside of the QW. We utilized the well known Fano approach for calculation of the matrix elements for the direct interband optical transitions in the QW. For such transitions the tunnel coupling of the 2D QW states with the impurity states leads to the drop of the luminescence spectral density at the frequency corresponding to the configuration resonance. This modification of the spectra leads to an integral circular polarization of the light emitted from the QW provided the bound hole state is split in the projection of the hole angular momentum. The key advantage of the approach used in the present study is that the unknown eigenfunctions of the system are expressed through those of the uncoupled states. Given the expansion (13) any effects on the localized state can be translated into effects for the whole coupled system. For this reason it is capable of describing other effects expected in such systems like anisotropy of the holes g-factor in the QW induced by the paramagnetic impurity or the indirect exchange interaction between the bound states provided by the 2D free carriers in the QW.

Acknowledgments

We thank V.D. Kulakovskii for very fruitful discussions and also express our thanks to B.A. Aronzon, P.I. Arseev, V.L. Korenev, M.M. Glazov, V.F. Sapega, S.V. Zaitsev for very useful and helpful comments. The work has been supported by RFBR (grants Nos. 11-02-00348, 11-02-00146, 12-02-00815, 12-02-00141), Russian Ministry of Education and Science (contract N 14.740.11.0892, contract N 11.G34.31.0001 with SPbSPU and leading scientist G.G. Pavlov), RF President Grant NSh-5442.2012.2.

1. U. Fano, *Phys. Rev*. **124**, 1866 (1961).
2. A.E. Miroshnichenko, S. Flach, and Y.S. Kivshar, *Rev. Mod. Phys*. **82**, 2257 (2010).
3. A. Blom, M.A. Odnoblyudov, I.N. Yassievich, and K.A. Chao, *Phys. Rev*. *B* **65**, 155302 (2002).
4. V.I. Okulov, A.T. Lonchakov, T.E. Govorkova, K.A. Okulova, S.M. Podgornykh, L.D. Paranchich, and S.Y. Paranchich, *Fiz. Nizk. Temp*. **37**, 281 (2011) [*Low Temp. Phys*. **37**, 220 (2011)].
5. V. Aleshkin, L. Gavrilenko, M. Odnoblyudov, and I. Yassievich, *Semiconductors* **42**, 880 (2008).
6. M. Dorokhin, S. Zaitsev, A. Brichkin, O. Vikhrova, Y. Danilov, B. Zvonkov, V. Kulakovskii, M. Prokofeva, and A. Sholina, *Phys. Solid State* **52**, 2291 (2010).
7. S. Zaitsev, M. Dorokhin, A. Brichkin, O. Vikhrova, Y. Danilov, B. Zvonkov, and V. Kulakovskii, *JETP Lett*. **90**, 658 (2010).
8. G. Lucovsky, *Solid State Commun*. **3**, 299 (1965).
9. J. Bardeen, *Phys. Rev. Lett*. **6**, 57 (1961).
10. I.V. Rozhansky, N.S. Averkiev, and E. Lähderanta, *Phys. Rev*. *B* **85**, 075315 (2012).
11. J. Schneider, U. Kaufmann, W. Wilkening, M. Baeumler, and F. Köhl, *Phys. Rev. Lett*. **59**, 240 (1987).
12. S.V. Zaitsev, *Fiz. Nizk. Temp*. **38**, 513 (2012) [*Low Temp. Phys*. **38**, 399 (2012)].
13. V.L. Korenev, I.A. Akimov, S.V. Zaitsev, V.F. Sapega, L. Langer, D.R. Yakovlev, Y.A. Danilov, and M. Bayer, *Nat. Commun*. **3**, 959 (2012).

PUBL. 7

I. V. ROZHANSKY, I. V. KRAINOV, N. S. AVERKIEV, and E. LÄHDERANTA, RESONANT EXCHANGE INTERACTION IN SEMICONDUCTORS, *Physical Review B*, **88**, 155326, 2013.

PHYSICAL REVIEW B **88**, 155326 (2013)

Resonant exchange interaction in semiconductors

I. V. Rozhansky,[1,2,3,*] I. V. Krainov,[1] N. S. Averkiev,[1] and E. Lähderanta[2]
[1]*A.F. Ioffe Physical Technical Institute, Russian Academy of Sciences, 194021 St.Petersburg, Russia*
[2]*Lappeenranta University of Technology, P.O. Box 20, FI-53851, Lappeenranta, Finland*
[3]*St. Petersburg State Polytechnic University, 29 Polytechnicheskaja, St. Petersburg 195251, Russia*
(Received 4 July 2013; published 29 October 2013)

We present a nonperturbative calculation of indirect exchange interaction between two paramagnetic impurities via two-dimensional (2D) free carriers gas separated by a tunnel barrier. The method takes into account the impurity attractive potential which can form a bound state. The calculations show that if the bound impurity state energy lies within the energy range occupied by the free 2D carriers the indirect exchange interaction is strongly enhanced due to resonant tunneling and exceeds by a few orders of magnitude what one would expect from the conventional Ruderman-Kittel-Kasuya-Yosida approach.

DOI: 10.1103/PhysRevB.88.155326 PACS number(s): 75.30.Et, 71.70.Gm

Semiconductor heterostructures with paramagnetic impurities spatially separated from the free charge carriers are coming into the focus of semiconductor-based spintronics. A number of recent experiments show that paramagnetic ions located at a tunnel distance from the quantum well (QW) induce substantial spin polarization of the two-dimensional (2D) carriers in the QW while preserving their high mobility.[1,2] Charge carriers tunneling between the bound impurity states and the continuum of delocalized states might also play an important role in the interaction between the paramagnetic ions themselves. The indirect exchange interaction between Mn ions mediated by the holes is believed to be the key mechanism underlying the ferromagnetic ordering in the InGaAs-based semiconductors doped with Mn.[3] For the uniformly doped samples there are different opinions whether the main contribution comes from the free holes of the valence band or from the localized carriers of the impurity band.[4,5] For the Mn δ-doped heterostructures experiments show that the QW located near the Mn layer affects its ferromagnetic properties,[6,7] most likely due to the free 2D holes in the QW.[8] The indirect exchange interaction via free carriers is usually described on the basis of the well known Ruderman-Kittel-Kasuya-Yosida (RKKY) theory, which utilizes the second-order perturbation calculation with account for the Pauli exclusion principle.[9] The RKKY theory, while perfectly applicable in many cases, ignores the fact that the attracting potential of the ion may have a bound state so that the scattering of the free carriers can be of a resonant character, at which point the perturbation theory fails. In this paper we report on a new approach to the indirect exchange pair interaction, which takes into account the resonance case in a nonperturbative way. The exactly solvable Fano-Anderson model is exploited to describe the tunnel coupling of the bound state with the continuum[10,11] with the spin configuration of the impurities being a parameter.

In order to rely on a certain model we consider a heterostructure containing a QW and δ layer of paramagnetic ions separated from the QW by a tunnel barrier. A paramagnetic ion is assumed to have a bound state characterized by its energy ε_0 while the QW has a continuum of 2D states starting from the single size quantization level and filled up to the Fermi level E_F. The resonant condition implies that ε_0 lies within the energy range of the continuum. Let us consider two paramagnetic ions located far enough from each other so that they do not interact directly. Both ions are located close to the QW so that the weak tunneling is allowed. The exchange interaction is described by:

$$H_J = J\widehat{\mathbf{S}}[\delta(\mathbf{r}-\mathbf{R}_1)\widehat{\mathbf{I}}_1 + \delta(\mathbf{r}-\mathbf{R}_2)\widehat{\mathbf{I}}_2], \tag{1}$$

where $\mathbf{R_{1,2}}$ are the ions positions, $\widehat{\mathbf{I}}_{1,2}, \widehat{\mathbf{S}}$ are the spin operators for the ion and the free carrier respectively, and J is the exchange constant. The RKKY theory[9] gives the interaction energy proportional to $J^2\langle\widehat{\mathbf{I}}_1\widehat{\mathbf{I}}_2\rangle$. In our theory we will show that the resonant tunnel coupling with the free carriers channel can substantially increase the interaction strength.

If we try to discard the perturbation theory limitation and consider exact solution for the Hamiltonian containing (1) the problem becomes far more complicated. Each of the free carriers spins is coupled with both ions and the only quantity that is conserved is the total spin of the whole system. The exact solution for this many-body problem is hard to find.[12] Here we suggest a simpler approach, which allows us to estimate the indirect exchange interaction including the resonant case. We shall neglect the ions' spin dynamics and consider them classically replacing the appropriate operators by the classical moments I_1, I_2. The strength of the indirect exchange interaction can be then evaluated as the energy difference between parallel and antiparallel spin configurations of the two impurity ions. For the (anti)parallel ion spin configuration H_J (1) does not mix the free carrier spin projections so we can replace $\widehat{\mathbf{S}}$ with a parameter $s = \pm|s|$. The total Hamiltonian consists of three terms:

$$H = H_0 + H_T + H_J, \tag{2}$$

where H_0 is the Hamiltonian of the system without tunnel coupling and spin-spin interaction, H_T is the Bardeen's tunnel term,[13] and H_J is the exchange interaction term (1). In the second quantization representation:

$$\begin{aligned} H_0 &= \varepsilon_0 a_1^+ a_1 + \varepsilon_0 a_2^+ a_2 + \int \varepsilon_\lambda c_\lambda^+ c_\lambda d\lambda, \\ H_T &= \int (t_{1\lambda} c_\lambda^+ a_1 + t_{2\lambda} c_\lambda^+ a_2 + h.c.) d\lambda, \\ H_J &= JA(I_1 s a_1^+ a_1 + I_2 s a_2^+ a_2), \end{aligned} \tag{3}$$

where $a^+_{1,2}, a_{1,2}$ are the creation and annihilation operators for the bound states at the impurity ions 1,2, characterized by the same energy ε_0 and localized wave functions ψ_1, ψ_2. c^+_λ, c_λ are the creation and annihilation operators for a continuum state characterized by the quantum number(s) λ, having the energy ε_λ and the wave function φ_λ, energy is measured from the QW size quantization level,

$$A = |\psi_1(\mathbf{R_1})|^2 = |\psi_2(\mathbf{R}_2)|^2. \tag{4}$$

The tunnel parameters are given by[11,13]

$$t_{1,2}(\lambda) = -\frac{\hbar^2}{2m_\perp}\int_{\Omega_S} dS\left(\varphi^*_\lambda \frac{d}{dz}\psi_{1,2} - \psi_{1,2}\frac{d}{dz}\varphi^*_\lambda\right), \tag{5}$$

where integration is over the plane Ω_S, parallel to the QW plane and passing through the ions centers, $m_\perp$ is the effective mass in the direction perpendicular to the QW plane. The hybridized eigenfunctions Ψ of the whole system can be expanded over the bound states and the delocalized states in the form:

$$\Psi = \nu_1\psi_1 + \nu_2\psi_2 + \Phi, \quad \Phi = \int \nu_\lambda \varphi_\lambda d\lambda. \tag{6}$$

Plugging (6) into the stationary Schrödinger equation $H\Psi = E\Psi$ with Hamiltonian (2) yields:

$$\begin{aligned} \nu_1(\varepsilon_0 - E + JAI_1 s) + \int t_{1\lambda}\nu_\lambda d\lambda = 0 \\ \nu_2(\varepsilon_0 - E + JAI_2 s) + \int t_{2\lambda}\nu_\lambda d\lambda = 0 \\ \nu_\lambda(\varepsilon - E) + \nu_1 t^*_{1\lambda} + \nu_2 t^*_{2\lambda} = 0. \end{aligned} \tag{7}$$

According to the Fano method[10] ν_λ is expressed from the last equation of (7) as follows:

$$\nu_\lambda = P\frac{\nu_1 t^*_{1\lambda} + \nu_2 t^*_{2\lambda}}{E-\varepsilon} + Z(\nu_1 t^*_{1\lambda} + \nu_2 t^*_{2\lambda})\delta(E-\varepsilon), \tag{8}$$

where P denotes principal value and $Z(E)$ is to be determined. Plugging (8) into (7) yields:

$$\begin{aligned} \nu_1(JAI_1 s + F_{11} + ZT_{11} - E') + \nu_2(F_{21} + ZT_{21}) = 0 \\ \nu_1(F_{12} + ZT_{12}) + \nu_2(JAI_2 s + F_{22} + ZT_{22} - E') = 0, \end{aligned} \tag{9}$$

where

$$\begin{aligned} F_{\alpha\beta} = P\int \frac{t^*_{\alpha\lambda}t_{\beta\lambda}}{E-\varepsilon}d\lambda, \quad T_{\alpha\beta} = \int t^*_{\alpha\lambda}t_{\beta\lambda}\delta(\varepsilon - E)d\lambda, \\ E' = E - \varepsilon_0, \quad \alpha,\beta = 1,2. \end{aligned} \tag{10}$$

For nontrivial solution of (9) one gets a dispersion equation for Z, which determines the energy-dependent phase shift due to the scattering at the bound state.[10] If the system is put in a box the phase shift affects the quantization condition for the wave vector and, in this way, the energy of the whole system. To proceed to the specific case let us consider two ions located at the same distance d from the QW having the distance R between them. The z axis is normal to the QW plane ($z = 0$ corresponds to the QW boundary), the x axis passes through the ions centers with $x = 0$ in the middle of them. Thus, the coordinates of the ions are:

$$\mathbf{R}_1 = (-R/2, 0, d); \quad \mathbf{R}_2 = (R/2, 0, d).$$

Because it is assumed $R \gg d$ and the localized wave functions ψ_1, ψ_2 do not overlap, their particular form is not important. It is convenient to take the localized wave functions in the form:

$$\psi_{1,2} = \left(\frac{2}{\pi r_0^2}\right)^{3/4} e^{-\left(\frac{x\pm R/2}{r_0}\right)^2} e^{-\left(\frac{y}{r_0}\right)^2} e^{-\left(\frac{z-d}{r_0}\right)^2}, \tag{11}$$

where r_0 is the localization radius. The continuum wave functions are taken as follows:

$$\varphi_{\mathbf{k}} = \eta(z)e^{i\mathbf{k}\rho}. \tag{12}$$

Here $\mathbf{k}$ is the in-plane wave vector, ρ is the 2D in-plane radius-vector, $\eta(z)$ is the envelope function of size quantization along z. Outside of the QW:

$$\eta(z) = \zeta a^{-1/2} e^{-qz}, \tag{13}$$

where $q = \sqrt{2m_\perp E_0}/\hbar^2$, E_0 is the binding energy of the bound state, which at the same time determines the height of the potential barrier between impurities and the QW,[14] a is the QW width, ζ is a dimensionless parameter weakly depending on q and a. For a realistic rectangular QW $\zeta \approx 0.5$. The calculation of (5) using (11) (assuming $r_0 \ll k^{-1}$) and (12) yields:

$$t_{1,2}(k) = \sqrt{\frac{\hbar^2 T}{2\pi m}} e^{-i\mathbf{k}\mathbf{R}_{1,2}}, \tag{14}$$

where T is the energy parameter for the tunneling:

$$T = (2\pi)^{3/2}\zeta^2 \frac{r_0 m}{a m_\perp} E_0 e^{-2qd}, \tag{15}$$

m is the effective mass along the QW plane. Plugging (14) into (10) we get:

$$\begin{aligned} T_{11} = T_{12} = T, \quad T_{12} = T_{21} \equiv t = TJ_0(kR), \\ F_{11} = F_{22} \equiv F, \quad F_{12} = F_{21} \equiv f = \pi T Y_0(kR), \end{aligned} \tag{16}$$

where J_0, Y_0 are the Bessel and Neumann functions of zeroth order, $k = \sqrt{2mE}/\hbar$. The quantity F represents the shift of the resonance position with respect to ε_0, its explicit calculation requires more accurate expression than (14) taking into account $k \sim r_0^{-1}$ to avoid the divergence. However, it will be not needed since F is of the order of T and does not depend on R. From (9) follows the dispersion equation for Z:

$$\begin{aligned} (ZT + F - E' + JAI_1 s)(ZT + F - E' + JAI_2 s) \\ = (f + Zt)^2. \end{aligned} \tag{17}$$

For the parallel spin configuration $I_1 = I_2 = I$ the two roots are

$$Z_\pm = -\frac{JAIs + F \pm f - E'}{T \pm t}. \tag{18}$$

$Z_\pm$ corresponds to $\nu_1 = \pm\nu_2$ so that the hybridized wave function (6) is either symmetric or antisymmetric with respect to $x \to -x$. This is due to the symmetry of the spin-spin interaction which holds only for the parallel spin configuration. With use of (6) and (8) the delocalized part of the hybridized wave function is given by:

$$\Phi_\pm = C_\pm \begin{bmatrix} J_0(k\rho_1)\cos\Delta_\pm - H_0(k\rho_1)\sin\Delta_\pm \\ \pm J_0(k\rho_2)\cos\Delta_\pm \mp H_0(k\rho_2)\sin\Delta_\pm \end{bmatrix}, \tag{19}$$

where J_0 and H_0 are Bessel and Struve functions of the zeroth order, $\rho_{1,2} = |\rho - \mathbf{R}_{1,2}|$,

$$\tan\Delta_\pm(E) = -\frac{\pi}{Z_\pm(E)}, \quad C_\pm = -\frac{\pi T \nu_1 \eta(d)}{\sin\Delta_\pm}.$$

The general solution is an arbitrary linear combination:

$$\Phi(\rho) = A\Phi_+(\rho) + B\Phi_-(\rho).$$

Let us put the system in a big cylindrical box of radius L and apply the boundary conditions $\Phi(L) = 0$. Using the asymptotic forms of Φ_+,Φ_- we obtain the following quantization condition for k:

$$\begin{aligned} k_\pm &= k_L - \frac{\widetilde{\Delta}_\pm}{L}, \\ \widetilde{\Delta}_+ &= -\operatorname{arccot}\left[\frac{\pi(T+t)}{JAIs + F - E' + f}\right], \\ \widetilde{\Delta}_- &= \arctan\left[\frac{\pi(T-t)}{JAIs + F - E' - f}\right], \end{aligned} \tag{20}$$

$k_L = \pi n/L$, $n = 1,2,3,\ldots$ is the quantized wave number in the absence of the tunnel coupling with the localized states. For the discrete energy levels in a box we have:[15]

$$\varepsilon_\pm = \varepsilon_L - \frac{\hbar^2 k_L \widetilde{\Delta}_\pm(\varepsilon_L)}{mL} + O\left(\frac{1}{L^2}\right), \tag{21}$$

where $\varepsilon_L = \hbar^2 k_L^2/2m$.

Let us now consider the antiparallel configuration of the ions spins $I_1 = -I_2 = I$. The dispersion equation (17) again has two roots Z_1, Z_2, but unlike the previous case the corresponding wave functions $\Phi_{1,2}$ are neither symmetric nor antisymmetric, they can be represented as a superposition of symmetric and antisymmetric parts:

$$\Phi_{1,2} = c_+(Z_{1,2})\Phi_+(Z_{1,2}) + c_-(Z_{1,2})\Phi_-(Z_{1,2}), \tag{22}$$

where

$$\frac{c_+(Z)}{c_-(Z)} = \frac{F - E' - f + Z(T-t) + JAIs}{F - E' + f + Z(T+t) + JAIs},$$

and Φ_+, Φ_- are given by (19). The general solution is a linear combination of Φ_1 and Φ_2. The quantization in a finite size box results in:

$$\begin{aligned} k_{1,2} &= k_L - \frac{\Delta_{1,2}}{L}, \\ \Delta_1 &= \arctan\left[\frac{\pi(F - E' + f)(T-t)}{(F-E')^2 - f^2 - (JAIs)^2}\right], \\ \Delta_2 &= -\operatorname{arccot}\left[\frac{\pi(F - E' - f)(T+t)}{(F-E')^2 - f^2 - (JAIs)^2}\right]. \end{aligned} \tag{23}$$

Given the discrete energy levels for the parallel and antiparallel ions spin configurations the indirect exchange energy can be calculated by summing the energy difference over all free carriers. Using (21) we have:

$$E_{\rm exc} = -\frac{1}{\pi}\sum_s \int_0^{E_F} [(\widetilde{\Delta}_+ + \widetilde{\Delta}_-) - (\Delta_1 + \Delta_2)]dE.$$

The evaluation neglecting terms of the order higher than T^2 yields:

$$E_{\rm exc} = \frac{1}{\pi}\int_0^{E_F} \arctan\left[\frac{8\pi^2 T^2 j^2 J_0(kR)Y_0(kR)}{((\varepsilon-\varepsilon_0)^2 - j^2)^2}\right]d\varepsilon, \tag{24}$$

where $k = \sqrt{2m\varepsilon}/\hbar$, $j = |JAIs|$. As seen from (24) the interaction energy $E_{\rm exc}$ oscillates with the distance between the impurities R. The argument of arctangent in (24) has poles at $\varepsilon = \varepsilon_0 \pm j$ and the result strongly depends on whether these resonances are within the range of integration $\varepsilon \in [0, E_F]$. If they are, from the width of the resonances the amplitude of the exchange interaction energy is estimated as:

$$E_{\rm res} \sim \sqrt{Tj}, \tag{25}$$

while the period of the oscillations is $\hbar/\sqrt{2m\varepsilon_0}$. The nonresonant case occurs if $\varepsilon_0 \gg E_F$, $j \ll E_F$. The integration (24) then results in:

$$\begin{aligned} E_{nr} &= \frac{8\pi T^2 j^2 E_F}{\varepsilon_0^4}\chi(R), \\ \chi(R) &= J_0(k_F R)Y_0(k_F R) + J_1(k_F R)Y_1(k_F R). \end{aligned} \tag{26}$$

The condition $j \ll E_F$ allows for the perturbation theory thus the expression (26) is what one would expect from the conventional RKKY approach. The functional dependence $\chi(R)$ is exactly the same as for the 2D RKKY interaction without tunneling[16] and the prefactor accounts for the particular model we have used to describe the tunneling and the bound impurity state. The interaction energy amplitude for the resonance case appears to be substantially higher than for the nonresonant one. Assuming for both cases $\varepsilon_0 \sim E_F$ we can roughly estimate the amplification as

$$\gamma \equiv \frac{E_{\rm res}}{E_{nr}} \sim \frac{\varepsilon_0^4}{8\pi T^{3/2} j^{3/2} E_F}. \tag{27}$$

For an estimate we take the parameters based on InGaAs-based heterostructures studied in Refs. 1, 2, 17. For $T \sim 0.01E_F$, $j \sim 0.1E_F$ γ can be as high as three orders of magnitude. Figure 1 shows the results of the numerical calculation according to (24). The domain of applicability starts from

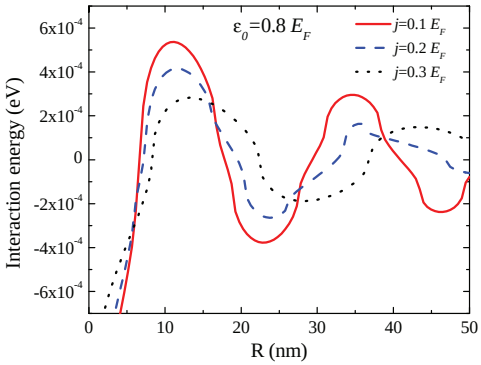

FIG. 1. (Color online) Indirect exchange interaction energy vs distance between ions in the resonant case.

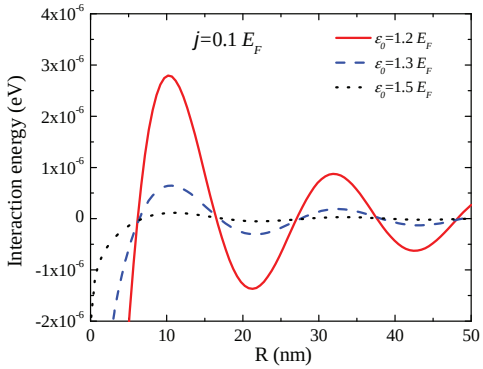

FIG. 2. (Color online) Indirect exchange interaction energy vs distance between ions in the nonresonant case.

$R > r_0$ (for real structures $r_0 \sim 1$ nm). We take $m = 0.1m_0$ (m_0 is the free electron mass), $E_F = 10$ meV, $\varepsilon_0 = 0.8E_F$, so for $j = 0.1E_F$ both integrand resonances are within the range $[0, E_F]$, for $j = 0.3E_F$ only one resonance is within the range and the interaction energy is decreased. The case $j = 0.2$ is an intermediate one—one of the resonances appears exactly at E_F. The nonresonant case is shown in Fig. 2. Here for all the curves both resonances $\varepsilon = \varepsilon_0 \pm j$ are above E_F. This strongly lowers the amplitude of the interaction energy by at least two orders of magnitude compared to the resonant case in Fig. 1. A very different nonresonant limiting case arises from (24) for $j \gg E_F, j \gg \varepsilon_0$:

$$E_{nrj} = \frac{8\pi T^2 E_F}{j^2}\chi(R). \tag{28}$$

While (28) has the same dependence on R as (26), this cannot be derived using the perturbation theory in j and describes the weakening of the interaction at large j due to the finite energy range of the free carriers available for the indirect exchange. This case along with the resonant case may be of importance for the diluted magnetic semiconductors. For GaAs heterostructures doped with Mn j (unlike in metals) is commonly assumed to be comparable or even substantially exceeding E_F.[3] However, the formula (28) must be regarded only as an estimate, because with $j \gg E_F$ the ions spins dynamics (neglected in our model) may be essential.

In our calculation we have obtained the interaction energy by analyzing the phase shift for scattering at the impurity potential and its effect on the density of states for the standing waves in a box. This approach allowed us to analyze the resonant case. For the bound-state energy being within the energy range occupied by the free carriers the indirect exchange interaction appears to be much stronger than expected from the RKKY approach. We believe that our results may shed light on ferromagnetic coupling in Mn layers in InGaAs-based heterostructures and other nanostructures with paramagnetic impurities.

The work has been supported by the Russian Foundation for Basic Research (RFBR) (Grants No. 11-02-00348, No. 11-02-00146, No. 12-02-00815, and No.12-02-00141), RF President Grant No. NSh-5442.2012.2, Dynasty Foundation.

*rozhansky@gmail.com

[1]V. Korenev, I. Akimov, S. Zaitsev, V. Sapega, L. Langer, D. Yakovlev, Y. A. Danilov, and M. Bayer, Nature Commun. **3**, 959 (2012).
[2]S. Zaitsev, M. Dorokhin, A. Brichkin, O. Vikhrova, Y. Danilov, B. Zvonkov, and V. Kulakovskii, JETP Lett. **90**, 658 (2010).
[3]T. Jungwirth, J. Sinova, J. Mašek, J. Kučera, and A. H. MacDonald, Rev. Mod. Phys. **78**, 809 (2006).
[4]T. Dietl, H. Ohno, and F. Matsukura, Phys. Rev. B **63**, 195205 (2001).
[5]J. Fujii, B. R. Salles, M. Sperl, S. Ueda, M. Kobata, K. Kobayashi, Y. Yamashita, P. Torelli, M. Utz, C. S. Fadley *et al.*, Phys. Rev. Lett. **111**, 097201 (2013).
[6]S. V. Zaitsev, Low Temp. Phys. **38**, 399 (2012).
[7]B. Aronzon, A. Davydov, M. Goiran, B. Raquet, A. Lashkul, and E. Lahderanta, J. Phys.: Conf. Ser. **456**, 012001 (2013).
[8]V. Tripathi, K. Dhochak, B. A. Aronzon, B. Raquet, V. V. Tugushev, and K. I. Kugel, Phys. Rev. B **85**, 214401 (2012).
[9]M. A. Ruderman and C. Kittel, Phys. Rev. **96**, 99 (1954).
[10]U. Fano, Phys. Rev. **124**, 1866 (1961).
[11]I. V. Rozhansky, N. S. Averkiev, and E. Lähderanta, Phys. Rev. B **85**, 075315 (2012).
[12]N. Andrei, K. Furuya, and J. H. Lowenstein, Rev. Mod. Phys. **55**, 331 (1983).
[13]J. Bardeen, Phys. Rev. Lett. **6**, 57 (1961).
[14]I. V. Rozhansky, N. S. Averkiev, and E. Lähderanta, Low Temp. Phys. **39**, 28 (2013).
[15]E. Mueller, http://people.ccmr.cornell.edu/~emueller/scatter.pdf (2002).
[16]D. N. Aristov, Phys. Rev. B **55**, 8064 (1997).
[17]V. Tripathi, K. Dhochak, B. A. Aronzon, V. V. Rylkov, A. B. Davydov, B. Raquet, M. Goiran, and K. I. Kugel, Phys. Rev. B **84**, 075305 (2011).

PUBL. 8

I. V. ROZHANSKY, N. S. AVERKIEV, I. V. KRAINOV, and E. LÄHDERANTA, RESONANT ENHANCEMENT OF INDIRECT EXCHANGE INTERACTION IN SEMICONDUCTOR HETEROSTRUCTURES, *physica status solidi (a)*, **211**, 1048-1054, 2014.

physica status solidi

pss

www.pss-journals.com

reprint

WILEY-VCH

Phys. Status Solidi A **211,** No. 5, 1048–1054 (2014) / **DOI** 10.1002/pssa.201300676

Part of Topical Section on
Nanoscaled Magnetism and Applications

physica status solidi a
www.pss-a.com
applications and materials science

Resonant enhancement of indirect exchange interaction in semiconductor heterostructures

I. V. Rozhansky[*,1,2,3], **N. S. Averkiev**[1], **I. V. Krainov**[1], **and E. Lähderanta**[2]

[1] A.F. Ioffe Physical Technical Institute, Russian Academy of Sciences, 194021 St. Petersburg, Russia
[2] Lappeenranta University of Technology, P.O. Box 20, 53851 Lappeenranta, Finland
[3] St. Petersburg State Polytechnic University, 29 Polytechnicheskaja, 195251 St. Petersburg, Russia

Received 15 October 2013, revised 16 December 2013, accepted 7 January 2014
Published online 17 February 2014

Keywords exchange interaction, diluted magnetic semiconductors, RKKY

[*] Corresponding author: e-mail rozhansky@gmail.com, Phone: +78 122927155, Fax: +78 122971017

We present an approach to calculate indirect exchange interaction between paramagnetic ions via free carriers in heterostructures. Unlike well-known Ruderman–Kittel–Kasuya–Yosida (RKKY) theory the suggested method is not a perturbation theory and thus can be used in the wider variety of cases, especially when resonant effects are important. The method is applied to standard 1D and 2D indirect exchange problems. We further focus on calculation of indirect exchange interaction between two ions mediated by 2D free carriers gas separated by a tunnel barrier. The calculations show that if the ion bound state energy lies within the energy range occupied by the free 2D carriers, the indirect exchange interaction is strongly enhanced due to resonant tunneling and far exceeds what one would expect from the conventional RKKY approach.

1 Introduction Ferromagnetic diluted magnetic semiconductors (DMS) have been in the focus of the extensively developing spintronics for quite a while. Of particular interest nowadays are the semiconductor heterostructures combining a quantum well (QW) and a narrow layer of magnetic impurities located nearby but not inside the QW. The general idea utilized in such structures is to preserve the high mobility of the 2D free carriers and at the same time to make use of the magnetic properties induced by the impurities layer. A number of interesting results have been obtained for the Mn-doped InGaAs-based heterostructures in the optical and transport experiments [1–3]. It was discovered that the spin polarization of the 2D carriers in an external magnetic field as well as the ferromagnetic properties of the samples show non-monotonic dependence on the QW depth [4, 5]. Analysis of the parameters of these GaAs/InGaAs/Mn heterostructures shows that the non-monotonic behavior originates from falling of the hole bound state at Mn ion into the energy range of occupied 2D heavy holes subband of the first QW size quantization level. In this case the resonant tunneling is allowed between the bound state and the continuum of the delocalized 2D states in the QW so that much stronger coupling of the hole localized at Mn with the 2D holes gas in the QW is expected. Both too shallow or too deep QW would break the resonant condition and decrease the mutual influence of the QW and the Mn ions. The effect of resonant tunnel coupling on the photoluminescence has been considered in [6, 7]. While the particular mechanism responsible for the ferromagnetism in diluted GaAs/Mn systems is still not clear [8], it is commonly believed that the exchange interaction between Mn ions is mediated by the holes. In particular, there are some experimental arguments in favor of the RKKY-type interaction in the Mn delta-doped heterostructures [9]. We believe that the non-monotonic dependence of the Curie temperature on the QW depth [5] is likely related to the resonant RKKY-type contribution to the Mn layer ferromagnetism mediated by the 2D holes in the QW. The main goal of this paper is to introduce a proper theory describing the indirect pair exchange interaction between two ions mediated by a 2D free carriers gas located at a tunnel distance. The tunnel coupling leads to the admixture of the bound ion state wavefunction to the 2D QW states. There has been an extensive studying of indirect exchange interaction in magnetic multilayers showing the effect of the energy spectrum and the carriers wavefunctions on the interlayer

coupling [10, 11]. However, inserting the exactly calculated free carriers wavefunctions into the RKKY formula is not valid when the wavefunctions are strongly modified, i.e. in the case of the resonant tunneling. It can be shown that the perturbation theory (RKKY) would deliver a divergent result when the resonant tunneling occurs near the Fermi level. The other approach well developed for the 1D case of magnetic multilayers is to solve one-particle electron problem exactly for the potential which takes the ions magnetic moments as parameters. The exchange interaction energy between the ions is then interpreted as the difference in the total system energy calculated for the different potentials [12–14]. In our calculations we will follow the latter approach and apply it both to 1D and 2D cases. Then in Section 5 we proceed to the case of the two magnetic ions interacting via a 2D electron gas separated from the ions by a tunnel barrier. It will be shown that when the condition for the resonant tunneling is met the interaction strength appears to be strongly enhanced.

2 Indirect exchange interaction. Non-perturbative approach The conventional RKKY theory describes pair interaction between two magnetic ions mediated by free carriers gas. The ions do not interact directly so the explicit exchange interaction is only between a magnetic ion spin and a free carrier spin. It is written in the form [15]

$$H_J = J\delta(\mathbf{r}-\mathbf{R}_1)\hat{\mathbf{I}}_1\hat{\mathbf{S}} + J\delta(\mathbf{r}-\mathbf{R}_2)\hat{\mathbf{I}}_2\hat{\mathbf{S}}, \tag{1}$$

where $\mathbf{R}_{1,2}$ is the ions positions, $\hat{\mathbf{I}}_{1,2}$, the spin operators for the ion and the free carrier, respectively, J the exchange constant. According to the RKKY approach, H_J is treated as perturbation and in the second-order one obtains the energy correction which is proportional to $J^2\mathbf{I_1}\mathbf{I_2}$ and depends on R in oscillating way. Here $\mathbf{I_1}$, $\mathbf{I_2}$ are the ion spins which are well defined for the non-perturbed state basis. If we try to discard the perturbation theory limitation and consider exact solution for the Hamiltonian containing (1) the problem becomes far more complicated. Each of the free carriers spins is coupled with both ions and the only quantity that is conserved is the total spin of the two ions and all the electrons. The exact solution for this many-body problem is hard to find. However, there is a certain room to improve the perturbative RKKY approach for the case when the direct exchange interaction determined by the constant J is still small compared to the free carriers Fermi energy E_F, but the modification of the coordinate parts of the wavefunctions is not small. In this case the total spin of the free carriers in the ground state would be small (otherwise due to the Pauli exclusion principle it would provide the energy correction of the order of E_F), thus, one can assume that the total spin of the ions $\mathbf{I_1}+\mathbf{I_2}$ is nearly conserved. Thus, the eigenstates can be classified by the total spin of the two impurities in the range 0–2I. The interaction energy can then be calculated by treating the ion spins classically as the energy difference between the states with zero total spin and with the total spin 2I, corresponding to the antiparallel and parallel configuration of the ion spins, respectively. As H_J (1) does not mix the free carrier spin projections we can further replace $\hat{\mathbf{S}}$ with a parameter $s=\pm|s|$. Finally, the interaction energy is calculated as

$$\Delta E = E_{\uparrow\uparrow} - E_{\uparrow\downarrow}, \tag{2}$$

where $E_{\uparrow\uparrow}, E_{\uparrow\downarrow}$ denote the energy of the system with parallel and antiparallel configurations with single-particle Hamiltonians being, respectively:

$$\begin{aligned} H_{\uparrow\uparrow} &= H_0 + JIs[\delta(\mathbf{r}-\mathbf{R}_1)+\delta(\mathbf{r}-\mathbf{R}_2)],\\ H_{\uparrow\downarrow} &= H_0 + JIs[\delta(\mathbf{r}-\mathbf{R}_1)-\delta(\mathbf{r}-\mathbf{R}_2)], \end{aligned} \tag{3}$$

where $H_0 = -(\hbar^2/2m)\Delta$ is the unperturbed Hamiltonian for the free carrier of the mass m. Once the single-particle Hamiltonian is fixed in the form (3) the appropriate solutions of the stationary Schrodinger equation can be found exactly. The appropriate difference in the total energy of an ensemble of electrons can be obtained by analyzing the solutions for $H_{\uparrow\uparrow}$, $H_{\uparrow\downarrow}$ in a finite-size box of size L with zero boundary conditions [13, 16]. The obtained spectra of single-particle states is filled with a fixed number of particles with account for Pauli exclusion principle and the total energy is calculated by summing the occupied states energies. The total energy difference between parallel and antiparallel ion spin configurations is interpreted as the indirect interaction energy between the ions. Here we present the results of such calculation for 1D and 2D cases and compare the exact solution with the known results of the perturbation theory (RKKY) [17].

3 Indirect exchange interaction in 1D For the 1D case it appears of particular importance to take into account the localized states $E<0$ whenever they occur in the spectra, i.e. when the contact interaction is represented by an attractive delta-function potential. Analyzing the 1D finite-box spectra of (3) and taking the continuous limit $L\to\infty$, we obtain

$$\Delta E = \frac{1}{2\pi}\int_0^{E_F} f(E,R)\mathrm{d}E + \Delta E_{\mathrm{loc}}, \tag{4}$$

where

$$\begin{aligned} f &= 2\arctan\frac{j^2\sin 2kR}{4k^2+2j^2\sin^2 kR}\\ &+\arctan\frac{4kj+j^2\sin 2kR}{4k^2-2j^2\sin^2 kR} - \arctan\frac{4kj-j^2\sin 2kR}{4k^2-2j^2\sin^2 kR}. \end{aligned} \tag{5}$$

$$j = JI|s|\frac{m}{\hbar^2},\ k=\frac{\sqrt{2mE}}{\hbar},\ R=|\mathbf{R}_1-\mathbf{R}_2|$$

E_F is the Fermi energy of the unperturbed free carriers gas. ΔE_{loc} stands for the difference in the bound states energy for the parallel and antiparallel configurations. The bound

state energy is determined from the following equation:

$$\left(\kappa\tanh\left(\frac{\kappa R}{2}\right)+\kappa+2j\right)\left(\kappa\coth\left(\frac{\kappa R}{2}\right)+\kappa\pm 2j\right)$$
$$=-\left(\kappa\tanh\left(\frac{\kappa R}{2}\right)+\kappa\pm 2j\right)\left(\kappa\coth\left(\frac{\kappa R}{2}\right)+\kappa+2j\right),$$

where $\kappa=\sqrt{2m|E_{\rm loc}|}/\hbar$, "+", "−" correspond to the parallel and antiparallel ion spin configurations, respectively. For the large distance between the ions $\kappa R>>1$:

$$E_{\rm loc}(\kappa R->\infty)=-\frac{(JIs)^2 m}{2\hbar^2}.$$

Always one such level exists for antiparallel ion spins configuration, for the parallel configuration there are no solutions for the repulsive double-delta potential and two bound states for the attractive double-delta potential. Figure 1 shows the indirect interaction energy calculated according to (4) and the result of the RKKY theory in 1D [17]:

$$E_{\rm RKKY}=E_0{\rm si}(2k_{\rm F}R),$$

where $E_0=4j^2\hbar^2/\pi m$, si(x) is the sine integral. The exchange constant is taken such that $j/k_{\rm F}=0.1$. In order to show the role of the localized states, we also plotted the part of interaction energy associated with delocalized states, i.e. neglecting $\Delta E_{\rm loc}$ (Fig. 1). As clearly seen from the figure at $R<1/j$ it is of key importance to take into account the overlapping of the localized states which strongly contribute to the indirect exchange. At large distance between the ions the interaction is only due to the plane waves and one gets the result of the RKKY theory. Interestingly, if we do take into account the localized states the exact solution perfectly matches the RKKY perturbation theory. This agreement remains very good up to $j/k_{\rm F}=1$ which is actually beyond the perturbation theory criteria.

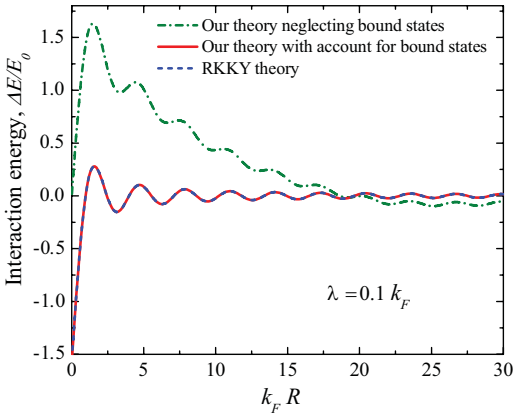

Figure 1 Indirect exchange energy in 1D case. The exact calculation with and without account of the bound states compared to the RKKY theory.

4 Indirect exchange interaction in 2D To solve the 2D case it is more convenient to write (3) in the momentum representation:

$$\begin{aligned}&\left(k^2-k_{\rm E}{}^2\right)\Psi(\mathbf{k})\\&+2\lambda_1 e^{-i\mathbf{k}\mathbf{R}_1}\Psi(\mathbf{R}_1)+2\lambda_2 e^{-i\mathbf{k}\mathbf{R}_2}\Psi(\mathbf{R}_2)=0,\end{aligned}\tag{6}$$

where

$$\lambda_{1,2}=JI_{1,2}s\frac{m}{\hbar^2},\quad k_{\rm E}=\frac{\sqrt{2mE}}{\hbar^2}.\tag{7}$$

Equation (6) gives $\Psi(\mathbf{k})$ only for $k\neq k_{\rm E}$. In order to get the solution for arbitrary k we follow the method introduced in Fano–Anderson model [18, 19]:

$$\begin{aligned}\Psi(\mathbf{k})=&\left(2\lambda_1 e^{-i\mathbf{k}\mathbf{R}_1}\Psi(\mathbf{R}_1)+2\lambda_2 e^{-i\mathbf{k}\mathbf{R}_2}\Psi(\mathbf{R}_2)\right)\\&\times\left[P\frac{1}{k_{\rm E}^2-k^2}+Z\delta\left(k_{\rm E}^2-k^2\right)\right],\end{aligned}\tag{8}$$

where P denotes the principal value, Z is an unknown function of $k_{\rm E}$ to be determined later. After inverse Fourier transformation and integration over the polar angle φ in k-space we obtain:

$$\begin{aligned}\Psi(\mathbf{r})=&\frac{1}{2}\lambda_1\left[\frac{Z}{\pi}J_0(k_{\rm E}\rho_1)+Y_0(k_{\rm E}\rho_1)\right]\Psi(\mathbf{R}_1)\\&+\frac{1}{2}\lambda_2\left[\frac{Z}{\pi}J_0(k_{\rm E}\rho_2)+Y_0(k_{\rm E}\rho_2)\right]\Psi(\mathbf{R}_2),\end{aligned}\tag{9}$$

where J_0, Y_0 are the Bessel and Neumann functions of zeroth order, $\rho_{1,2}=|\mathbf{r}-\mathbf{R}_{1,2}|$. Substituting $\mathbf{r}=\mathbf{R}_{1,2}$ yields:

$$\begin{aligned}\Psi(\mathbf{R}_1)&=\lambda_1\Psi(\mathbf{R}_1)(F+ZT)+\lambda_2(f+Zt)\Psi(\mathbf{R}_2),\\\Psi(\mathbf{R}_2)&=\lambda_1\Psi(\mathbf{R}_1)(f+Zt)+\lambda_2(F+ZT)\Psi(\mathbf{R}_2),\end{aligned}\tag{10}$$

where

$$\begin{aligned}&F=\frac{1}{\pi}P\int_0^\infty\frac{1}{k_{\rm E}^2-k^2}k{\rm d}k;\quad T=\frac{1}{2\pi},\\&f=\frac{1}{\pi}P\int_0^\infty\frac{J_0(kR)}{k_{\rm E}^2-k^2}k{\rm d}k;\quad t=\frac{1}{2\pi}J_0(k_{\rm E}R),\\&R=|\mathbf{R}_1-\mathbf{R}_2|.\end{aligned}\tag{11}$$

The quantity F diverges logarithmically resembling the known issue of dimension deficiency for the delta-potential in 2D [20, 21]. The issue is resolved by renormalization:

$$\frac{1}{\lambda_{1,2}}\to\frac{1}{\lambda_{1,2}}+F.\tag{12}$$

From (10) with (12) requiring $\Psi(\mathbf{R}_{1,2}) \neq 0$ we get the equation for Z:

$$(\lambda_1 ZT - 1)(\lambda_2 ZT - 1) = \lambda_1 \lambda_2 (f + Zt)^2. \tag{13}$$

Each of the two roots $Z_{1,2}$ determines the solutions $\Psi_{Z_{1,2}}(\mathbf{r})$ and the general solution is a linear combination of the two:

$$\Psi(r) = A\Psi_{Z_1}(r) + B\Psi_{Z_2}(\mathbf{r}). \tag{14}$$

Let us put the system in a big cylindrical box of radius L and apply the boundary conditions $\Psi(L, \varphi) = 0$. Using the asymptotic of $\Psi(\mathbf{r})$ from (9)–(14) we obtain:

$$\Psi(L,\varphi) = \begin{bmatrix} AC_1^+ \cos(k_E L + \delta_1) \\ +BC_2^+ \cos(k_E L + \delta_2) \end{bmatrix} \cos(k_E R \cos\varphi) + \begin{bmatrix} AC_1^- \sin(k_E L + \delta_1) \\ +BC_2^- \sin(k_E L + \delta_2) \end{bmatrix} \sin(k_E R \cos\varphi), \tag{15}$$

where

$$\tan\delta_{1,2} = -\frac{\pi}{Z_{1,2}}, \qquad C_{1,2}^{\pm} = \frac{\lambda_1 \Psi_{Z_{1,2}}(\mathbf{R}_1) \pm \lambda_2 \Psi_{Z_{1,2}}(\mathbf{R}_2)}{2\sin\delta_{1,2}}. \tag{16}$$

Imposing the zero boundary condition yields:

$$\begin{bmatrix} k_E = \dfrac{\pi n}{L} + \dfrac{\Delta_1}{L}, \\ k_E = \dfrac{\pi n}{L} + \dfrac{\Delta_2}{L} \end{bmatrix},$$

here $\Delta_{1,2}$ are functions of $\lambda_{1,2}$, f, T, t. Assuming zero temperature and Fermi distribution of the electrons the total energy shift for the system is given by[16]:

$$\Delta E = \frac{1}{\pi} \int_0^{E_F} [\Delta_1(E) + \Delta_2(E)] \mathrm{d}E, \tag{17}$$

where E_F is the Fermi level. The phase shifts $\Delta_{1,2}$ depend on $\lambda_{1,2}$, thus ΔE is different for different configurations of the ions and electrons spins. The exchange energy is given by

$$E_{ex} = \left(\Delta E_{\uparrow\uparrow -} + \Delta E_{\uparrow\uparrow +}\right) - \left(\Delta E_{\uparrow\downarrow -} + \Delta E_{\uparrow\downarrow +}\right). \tag{18}$$

Here in the indices the arrows denote ion spin projection and the signs stand for the electron spin projection. Substituting (17) into (18) we finally arrive at

$$E_{ex} = \frac{1}{\pi} \int_0^{E_F} \arctan[2\zeta(j) Y_0(k_E R) J_0(k_E R)] \mathrm{d}E, \tag{19}$$

where $\zeta(j)$ is the known function

$$\zeta(j) = j^2 - \frac{j^4}{2} + O\left(j^6\right), \qquad j = JI|s|\frac{m}{\hbar^2}. \tag{20}$$

For $j << 1$ from (19) follows the known result of $2D$ RKKY theory [17]:

$$E_{RKKY} = \frac{{k_F}^2 (JIs)^2}{\pi m \hbar^2} \chi(R), \qquad \chi(R) = J_0(k_F R) Y_0(k_F R) + J_1(k_F R) Y_1(k_F R). \tag{21}$$

5 Resonant indirect exchange interaction Let us now address the problem of indirect exchange interaction mediated by a free carriers gas separated by a tunnel barrier from the paramagnetic ions. Because the spin–spin interaction operator contains the delta-function (1), its matrix elements are proportional to the product of the basis wave function amplitudes at the ions site. For a wavefunction amplitude decaying inside the tunnel barrier one would simply expect a suppression of the indirect exchange interaction by a factor of $\exp(-4\kappa d)$, where $\kappa = \sqrt{2mU_0}/\hbar$, U_0 and d are the barrier height and width, respectively. However, if the ion has its own spin-independent attracting potential forming a bound state, the particle form the conducting layer with the same energy can effectively tunnel to the ions bound state. In terms of quantum mechanics it means that for the energy coinciding with that of the bound state the single-particle stationary wave function has an enhanced amplitude at the ion site due to the resonant tunneling. In this section, we shall consider this case and see how the resonant tunneling affects the indirect exchange. We consider two magnetic ions located at the same distance d from the the QW and coupled with the 2D electron gas of the QW through a tunnel barrier. The distance R between the ions is assumed to be large enough so that they do not interact directly. The ions are assumed to have a bound state which may lie within the energy range of the occupied states of the 2D gas. In this case, the resonant tunneling can occur between the delocalized state of the QW 2D subband and the ion bound state. We consider the total Hamiltonian consisting of three terms:

$$H = H_0 + H_T + H_J, \tag{22}$$

where H_0 is the Hamiltonian of the system without tunnel coupling and spin–spin interaction, H_T the Bardeen's tunnel

term [22], H_J the exchange interaction term (1). In the second quantization representation:

$$\begin{aligned} H_0 &= \varepsilon_0 a_1^+ a_1 + \varepsilon_0 a_2^+ a_2 + \int \varepsilon_\lambda c_\lambda^+ c_\lambda \mathrm{d}\lambda, \\ H_T &= \int \left(t_{1\lambda} a_1^+ c_\lambda + t_{2\lambda} a_2^+ c_\lambda + \text{h.c.}\right)\mathrm{d}\lambda, \\ H_J &= JA\left(I_1 s a_1^+ a_1 + I_2 s a_2^+ a_2\right), \end{aligned} \tag{23}$$

where $a_{1,2}^+, a_{1,2}$ are the creation and annihilation operators for the bound states at the impurity ions 1,2, characterized by the same energy ε_0 and localized wavefunctions ψ_1, ψ_2. c_λ^+, c_λ are the creation and annihilation operators for a continuum state characterized by the quantum number(s) λ, having the energy ε_λ and the wavefunction φ_λ, energy is measured from the QW size quantization level,

$$A = |\psi_1(\mathbf{R}_1)|^2 = |\psi_2(\mathbf{R}_2)|^2. \tag{24}$$

The tunnel parameters are given by [6, 22]

$$t_{(1,2),\lambda} = -\frac{\hbar^2}{2m_\perp}\int_{\Omega_S} \mathrm{d}S\left(\varphi \frac{\mathrm{d}}{\mathrm{d}z}\psi_{1,2}^* - \psi_{1,2}^* \frac{\mathrm{d}}{\mathrm{d}z}\varphi_\lambda\right), \tag{25}$$

where integration is over the plane Ω_S, parallel to the QW plane and passing through the ions centers, $m_\perp$ is the effective mass in the direction perpendicular to the QW plane. Let the z-axis be normal to the QW plane ($z=0$ corresponds to the QW boundary), the x-axis passes through the ions centers so that their coordinates are

$$\mathbf{R}_1 = (-R/2, 0, d);\ \mathbf{R}_2 = (R/2, 0, d).$$

We assume that the localized wavefunctions ψ_1, ψ_2 do not overlap, thus, their particular form is not important. It is convenient to take them in the form

$$\psi_{1,2} = \left(\frac{2}{\pi r_0^2}\right)^{3/4} \mathrm{e}^{-((x\pm R/2)/r_0)^2} \mathrm{e}^{-(y/r_0)^2} \mathrm{e}^{-(z-d/r_0)^2}, \tag{26}$$

where r_0 is the localization radius. The continuum wavefunctions are taken as follows:

$$\varphi_{\mathbf{k}} = \eta(z)\mathrm{e}^{i\mathbf{k}\rho}. \tag{27}$$

Here $\mathbf{k}$ is the in-plane wave vector, ρ is the 2D in-plane radius-vector, $\eta(z)$ is the envelope function of size quantization along z. Outside of the QW:

$$\eta(z) = \zeta a^{-1/2}\mathrm{e}^{-qz}, \tag{28}$$

where $q = \sqrt{2m_\perp U_0}/\hbar^2$, U_0 is the binding energy of the bound state, which at the same time determines the height of the potential barrier between impurities and the QW [7], a is the QW width, ζ is a dimensionless parameter weakly depending on q and a. For a realistic rectangular QW $\zeta \approx 0.5$. The calculation of (25) using (26) (assuming $r_0 << k^{-1}$) and (27) yields

$$t_{1,2}(k) = \sqrt{\frac{\hbar^2 T}{2\pi m}}\mathrm{e}^{i\mathbf{k}\mathbf{R}_{1,2}}, \tag{29}$$

where T is the energy parameter for the tunneling,

$$T = (2\pi)^{3/2}\zeta^2 \frac{r_0 m}{a m_\perp} U_0 \mathrm{e}^{-2qd}, \tag{30}$$

m is the effective mass along the QW plane.

In order to tackle the resonance tunnel coupling of the bound state with the 2D continuum we use exactly solvable Fano–Anderson model [18]. The hybridized eigenfunctions ψ of the whole system are expanded over the bound states and the delocalized states in the form:

$$\Psi = \nu_1\psi_1 + \nu_2\psi_2 + \Phi, \quad \Phi = \int \nu_{\mathbf{k}}\varphi_{\mathbf{k}}\mathrm{d}\mathbf{k}. \tag{31}$$

Plugging (31) into the stationary Schrödinger equation $H\Psi = E\Psi$ with Hamiltonian (22) yields:

$$\begin{aligned} &\nu_1(\varepsilon_0 - E + \lambda_1) + \int t_{1\mathbf{k}}\nu_{\mathbf{k}}\mathrm{d}\mathbf{k} = 0, \\ &\nu_2(\varepsilon_0 - E + \lambda_2) + \int t_{2\mathbf{k}}\nu_{\mathbf{k}}\mathrm{d}\mathbf{k} = 0, \\ &\nu_{\mathbf{k}}(\varepsilon - E) + \nu_1 t_{1\mathbf{k}}^* + \nu_2 t_{2\mathbf{k}}^* = 0, \end{aligned} \tag{32}$$

where

$$\lambda_{1,2} = JAI_{1,2}s, \quad \varepsilon = \frac{\hbar^2 k^2}{2m}.$$

$\nu_{\mathbf{k}}$ is expressed from the last equation of (32) as follows:

$$\begin{aligned} \nu_{\mathbf{k}} = P\frac{\nu_1 t_{1\mathbf{k}}^* + \nu_2 t_{2\mathbf{k}}^*}{E-\varepsilon} \\ + Z\left(\nu_1 t_{1\mathbf{k}}^* + \nu_2 t_{2\mathbf{k}}^*\right)\delta(E-\varepsilon), \end{aligned} \tag{33}$$

where P denotes principal value and $Z(E)$ is to be determined. Plugging (33) into (32) yields

$$\begin{aligned} &\nu_1(\lambda_1 + F_{11} + ZT_{11} - E') + \nu_2(F_{21} + ZT_{21}) = 0, \\ &\nu_1(F_{12} + ZT_{12}) + \nu_2(\lambda_2 + F_{22} + ZT_{22} - E') = 0, \end{aligned} \tag{34}$$

where

$$\begin{aligned} &F_{\alpha\beta} = P\int \frac{t_{\alpha\lambda}^* t_{\beta\lambda}}{E-\varepsilon}\mathrm{d}\lambda, \quad T_{\alpha\beta} = \int t_{\alpha\lambda}^* t_{\beta\lambda}\delta(\varepsilon - E)\mathrm{d}\lambda, \\ &E' = E - \varepsilon_0; \quad \alpha, \beta = 1, 2. \end{aligned} \tag{35}$$

Plugging (29) into (35) we get

$$\begin{aligned} &T_{11} = T_{12} = T, \quad T_{12} = T_{21} \equiv t = TJ_0(k_E R), \\ &F_{11} = F_{22} \equiv F, \quad F_{12} = F_{21} \equiv f = \pi T Y_0(k_E R), \end{aligned} \tag{36}$$

where $k_E = \sqrt{2mE}/\hbar$. F represents the shift of the resonance position with respect to ε_0 and plays the same role as in (11). It can be explicitly evaluated given more accurate expression than (29) taking into account $k \sim r_0^{-1}$ to avoid the divergence. This is, in fact, the same as the renormalization procedure (12) for the true delta-potential. The finite F still contains extra degree of the tunneling parameter T, does not depend on R and can be neglected in the lowest order in T. From (34) follows the equation for Z:

$$(ZT - E' + \lambda_1)(ZT - E' + \lambda_2) = (f + Zt)^2. \tag{37}$$

With use of (31) and (33) the delocalized part of the hybridized wavefunction is given by

$$\Phi(E) = \pi\sqrt{\frac{2\pi mT}{\hbar^2}}\left[\begin{array}{l}\nu_1\left(\dfrac{Z}{\pi}J_0(k\rho_1) + Y_0(k\rho_1)\right)\\ +\nu_2\left(\dfrac{Z}{\pi}J_0(k\rho_2) + Y_0(k\rho_2)\right)\end{array}\right], \tag{38}$$

where $\rho_{1,2} = |\mathbf{r} - \mathbf{R}_{1,2}|$.

Proceeding analogously to (14)–(19) we, however, keep only the leading order in the tunneling parameter which appears to be T^2. Then we end up with the exchange energy for the tunneling case:

$$E_{\mathrm{ex}} = \frac{1}{\pi}\int_0^{E_F} \arctan\left[\frac{8\pi^2T^2j^2J_0(kR)Y_0(kR)}{\left((\varepsilon-\varepsilon_0)^2 - j^2\right)^2}\right]\mathrm{d}\varepsilon, \tag{39}$$

where $j = |JAIs|$. The expression (39) is somewhat similar to (19), but now the argument of arctangent in (39) has poles at $\varepsilon = \varepsilon_0 \pm j$ and the result strongly depends on whether these resonances are within the range of integration $\varepsilon \in [0, E_{\mathrm{F}}]$. If they are, from the width of the resonances the amplitude of the exchange interaction energy is estimated as

$$E_{\mathrm{res}} \sim \sqrt{Tj}, \tag{40}$$

while the period of the oscillations is $\hbar/\sqrt{2m\varepsilon_0}$. The limiting non-resonant case occurs if $\varepsilon_0 \gg E_{\mathrm{F}}$, $j \ll E_{\mathrm{F}}$. The integration (39) then results in

$$\begin{aligned} E_{\mathrm{nr}} &= \frac{8\pi T^2 j^2 E_{\mathrm{F}}}{\varepsilon_0^4}\chi(R),\\ \chi(R) &= J_0(k_{\mathrm{F}}R)Y_0(k_{\mathrm{F}}R) + J_1(k_{\mathrm{F}}R)Y_1(k_{\mathrm{F}}R). \end{aligned} \tag{41}$$

The condition $j \ll E_{\mathrm{F}}$ allows for the perturbation theory thus the expression (41) is what one would expect from the conventional RKKY approach. The functional dependence on R is exactly the same as for 2D RKKY interaction without tunneling [17] and the prefactor accounts for the particular model we have used to describe the tunneling and the bound impurity state. The interaction energy amplitude for the resonance case appears to be substantially higher than for the non-resonant one. Assuming for both cases $\varepsilon_0 \sim E_{\mathrm{F}}$ we can roughly estimate the amplification

$$\gamma \equiv \frac{E_{\mathrm{res}}}{E_{\mathrm{nr}}} \sim \frac{\varepsilon_0^4}{8\pi T^{3/2}j^{3/2}E_{\mathrm{F}}}. \tag{42}$$

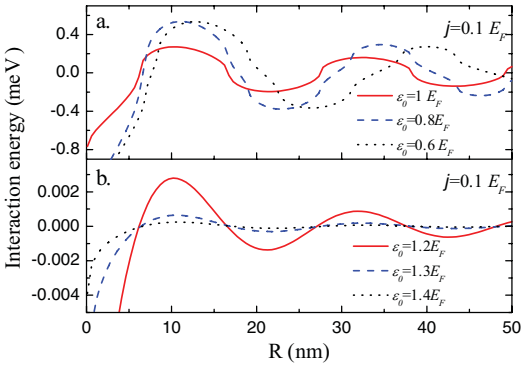

Figure 2 Indirect exchange interaction energy vs. distance between ions in the resonant (a) and non-resonant (b) case.

For an estimate we take the parameters based on InGaAs-based heterostructures studied in [1, 3, 23]. For $T \sim 0.01E_{\mathrm{F}}$, $j \sim 0.1E_{\mathrm{F}}$, γ can be as high as three orders of magnitude. Figure 2 shows the results of the numerical calculation according to (39) for different positions of the bound state energy ε_0 related to the Fermi level E_{F}. The domain of applicability starts from $R > r_0$ (for real structures $r_0 \sim 1$ nm). We take $m = 0.1m_0$ (m_0 is the free electron mass), $E_{\mathrm{F}} = 10$ meV, $j = 0.1E_{\mathrm{F}}$. The upper panel (Fig. 2a) represents the resonant case. For all the curves the resonances are within the integration range. In the case of $\varepsilon_0 = E_{\mathrm{F}}$ one of the two resonances goes outside of the range and the exchange energy is somewhat decreased. For the nonresonant case shown in (Fig. 2b) the argument of arctangent in (39) has no poles and the amplitude of the oscillations is dramatically decreased by two orders of magnitude. Figure 3 shows the dependence of the exchange energy on j. While for the non-resonant case it resembles the expected dependence $E_{\mathrm{ex}} \sim j^2$, for the resonant case the interaction energy may even decrease with increase of j when one of the resonances leaves the range $[0, E_{\mathrm{F}}]$. This very case occurs for $j = 0.3\ E_{\mathrm{F}}$ in Fig. 3a.

The formula (39) has another non-resonant limiting case for $j \gg E_{\mathrm{F}}$, $j \gg \varepsilon_0$. However, its applicability in this case remains questionable because with $j \gg E_{\mathrm{F}}$ the ion spins dynamics (neglected in our model) may be essential. It seems, however, the small tunneling parameter T allows for the case when the exchange constant is of the order of E_{F} while the ion spins dynamics yet does not play a role. This issue requires further investigation.

ACTA UNIVERSITATIS LAPPEENRANTAENSIS

544. MARTTONEN, SALLA. Modelling flexible asset management in industrial maintenance companies and networks. 2013. Diss.

545. HAKKARAINEN, JANNE. On state and parameter estimation in chaotic systems. 2013. Diss.

546. HYYPIÄ, MIRVA. Roles of leadership in complex environments
Enhancing knowledge flows in organisational constellations through practice-based innovation processes. 2013. Diss.

547. HAAKANA, JUHA. Impact of reliability of supply on long-term development approaches to electricity distribution networks. 2013. Diss.

548. TUOMINEN, TERHI. Accumulation of financial and social capital as means to achieve a sustained competitive advantage of consumer co-operatives. 2013. Diss.

549. VOLCHEK, DARIA. Internationalization of small and medium-sized enterprises and impact of institutions on international entrepreneurship in emerging economies: the case of Russia. 2013. Diss.

550. PEKKARINEN, OLLI. Industrial solution business – transition from product to solution offering. 2013. Diss.

551. KINNUNEN, JYRI. Risk-return trade-off and autocorrelation. 2013. Diss.

552. YLÄTALO, JAAKKO. Model based analysis of the post-combustion calcium looping process for carbon dioxide capture. 2013. Diss.

553. LEHTOVAARA, MATTI. Commercialization of modern renewable energy. 2013. Diss.

554. VIROLAINEN, SAMI. Hydrometallurgical recovery of valuable metals from secondary raw materials. 2013. Diss.

555. HEINONEN, JARI. Chromatographic recovery of chemicals from acidic biomass hydrolysates. 2013. Diss.

556. HELLSTÉN, SANNA. Recovery of biomass-derived valuable compounds using chromatographic and membrane separations. 2013. Diss.

557. PINOMAA, ANTTI. Power-line-communication-based data transmission concept for an LVDC electricity distribution network – analysis and implementation. 2013. Diss.

558. TAMMINEN, JUSSI. Variable speed drive in fan system monitoring. 2013. Diss.

559. GRÖNMAN, KAISA. Importance of considering food waste in the development of sustainable food packaging systems. 2013. Diss.

560. HOLOPAINEN, SANNA. Ion mobility spectrometry in liquid analysis. 2013. Diss.

561. NISULA, ANNA-MAIJA. Building organizational creativity – a multitheory and multilevel approach for understanding and stimulating organizational creativity. 2013. Diss.

562. HAMAGUCHI, MARCELO. Additional revenue opportunities in pulp mills and their impacts on the kraft process. 2013. Diss.

563. MARTIKKA, OSSI. Impact of mineral fillers on the properties of extruded wood-polypropylene composites. 2013. Diss.

564. AUVINEN, SAMI. Computational modeling of the properties of TiO2 nanoparticles. 2013. Diss.

565. RAHIALA, SIRPA. Particle model for simulating limestone reactions in novel fluidised bed energy applications. 2013. Diss.

566. VIHOLAINEN, JUHA. Energy-efficient control strategies for variable speed controlled parallel pumping systems based on pump operation point monitoring with frequency converters. 2014. Diss.

567. VÄISÄNEN, SANNI. Greenhouse gas emissions from peat and biomass-derived fuels, electricity and heat – Estimation of various production chains by using LCA methodology. 2014. Diss.

568. SEMYONOV, DENIS. Computational studies for the design of process equipment with complex geometries. 2014. Diss.

569. KARPPINEN, HENRI. Reframing the relationship between service design and operations: a service engineering approach. 2014. Diss.

570. KALLIO, SAMULI. Modeling and parameter estimation of double-star permanent magnet synchronous machines. 2014. Diss.

571. SALMELA, ERNO. Kysyntä-toimitusketjun synkronointi epävarman kysynnän ja tarjonnan toimintaympäristössä. 2014. Diss.

572. RIUNGU-KALLIOSAARI, LEAH. Empirical study on the adoption, use and effects of cloud-based testing. 2014. Diss.

573. KINNARINEN, TEEMU. Pressure filtration characteristics of enzymatically hydralyzed biomass suspensions. 2014. Diss.

574. LAMMASSAARI, TIMO. Muutos kuntaorganisaatiossa – tapaustutkimus erään kunnan teknisestä toimialasta. 2014. Diss.

575. KALWAR, SANTOSH KUMAR. Conceptualizing and measuring human anxiety on the Internet. 2014. Diss.

576. LANKINEN, JUKKA. Local features in image and video processing – object class matching and video shot detection. 2014. Diss.

577. AL-SAEDI, MAZIN. Flexible multibody dynamics and intelligent control of a hydraulically driven hybrid redundant robot machine. 2014. Diss.

578. TYSTER, JUHO. Power semiconductor nonlinearities in active d*u*/d*t* output filtering. 2014. Diss.

579. KERÄNEN, JOONA. Customer value assessment in business markets. 2014. Diss.

580. ALEXANDROVA, YULIA. Wind turbine direct-drive permanent-magnet generator with direct liquid cooling for mass reduction. 2014. Diss.

581. HUHTALA, MERJA. PDM system functions and utilizations analysis to improve the efficiency of sheet metal product design and manufacturing. 2014. Diss.

582. SAUNILA, MINNA. Performance management through innovation capability in SMEs. 2014. Diss.

583. LANA, ANDREY. LVDC power distribution system: computational modelling. 2014. Diss.

584. PEKKARINEN, JOONAS. Laser cladding with scanning optics. 2014. Diss.

585. PELTOMAA, JYRKI. The early activities of front end of innovation in OEM companies using a new FEI platform as a framework for renewal. 2014. Diss.